Published in final edited form as:
Chem Rev. 2010 May 12; 110(5): 2858–2902. doi:10.1021/cr900325h.

Coordinating Radiometals of Copper, Gallium, Indium, Yttrium and Zirconium for PET and SPECT Imaging of Disease

Thaddeus J. Wadas, Ph.D. *,
Mallinckrodt Institute of Radiology, Washington University School of Medicine, 510 S. Kingshighway Blvd., Campus Box 8225, St. Louis, MO. 63110 USA

Edward H. Wong, Ph.D.,
Department of Chemistry, University of New Hampshire, Durham, NH 03824-3598 USA, Phone: 603-862-1788, Fax: 603-862-4278, ehw@cisunix.unh.edu

Gary R. Weisman, Ph.D., and
Department of Chemistry, University of New Hampshire, Durham, NH 03824-3598 USA, Phone: 603-862-2304, Fax: 603-862-4278, gary.weisman@unh.edu

Carolyn J. Anderson, Ph.D. *
Mallinckrodt Institute of Radiology, Washington University School of Medicine, 510 S. Kingshighway Blvd., Campus Box 8225, St. Louis, MO. 63110 USA

1.0. Introduction

Molecular imaging is the visualization, characterization and measurement of biological processes at the molecular and cellular levels in humans and other living systems. Molecular imaging agents are probes used to visualize, characterize and measure biological processes in living systems. These two definitions were put forth by the Sociey of Nuclear Medicine (SNM) in 2007 as a way to capture the interdisciplinary nature of this relatively new field. The emergence of molecular imaging as a scientific discipline is a result of advances in chemistry, biology, physics and engineering, and the application of imaging probes and technologies has reshaped the philosophy of drug discovery in the pharmaceutical sciences by providing more cost effective ways to evaluate the efficacy of a drug candidate and allowing pharmaceutical companies to reduce the time it takes to introduce new therapeutics to the marketplace. Finally the impact of molecular imaging on clinical medicine has been extensive since it allows a physician to diagnose a patient's illness, prescribe treatment and monitor the efficacy of that treatment non-invasively.

Single Photon Emission Computed Tomography (SPECT) and Positron Emission Tomography (PET) were the first molecular imaging modalities used clinically. SPECT requires the use of a contrast agent labeled with a gamma emitting radionuclide, which should have an ideal gamma energy of 100-250 keV. These gamma rays are recorded by the detectors of a dedicated gamma camera or SPECT instrument and after signal processing can be converted into an image indentifying the localization of the radiotracer. PET requires the injected radiopharmaceutical to be labeled with a positron emitting radionuclide. As the radionuclide decays it ejects a positron from its nucleus which travels a short distance before being annihilated with an electron to release two 511 keV gamma rays 180° apart that are detected by the PET scanner (Figure 1). After sufficient acquisition time the data are reconstructed using

*Phone: 314.362.8427, Fax: 314.362.9940, andersoncj@wustl.edu. *Corresponding Author: Phone: 314.362.8441, Fax: 314.362.9940, wadast@wustl.edu.

computer based algorithms to yield images of the radiotracer's location within the organism. When compared to SPECT, PET has greater advantages with respect to sensitivity and resolution and has been gaining in clinical popularity, with the number of PET-based studies expected to reach 3.2 million by 2010.[1] While SPECT and PET technology has been around for decades, its use remained limited because of the limited availability of relevant isotopes which had to be produced in nuclear reactors or particle accelerators. However, the introduction of the small biomedical cyclotron, the self-contained radionuclide generator and the dedicated small animal or clinical SPECT and PET scanners to hospitals and research facilities has increased the demand for SPECT and PET isotopes.

Traditional PET isotopes such as ^{18}F, ^{15}O, ^{13}N and ^{11}C have been developed for incorporation into small molecules, but due to their often lengthy radio-syntheses, short half-lives and rapid clearance, only early time points were available for imaging, leaving the investigation of biological processes, which occur over the duration of hours or days, difficult to explore. With the continuing development of biological targeting agents such as proteins, peptides, antibodies and nanoparticles, which demonstrate a range of biological half-lives, a need arose to produce new radionuclides with half-lives complementary with their biological properties. As a result, the production and radiochemistry of radiometals such as Zr, Y, In, Ga and Cu have been investigated as radionuclide labels for biomolecules since they have the potential to combine their favorable decay characteristics with the biological characteristics of the targeting molecule to become a useful radiopharmaceutical (Tables 1 and 2).[2]

The number of papers published describing the production or use of these radiometals continues to expand rapidly, and in recognition of this fact, the authors have attempted to present a comprehensive review of this literature as it relates to the production, ligand development and radiopharmaceutical applications of radiometals (excluding ^{99m}Tc) since 1999. While numerous reviews have appeared describing certain aspects of the production, coordination chemistry or application of these radiometals,[2-18] very few exhaustive reviews have been published.[10,12] Additionally, this review has been written to be used as an individual resource or as a companion resource to the review written by Anderson and Welch in 1999.[12] Together, they provide a literature survey spanning 50 years of scientific discovery. To accomplish this goal, this review has been organized into three sections: the first section discusses the coordination chemistry of the metal ions Zr, Y, In, Ga and Cu and their chelators in the context of radiopharmaceutical development; the second section describes the methods used to produce Zr, Y, In, Ga and Cu radioisotopes; and the final section describes the application of these radiometals in diagnostic imaging and radiotherapy.

2.0. The Coordination Chemistry of Cu, Ga, Y, In and Zr

2.1. General Considerations

The development of metal-based radiopharmaceuticals represents a dynamic and rapidly growing research area which requires an intimate knowledge of metal coordination chemistry and ligand design. This section of the review covers general considerations regarding the parameters that are important in developing stable, kinetically inert radiometal complexes that can be incorporated into radiopharmaceuticals. Additionally, the aqueous coordination chemistry of these metals and their coordination complexes which are most relevant to radiopharmaceutical development are discussed below.

Relevant properties in aqueous solution of the five metal cations covered in this review are presented in Table 3. The acidic cations Ga(III), In(III), and especially Zr(IV) present precipitation problems at neutral pH in the absence of suitable complex formation. In terms of plausible aqueous redox processes relevant to radiopharmaceutical applications, only Cu(II) and its complexes are susceptible to reduction chemistry, although the possibility of an ascorbic

acid reduction of a ^{89}Zr(IV) complex has been postulated.[19] Based on Pearson's Hard-soft Acid-base theory, the tetravalent Zr(IV) is an extremely hard acidic cation, followed by Y(III), Ga(III), and In(III). The Cu(II) cation is considered a borderline acid.

Since the preponderance of radiometal complexes of note feature at least tetradentate ligands, we have restricted our discussion here to ligands with four or more donor sites coordinating the cation of interest. Rather than exhaustive coverage of all chelators of potential interest, we will discuss only selected representatives of the most-frequently reported ligands, especially those with more complete data of relevance. For the chosen representative chelators of each cation, we have listed available pertinent data on their denticity, coordination geometry, and thermodynamic stability. Where X-ray structural data are available, geometrical data on the coordination mode can provide useful insight into the "goodness of fit" for a specific cation-chelator pairing, the caveat being that actual solution structures or indeed number of species may be distinct from solid-state observations. For the four diamagnetic cations, solution NMR spectroscopic studies can be used to supplement X-ray data. Despite the difficulty of comparing stability constants of complex formation between ligands of different basicity and denticity, the listed log $\mathbf{K_{ML}}$'s provide a convenient gauge of their relative affinities for a specific metal.

For *in vivo* applications, kinetic inertness of metal-chelator complexes or conjugates can be more relevant than thermodynamic stability.[12,20,21] In general, acyclic chelator complexes are less kinetically inert than macrocyclic complexes of comparable stability.[22-26] By the same token, acyclic chelators typically have faster metal-binding kinetics compared to their macrocyclic analogues, which can be a significant advantage for shorter-lived radiometals.[27-30] There have been efforts to enhance the binding rate of macrocycles by incorporation of an acyclic polydentate pendant.[31]

A variety of *in vitro* assays of metal-chelator complex integrity can be found in the literature.[32-35] A popular assay of aqueous kinetic inertness is acid decomplexation. This has some relevance in biological environments that are relatively acidic such as in hypoxic tissues and certain cell vesicles. However, the extremely high acidities, e.g. 1-5 M HCl, often required to decompose relatively inert complexes clearly have no parallel to any *in vivo* conditions. Nor can such data be relied upon, without considerations of other factors, as the sole predictor of biological behavior.[36] Typically, the decomplexation of Cu(II) complexes is readily monitored through their electronic spectra. Demetallation of the diamagnetic Ga(III), In(III), Y(III), and Zr(IV) complexes can usually be followed by proton and ^{13}C NMR spectroscopy in acidified D_2O solutions. Where practicable, ^{71}Ga, ^{115}Ga, In, and ^{89}Y NMR studies can also be undertaken.[37-39] Although detailed mechanistic investigations are sometimes reported, more commonly only *pseudo*-first order half-lives are reported which should only be used to rank inertness qualitatively. Nonetheless, such data remain useful as a preliminary indicator of the *in vivo* viability of specific metal-based radiopharmaceuticals.

Competition or challenge assays of complexes of interest with excess biometals and biochelators are relevant since their typical concentrations are orders of magnitude higher than the radiolabeled complex's, requiring high chelator selectivity for the radiometal. For example, copper homeostasis is tightly regulated in biology,40 and as a result a variety of copper-binding biomolecules are present in extracellular (e.g. serum albumin, ceruloplasmin, transcuprin, etc.) as well as intracellular (e.g. transporters, chaperones, metallothioneins, superoxide dismutase, cytochrome c oxidase, etc.) environments.41-43 A viable Cu(II) chelator should therefore be both thermodynamically stable and kinetically inert to transchelation challenges by these species. Highly-charged cations like Y(III) and Zr(IV) may also have high affinity for bone tissues while the avid Ga(III) binding of transferrin is well-established.44-46 Serum stability studies using radiometal-labeled chelator complexes or their bioconjugates are routinely used in inertness assays. These are readily monitored by radio-TLC, HPLC and LC-MS techniques.

47-49 *In vitro* uptake studies using specific cell lines have also been carried out in many assays. While simulating extracellular environments to an extent, these studies cannot always accurately forecast *in vivo* behavior. Ultimately studies of animal biodistribution and bioclearance using radiometal-labeled complexes or bioconjugates need to be carried out to obtain realistic data on their *in vivo* performance.

The following discussion of pertinent acyclic and macrocyclic ligands and their specific metal coordination chemistry is organized according to their denticity. Most of these ligands have been designed to provide a minimum of four donor atoms, usually also incorporating anionic sites for charge balance (See Figures 2 and 3.). While all are given numerical "**L(number)**" designations, many have been labeled additionally with their respective acronyms. Published X-ray crystal structures of Cu, In, Ga, Y and Zr coordination complexes involving these ligands are also provided where appropriate. They were prepared from published CIF files using CrystalMaker 8.2 for Mac (CrystalMaker Software Ltd., Centre for Innovation & Enterprise, Oxford University Begbroke Science Park, Sandy Lane, Yarnton, Oxfordshire, OX5 1PF, UK; http://www.crystalmaker.com). Each atomic sphere is scaled to 0.4 times the covalent atomic radius, using the recently updated radii of Alvarez and coworkers.[50] In addition to the labeled and uniquely colored metal atoms, common elements are color coded as follows: C = gray, Cl = green, F = light green, N = blue, O = red, P = orange, and S = yellow. Hydrogen atoms have been omitted from the structures for clarity.

2.2. Aqueous Copper Coordination Chemistry

While +1 and +3 oxidation states are both accessible for copper in the presence of suitable donors, 3d9 Cu(II) remains the predominant state for radio-copper chemistry in protic media. The aqueous cupric ion was long believed to have a tetragonally distorted hexa-aqua structure until a 2001 report suggested only five-coordination.51 Its water-exchange rate has been found to be very rapid compared to most common first-row transition metal cations and as a result it has relatively facile substitution chemistry despite having some crystal-field stabilization. This is usually ascribed to the Jahn-Teller distortion that elongates one or more of its coordinated ligands. Classified as a cation of borderline hardness, the high affinity of Cu(II) for borderline nitrogen donors is well-established. With a relatively small ionic radius of between 57 to 73 pm for coordination numbers 4 through 6, it is particularly suitable for the formation of 5-membered chelate rings; indeed the chelate effect is epitomized in its ethylenediamine family of complexes.52 The popular use of polyazamacrocycles, especially cyclen and cyclam, for strong binding of Cu(II) is a consequence of the added advantage of the macrocyclic effect, 53 as borne out by their extensive coordination literature.54-57

The importance of *in vivo* redox activation of metallodrugs incorporating Pt(IV), Ru(III), and Co(III) has received increasing attention.[58-61] The role of bioreduction in copper radiopharmaceutical efficacy has been intensively studied in their thiosemicarbazone complexes, especially Cu-**ATSM** (**L9**).62-64 Convincing evidence for the formation and selective retention/decomplexation of Cu(I)-intermediates from Cu(II) precursors in hypoxic tissues has been presented.65,66 Whether Cu(II)/Cu(I) bioreduction is also a viable pathway for irreversible *in vivo* radio-copper loss from other chelator complexes and their bioconjugates is an intriguing possibility. There is some compelling evidence for the deteriorated *in vivo* performance of related Cu(II) complexes differing only in their reduction propensities. Specifically, the "long arm" dicarboxyethyl pendant-armed Cu(II) complex of cross-bridged cyclam has an E_{red} almost 400 mV higher (or more positive) than that its carboxymethyl-armed analogue, Cu-**CB-TE2A** (**L57**).[67] The former has been found to exhibit significantly inferior bioclearance behavior despite very similar coordination geometry and acid-inertness. More structure-activity studies, including the consequence of protonation on reduction feasibility, are warranted. Most polyazamacrocyclic complexes of Cu(II), however, have rather negative

reduction potentials that are well below the estimated −0.40 V (NHE) threshold for typical bioreductants. It should be further noted that an appropriate *in vivo* donor able to alter the first or, perhaps even second coordination sphere around a metal cation can dramatically facilitate its redox processes. The relevance of this tuning of redox-active metal lability during biological iron transfer has been substantiated.[68,69] Whether such ternary interactions can play a role in the reductive demetallation of thermodynamically-stable Cu(II) complexes *in vivo* has not been explored.

2.3. Copper(II) Complexes of Selected Chelators

The plasticity of the Cu(II) coordination geometry can be gleaned from a literature survey of 89 of its complexes with cyclen and cyclam derivatives.[70] Coordination numbers (CN) ranging from 4 through 6 were found with geometries approximating square planar, square pyramidal, trigonal bipyramidal, as well as octahedral. Tetradentate chelators are usually designed to cater to Cu(II)'s strong affinity for ligands favoring a square-planar geometry. Common donor sets include two amino or imino nitrogens combined with two charge-neutralizing anionic amido, oxo, or thiolato sites. These include numerous Schiff-base or amino-acid derived chelators. Full envelopment of Cu(II) in its maximum six-coordinate mode is much sought after. As a result, hexadentate chelators have become the most investigated in radio-copper chemistry. Popular scaffolds include triaza- or tetraazamacrocycles, especially **TACN** (**L26**), cyclen (**L38**), and cyclam (**L48**). Methodologies for selective attachment of appropriate pendant arms to their secondary amine nitrogen sites as well as to the carbon backbone have been developed.[71-79] Resulting donor sets usually incorporate anionic carboxylate or thiolate sites to provide a medley of charge-neutralizing N_3O_3, N_3S_3, or N_4O_2 coordination spheres. Data for selected Cu(II)-chelator complexes are listed in Table 4.

2.3.1. Acyclic Tetradentate Chelators—A dimethyl ester of *N,N'*-ethylenediamine-di-L-cysteinato **EC** (**L5**) was reacted with Cu(II) and the resulting complex structurally characterized and found to be substantially twisted (21°) from a square planar geometry (Figure 4).[80]

Bis(thiosemicarbazonato) complexes of cold and radio-Cu(II) have been intensely investigated for hypoxia imaging (*vide infra*).[62,63,81] A series of X-ray structures of these complexes have been determined and near square-planar geometries were typically observed (e.g. **Cu-GTS** (Cu-**L7)** and **Cu-PTSM** (Cu-**L8)** in Figures 5 and 6). Alkylation at the backbone C atoms was found to increase the backbone C-C bond length and allow the metal to fit better into the ligand cavity with shorter Cu-S bonds.[82] Their Cu(II)/Cu(I) reduction potentials have been shown to have significant bearing on their *in vivo* biological behavior.[62,63,66]

2.3.2. Acyclic Hexadentate Chelators—The Cu(II)-**EDTA** (**L10**) structure has been reported to be a tetragonally-distorted N_2O_4 octahedron along one O-Cu-O axis (Figure 7).[83] A **DTPA** (**L12**) analogue also features a hexadentate chelator but with an N_3O_3 coordination environment (Figure 8).[84]

Rigid **BISPIDINE** (3,7-diazabicyclo[3.3.1]nonane) derivatives with two appended pyridyl functions have been shown to be tetradentate in five-coordinate Cu(II) complexes (Cu-**L17**, Figure 9).[85] Variations with four pyridyl as well as two non-coordinating carboxylate groups for charge neutralization are hexadentate chelators which were found to bind Cu(II) rapidly. An X-ray structure revealed a distorted octahedral N_6 coordination mode (Cu-**L18**, Figure 10). This chelator was conjugated to bombesin, radiolabeled with ^{64}Cu and studied in rats.[86]

Hexadentate ligands based on the 1,3,5-triaminocyclohexane backbone appended with three methylpyridines (**TACHPYR, L19**) have been investigated as radio-copper chelators.[87,88] These form tetragonally-distorted octahedral Cu(II) complexes (Figure 11).

2.3.3. Macrocyclic Chelators—The 14-membered N_2S_2 macrocycle **L24** was found to form the most inert Cu(II) complex compared to other ring sizes.[89] New N_2S_2 macrocycles with two appended carboxymethyl arms (**L25**) have been synthesized and complexed with both Cu(II) and ^{64}Cu(II).[90] Molecular modeling suggested that only the 13-membered macrocycle can form a six-coordinate complex while the 14-membered analogue can only coordinate with its O_2S_2 donors.

Derivatives of **TACN** with either two (**NO2A, L28**) or three (**NOTA, L29**) carboxymethyl pendant arms both complex Cu(II) with good affinity. Their structures (Figure 12 and 13) reflect the ability of the cation to adopt either 5 or 6-coordination modes. The former has an N_3O_2 square pyramidal geometry with one N axial.[91] The latter N_3O_3 donor set forms a distorted trigonal prismatic geometry.[92] A **TACN** derivative with three oxime arms (**L31**) yielded a 5-coordinate Cu(II) complex with one oxime arm uncoordinated but held by a strong OH3···O hydrogen bond to a coordinated oxime (Figure 14).[93]

Monocationic diimine dioxime (**L32**) complexes of Cu(II) were labeled with ^{64}Cu and their biodistributions studied.94-[96] The X-ray structure of a Cu(II) complex of a pyridyl-tethered derivative revealed a tetradentate ligand (**L33**) forming the base of a square pyramid with an axial water but no pyridyl coordination (Figure 15).[97] Propylenediamine dioxime ligands have also been examined for their Cu(II) complexation in order to model radiopharmaceuticals.[98] The cation was again found to adopt a square pyramidal coordination geometry featuring an apical water.

Dioxotetraazamacrocyclic Cu(II) complexes have been investigated for their radio-copper chelation potential.[99] Of the chelators with varying ring sizes studied, dioxocyclam (**L34**) was shown to form the most stable complex. A methylquinoline pendant-armed dioxocyclam (**L35**) was found to doubly deprotonate at its amide N's upon Cu(II) binding. Its structure has a distorted square-planar coordination geometry (Figure 16).[82] Recently, a benzo-annelated dioxocyclam (**L36**) was synthesized and its Cu(II) complexation and ^{64}Cu radiolabeling investigated.[100] A four-coordinate distorted square planar structure was found. This complex has an extremely low reduction potential but can be reversibly oxidized.

Carboxymethyl pendant-armed derivatives of cyclen including **DOTA**(**L39)** and **DO3A** (**L42**) have been investigated for their Cu(II) binding. An X-ray structure of Cu-**DOTA** (Cu-**L39)** shows the expected *pseudo*-octahedral geometry with all cyclen N's and two carboxymethyl arms from non-adjacent N's coordinating *cis* to each other (Figure 17).[101] An analogous geometry was found for the Cu-**DO3A**(**L42**) structure.[102] The dicarboxymethyl armed cross-bridged cyclen (**CB-DO2A, L37**) was shown to envelop the Cu(II) in a very distorted octahedral geometry with the carboxylate donor sites *cis* to each other (Figure 18).[21] It was pointed out that the metal center is significantly distended from the chelator cavity, which may account for its significantly lower inertness compared to its cyclam analogue Cu-**CB-TE2A** (Cu-**L57**) (*vide infra*).

Cyclen appended with methanephosphonate pendant arms such as **DO2P** (**L46**) and **DOTP** (**L47**) have been synthesized and chelated to Cu(II) and ^{64}Cu.[103] Mixed phosphonate- and acetate-armed cyclen (e.g. **DO2A2P**, **L45**) have also been studied with the highest log $\mathbf{K_{ML}}$ found for Cu-**DO2P** (Cu-**L46**).[104]

Due to the good cation/cyclam match, numerous Cu(II) complexes of cyclam and its derivatives with at least one carboxymethyl pendant arm on N have been prepared and studied. As expected, the singly-armed chelator C-hexamethyl-**TE1A** (Me_6-**L50**) yielded a square-pyramidal Cu(II) structure (Figure 19).[105] Several structures of the doubly-armed ligand complexes have been determined. The first features carboxylates on adjacent ring N's (**1,4-**

TE2A, **L51**, Figure 20),[106] while the latter on non-adjacent N's (**1,8-TE2A**, **L52**, Figure 21).[107] Two diprotonated Cu-**TETA** (**L49**) structures were shown to have their axial-elongations either along the acetate O's or across two cyclam ring N's (Figure 22).[108] A C-functionalized **TETA** Cu(II) complex, Cu-**L55** also has a *pseudo*-octahedral metal coordination mode (Figure 23).[109]

Two cross-bridged cyclam chelators, one with two carboxymethyl arms (**CB-TE2A, L57**), the other with one carboxymethyl and one acetamide arm (**CB-TEAMA**, **L58**) have been prepared to compare the *in vivo* behavior of their ^{64}Cu complexes.[110] The former structure revealed full envelopment of the Cu(II) in a *pseudo*-octahedral geometry with elongation along one N-Cu-O axis (Figure 24).[111] While the latter has a very similar geometry, a weaker amide O-coordination is observed (Figure 25).[110] The Cu-**CB-TE2A** complex has been shown to have remarkable kinetic inertness towards acid decomplexation, with a half-life of almost a week in 5 M HCl, even at 90°.[112] A derivative of this chelator with a C-functionalized *p*-isothiocyanatobenzyl group has been prepared and successfully conjugated to biotin.[113]

The diphosphonate pendant-armed cyclam **TE2P** (**L54**) has been reported to form a very stable Cu(II) complex with a tetragonally-distorted octahedral geometry (Figure 26).[114] This complex also has a respectable acid inertness compared to typical cyclam copper complexes.

Pendant-armed derivatives of adjacent or side-bridged cyclam (**L58**, **L59**) have been prepared and complexed with Cu(II).[108] These chelators strongly favor square planar coordination of the cation by the macrocycle with axial coordination by a pendant arm to give square pyramidal geometries. A recent novel side-bridged cyclam with one acetate and one phosphonate pendant arm (**L60**) has been synthesized, labeled with ^{64}Cu and studied *in vivo*. It was reasoned that, unlike **CB-TE2A**, this bifunctional chelator (BFC) will form a charge-neutral Cu(II) complex despite conjugation of one acetate arm.[115]

The venerable hexaamine cryptand, Sarcophagine, is well known for its strong binding of Cu (II) and inertness of its complexes.[116-118] Its derivatives **DIAMSAR** (**L62**) and **SARAR** (**L65**) have been investigated as ligands for copper radiopharmaceuticals by several research groups.[119-124] Diprotonated **DIAMSAR** (**L62**) was found to have a Cu(II) coordination mode halfway towards trigonal prismatic but with two elongated *trans*-Cu-N bonds (Figure 27).[118] A related carboxymethyl pendant armed complex (Cu-**L63**) is closer to an octahedral coordination mode again with two long *trans*-bonds (Figure 28),[125] while a doubly carboxymethylated **DIAMSAR** Cu(II) complex (Cu-**L64**) has two elongated *cis*-bonds (Figure 29).[126] Recently the Cu(II) complex of a glutaric acid **DIAMSAR** derivative suitable for peptide conjugation was synthesized. Its coordination geometry is again distorted octahedral with axial Jahn-Teller elongations.[124]

2.4. Aqueous Gallium(III) Coordination Chemistry

The prevalent gallium oxidation state in aqueous solution is +3. This small and highly-charged cation of ionic radius 47-62 pm (CN 4-6) is quite acidic with a *pKa* of 2.6 in its hydrated form. As a result it has low solubility in normal pH media in the absence of suitable donors. Due to its strong affinity for hydroxide, at very high pH it also has a propensity to demetallate from its complexes and form the gallate anion $Ga(OH)_4^-$. Among the four water-soluble metal cations discussed in this review, aqueous Ga(III) has the most sluggish water exchange rate due to its small size and high charge.

As a classic hard acidic cation, Ga(III) is strongly bound to ligands featuring multiple anionic oxygen donor sites, although it has also been shown to have good affinity for thiolates. Typically chelators have been developed to sequester Ga(III) up to its maximum coordinate

number of 6 in a *pseudo*-octahedral geometry. A comprehensive review of six-coordinate Ga (III) complexes has appeared recently.[127]

It is well known that the biological iron transporter transferrin has a strong affinity for Ga(III) (Table 5). [46,128] Radio-gallium chelator complexes must therefore be sufficiently inert to transchelation by this biomolecule to have efficacy for *in vivo* applications. Data for selected Ga(III)-chelator complexes are presented in Table 5.

2.4.1. Tetradentate Ligands—Tetradentate *o*-hydroxybenzyl derivatives of iminodiacetic acid (**L1**) were designed to provide an NO_3 donor set which completes the distorted octahedral coordination around their Ga(III) center together with two *cis*-coordinated waters (Figure 30).[129] In accordance with substituent effects, the *p*-OMe derivative has the highest stability constant while *p*-NO_2 has the lowest.

The tripodal NS_3 chelator *tris*(2-mercaptobenzyl)amine (**L2**) formed a stable 4-coordinate Ga (III) complex with a distorted tetrahedral structure (Figure 31).[130] Under similar preparative conditions, the analogous In(III) complex was found to be 5-coordinate with additional solvent binding.

A *bis*(aminothiolate) N_2S_2 chelator yielded a distorted square pyramidal GaCl complex with one S donor in the axial site.[131] A similar structure was determined for the related GaCl-**BAT-TM** (GaCl-**L4**) except that chloride is the axial ligand (Figure 32).[132] In aqueous acetonitrile solution, however, NMR spectra revealed the presence of two different N_2S_2–coordinated species.

2.4.2. Hexadentate Ligands—An acyclic hexadentate chelator *N,N'*-ethylene-di-*L*-cysteine (**EC, L5**) with $N_2O_2S_2$ donor sites has been found to form a very stable complex with Ga(III) (Table 5).[133] This structure is a distorted octahedron with the two carboxylate O's in *trans* arrangement (Figure 33). Additionally, the [Ga-**EDTA, L10**]$^-$ structure has been reported in which the acyclic chelator is fully hexadentate in a distorted octahedral coordination sphere (Figure 34).[134]

The aminophenolate chelator N,N'-*bis*(2-hydroxybenzyl)ethylenediamine-N,N'-diacetic acid (**HBED, L11**) has an N_2O_4 donor set and its Ga(III) complex has a very high stability constant (Table 5).[135] As a consequence, it has generated considerable interest as a bifunctional chelator. The derivative N,N'-*bis*[2-hydroxy-5-carboxyethyl)-benzyl]ethylene diamine-N,N'-diacetic acid (**HBED-CC**)[136] and its tetrafluorophenyl ester derivative have been described to promote facile coupling to both scFV and anti-Ep-CAM diabodies.[137] Using this BFC these biomolecules could be labeled with ^{68}Ga to give specific activities of 142 GBq/μmol. Interestingly, a potentially octadentate **DTPA (L12)** derivative gave a less stable complex likely due to its structural constraints.[138] Linear tetraamines end-capped with phenols, like **SBAD** (**L15**), have been synthesized and their Ga(III) complexations investigated.[139] These were all found to favor Ga(III) over In(III) binding.

Although numerous complexes of both cold and radio-Ga(III) with **DTPA** (**L12**) and its derivatives have been prepared and studied, surprisingly no X-ray structure of the parent complex has yet been published. It is noteworthy that both **EDTA (L10)** and **DTPA (L12)** bind In(III) more avidly than Ga(III) (Tables 5 and 6). Recently, a variant of **DTPA (L12)** incorporating the *trans*-1,2-diaminocyclohexane backbone, **CHX-A"-DTPA (L14)**,[140] has been bioconjugated and studied as a chelator for ^{68}Ga, ^{86}Y, and ^{111}In in melanoma imaging.[141]

A family of hexadentate *bis*(salicylaldimine) chelators, **BAPEN** (**L16**), have been developed as carriers for ^{68}Ga radiopharmaceuticals.[142-144] These all feature a set of N_4O_2 donors enveloping the Ga(III) in a *pseudo*-octahedral coordination sphere. The structure of one of these is shown (Figure 35).

The *tris*-acetate pendant armed 1,4,7-triazacyclononane (**TACN**) derivative, **NOTA (L29)**, and its relatives have been found to form highly stable Ga(III) complexes.[145] An X-ray structure of Ga-**NOTA** (Ga-**L29**) confirmed the distorted octahedral N_3O_3 envelopment of the cation (Figure 36).[37,146] Remarkably, Ga-**NOTA** (Ga-**L29**) showed such high acid inertness that it survived 5M HNO_3 for over 6 months.[37] This is in stark contrast to In-**NOTA** (In-**L29**) which demetallated irreversibly within minutes at pD < 0. The *tris*(2-mercaptoethyl) pendant-armed **TACN** chelator, **TACN-TM (L27)**, also formed a distorted octahedral structure with Ga(III), again with impressive stability (Figure 37).[146] The superb stability of Ga(III)-**NOTA** (Ga-**L29**) (log K = 30.1; pM = 26.4) [147] underscores the use of this agent in radiopharmaceutical chemistry. This exceptional stability is believed to arise from the effective encapsulation of the gallium ion, which has an ionic radius of 0.76 Å within the macrocyclic cavity. Additional protection is afforded by the pendant carboxymethyl arms that help to protect the Ga ion from nucleophilic attack, which would cause complex instability and transchelation *in vitro* or *in vivo*. Since its synthesis, several **NOTA** (**L29**), analogues have been prepared with modified pendant groups for coupling to biological molecules, to influence the charge on the complexes once complexation has occurred or to facilitate coupling during peptide synthesis.[148-154]

Since the potentially octadentate **DOTA** (**L39**) can more than saturate Ga(III)'s usual 6-coordination sphere, both its mono- and diprotonated structures feature a similar distorted octahedral coordination composed of two *cis*-carboxylates and four macrocyclic N's (Figure 38).[155,156] It is advantageous that a free carboxymethyl arm can be available for conjugation to targeting moieties. A variety of such complexes have appeared in the literature. The Ga-**DOTA-D-PheNH$_2$** (Ga-**L40**) coordination mode is again *pseudo*-octahedral with *cis*-carboxylate coordination while the remaining acetate and amide arms are unbound (Figure 39).[157] It was therefore postulated that the better kidney clearance of the radiolabeled **DOTA**^{0}-D-Phe^1-Tyr^3-octreotide, ^{67}Ga-**DOTA(L39)-TOC,** compared to its ^{90}Y-labeled analogue was due to their different coordination modes. Whereas the former has uncoordinated amide and carboxylate arms, the latter is likely fully octa-coordinated. When **DOTA (L39)** was linked to a mitochondrion-targeting triphenylphosphonium moiety to give **DO3A-TPP** (**L44**), its Ga (III) complex again retained the 6-coordinate *pseudo*-octahedral geometry (Figure 40).[158] Unfortunately, **DOTA (L39)** has many potential drawbacks as a BFC for gallium radiometals, which include an overly large cavity size that can lead to lower thermodynamic stability as well as non-selectivity as a metal chelator.[159] Additionally, the complexation kinetics are slower, and as a result the complexation reactions often require elevated temperatures and longer reaction times, which are counterproductive given the short half-life of the ^{68}Ga radionuclide. The thermodynamic stability of Ga(III)-**DOTA** (Ga-**L39**) is approximately 10 orders of magnitude lower than Ga(III)-**NOTA** (Ga-**L29**), with a log K of 21.3 and a pM of 15.2.[160] Given the low pM values, it is interesting that radio-gallium DOTA (**L39**) complexes have shown *in vivo* stability in agents such as $^{67/68}$Ga-**DOTA**(**L39**)-TOC. However, there are reports that radio-gallium **DOTA**(**L39**)-RGD peptides have demonstrated compromised stability *in vivo*, with the radio-gallium demonstrating binding to plasma proteins.[161]

Related to Ga-**DOTA (Ga-L39)** is the complex Ga-**TETA (Ga-L49)** but, no structural data has been reported for it. Further, Ga-**TETA (Ga-L49)** has a lower stability constant than the former complex (log K = 19.7; pM = 14.1).[160] It should be noted that **TETA (L49)**, unlike **DOTA (L39)**, does not have a favorable *fac*-coordinating conformation.

Both dicarboxymethyl pendant-armed cross-bridged cyclen (**CB-DO2A**, **L37**) and cross-bridged cyclam (**CB-TE2A**, **L57**) gallium complexes have been synthesized and structurally characterized.[162,163] As expected, distortions from an octahedral geometry are much more pronounced in the former (Figures 41 and 42). Of these two, only Ga-**CB-TE2A** (Ga-**L57**) showed impressive acid inertness. A sample of it in 5M DCl at 90° was less than 20% demetallated even after 6 months.

The high thermodynamic stability of Ga(III) complexes of preorganized O_6 trihydroxamate chelators, especially Desferal or Deferrioxamine-B, **DFO** (**L23**) (log K = 28.6), has spurred much activity towards their biological and radiopharmaceutical applications.[164-169] Early solution NMR spectroscopic studies had revealed the presence of two major isomeric forms of Ga-**DFO** (Ga-**L23**).[170] An X-ray structure that can model Ga-**DFO** (Ga-**L23**) has been obtained in a Ga-*tris*(benzohydroxamate) complex which has a *fac*-octahedral coordination sphere (Figure 43).[171] The stability constants of Ga(III) complexes of a *tris*(hydroxamate) cryptate, **L63**, as well as two acyclic analogues, **L21** and **L22**, were compared with the cryptate complex and found to be the most stable of the three (log Ks = 27.5, 25.6 and 27.3, respectively).[172] An Enterobactin model **DiP-LICAM** (**L20**) has been reported to bind ^{67}Ga(III) with a very high stability constant (log K = 38.6; Table 5).[185]

2.5. Aqueous Indium(III) Coordination Chemistry

Like gallium, the only stable aqueous indium oxidation state is +3. The significantly larger size of In(III) at 62-92 pm for CN 4-8, however, results in its attainment of coordination numbers of 7 and even 8 in its complexes. While still a hard acid, its higher *pKa* of 4.0 and faster water exchange rate also reflect its distinction from Ga(III). A slightly enhanced affinity for softer donor types compared to Ga(III) can be noted in In(III) coordination chemistry. For example, acyclic N_4O_2 aminophenols as well as the biological iron transporter transferrin bind Ga(III) more avidly than In(III). By contrast, the tripodal NS_3 chelators, **EDTA** (**L10**), **DTPA** (**L12**), and **DOTA** (**L39**) all complex In(III) more securely as well as with higher denticity than Ga(III). Such differences in fundamental coordination preferences can have significant consequences in their biological behavior.[157] Data for selected complexes are listed in Table 6.

2.5.1. Tetradentate Chelators—A variety of acyclic tetradentate chelators featuring mixed amine and thiolate donor sets have been synthesized for In(III) complexation. The InCl-*bis*(aminothiolate), InCl-**BAT-TM** (**L4**), structure is 5-coordinate and near square pyramidal with an axial chloride (Figure 44).[132] While the complex was found to be stable in aqueous acetonitrile at *pD* 4.6, NMR spectra revealed the presence of two isomeric solution species. Tripodal NS_3 chelators such as *tris*(2-mercaptobenzyl)amine (**L2**) favor a trigonal bipyramidal coordination including an axial solvent dimethylformamide (DMF) at the metal center (Figure 45).[130] This can be contrasted with the ready isolation of a 4-coordinate Ga(III) analogue.[130] Both the synthesis and structural determination of a related *tris*(mercaptoethyl)amine (**L3**) complex of In(III) have also been reported.[173]

2.5.2. Hexa- to Octadentate Chelators—A hexadentate chelator boasting $N_2O_2S_2$ donors, N,N'-ethylenedi-*L*-cysteine (**EC**, **L5**), was found to form a distorted octahedral complex of In(III) with both carboxylate donors at axial sites (Figure 46).[133] This has an impressively high stability constant and was not demetallated by transferrin. The related *N,N'-bis*(2-hydroxybenzyl)ethylene-diamine-N,N'-diacetic acid (**HBED**, **L11**) has also been found to bind In(III) strongly, though still with much lower affinity when compared to Ga(III) (Tables 5 and 6).[138]

Popular acyclic chelators **EDTA** (**L10**) and **DTPA** (**L12**) form very thermodynamically stable complexes with indium (Table 6). The 7-coordinate In-**EDTA** (In-**L10**) structure features a hexadentate chelator and approximates a pentagonal bipyramidal geometry with a single water at an equatorial position (Figure 47).[174] In-**DTPA** (In-**L12**) structures feature both 7-as well as full 8-coordination by the chelator in distorted pentagonal bipyramidal and square antiprismatic geometries respectively; the latter is shown in Figure 48.[175,176] A $^{13}C\{^{1}H\}$NMR spectroscopic study of Na_2[In-**DTPA**] [Na_2(In-**L12**)] in D_2O confirmed retention of its square antiprismatic geometry in neutral aqueous solution.[176] The *N,N"-bis*(benzylcarbamoyl-methyl) derivative of **DTPA** (**L12**), **DTPA-BA$_2$** (**L13**), was first designed as a model for a doubly-bioconjugated chelator.[177] An X-ray structure of its In(III) complex also features an 8-coordinated cation in a distorted square antiprismatic envelopment (Figure 49).[178] Unlike In-**DTPA** (In-**L12**), however, its solution NMR spectrum revealed the presence of at least three isomeric species. It was proposed that the two amide carbonyls are no longer coordinated in solution, thus rendering this complex more hydrophilic in its HPLC retention behavior compared to its Y(III) analogue. A **DTPA** derivative with a *trans*-1,2-diaminocyclohexane backbone, **CHX-A"-DTPA** (**L14**), has been conjugated to a targeting peptide and found to be a viable ligand for ^{68}Ga, ^{86}Y, and ^{111}In radiometals for melanoma imaging.[141]

Linear N_4O_2 aminophenols such as **SBAD** (**L15**) have been prepared and their complexations with Ga(III) and In(III) studied.[139] These consistently bind the former cation more tenaciously. Additionally, several In(III) complexes of pendant-armed triazacyclononane (**TACN, L26**) derivatives have had their solid-state structures determined. An InCl-**NOTA** (InCl-**L29**) complex protonated at one carboxylate arm was found to have a near pentagonal bipyramidal geometry with the chelator hexadentate (Figure 50).[37,179] In aqueous solution, however, NMR spectral data suggested a time-averaged six-coordinate C_3-symmetric species instead. At $pD < 0$, this complex decomposed irreversibly. The related In-(R)-1,4,7-*tris*(2′-methylcarboxymethyl)-triazacyclononane structure has a more typical *pseudo*-octahedral coordination sphere (Figure 51).[180] A *tris*(phenylphosphinate)-armed derivative of **TACN (L26)**,[181] as well as the *tris*(mercaptoethyl)-armed derivative **TACN-TM** (**L27**) can both bind In(III) in a similar mode (Figure 52).[182]

The valuable octadentate chelator **DOTA** (**L39**) has also been shown to form a robust complex with In(III) (Table 6).[183] Surprisingly, no X-ray structural data are yet available for the parent In-**DOTA** (In-**L39**) complex. There are, however, several reported structures of its amide-armed derivatives. The In(III) complex of the *p*-aminoanilide, **DOTA-AA** (**L41**), was found to have a twisted (~28°) square antiprismatic geometry (Figure 53).[184] Inside the chelator cavity the cation is approximately 1.2 and 1.3 Å from the O_4 and N_4 coordination planes respectively. This indicates that its fit may not be as ideal as that for the larger Y(III) cation (*vide infra*). With one fewer carboxymethyl pendant arm than **DOTA** (**L39**), the chelator **DO3A** (**L42**) has also been complexed to In(III) and its structure adopts the expected 7-coordinate geometry.[185] Biodistribution studies using **DOTA** (**L39**) conjugated to D-Phe^1-Tyr^3-octreotide, **DOTATOC** (**L39**-TOC), and labeled with ^{67}Ga, ^{111}In, and ^{90}Y revealed that the Ga-**DOTATOC** (Ga-**L39**-TOC) had the best tumor uptake and kidney clearance.[157] It was postulated that this may be the result of a hexacoordinate Ga(III) compared to the higher coordination requirements for the In(III) and Y(III) analogues. Another 7-coordinate In(III) geometry, described as monocapped trigonal prismatic, was found for In-**DO3A-TPP** (**L44**) which features **DOTA** (**L39**) linked to a triphenylphosphonium moiety to target mitochondria (Figure 54).[158] Proton NMR data supported retention of this heptadentate chelation mode in aqueous solution.

A *tris*(carboxymethyl)-armed cyclam chelator, **TE3A** (**L53**) has also been found to complex In(III) in a heptadentate mono-capped trigonal prismatic geometry (Figure 55).[185] No structure of In-**TETA** (In-**L49**) has been reported though its stability constant has been determined to

be 2 orders of magnitude lower than that of In-**DOTA** (In-**L39**) due to a poorer cation-chelator match.[186]

An early report of ^{111}In-labeling of tricatecholamide analogues of Enterobactin (**DiP-LICAM** (**L20**) yielded impressive stability constants (Table 4). However biodistribution studies were not performed.[187]

2.6. Aqueous Yttrium(III) Coordination Chemistry

Aqueous yttrium chemistry is often discussed together with that of the lanthanides because of their common tricationic state and similar ionic radii. Yttrium (III), 90-108 pm (CN 6-9), is significantly larger than the other four metal cations discussed in this review and can readily reach coordination numbers of 8 and 9 in its complexes. With a closed-shell electron configuration, it is also considered a harder acidic cation than Ga(III) or In(III). This can be seen in its higher Drago-Wayland parameter $\mathbf{I_A}$ which is an indicator of the relative significance of the electrostatic versus covalent component of its coordination interaction.[579,580] Data for selected complexes are presented in Table 7.

Both **EDTA** (**L10**) and **DTPA** (**L12**) have been shown to form reasonably stable complexes with Y(III). Several solid-state structures of these have been determined and two selected examples are shown in Figures 56 and 57. The YF_2-**EDTA** (YF_2-**L10**) structure approximates a dodecahedron with a hexadentate **EDTA** (**L10**),[188] while Y-**DTPA** (Y-**L12**) is 9-coordinate with a monocapped anti-prismatic geometry including an octadentate **DTPA** (**L12**) and one coordinated water.[189] Two related structures are of Y-**DTPA-BA$_2$** (**L13**), a N,N"-*bis* (benzylcarbamoylmethyl) derivative of **DTPA** (**L12**) which served as a model for a dual biomolecule-labeled chelator.177,[178] In each case, the 9-coordinate Y(III) adopts a distorted tricapped trigonal prismatic geometry featuring an octadentate chelator plus a coordinated solvent (methanol) molecule (Figure 58). In D_2O solution, however, NMR spectroscopy revealed the presence of at least three isomers up to 85 °C. It was suggested that these accessible structural variations may account for the relatively low inertness of typical Y-**DTPA** (Y-**L12**) complexes.

The structure of a Y(III) triflate complex of a *tris*(carbamoylmethyl) derivative of **TACN** (**L26**), **NOTAM** (**L30**), has been reported.[190] This 9-coordinate geometry can be viewed as a capped square anti-prism, although alternative descriptions are also viable (Figure 59). NMR spectroscopic studies showed that this complex is fluxional in acetonitrile solution.

A number of yttrium(III) complexes of **DOTA** (**L39**) and its derivatives have been prepared. An X-ray structure of [Y-**DOTA**]$^-$ (Y-**L39**$^-$) is shown in Figure 60.177,[191] The 9-coordinate Y(III) center has a monohydrate capped square antiprismatic (SA) coordination sphere (often referred to as the "*M*" isomeric geometry) featuring an octadentate **DOTA (L39)** with the cation held significantly closer to the O_4 plane than the N_4 plane (0.72 versus 1.62 Å respectively). A related structure of a **DOTA** (**L39**) derivative with one carboxymethyl arm conjugated to phenylalanine, Y-**DOTA-*D*-PheNH$_2$** (Y-**L40**), has also appeared (Figure 61). This adopts instead a twisted square anti-prismatic (TSA) geometry (or "*m*" isomer) with four macrocyclic amine nitrogens, three carboxylate oxygens, and an amide oxygen coordinating.[157] As mentioned in the gallium section, octreotide-conjugated ^{90}Y-**DOTATOC** (^{90}Y-**L39-TOC**) was found to have inferior biological behavior compared to its ^{67}Ga analogue, possibly as a result of the higher coordination requirement of Y(III). According to solution NMR spectroscopic data, a similar complex with a **DOTA** (**L39**) *p*-aminoanilide was found to retain the chelator's full N_4O_4 coordination mode.[47] The consequence of substituting a carboxylate pendant arm with a phosphonate in a **DOTA** (**L39**) derivative, **DO3AP** (**L43**), can be seen in its yttrium complex geometry (Figure 62). A twisted square antiprismatic configuration

(*TSA* twist angle ~ 25°) can be noted while the cation remains closer to the O_4 plane (1.04 Å) than the N_4 plane (1.52 Å).[192]

A very interesting crystal structure of the yttrium(III) complex of a chiral **DOTA** (**L39**) derivative bound to the antibody 2D12.5 Fab has been reported,[193] but no direct complex-protein interactions were found. Likely as a result of the symmetrical nature of this type of complex, only modest differences in binding affinities were found for enantiomers of opposite helicity. Additionally, C-functionalized **DOTA** (**L39**) chelators have recently been investigated as BFC's for yttrium-86.[194] The (*S*)-*p*-aminobenzyl derivative's Y(III) complex was successfully separated into *SA* (major M) and *TSA* (minor m) isomeric forms which were assigned by solution 2-D NMR as well as CD spectroscopy.

The cyclam analog, **TETA** (**L49**), has been reported to bind Y(III), though with far less affinity than either **DOTA** (**L39**) or even the acyclic **DTPA (L12)** indicating a poorer cation/chelator match (Table 7).[195] Both the labeling efficiency and acid inertness of ^{90}Y-**TETA** (^{90}Y-**L49**) (half life at pH 3.6 ~ 5 min) have been found to be inferior to that of its **DOTA** (**L39**) analogue (no decomplexation after 3 months).[196] Although no Y-TETA (Y-**L49**) structure has been reported to date, it is likely to resemble that of Tb-**TETA** (Tb-**L49**) and (Eu-**L49**). Both of these were described as having a highly-distorted octadentate dodecahedral geometry with the metal cation significantly distended from the cyclam cavity.[197,198]

Although often used as a surrogate for Y(III) in ^{90}Y-radiopharmaceutical studies, In(III) can exhibit appreciably different coordination chemistry due to its smaller ionic radius and typical coordination numbers of less than 8. Acyclic aminopolycarboxylates like **EDTA** (**L10**) and **DTPA** (**L12**) form far more stable complexes with In(III) than Y(III). By contrast, the octadentate **DOTA** (**L39**) binds Y(III) with more avidity. While Y-**DOTA-*D*-PheNH$_2$** (Y-**L40**) adopts the twisted square antiprismatic (*TSA*) solid-state geometry, In-**DOTA-*D*-Phe-NH$_2$** (In-**L40**) has the square antiprismatic (*SA*) configuration.[157,199] These complexes also have distinct NMR spectral behavior in solution with only the indium complex showing fluxional behavior. Another Y-**DOTA** (Y-**L39**) derivative with a single amide pendant arm, Y-**DOTA-AA** (Y-**L41**), was observed to retain a rigidly octadentate chelator coordination sphere in solution at ambient temperature, while its In(III) analogue again exhibited dynamic behavior suggestive of an uncoordinated amide pendant arm.[184] Consistent with the observation, this and related indium **DOTA** (**L39**) complexes were found to be more hydrophilic in their RP-HPLC retention data.[184,200] Similar discrepancies were also noted for the corresponding **DTPA**-RGD (**L12**-RGD) and **DTPA-BA$_2$** (**L13**) complexes of these cations.[178,201] Although potentially significant, no general conclusions about the relevance of these differences to the *in vivo* properties of these species can yet be made. Finally, the antibody 2D12.5 was reported to bind Y-**DOTA** (**L39**) with much higher affinity than In-**DOTA** (In-**L39**).[193]

2.7. Aqueous Zirconium(IV) Coordination Chemistry

With its high charge and small radius (59-89 pm for CN 4-9), hydrated Zr(IV) likely exists only at high dilution in very acidic solutions. Multiple monomeric as well as polynuclear oxo/hydroxy species are believed to be present before onset of precipitation as the pH is raised.[202,203]

In consequence of its extreme hardness, a strong preference of Zr(IV) for polyanionic hard donor chelators can be expected. This predilection can be seen in the very impressive stability constants of its **EDTA** (**L10**) and **DTPA** (**L12**) complexes (Table 8). A total coordination number of 8 is typical in their X-ray structures (Figures 63 and 64). The Zr-**EDTA** (Zr-**L10**) geometry approximates a dodecahedron including a hexadentate chelator,[204] while **DTPA** (**L12**) is fully octadentate in its Zr(IV) envelopment.[205] The use of ibritumomab tiuxetan, a

MX-DTPA (**MX-L12**)-conjugated monoclonal antibody to chelate ^{89}Zr has been reported. No solid-state structure of Zr-**DOTA** (Zr-**L39**) has yet been reported. Although its D_2O solution $^{13}C\{^1H\}$ NMR spectral data were consistent with a time-averaged symmetric C_4 species implying full N_4O_4 chelator coordination, its proton NMR spectrum actually revealed a lower symmetry species in equilibration with a second minor isomer.[177]

The hydroxamate-based iron chelator *Desferal* **DFO** (**L23**) and its derivatives have been frequently used to bind Zr(IV),[19,44,206-210] yet no structural characterization or stability constant data of resulting complexes are available. With the current interest in zirconium-based radiopharmaceuticals, future investigations of other hard metal cation-binding chelators likely to have high affinity for Zr(IV) such as catecholates, and catecholamides should be timely. The family of tripodal hydroxypyridinone (HOPO) chelators developed recently for lanthanide complexation towards MRI applications also merits attention.[211]

2.8. Summary

Viable chelators for Cu(II) range from tetradentate N_2O_2, N_2S_2, and N_4 ligands favoring square-planar coordination to fully encapsulating N_3O_3, N_4O_2, and N_6 hexadentate ligands giving distorted octahedral binding modes. Especially high thermodynamic stabilities as well as acid inertness are realized using polyazamacrocycles and cryptands, often appended with ionizable carboxylate or phosphonate arms. Highly stable Ga(III) complexes have been attained with hexadentate chelators featuring $N_2O_2S_2$, N_2O_4, N_3O_3, N_3S_3, N_4O_2, and O_6 donor sets, usually in a *pseudo*-octahedral coordination geometry. Selected macrocyclic N_3O_3 and N_4O_2 chelator complexes also have remarkable inertness in strong acids. Although it is possible for the larger In(III) cation to adopt higher coordination numbers of 7 and 8, its most robust complexes are formed by hexadentate chelators similar to those for Ga(III) containing $N_2O_2S_2$, N_2O_4, N_3O_3, N_3S_3, N_4O_2, and O_6 donor motifs. Due to the higher coordination number requirement of Y(III), the octadentate lanthanide chelator **DOTA** (**L39**) provides an almost ideal fit with associated high affinity. Only limited thermodynamic, kinetic, and structural data are available for Zr(IV)-chelator complexes in comparison to the other four metals discussed in this review. These indicate a strong preference for octadentate chelators with hard anionic oxygen donors. Finally, as demonstrated from the examples contained in this section, the affinity between metal and chelator play an integral role in the development of useful radiopharmaceuticals.

3.0. Radioisotope Production

The availability of radiometals that are carrier free and radionuclidically pure is essential to the development of effective radiopharmaceuticals for diagnostic imaging and radiotherapy. While the production of Zr, Y, In, Ga and Cu radiometals require a thorough understanding of the nuclear reactions and decay schemes available, their processing methods rely upon an intimate knowledge of their aqueous solution chemistry. The next section describes these methods.

3.1. Production of Copper Radiometals

The production of copper radiometals has been an area of intense research since they offer a variety of half-lives and decay energies that are applicable to diagnostic imaging and radiotherapeutic applications. Additionally, depending upon the application, copper radionuclides can be utilized by facilities with limited resources.

Copper-62 ($t_{½}$ = 0.16 h, β^+: 98% E_{β^+max}: 2.19 MeV; EC: 2%) can be produced in a small cyclotron,[212] and is the only generator-produced copper radionuclide, resulting from the decay of its parent, ^{62}Zn. Zn-62 is produced by irradiation of an enriched Cu target with protons

according to the nuclear reactions $^{63}Cu(p,n)^{62}Zn$ or $^{65}Cu(p,4n)^{62}Zn$.[213] Numerous $^{62}Zn/^{62}Cu$ generator configurations were produced before 1999, using a glycine solution or other aqueous and organic mixtures to elute the ^{62}Cu in a form suitable for radiopharmaceutical preparation.[214,215] Haynes and coworkers developed a method for the direct labeling of PTSM (**L8**) to produce a patient-ready dose using a generator system designed to simultaneously deliver the ^{62}Cu eluate, NaOAc buffer and PTSM (**L8**) ligand solution into a dedicated syringe.[216] While the life span of a ^{62}Cu generator is only 24 h, a clinically useful dose can be prepared every 30 minutes, which can be economical for hospitals that do not have the resources for an onsite cyclotron. Additional improvements in generator preparation by Fukumura et al. have increased the probability of ^{62}Cu use in the clinic.[217]

Copper 60 ($t_{½}$ = 0.4 h, β^+: 93% E_{β^+max}: 3.9 MeV and 3.0 MeV; EC: 7%, $E_{\gamma\ max}$: 2.0 MeV) is another potentially useful copper radionuclide since high quality images can be obtained due to the high percentage of positron decay, despite its high β^+ energy and prompt gamma emission.[218] Additionally, ^{61}Cu ($t_{½}$ = 3.3 h, β^+: 62% $E_{\beta+\ max}$: 1.2 MeV and 1.15 MeV; EC: 38%, $E_{\gamma\ max}$: 940 MeV and 960 MeV) also has potential applications in medical imaging since its half-life is suitable for biological applications which occur between 1 and 4 hours after injection.[218] Both isotopes can be produced using targetry systems which were designed for the production of ^{64}Cu. Copper-60 can be prepared by the $^{60}Ni(p,n,)^{60}Cu$ reaction while ^{61}Cu can be prepared by the $^{61}Ni(p,n)^{61}Cu$ or $^{61}Ni(d,n)^{61}Cu$ nuclear reactions[219] on a biomedical cyclotron using 14.7 MeV protons or 8.1 MeV deuterons respectively and using natural or enriched nickel targets. Approximately 16.7 GBq of ^{60}Cu and up to 3.7 GBq of ^{61}Cu can be produced after the isotopic products are separated from the target material by ion exchange chromatography. However, the need for enriched target materials, which increases production costs, presents a significant limitation to the cost-effective production of these two radiometals and has prompted investigators to develop other production methods using the nuclear reactions $^{59}Co(^3He,2n)^{60}Cu$ and $^{59}Co(^3He,n)^{61}Cu$, which can be carried out on Co foil using beam energies of 70 MeV.[220-222]

Copper-67 ($t_{½}$ = 62.01 h, β^-: 100% E_{β^-max}, 0.577 MeV; $E_{\gamma\ max}$: 0.185 MeV) decays by β emission. These particles have sufficient energy to penetrate small tumors, and the medium range half-life of ^{67}Cu makes it an attractive radiometal for radioimmunotherapy with intact antibodies. It can be produced on a cyclotron or high energy accelerator using the nuclear reactions $^{65}Zn(p,2p)^{67}Cu$ and $^{68}Zn(p,2p)^{67}Cu$ or $^{65}Zn(n,p)^{67}Cu$, respectively.[223] While several different Zn target materials are used, ^{68}Zn targets are preferred since their irradiation leads to substantial increases in ^{67}Cu yields.[224,225] However production yields are relatively low, since numerous contaminants such as ^{62}Zn, ^{67}Ga, ^{65}Zn, ^{55}Co, ^{58}Co and ^{57}Ni have to be removed by numerous ion exchange chromatography steps. Despite the availability of these purification methods, high specific activity ^{67}Cu is still difficult to obtain because of the ubiquity of natural copper and zinc in the environment.[224,226] The need for the high energy cyclotron or accelerator, which drives up the cost, has also prevented mass production of this radiometal. Accordingly, interest in the applications of this radiometal remains limited.[227-235]

The production and preparation of ^{64}Cu ($t_{½}$ =12.7 h, β^+: 19% $E_{\beta+\ max}$, 0.656 MeV; EC: 41%; β^-: 40%) has been extensively reviewed and discussed.[236-238] Briefly, copper-64 can be prepared in a nuclear reactor by several reactions including $^{63}Cu(n,\gamma)^{64}Cu$, though the product cannot be isolated in a carrier-free state. A second method which can lead to carrier-free ^{64}Cu involves bombarding the target in a reactor with fast neutrons according to the nuclear reaction $^{64}Zn(n,p)^{64}Cu$. Two other methods involve the nuclear reaction $^{64}Ni(p,n)^{64}Cu$ and $^{64}Ni(d,2n)^{64}Cu$,[239,240] which can be carried out on a biomedical cyclotron to yield carrier-free copper-64, but an enriched nickel target must be irradiated to increase the yield of copper-64,[241,242] and has spurred the development of ^{64}NiO targets to enhance ^{64}Ni recovery.[243] Recently, Obata and colleagues described the production of ^{64}Cu using 12 MeV proton

irradiation via ^{64}Ni(p,n)^{64}Cu.[244] Automated processing and purification of the ^{64}Cu by AG1-X8 anion exchange chromatography allowed for the recycling of the ^{64}Ni target material and the generation up to 185 GBq of ^{64}Cu depending upon target thickness.

Avila-Rodriquez et al. were able to simultaneously produce ^{64}Cu and ^{61}Co with a 11.4 MeV proton beam on a biomedical cyclotron using the ^{64}Ni(p,n)^{64}Cu reaction.[245] A single chromatography step using an anion exchange column separated the chloride salts of Ni, Cu and Co, providing carrier-free ^{64}Cu with higher specific activities than previously reported.[237,244,246]

While Van So et al. attempted to produce ^{64}Cu from a ^{68}Zn target,[247] others have explored making ^{64}Cu with ^{64}Zn targets using the nuclear reaction ^{64}Zn(d,2p)^{64}Cu, but the production of other radionuclide contaminants has remained problematic.[248-250] Recently, Kozempel and colleagues reported the production of no-carrier-added (NCA) ^{64}Cu using the ^{64}Zn(d, 2pn)^{64}Cu reaction with a 19.5 MeV deuteron beam.[251] After irradiation the radioactive target material is subjected to dual ion exchange chromatography using a strong cation exchange resin to remove any Ga-based radio-impurities and a strong anion exchange column to retain the ^{64}Cu and ^{64}Zn target material, while allowing other impurities such as ^{24}Na and ^{58}Co to flow through the column. The ^{64}Cu is then eluted in 2 M HCl while the Zn fraction is eluted in neutral water. Additionally, Hassanein and coworkers separated ^{64}Cu from the zinc target using a gel matrix consisting of 6-tungstocerate(IV), which is highly insoluble in water and has a mean particle size of 230-464 μm.[252] The matrix's affinity for metal ions such as Zn(II) and Cu(II) is dependent on the hydrogen ion concentration in the column with the distribution of both cations decreasing with decreasing pH. In dilute acid the Cu ions have an increased affinity towards the matrix compared to Zn ions, which can be washed from the column using 1mM HCl while the ^{64}Cu can be eluted in a carrier-free stat using 1 M HCl.[252]

3.2. Production of Gallium Radiometals

Three gallium radioisotopes have suitable properties to be used in radiopharmaceutical applications. ^{67}Ga is used in SPECT and gamma scintigraphy while ^{66}Ga and ^{68}Ga are used in the development of PET radiopharmaceuticals. This next section will discuss the production and purification of these three radioisotopes.

Gallium-67 ($t_{½}$ = 78.3 h, γ: 93.3 keV, 37%, γ: 184.6 keV, 20.4%, γ: 300.2 keV, 16.6%) is produced using a cyclotron by bombarding a zinc or copper target with protons using the ^{67}Zn (p,xn)^{67}Ga reaction,[253,254] deuterons by the ^{67}Zn(d,2n)^{67}Ga reaction,[255] alpha particles by the ^{64}Zn(^{4}He,n)^{67}Ga or ^{65}Cu(^{4}He,2n)^{67}Ga reactions.[254,256] Additionally, it can be produced using a tandem ^{Nat}Ge-^{Nat}Zn target, where separation of the ^{67}Ga from the target material is accomplished by acid dissociation followed by resin-based chromatography on an organic polymer to achieve high radionuclidic purity.[256] In some cases however, iron contamination can be problematic, but the use of a reducing agent such as $TiCl_3$ can resolve this issue.[257] Recently, ^{67}Ga was produced from the irradiation of a target consisting of natural cobalt foil with 52 MeV $^{11}B^{4+}$ and 73 MeV $^{12}C^{6+}$ ions through one of the following reactions: ^{59}Co (^{11}B,3n)^{67}Ge or ^{59}Co(^{12}C, 4n)^{67}As.[258] The ^{67}Ge and ^{67}As products are short lived radionuclides which decay to ^{67}Ga after a short "cooling" time. Separation of the target material is achieved by liquid-liquid extraction using concentrated acid and trioctylamine (TOA), which is then back-extracted using a basic solution of DTPA or EDTA. Alternatively, ^{67}Ga has been purified from cobalt target materials using alginate biopolymers,[259] which are naturally occurring polymers extracted from microalgae, shrimp, crab and fungi that are known to bind strongly to metal ions.[260] Upon addition of the radioactive target material, nearly 90% of the ^{67}Ga is retained in the biopolymeric matrix while the cobalt target material is removed from the column using an aqueous solution of $NaNO_2$. After all of the target material is removed, elution of the no-carrier-added ^{67}Ga occurs using 0.1 M HCl, which is suitable for

radiopharmaceutical applications. In many medical centers that have PET scanners, the use of ^{67}Ga has been replaced by [^{18}F]FDG-PET.[261]

Gallium-68 ($t_{½}$ = 67.71 min, β^+: 89%, E_{β^+max}, 1.9 MeV; EC: 11%, $E_{\gamma\ max}$: 4.0 MeV) is an important positron emitting radiometal that is produced by electron capture decay of its parent radionuclide ^{68}Ge ($t_{1/2}$ = 270.95 days),[159] and it can be produced from a compact generator system which contains the parent radionuclide. The ^{68}Ge/^{68}Ga generator system provides a continuous source of Ga-based PET radiopharmaceuticals for approximately 1 year, it has been extensively reviewed,[262-264] and numerous commercial systems are available. Cyclotron Co. (Obninsk, Russia) has recently produced a popular TiO_2-based generator system which can contain 370-18500 MBq ^{68}Ge.[159] This system is eluted with 0.1 M HCl to provide the user with ionic $^{68}GaCl_3$; however, there are drawbacks, including ^{68}Ge breakthrough, large eluate volume, high HCl concentration and the presence of metallic impurities such as Zn^{2+}, Ti^{4+} and Fe^{3+}, which can lead to difficulties in synthesizing the ^{68}Ga radiopharmaceutical. To circumvent these difficulties research groups have explored purification protocols using anion and cation exchange micro-chromatography[264,265] and fractionation,[266] while additional work has sought to develop facile synthetic routes to radiopharmaceuticals that complement this generator system including infrared (IR) and microwave supported syntheses.[265,267]

Gallium-66 ($t_{½}$ = 9.49 h, β^+: 56.5%, $E_{\beta+\ max}$, 4.15 MeV; EC: 43.5%, $E_{\gamma\ max}$: 4.0 MeV) is another radiometal that is relevant in nuclear medicine and molecular imaging applications. As a positron emitter it can be used in PET imaging, and its longer half-life allows for data collection at later time points, which is not possible with the positron emitting isotope ^{68}Ga. Gallium-66 can be produced and purified using methods similar to those that have been described for ^{67}Ga[258] (*vide supra*). An alternative method for ^{66}Ga production has been accomplished using the ^{66}Zn(p,n)^{66}Ga nuclear reaction on a small biomedical cyclotron.[268] This publication also compared purification of the ^{66}Ga by cation exchange chromatography with the traditional purification method involving diisopropyl ether extraction using 20% $TiCl_3$ in 3% HCl. The authors report that using cation exchange chromatography to purify the ^{66}Ga has several advantages. Firstly, 200 mCi of ^{66}Ga can be prepared and purified in this manner. Secondly it can be automated, and the processing time was more than twice as fast when compared to the diisopropyl ether extraction protocol. However a potential limitation lies in the high concentration of metal impurities in the cation exchange column, which will need to be reduced if this process is to be used to regularly prepare ^{66}Ga radiopharmaceuticals. Additionally, although the longer half-life of ^{66}Ga compared to ^{68}Ga provides more flexibility with respect to the types of biomolecules to be investigated and the amount of time required for radiochemistry, the very high energy of the positron (4.15 MeV) as well as a high energy gamma emission (4.0 MeV) provide a prohibitively high absorbed dose to the subject being imaged, as well as to the personnel working with this radiometal. These intrinsic physical properties of this radiometal have severely limited its practical use.

3.3. Production of Indium Radiometals

The production, purification and application of indium radiometals are active areas of research in the nuclear medicine, radiochemistry and molecular imaging communities. While numerous reports exist which involve the use of ^{110}In[269,270] ^{110m}In[271] and ^{114m}In[272], this review will focus on the production, purification, and radiopharmaceutical applications of ^{111}In, since it is the most widely used and extensively studied indium radiometal.

Indium-111 ($t_{½}$ = 2.8 d; γ: 171 keV, γ: 245 keV (EC 100%)) is produced commercially by irradiating a natural cadmium target with energetic protons according to the reaction ^{111}Cd (p,n)^{111}In or ^{112}Cd(p,2n)^{111}In, and both remain the most widely used production methods of ^{111}In.[273] Indium-111 can be separated from the cadmium target by ion exchange or solvent extraction, with both techniques providing similar yields.[270] Alternatively, ^{111}In can also be

produced in an accelerator by irradiating a rhodium target with ^{12}C ion beam[274] or irradiating silver targets with 55 MeV ^{11}B ions by the $^{107,109}Ag(^{11}B,3pxn)^{111}In$ nuclear reaction.[275] In this process, the ^{111}In is separated from the target material by first dissolving it with HNO_3, aliquat-336 (a phase transfer catalyst), and 0.001 M HCl, which are used to separate the silver target and the radiometal. A second extraction step involving 1 M HCl and 0.1 M trioctylamine (TOA) separates the ^{111}In, which remains in the organic phase while impurities such as $^{116/117}Te$, and $^{116/116m/117}Sb$ remain in the aqueous phase. A final extraction using a basic solution of 0.1M EDTA isolates the ^{111}In in a carrier free state.

3.4. Production of Yttrium Radiometals

The most abundant source of yttrium (Y) is found in the naturally occurring isotope ^{89}Y. Additionally there are numerous radioisotopes of Y, which are synthetically produced during the nuclear fission process and have half-lives that range from nanoseconds to months. For example, ^{88}Y ($t_{½}$ = 106.62 days) is produced by irradiating a strontium target with 16 MeV protons or a rubidium carbonate target with 7.3 MeV deuterons, 19 MeV ^{3}H ions and 12.4 MeV ^{4}He ions.[276] This radiometal has been used in place of ^{90}Y for determining biodistribution of radio-yttrium compounds,[277] is often considered invaluable as an active component of the ^{88}Y-Be photoneutron source,[278] and is important in the characterization of electrical materials. Additionally, ^{87}Y, which serves as the parent radionuclide in a $^{87}Y/^{87m}Sr$ generator, can be prepared by irradiating a rubidium target with alpha particles or by irradiating an enriched ^{87}Sr target with protons.[279,280] While a discussion of the production and purification of all of the Y radiometals is beyond the scope of this text, the remainder of this section will be devoted to the production and purification of the most medically relevant yttrium radiometals ^{90}Y and ^{86}Y.

Yttrium-90 ($t_{½}$ = 64.1 h, β^-: 100%, E_{β^-max} = 2.3 MeV) is currently used as a therapeutic radionuclide in nuclear medicine because it has a half-life of 64.2 h and emits β^- radiation (E_{β^-max} = 2.28 MeV) with no accompanying gamma rays, reducing the received radiation dose to both patients and hospital staff.[281] Yttrium-90 can be produced by (n,γ) reactions on yttrium metal or yttrium oxide, but the resulting product is obtained with a low specific activity.[281] Additionally, it can be produced by the $^{90}Zr(n,p)^{90}Y$ reaction in a nuclear reactor.[281] Following irradiation of the Zr starting material, it is extracted with HNO_3 and mandelic acid leaving a solution containing the ^{90}Y product and the ^{90} Sr parent, which can be separated from the ^{90}Y product by its retention on a DOWEX cation exchange column. The radiochemical yield of this method is 90±8%.

Since large quantities are needed for nuclear medicine applications, the majority of the ^{90}Y obtained by hospitals is from facilities that manage nuclear materials produced within fission reactors. In this fissile material, ^{90}Y is associated with its parent ^{90}Sr ($t_{½}$ = 29 years), which must be separated in sufficient purity to meet hospital quality control standards. This has previously been accomplished with the use of co-precipitation[282] or solid-supported solvent-extraction chromatography.[283]

Recently, Happell et al. used nuclear track micro filters (NTMF) as supported liquid membranes by impregnating them with 1:1 bis-(2-ethylhexyl)-phosphate (HDEHP) and tributylphosphate (TBP).[284] ^{90}Y separation from its parent ^{90}Sr is achieved by its selective transport through the pores of the impregnated NTMF. While initial ^{90}Y recovery was good, the system lacked long term stability and ^{90}Sr breakthrough was problematic.

Although ^{90}Y is becoming more commonly used as a radiotherapeutic, not every hospital has access to ^{90}Y on a routine basis. However, since ^{90}Y and ^{90}Sr have such distinctly different half-lives, they represent a daughter/parent radionuclide combination that is ideal for incorporation into a generator system. Numerous generator systems have been developed

where the ^{90}Sr is adsorbed onto a solid support and the ^{90}Y is eluted using lactate,[285] methanol and acetate,[286] oxalate,[287] citrate[288] or EDTA.[289,290] Recently, Chakravarty et al. developed the Kamadhenu generator.[291] This ^{90}Y generator uses a dual electrochemical separation technique to separate ^{90}Y from the ^{90}Sr parent in very high radionuclidic purity by performing both electrolytic steps potentiostatically, and the constant voltage minimizes the level of ^{90}Sr contamination to 30 kBq per 37 GBq ^{90}Y, which is well below 74 kBq, the upper limit of exposure defined by international regulatory agencies. This method offers several advantages over conventional column based generator systems. Firstly, this generator can constantly be supplied by a ^{90}Sr feed solution, and there is an insignificant loss of ^{90}Sr except by natural decay. There is minimal radioactive and non-radioactive waste production, and minimal amounts of chemicals are used in the entire process. Finally, the ^{90}Y is obtained in acetate buffer making it suitable for labeling biological molecules without further modifications.

Yttrium-86 ($t_{½}$ = 14.7 h, β^+: 34%, E_{β^+max} = 1.2 MeV) has gained attention as a new imaging surrogate for ^{90}Y and as a positron emitting radioisotope for diagnostic PET imaging because of its favorable half-life and decay characteristics. This increased demand for ^{86}Y has led to an intense research effort to develop efficient and high yielding production methods. Several methods for the production and purification of ^{86}Y have been investigated which involve irradiation of germanium targets with accelerator produced heavy ion particles such as 15 MeV $^{16}O^{+6}$,[292] but most ^{86}Y production protocols have used $SrCO_3$ or SrO as the target material and protons with energies from 8-15 MeV. Separation of the ^{86}Y has been accomplished using co-precipitation and ion exchange chromatography,[293] ion exchange chromatography,[294,295] a Sr-selective resin,[296,297] and electrolysis, which separated the ^{86}Y from the $SrCO_3$ target material resulting in high yields of no-carrier added ^{86}Y in only 2 hours.[298]

Yoo et al. published a report that described the production of ^{86}Y using either an enriched $SrCO_3$ or SrO target on a small biomedical cyclotron via the ^{86}Sr(p,n)^{86}Y nuclear reaction.[299] The authors demonstrated that the use of SrO coated onto a platinum disk target and two electrolytic steps allowed for a more efficient preparation of ^{86}Y with 99% of the available ^{86}Y being recovered. Specific activities with this method were observed to be as high as 282 GBq/μmol, and since no co-precipitates are formed or exchange resins are used in the purification process, the introduction of carrier species is greatly reduced. Furthermore, electrolysis requires fewer steps, is easier to handle, can be adopted for automation and can produce no-carrier-added (NCA) ^{86}Y sufficient for biological studies in less than three hours. Recently, further modifications to the electrolytic procedures have been published which have optimized the electrochemical separation of ^{86}Y, resulting in reliable yields of 91% in only 60 minutes.[300]

3.5. Production of Zirconium Radiometals

Several isotopes of Zr can be produced on a cyclotron using a variety of nuclear reactions with particle energies between 5-85 MeV, and include ^{86}Zr ($t_{½}$ =17 h, γ: 100%, $E_γ$ = 241 keV), ^{88}Zr ($t_{½}$ = 85 d, γ: 100%, $E_γ$ = 390 keV) and ^{89} Zr ($t_{½}$ = 78.4 h, β^+: 22.8 %, E_{β^+max} = 901 keV; EC: 77%, $E_γ$ = 909 keV).[301] However, for radiopharmaceutical development and radioimmunotherapy applications ^{89}Zr has received considerable attention owing to its favorable decay characteristics and longer half-life, which make it useful in the labeling of antibodies for PET imaging at relatively long time points. A caveat to ^{89}Zr is the high abundance of the 909 keV gamma photons, which contribute greatly to the absorbed dose of ^{89}Zr radiopharmaceuticals, especially in slower clearing agents such as mAbs.

Zirconium-89 was first produced by Link et al. in 1986 by a (p,n) reaction by bombarding ^{89}Y on Y foil with 13 MeV protons.[302] After irradiation, ^{89}Zr was purified by a double extraction protocol. The target was first mixed with 4,4,4-trifluoro-1-(2-thienyl)-1,3-

butanedione (TTA) in xylene to remove the Zr(IV) from the foil followed by a second extraction step involving HNO_3/HF to return the Zr(IV) to the aqueous phase. Anion exchange using 1M HCl/0.01 M oxalate completes the purification procedure to afford ^{89}Zr in an 80% yield and with a purity of 99.99 %. A similar method reported by Dejesus et al. yielded similar results.[303]

A third method of production involves the irradiation of ^{89}Y pellets, prepared from high purity powder, with 16 MeV deuterons (^{89}Y(d,2n)^{89}Zr reaction).[304] Unlike the previous two methods, which relied upon solvent-solvent extraction as a means to purify the ^{89}Zr, this method relied solely upon the differences in the distribution coefficients of these two elements on an anion exchange resin at different HCl concentrations. The authors reported that the overall radionuclidic yield was 80%. The purification protocol is simpler than the procedures proposed by Link, but the precipitation of YCl_3 before and after anion-exchange chromatography has been problematic.[305]

Finally, using a Philips AVF cyclotron, Meijs and coworkers were able to produce ^{89}Zr using the (p,n) reaction, 14 MeV protons and ^{89}Y (300 μmol), which was sputtered onto a natural copper target that was cooled by water during bombardment.[306] These simple modifications led to the production of 8140 MBq ^{89}Zr after 2 h. After oxidation of the ^{89}Zr to the M^{4+} oxidation state using H_2O_2, it was separated from other metal impurities such as ^{89}Y, ^{88}Y, ^{65}Zr, ^{48}V and ^{56}Co using an anion exchange column chemically modified with hydroxamate groups. Hydroxamate was chosen because of its ability to form complexes with ^{89}Zr under highly acidic conditions, which allows the ^{89}Zr to be retained in the column while the other metal impurities are removed with highly concentrated HCl. The purified ^{89}Zr can then be eluted in 95% yield using 1 M oxalic acid, which is removed by sublimation under vacuum. However, newly established purification and labeling protocols have improved the separation efficiency of the hydroxamate column and rendered this sublimation step obsolete.[19]

4.0. Applications of Zr, Y, Ga, In and Cu Radiopharmaceuticals

As new production and processing methods of Cu, Ga, In, Y and Zr radiometals become available, their use in radiopharmaceutical development has allowed researchers and physicians to utilize the variable half-lives and emission energies to explore a variety of research problems including imaging multidrug resistance[143,307,308] and treating refractory arthritis and synovitis.[309,310] However, a thorough discussion of every application is beyond the scope of this text. To make this review more manageable for the reader, only applications involving oncology, gene expression, infection and inflammation and hypoxia and perfusion will be emphasized. A representative summary of applications can be found in Table 9.

4.1. Oncology

Each year 10.9 million people are diagnosed with cancer worldwide.[311] Cancer is caused by the effects of genetic mutation and environmental stress, either individually or in concert. Additionally, the aggressiveness and responsiveness to therapy displayed by each malignancy varies, and while satisfactory progress continues to be made in the successful diagnosis and treatment of some cancers, the overall success rate remains low. While several of the radiometals such as ^{67}Cu[227-235] and ^{90}Y[312-345] are used in oncology as radiotherapeutics, the remainder of this discussion will focus on the incorporation of In, Cu, Ga, Y, and Zr radiometals into radiopharmaceuticals for the diagnostic imaging of cancer. Moreover, while numerous radiopharmaceuticals have been prepared to detect biomarkers such as the folate receptor,[166,346,347] the neurotensin receptor,[348,349] oxytocin receptor expressing tumors,[350] apoptosis using Annexin-5,[351-355] Urokinase-Type Plasminogen Activator Receptor (uPAR),[356] matrix metalloproteinases (MMPs),[357,358] Met-expression,[359] antigens in head-and-neck

cancer,208,[360-362] lymphoma,[363-371] non-Hodgkin's lymphoma,[45] and esophageal and pancreatic cancer,[372,373] the remainder of this discussion will be further confined to several biomarkers which have received the most attention and include the integrin $\alpha_v\beta_3$, the somatostatin receptor, the gastrin-releasing peptide receptor, melanoma and melanocortin-1 receptor, HER-2/neu receptor, VEGF receptor and EGF receptor.

4.1.1. Integrin Imaging—Integrins are a family of cell surface heterodimeric transmembrane glycoproteins that mediate the attachment of cells to the extracellular matrix.[374,375] They consist of α and β subunits which are needed for adhesion to the extracellular domain. The cytoplasmic domain of both subunits anchors the cytoskeleton to the plasma membrane and is required to mediate signaling events. While imaging agents that target several different integrins have been reported,[376-378]the most widely investigated in this superfamily of proteins has been the vitronectin receptor, $\alpha_v\beta_3$, since it has been observed to be involved in tumor growth, local invasiveness, metastatic potential, and it is highly expressed on endothelial cells undergoing angiogenesis.[379,380] While several different protein, peptide and peptidomimetic motifs have been used to image this biomarker,200,381-387 the vast majority of published reports have targeted this receptor using an arginine-glycine-aspartic acid (RGD) peptide motif (Figure 65). For example, Yoshimoto et al. prepared ^{111}In-**DOTA**(**L39**)-c(RGDfK)[388] and demonstrated that this radiopharmaceutical had rapid tumor uptake and renal clearance in SKOV-3 human ovarian carcinoma cells implanted in female BALB/c nu/nu mice, while van Hagen et al. used ^{111}In-**DTPA**(**L12**)-c(RGDyK) to investigate the imaging of neoangiogenesis in CA20948 rat pancreatic tumors.[389] Receptor-specific, but dose-dependant accumulation of the tracer was observed in these tumors with more accumulation being observed when the mass of the injected radiopharmaceutical was reduced. Additionally, several ^{64}Cu-**DOTA**(**L39**)-RGD based radiopharmaceuticals have been developed to target $\alpha_v\beta_3$ expression in order to monitor dasatinib therapy[390] and image glioma,[391] inflammation,[392] lung cancer,[393] and teratoma.[394] Additional research has been conducted to improve $\alpha_v\beta_3$ positive tumor targeting using RGD multimers,[395] enhance the biokinetics of RGD based radiopharmaceuticals using PEG linkers[396] and develop multimodal imaging agents for PET/MR[397] or PET/NIR applications.[398]

Since ^{64}Cu-**DOTA (L39)** complexes were previously shown to be unstable *in vivo*,[21] Wei and colleagues compared the properties of ^{64}Cu-**CB-TE2A**(**L57**)-c(RGDyK) and ^{64}Cu-**DIAMSAR**(**L62**)-c(RGDfD) in M21 ($\alpha_v\beta_3$ positive) and M21L ($\alpha_v\beta_3$ negative) melanoma bearing mice.[399] These ligands were developed to form more kinetically inert Cu(II) complexes with the hope of preventing Cu transchelation *in vivo*. While both radiopharmaceuticals exhibited similar binding affinities for $\alpha_v\beta_3$ integrin, ^{64}Cu-**CB-TE2A**(**L57**)-c(RGDyK) demonstrated better tumor targeting at all time points examined, and demonstrated more rapid liver and blood clearance resulting in lower liver and blood concentrations at 24 h p.i.

In another interesting application using **CB-TE2A**(**L57**), Sprague et al. used the radiopharmaceutical ^{64}Cu-**CB-TE2A**(**L57**)-c(RGDyK) to image osteoclasts, which express high levels of $\alpha_v\beta_3$ integrin and are a component of osteolytic bone metastases.[400] This radiopharmaceutical was observed to have a 30-fold greater affinity for $\alpha_v\beta_3$ than $\alpha_v\beta_5$, and was observed to bind to osteoclasts through $\alpha_v\beta_3$-mediated interactions. Biodistribution and small animal imaging of a pharmacologically induced mouse model of osteolysis demonstrated increased uptake at the mouse calvarium, which was the site of pharmacological induction (Figure 66). This increased uptake could be blocked with a co-injection of c(RGDyK) demonstrating that imaging of $\alpha_v\beta_3$-expressing osteoclasts was possible.

Gallium-based imaging agents have been developed for imaging $\alpha_v\beta_3$. Jeong et al. labeled **NOTA**(**L29**)-c(RGDyK) with ^{68}Ga.[401] Although some purification was necessary, the purified complex could be obtained with a specific activity of 17.4 GBq/μMol, and biodistribution

studies in nude mice bearing human colon cancer (SNUC4) xenografts demonstrated appreciable receptor-mediated tumor uptake. Additionally, small animal PET studies were performed, which demonstrated excellent tumor uptake that was significantly reduced by the coadministration of c(RGDyK); however, quantification of the microPET imaging was not reported. In another report, Li et al. examined the differences between ^{68}Ga-**NOTA**(**L29**)-(RGD)$_4$, ^{68}Ga-**NOTA**(**L29**)-(RGD)$_2$, and ^{68}Ga-**NOTA**(**L29**)-RGD.[402] In all cases, nearly quantitative labeling of these conjugates was achieved, and specific activities of 12-17 MBq/nmol were achievable. The ^{68}Ga-**NOTA**(**L29**)-(RGD)$_4$ demonstrated the highest receptor affinity and tumor uptake based upon biodistribution and small animal PET studies, but it also demonstrated the highest kidney uptake, which can be problematic since the kidney is a dose limiting organ. Similarly, a recent study by Liu et al. examined the effects PEG and glycine linkers had on the affinity of RGD dimers for $\alpha_v\beta_3$ positive tumors xenografts.[403]

4.1.2. Somatostatin Receptor Imaging—Somatostatin (SST), which consists of 14 amino acid (aa) and 28 aa peptides, affects several organ systems including the central nervous system, hypothalamopituitary system, the gastrointestinal tract, the exo- and endocrine pancreas and the immune system.[404] Currently five different somatostatin receptor subtypes have been discovered. While many human tumors express these membrane bound receptors, the subtype expression pattern is dependent on the origin and type of tumor.405 This information has led to a continuing flurry of activity, seeking to develop new diagnostic imaging agents for somatostatin receptors and evaluate them in preclinical and clinical settings.

Numerous somatostatin analogues have been prepared, conjugated to various chelators such as **DTPA** (**L12**) and **DOTA** (**L39**), labeled with ^{111}In and have been evaluated in both laboratory and in the clinic (Figure 67). [9,406-425] de Jong et al. investigated tumor uptake of ^{111}In-**DOTA**(**L39**)-Y^3-octreotide as a function of injected radiopharmaceutical mass, which is an important factor when seeking to maximize tumor uptake while trying to minimize non-target organ radiotoxicity.[426] ^{111}In-**DOTA**(**L39**)-Tyr^3-octreotide was injected into male Lewis rats bearing CA20949 pancreatic carcinoma tumors with the mass of the radiopharmaceutical varying between 0.05-12 μg peptide. Higher specific uptake was observed only in somatostatin receptor subtype 2 (SSTR(2)) positive organs when the mass of the injected radiopharmaceutical was low, illustrating that this parameter is more important in determining radiopharmaceutical uptake in tumor and non-target organs than its specific activity. Another report by Lewis et al. described the evaluation of the somatostatin analogues ^{64}Cu-**TETA**(**L49**)-Y^3-OC, ^{64}Cu-**TETA**(**L49**)-TATE, ^{64}Cu-**TETA**(**L49**)-OC and ^{64}Cu-**TETA**(**L49**)-Y^3-TATE to correlate the *in vivo* changes in biokinetics of these molecules that occurred when a substitution of tyrosine for phenylalanine is induced at position 3 of the peptide sequence and when the C-terminal alcohol is oxidized to a carboxylic acid functional group.[427] The analogue ^{64}Cu-**TETA**(**L49**)-Y^3-TATE displayed significantly higher affinity to somatostatin receptor positive CA20948 rat pancreatic tumor membranes and demonstrated up to 3.5-fold more tumor retention than the other tracers examined. These findings led to further investigations of this radiopharmaceutical as a diagnostic imaging agent using a non-human primate model[428] and has led to preliminary dosimetry studies in a rat model.[427] However the experimental evidence of copper transchelation *in vivo* has led to the use of other chelators that form more kinetically inert copper complexes.[20] One such chelator currently being investigated is the cross-bridged chelator **CB-TE2A** (**L57**).[429] To demonstrate its superiority, Sprague et al. prepared the radiopharmaceuticals ^{64}Cu-**CB-TE2A**(**L57**)-Y^3-TATE and ^{64}Cu-**TETA**(**L49**)-Y^3-TATE, which differ only in the copper chelator conjugated to the peptide.[430] While both radiotracers had similar binding affinity to SSTR(+) AR42J tumor cell membranes, blood, liver and non-specific uptake was lower for the cross-bridged analog. Additionally at 4 h, the non-cross bridged tracer had 4-fold and 2-fold higher blood and liver uptake while ^{64}Cu-**CB-TE2A**(**L57**)-Y^3-TATE demonstrated 4-fold greater tumor uptake at the same time point. These interesting properties led Eiblmaier and colleagues to examine the difference in internalization

of these two radiopharmaceuticals in A427-7 cells, which were stably transfected for the SSTR (2) to evaluate their radiotherapeutic and cell killing potential.[431] Cellular internalization and efflux experiments demonstrated that ^{64}Cu-**CB-TE2A**(**L57**)-Y^{3}-TATE internalized more rapidly than ^{64}Cu-**CB-TETA**(**L49**)-Y^{3}-TATE, however more ^{64}Cu-**TETA**(**L49**)-Y^{3}-TATE localized in the nucleus leading the authors to conclude that the difference in kinetic inertness between the two ^{64}Cu complexes led to the higher localization of activity in the nucleus.

In 2004 Milenic, et al. reported the development of a **DTPA** (**L12**) analogue **CHX-A"-DTPA**, (**L14**), which forms stable complexes with a variety of radiometals and is capable of achieving rapid complex formation at room temperature.[432] In order to evaluate this bifunctional chelator, it was coupled to octreotide (OC), labeled with ^{86}Y and injected into rats bearing AR42J pancreatic tumors which over express the somatostatin subtype 2 receptor (SSTr2).[433] ^{86}Y-**CHX-A"-DTPA**(**L14**)-OC demonstrated high tumor uptake along with uptake in the kidneys associated with the renal clearance of the agent. Imaging of the tumor was easily visualized using small animal PET at 4 h, but effective clearance from the tumor was demonstrated with only 25% of the activity remaining at 24 h compared to the 4 h time point in biodistribution studies.

Several ^{68}Ga-radiopharmaceuticals have also been developed to the somatostatin receptor on neuroendocrine tumors.[434-440] Henze et al. examined the diagnostic utility of ^{68}Ga-**DOTA** (**L39**)-D-Phe^{1}-Tyr^{3}-octreotide in patients with meningiomas.[441] During the study, rapid blood clearance and high uptake in the meningioma lesions of various sizes could be observed while no tracer accumulation was found in healthy brain tissue allowing for excellent visualization of these lesions. Additionally, Hofmann and co-workers evaluated ^{68}Ga-**DOTA**(**L39**)-TOC in patients with somatostatin receptor-positive tumors, and compared their results to those obtained with ^{111}In-**DTPA**(**L12**)-octreotide with planar and SPECT imaging.[439] Based upon this study, ^{68}Ga-**DOTA**(**L39**)-TOC was able to clearly delineate 100% of the lesions predefined with CT or MRI, and an additional 30% more lesions were detected when compared with SPECT using ^{111}In-**DOTA**(**L39**)-octreotide. Conversely, only 85% of the lesions previously identified using CT or MRI were correctly identified with the gamma-emitting radiopharmaceutical demonstrating the utility of ^{68}Ga-**DOTA**(**L39**)-TOC in PET imaging and preclinical experiments. Kayani et al. demonstrated that PET/CT using ^{68}Ga-**DOTA**(**L39**)-TATE was superior to [^{18}F]-FDG for imaging well-differentiated neuroendocrine tumors, but [^{18}F]-FDG was more sensitive in detecting high-grade tumors.[442] Additionally, the authors note that the combination use of ^{68}Ga-**DOTA**(**L39**)-TATE, [^{18}F]-FDG and PET/CT has the potential for more comprehensive tumor assessment in intermediate and high-grade tumors. Finally, Ugur et al. investigated the potential of ^{66}Ga-**DOTA**(**L39**)-D-phe^{1}-Tyr^{3}-octreotide as a potential PET agent and radiotherapeutic for somatostatin receptor-positive tumors in AR42J rat pancreatic tumors implanted in nude mice.[443] The authors radiolabeled this radiopharmaceutical precursor with ^{66}Ga, ^{67}Ga and ^{68}Ga. Radiochemical purity of more than 95% was achieved for each radiotracer, and tissue biodistribution demonstrated comparable uptake for the ^{66}Ga, ^{67}Ga and ^{68}Ga complexes. Small animal PET experiments demonstrated efficient tumor retention, but high radioactivity accumulation in the kidney also was observed, suggesting that effective measures to block renal uptake will be needed before therapeutic and imaging protocols using this radiotracer can be implemented.

Targeted radiopharmaceuticals having high specificity and affinity for individual SST subtypes have also been reported. Recently, Ginj et al. compared somatostatin receptor agonists and antagonists as targeting ligands and their specific affinity for the five different subtypes of the somatostatin receptor.[444] The somatostatin receptor subtype 2 (SSTR(2)) selective antagonist sst$_2$-ANT was determined to have a high affinity for the SSTR(2), which was not decreased by the presence of conjugated **DOTA**(**L39**) or a conjugated ^{nat}In-**DOTA**(**L39**) complex. Internalization of the SSTR(2) was not observed using immunofluorescence internalization

assays even when the concentration of the antagonist exceeded 9 μM. Biodistribution studies using ^{111}In-**DOTA**(**L39**)-sst$_2$-ANT revealed high uptake and a slow clearance of the radiopharmaceutical in nude mice bearing tumors comprised of human embryonic kidney (HEK) cells that were stably transfected to only express SSTR(2). Wadas et al. further expanded upon this approach by developing the PET analogue ^{64}Cu-**CB-TE2A**(**L57**)-sst$_2$-ANT and comparing its properties as a PET radiopharmaceutical to the agonist ^{64}Cu-**CB-TE2A**(**L57**)-Y^3-TATE.[445] Biodistribution studies revealed that the PET antagonist demonstrated rapid blood clearance but slower clearance from the liver and kidney. Both radiotracers demonstrated substantial uptake in SSTR(+) tissues and AR42J tumors, which was reduced upon the co-injection of blockade indicating that interaction between the radiopharmaceuticals and the tissues are a receptor-mediated process (Figure 68). ^{64}Cu-**CB-TE2A**(**L57**)-sst$_2$-ANT demonstrated higher tumor:blood and tumor:muscle ratios at the latest time point of 24 h and excellent tumor visualization during small animal PET imaging experiments, which was believed to reflect the antagonist's increased chemical stability and increased hydrophobicity. Interestingly, the relative tumor uptake observed by Wadas and colleagues was much lower than what was reported by Ginj et al.[444] In the studies by Ginj and coworkers, HEK229 cells that were stably transfected to express SSTR(2) were used, while Wadas and colleagues performed their studies using the SSTR(2) endogenously expressing AR42J rat pancreatic carcinoma cell line. This illustrates the variability in results that can occur when cell lines engineered for receptor expression are used rather than cell lines with a natural phenotype for the receptor of interest.

4.1.3. HER-2/neu Receptor Imaging—HER-2/neu proto-oncogene, which is also called erbB-2 was first identified by transfection studies, when NIH3T3 cells were transformed with DNA from chemically-induced rat neuroglioblastomas.[446] It encodes a protein that has extracellular, transmembrane and intracellular domains, and is over-expressed in 25-30% of human breast cancers. Approximately 90-95% of these cases are the result of uncontrolled gene amplification, which produces a malignant phenotype that correlates with shorter disease free survival and shorter overall survival.[447] Several groups have attempted to image this biomarker by developing SPECT imaging agents such as ^{111}In-labeled trastuzimab,[140,448,449] or by developing multimodal imaging agents[450] which will bind tumor cells that over express the HER-2/neu receptor. However, the slow elimination of intact monoclonal antibodies from the body yields low tumor/blood and tumor/normal tissue ratios and has forced researchers to investigate smaller targeting systems to improve the biokinetics of these imaging agents without sacrificing specificity. For example, Tang et al. prepared ^{111}In-**DTPA**(**L12**)-trastuzumab Fab fragments with high radiochemical purity. Although, the measured K_d values for these ligands were 2-fold less than observed for trastuzumab immunoglobulin gamma (IgG), the maximum number of labeled cell sites was 1.5-fold greater.[451,452] Moreover, biodistribution studies revealed significant tumor to non-target ratios but high kidney uptake after 72 h, and small animal imaging studies revealed the clear visualization of HER-2/neu positive BT474 human breast cancer xenografts implanted in athymic mice. Similarly, Dennis and colleagues developed ^{111}In-**DOTA**(**L39**)-AB.Fab4D5, a Fab fragment derived from trastuzumab, which was designed to bind albumin and HER-2/neu simultaneously.[453] Small animal SPECT imaging of MMTV/HER-2 transgenic mice, which develop mammary tumors expressing elevated levels of HER-2, revealed rapid accumulation of ^{111}In-**DOTA**(**L39**)-AB.Fab4D5 in these tumors, which was comparable with other ^{111}In-**DOTA**(**L39**)-trastuzumab Fab fragments, but had better kidney clearance. Finally, Orlova and co-workers described the radiolabeled affibody molecule ^{111}In-**DOTA**(**L39**)-$Z_{HER2:342\text{-}pep2}$.[454] High uptake in SKOV-3 tumor bearing mice at 72 h p.i. was observed, but also unusually high kidney retention. Additionally, cell internalization properties of this imaging agent were examined by Wållberg et al., who demonstrated that between 20-40% of ^{111}In-**DOTA**(**L39**)-$Z_{HER2:342\text{-}pep2}$ was internalized in several HER-2/neu positive cell lines.[455]

4.1.4. Gastrin Releasing Peptide Receptor Imaging—Bombesin (BBN), a 14 aa peptide present in amphibian tissues and gastrin releasing peptide (GRP), its human analogue, which consists of 27 amino acids belong to a family of brain gut peptides that share very similar activities and occur primarily in the central nervous system.[404] GRP receptors have been observed on a wide variety of human cancers including cancers of the GI tract, lung, prostate, breast and neuroblastomas,404 and represent attractive targets for radiopharmaceutical development. Consequently numerous bombesin analogues have been developed and labeled with In,456-458 Ga,[459,460] Y[461] and Cu[461-466] radiometals in order to evaluate the influence of ligand or chelator structure on the biokinetics of these radiopharmaceuticals (Figure 69). For example, Hoffman et al. examined several **DOTA**(**L39**)-X-BBN[7-14]-NH_2 peptides where X was a carbon spacer which was either 2, 5, 8 or 11 carbons in length, in order to optimize the pharmacokinetics for specific targeting of human cancers.[457] Once synthesized, these compounds were radiolabeled with ^{111}In and evaluated in cellular assays that utilized the human prostate carcinoma cell line (PC-3). Biodistribution studies on the 8 carbon analogue, which were conducted in SCID mice bearing PC-3 tumors, demonstrated rapid blood clearance with high tumor uptake occurring 15 minutes p.i. However, washout of the radiotracer was also rapid with only 20% of the injected activity remaining in the tumor by 24 h p.i. Garrison et al. further evaluated the pharmacokinetic changes induced by aliphatic, aromatic and polyethylene glycol ether functional groups in these analogues.[458] Biodistribution studies and small animal SPECT/CT imaging demonstrated that radiopharmaceuticals containing aromatic groups as linkers exhibited the highest percentage of tumor retention 15 minutes p.i., but also exhibited higher uptake in the pancreas and in the GI tract especially at later time points, demonstrating that care needs to be taken when designing radiopharmaceuticals that require chemical linkers between the targeting molecules and the bifunctional chelator.

Recently, Prasanaphich and colleagues explored the Bombesin-based radiopharmaceutical ^{64}Cu-**NOTA(L29)**-8-Aoc-BBN(7-14)NH_2 for the PET imaging of GRPR-expressing tissues.[467] This bioconjugate demonstrated high affinity with an IC_{50} of 3.1 nM while *in vivo* biodistribution studies in PC3 tumor bearing mice demonstrated high uptake in tumor tissue with retention evident at 24 h p.i. Small animal PET/CT corroborated biodistribution studies demonstrating excellent image quality and tumor visualization especially when compared to the ^{64}Cu-**DOTA**(**L39**) analogue. Additional work by the authors have sought to extend this radiopharmaceutical's utility by examining its potential as an imaging agent for breast cancer.[468]

4.1.5. Epidermal Growth Factor Receptor Imaging—The Epidermal Growth Factor Receptor (EGFR) family consists of four related transmembrane receptor tyrosine kinases, which can be activated by a variety of ligands including epidermal growth factor (EGF), causing enhanced cellular proliferation, motility and evasion of apoptosis through downstream pathways.[469] Its over-expression has been observed in up to 60% of human breast cancers with the receptor concentration on these cells being 100 times higher than on normal epithelial tissues, and several studies have associated this cellular phenotype with poor long term survival.470 While some groups have attempted to image other malignancies,44,471,[472] extensive research has been conducted to target EGFR in an attempt to develop imaging agents for breast cancer. For example, Reilly et al. compared the biodistribution properties of ^{111}In-**DTPA**(**L12**)-hEGF, where hEGF is a 53 aa peptide analogue of human epidermal growth factor, and ^{111}In-**DTPA**(**L12**) conjugated anti-EGFR monoclonal antibody in cell lines that were known to have low (MCF-7), medium (MDA-MB-231) and high (MDA-MB-468) EGFR expression.[473] As expected, both radiopharmaceuticals bound to MDA-MB-468 cells with high affinity, and the peptide-based radiopharmaceutical cleared more rapidly from the blood of the mice that were implanted with MDA-MB-468, MDA-MB-231 and MCF-7 tumors. However, 72 h after radiopharmaceutical injection, no direct correlation between the level of tumor uptake

and EGFR receptor expression on the cell surface could be made, while localization of the peptide radiopharamcetical was up to 10-fold lower than that observed with the mAb-based radiopharmaceutical. Small animal imaging demonstrated relatively high accumulation of both radiopharmaceuticals in normal tissue such as liver and kidney and sufficient accumulation in MDA-MB-468 human breast cancer xenografts to visualize the tumor at 72 h p.i. Despite the differences in biokinetics, the mAb based radiopharmaceutical was deemed worthy of future study since its longer circulation time led to high tumor uptake and better tumor visualization at longer time points. Reilly and coworkers have sought to expand upon these interesting results by examining the radiotoxic effect of ^{111}In-**DTPA**(**L12**)-hEGF on breast cancer cells over-expressing EGFR,[474] and comparing the effects of ^{111}In-**DTPA**(**L12**)-hEGF on normal and malignant tissues in EGFR-positive tumor-bearing mice.[475] Additional reports from this group have evaluated the preclinical pharmacokinetic, toxicologic and dosimetric properties of ^{111}In-**DTPA**(**L12**)-hEGF,[476] have correlated the EGFR receptor diversity with nuclear importation,[477] and described the development of a GMP compliant kit, which allows for the clinical preparation of ^{111}In-**DTPA**(**L12**)-hEGF.[478]

A ^{68}Ga-labeled analogue, ^{68}Ga-**DOTA**(**L39**)-hEGF, was also described by Velikyan and colleagues to image EGFR expression in malignant tumors.[479] This radiopharmaceutical demonstrated high affinity for EGFR on A431 cells and biodistribution results established significant uptake during small animal PET imaging; however, liver and kidney uptake were extremely high and may prevent further investigation of this complex as an imaging agent for hepatic metastases.

Investigations to monitor EGFR expression using ^{64}Cu-**DOTA**(**L39**)-cetuximab have also been reported.[480] Cai *et al.* reported the evaluation of ^{64}Cu-**DOTA**(**L39**)-cetuximab in several tumor-bearing mouse models,[481] and using Western blot analysis, a positive correlation was shown to exist between the expression of EGFR and uptake of ^{64}Cu-**DOTA**(**L39**)-cetuximab. Li et al. also evaluated ^{64}Cu-**DOTA**(**L39**)-cetuximab as a PET imaging agent for EGFR positive tumors.[482] Using A431 cells it was determined that this radiopharmaceutical had a k_d of 0.28 nm, while biodistribution and small animal imaging studies revealed good tumor uptake. More importantly, tumor-to-blood and tumor-to-muscle ratios were comparable to those values reported by Perk et al. using ^{89}Zr-**DFO**(**L23**)-cetuximab[44] and were observed to have a better biodistribution profile than an ^{111}In-**DTPA**(**L12**) conjugated cetuximab at 48 h p.i.[483] Eiblmaier and colleagues correlated EGFR expression with ^{64}Cu-**DOTA**(**L39**)-cetuximab affinity and internalization in cervical cancer using cellular assays and microarray analysis of EGFR gene expression.[484] EGFR mRNA expression was found to correlate with EGFR cell surface populations in five human cancer cell lines while the amount of internalized radiopharmaceutical correlated with EGFR mRNA expression and observed protein levels. This radiopharmaceutical demonstrated high uptake in Caski cervical cancer tumors 24 h after being injected into nude mice while small animal imaging revealed excellent image quality comparable to other investigations using ^{64}Cu-labeled cetuximab.[481]

4.1.6. Vascular Endothelial Growth Factor Receptor Imaging—The Vascular Endothelial Growth Factor (VEGF) family of growth factors includes VEGF receptors A, B, C, and D, as well as Placental Growth Factor (PlGF). These ligand/receptor pairs are important for the directed proliferation and migration of endothelial cells that occur during embryonic development and other important biological processes such as wound healing and muscle growth.[485] However, they also play a role in the pathological angiogenesis that accompanies the induction and progression of numerous malignancies. More importantly, several VEGF receptors have been shown to play critical roles in tumor progression, metastasis and angiogenesis and offer scientists a valuable target against which to develop molecular imaging agents.[486,487] For example, Nagengast and coworkers evaluated ^{111}In-**DTPA**(**L12**)-bevacizumab, a monoclonal antibody that recognizes all VEGF isoforms and blocks tumor

angiogenesis, in nude mice bearing human SKOV-3 ovarian tumors xenografts. They demonstrated increasing tumor uptake even after 7 days, with appreciable activity still found in the blood, liver and kidney.[210] This antibody was also labeled with ^{89}Zr and compared to ^{89}Zr-IGg in ovarian tumor xenografts.[210] Tumors were easily visualized at 24 h p.i., and after 168 h p.i. accumulation of the ^{89}Zr-bevacizumab was still observed to be increasing in the tumor (Figure 70). Based upon PET analysis, significantly more activity had accumulated after several days in the tumors of animals that received ^{89}Zr-bevacizumab than those that received ^{89}Zr-IgG. *Ex vivo* determination of tumor uptake correlated well with the *in vivo* data, and demonstrated that quantitative measurement of the tracer in the tumor was possible.

Others have explored the use of radiolabeled recombinant fusion proteins as imaging agents. Chan and coworkers described a novel recombinant fusion protein, composed of $VEGF_{165}$ fused to human transferrin (hnTrf), which was used to chelate ^{111}In.[488] This radiopharmaceutical accumulated through receptor-mediated processes in highly vascularized U87MG glioblastoma xenografts allowing imaging as early as 24 h p.i. However, since the ^{111}In was bound to hnTrf without the use of a traditional chelator, approximately 65% of the incorporated activity was observed to be transchelated under physiological conditions after 72 h. Additional work has focused on the preparation of ^{64}Cu-**DOTA**(**L39**)-$VEGF_{121}$,[489] ^{64}Cu-**DOTA**(**L39**)-$VEGF_{DEE}$, (which is specific for VEGFR2)[490] and ^{64}Cu-**DOTA**(**L39**)-QD-VEGF, which was developed as a multimodal imaging agent combining the PET reporter ^{64}Cu-**DOTA**(**L39**) and the optical properties of quantum dots (QDs).[491,492] Backer et al. developed a single chain, cysteine-tagged VEGF ligand, which is a fusion protein combining two fragments of human $VEGF_{121}$ cloned head to tail.[493] Upon folding, a single cysteine was engineered to be available for chelator conjugation so that the molecule could be radiolabeled with +2 and +3 metal radionuclides. This molecule was also engineered to contain a PEG moiety to increase its blood circulation time. After attaching the chelator **DOTA**(**L39**), the molecule was labeled with ^{64}Cu and biodistribution was determined in female Balb/C mice with 4T1/luc murine mammary carcinoma cells implanted in their mammary fat pads. Data at 2 h p.i. showed prolonged blood circulation due to the addition of the PEG linker and appreciable tumor uptake. Unfortunately, kidney uptake was observed to be extremely high approaching 60% ID/g at this time point.

4.1.7. Melanoma Imaging—Malignant melanoma is the sixth most commonly diagnosed cancer and the most lethal form of skin cancer.[494] To improve diagnosis and survival rates, the melanoma cortin-1 (MC-1) receptor has been a very promising melanoma-specific target for the development of imaging probes based upon the alpha melanocyte stimulating hormone (α-MSH), which binds this receptor with nanomolar affinity (Figures 71 and 72).[141,495-503] Chen et al. synthesized several **DOTA**(**L39**) conjugated α-MSH analogues including **DOTA**(**L39**)-[Nle^4, D-Phe^7]α-MSH (NDP), **DOTA**(**L39**)-CCMSH, a linear analogue, **DOTA**(**L39**)-CMSH, a disulfide bonded analogue and **DOTA**(**L39**)-Re-CCMSH, a rhenium-cyclized analogue in order to optimize the *in vivo* biological properties through structure modification.[496] Of these, ^{111}In-**DOTA**(**L39**)-ReCCMSH had significantly higher tumor accumulation and displayed lower radioactivity accumulation in the kidney and other normal tissues when compared to the linear or disulfide cyclized analogues. This led Cheng et al. to expand on this work by examining the relationship between the structure of the rhenium metallopeptide and its biological properties.[497-499] One derivative, ^{111}In-**DOTA**(**L39**)-ReCCMSH(Arg^{11}), which replaced the lysine at position 11 with arginine demonstrated slightly higher affinity than the ^{111}In-**DOTA**(**L39**)-ReCCMSH *in vitro*, had significantly higher tumor uptake and lower kidney retention at almost every time point investigated when evaluated in a B16/F1 murine melanoma tumor model.

McQuade, et al. evaluated the analogous PET radiopharmaceuticals ^{86}Y-**DOTA**(**L39**)-ReCCMSH(Arg^{11}) and ^{64}Cu-**DOTA**(**L39**)-ReCCMSH(Arg^{11}) using a B16/F1 melanoma

model.[500] Biodistribution studies demonstrated that uptake in the tumor peaked at 30 minutes and remained stable after 4 h, but by 24 h tumor uptake had decreased by 94% and 68%, respectively. Even with significant clearance from the tumor at 24 h, small animal PET experiments revealed good tumor visualization due to low uptake in non-target tissues.

Wei et al. further modified this radiopharmaceutical by replacing **DOTA**(**L39**) with the ^{64}Cu chelator **CB-TE2A**(**L57**), whose Cu(II) complex is highly kinetically inert (*vide supra*).[504] While tumor uptake and retention was similar to that observed by McQuade and coworkers, the advantages of the cross-bridged chelator were clearly evident, since it exhibited more rapid renal clearance than either the ^{64}Cu-**DOTA**(**L39**) or ^{86}Y-**DOTA**(**L39**) analogues with lower accumulation in non-target tissues. This low level of background radioactivity provided excellent contrast resulting in high quality PET images, making ^{64}Cu-**CB-TE2A**(**L57**)-ReCCMSH(Arg^{11}) a promising melanoma imaging agent.

4.2. Imaging Gene Expression

While numerous cell surface molecules have been successfully targeted for imaging, they represent a small fraction of the proteome of a living cell.[505] Since numerous intra- and intercellular regulatory proteins are implicated in cancer initiation and progression, molecular imaging of these biomolecules found within the cytoplasm and nucleus of the cell would provide valuable insight into the phenotype and aggressiveness of cancerous tumors[506] and has become an active area of imaging research.

There are several reports in the literature of the use of ^{86}Y, ^{68}Ga and ^{64}Cu radiometals to image mRNA expression.[194,507-510] Schlesinger et al. investigated the application of ^{86}Y labeled L-oligonucleotides.[194,509] These mirror-image oligonucleotides have an extended biological half-life due to their high resistance to enzyme degradation. Labeled oligonucleotides had a radiochemical purity which fell within a range of 73-98% depending upon the isomer examined. Biodistribution of these systems in normal wistar rats revealed that the radiopharmaceuticals are renally excreted and that they demonstrate appreciable uptake in the adrenal glands, liver and bone. Additionally, Roivainen et al. labeled **DOTA (L39)**-conjugated antisense oligonucleotides, which were designed to target activated human k-ras oncogene with ^{68}Ga, and these radiopharmaceuticals were evaluated in mice bearing A549 lung carcinoma tumors containing a mutated form of the k-ras oncogene and BxPC3 pancreatic adenocarcinoma cell tumors exhibiting wild type expression of k-ras.[511] Radiolabeling did not alter the hybridization properties or protein binding of these systems and small animal PET imaging revealed exceptional visualization of tumors bearing WT k-ras expression, while tumors with the k-ras mutations were barely visible above background. Unfortunately, no quantification of the PET data was provided.

Wang et al. developed a **DTPA**(**L12**)-conjugated, 18-mer phosphothioated antisense oligodeoxynucleotide (ODNS) that could be labeled with ^{111}In to image p21$^{waf-1/CIP-1}$ gene expression at the RNA level.[510] The p21$^{waf-1/CIP-1}$ gene is a prominent early response gene for DNA damage, which encodes a cyclin-dependent kinase inhibitor that regulates progress through the eukaryotic cell cycle. These oligonucleotide imaging agents were evaluated in athymic mice bearing MDA-MB-468 tumor xenografts where the expression of p21$^{waf-1/CIP-1}$ is induced following the subcutaneous injection of epidermal growth factor (EGF) directly into the tumor. Forty-eight hours after the induced p21$^{waf-1/CIP-1}$ gene expression, biodistribution studies revealed tumor-to-muscle ratios that were approximately 3- and 2-fold greater than that seen in tumors where EGF induction was not performed or where random ODNS were injected, respectively. Moreover, tumors were easily visualized via gamma camera scintigraphy.

Developing protein nucleic acid based radiopharmaceuticals has also been investigated. Tian and co workers developed ^{64}Cu-**DOTA**(**L39**)-PNA-peptide radiopharmaceuticals to image the over-expression of CCND1 mRNA, which is translated into cyclin D1, a key regulator in cell proliferation.[512] This radiopharmaceutical was designed with dual specificity, containing a peptide sequence that binds to the insulin-like growth factor receptor (IGFR), which allows the radiopharmaceutical to be internalized into the cell, as well as a nucleic acid sequence that can hybridize to the CCND1 mRNA once in the cytosol. These ^{64}Cu-**DOTA**(**L39**)-PNA-peptide radiopharmaceuticals were observed to be stable to transchelation challenge using 100-fold molar excess **DTPA** (**L12**), human serum albumin or cysteine at 22°C for 30 minutes, and once injected *in vivo*, no transchelation to proteins such as superoxide dismutase was observed. Additionally, appreciable tumor uptake was noted that could be blocked with a co-injection of insulin-like growth factor (IGF) and washout was observed to be rapid by 24 h. Moreover tumor-to-muscle ratios were not significantly different between cohorts that received the radiopharmaceutical and the cohorts that received the PNA or peptide mismatch, respectively. Small animal PET/CT imaging of MCF-7, ER$^+$ breast cancer xenografts implanted in female SCID mice revealed significantly faster and higher uptake in these tumors than CCND1 scintographic probes previously described.[513] Additional work in this area by this group has also led to the development of ^{111}In-**DTPA**(**L12**) conjugated protein nucleic acid (PNAs) antisense molecules that could cross the blood-brain-barrier (BBB) and tumor cell membrane to image either rat glial fibrillary acidic protein (GFAP) or rat caveolin-1 α (CAV).[514,515] Together these results demonstrate that it is possible to image endogenous gene expression in brain cancer with sequence specific PNA antisense radiopharmaceuticals conjugated to a drug targeting system.

4.3. Imaging Inflammation and Infection

The imaging of any infection or inflammatory foci which are characterized by enhanced blood flow, enhanced vascular permeability and an influx of white blood cells, has become a valuable tool that physicians can utilize to diagnose disease and monitor therapy.[516] There are numerous examples in the literature of non-specific imaging agents that rely on the differences in vascular dilation between healthy and diseased tissue, or targeted radiopharmaceuticals that bind to specific targets present in the inflammation[516-519] or infection[413-417] process. For example, Lazzeri et al. exploited the high affinity between avidin and biotin for inflammation imaging in patients with skeletal lesions that included orthopedic conditions, osteomyelitis of the trunk, infection/inflammation of prosthetic joint replacements, and patients with suspected osteomeylitis of appendicular bones.[520,521] This technique involves an infusion of avidin, which was allowed to localize at the infection site followed 4 h later by an injection of ^{111}In-**DTPA**(**L12**)-biotin. Imaging was conducted at 30 minutes and 16-18 h p.i., and to assess its effectiveness it was compared to ^{99m}Tc-HMPAO labeled leukocytes scintigraphy. Based upon the results of this study, the ^{111}In-biotin-avidin system was more sensitive at detecting lesions than ^{99m}Tc-leukocytes scintigraphy in patients with prosthetic joint replacement, osteomyelitis of appendiuclar bones and osteomyelitis of the trunk, and was determined to be more practical since these procedures reduce patient burden by 50%.

Receptor-specific radiopharmaceuticals that target the cells involved with immune and inflammatory processes have also been designed. For example, van Erd et al.[522] and Broekema et al.[523] investigated the new imaging agent ^{111}In-**DTPA**(**L12**)-DPC11870, where DPC11870 is an antagonist of leukotriene B4 (LTB4) receptor, expressed on the surface of neutrophils (Figure 73). This molecule was evaluated in a model of acute colitis, which was induced in New Zealand white rabbits by infusion of trinitrobenzene sulfonic acid in the descending colon, and was compared to [^{18}F]-FDG and ^{99m}Tc-HMPAO granulocytes, which measure metabolic activity and infection response, respectively. Based upon these experiments all three radiotracers revealed the inflamed colon upon scanning, but ^{111}In-**DTPA**(**L12**)-DPC11870

was superior to both ^{99m}Tc-HMPAO-granulocytes and [^{18}F]-FDG because it exhibited high uptake in the colonic lesions, while generating a low background signal in non-inflamed colon. Additionally, Bhargava et al. was able to label leukocytes with ^{64}Cu using a dual chelator method, which demonstrated an equal efficiency to labeling leukocytes with ^{111}In and was superior to labeling leukocytes with ^{18}F-FDG,[524] while Locke and colleagues examined ^{64}Cu-**DOTA**(**L39**)-PEG-c(FLFLFK). This radiopharmaceutical targets the Formyl peptide receptor (FPR) located on leukocytes, and acts as an antagonist by selectively binding to neutrophils with a k_d of 18 nM, but without inducing neutropenia.[525] Small animal imaging studies were performed on mice that were exposed to *Klebsiella pneumoniae*. Eighteen hours after exposure small animal PET/CT and SUV analysis revealed a 5-fold increase in radiopharmaceutical uptake in animals exposed to the bacteria when compared to the control cohort, and this was corroborated by an examination of the lung myeloperoxidase activity which was determined in both groups of animals.

4.4. Imaging Hypoxia and Perfusion

Perfusion and hypoxia imaging have developed into robust research areas since they allow scientists and clinicians to monitor changes in blood flow and image changes in oxygen demand. Both have important implications in the *in vivo* imaging of myocardial infarction and neurological stroke since changes in perfusion often lead to changes in tissue oxygenation and ischemia.[526,527] Imaging hypoxia also has important implications in cancer since tumor hypoxia is believed to increase a tumor's metastatic potential while reducing its sensitivity to radio- and chemotherapeutic agents.[528] Both perfusion and hypoxia imaging have been exhaustively reviewed.[63,529-531]

Numerous perfusion agents have been developed and evaluated using Ga and Cu radiometals because of their short half lives.[532-537] Cutler et al. evaluated the small neutral lipophilic complex ^{68}Ga-*tris*(2-mercaptobenzyl)amine (**L2**) as a potential coronary and neurological perfusion agent.[538] Radiolabeling of this ligand with ^{68}Ga was observed to be facile and biodistribution studies of this complex in rats demonstrated high uptake in brain and heart after 60 minutes. PET imaging of canines and non-human primates demonstrated that this imaging agent is taken up in normal myocardium and has the potential to be used as a diagnostic PET agent for cerebral blood flow.

Because of the short half lives of $^{60/61/62}$Cu, research to develop perfusion agents with these radiometals has also been explored, and the most extensively studied of these perfusion agents is (Cu-**PTSM** (Cu-**L8**). Its popularity is attributed to its higher reduction potential when compared to other copper thiosemicarbazone complexes, which have been developed to image tumor hypoxia (*vida infra*). This physical property facilitates the reduction of Cu(II) to Cu(I) by the normal electron transport chain found in the mitochondria of both normoxic and hypoxic tissues.[535,536] This reductive process and its low membrane permeability after reduction explain its utility as a perfusion agent of healthy and diseased tissues. For example, Wallhaus and colleagues demonstrated that flow defects identified by ^{62}Cu-**PTSM** (^{62}Cu-**L8**) correlated well with angiography in patients with significant coronary artery disease and the results were comparable to those obtained with ^{99m}Tc-Sestamibi and ^{82}Ru.[539] Additionally, Flower et al. examined the possibility of using ^{64}Cu-**PTSM** (^{64}Cu-**L8**) to monitor blood flow changes in patients who presented with colorectal liver metastases and were prescribed vascular manipulation as a component of loco regional chemo- and radiotherapy. Efficacy rates were as high as 78% in patients receiving these treatments.[540] Moreover, Holschenider and colleagues attempted to determine if ^{64}Cu-**PTSM** (^{64}Cu-**L8**) could be used to distinguish between active and passive brain function by comparing it to [^{14}C]-iodoantipyrine, a traditional perfusion agent, in Sprague Dawley rats which were being subjected to a motor skills challenge after being injected with each tracer.[541]

While research had been conducted to develop Ga-based radiopharmaceuticals for hypoxia imaging,[534,542,543] the vast majority has been focused on Cu radiopharmaceuticals, which are based upon the hypoxia-selective imaging agent Cu-**ATSM** (Cu-**L9**) first reported by Fujibayashi and colleagues.[544] Since then, much research has been published on the non-radioactive chemistry of this complex in order to develop new **ATSM** (**L9**) derivatives,[545-554] and elucidate the relationships between molecular structure and the hypoxia mechanisms active within the living cell.[34,64,65,81,555-557] Additionally, **ATSM** (**L9**) has been labeled with several different Cu radiometals,[558-561] and studied as a PET radiopharmaceutical for hypoxia imaging in lung cancer,[562] cervical cancer[563-566] and to monitor therapy response after laparoscopic surgery.[567] Preclinically, it has been examined as an agent for targeted radiotherapy,[62,568-570] examining multidrug resistant tumors,[571] and in conjunction with perfusion imaging.[572,573] Moreover, ^{64}Cu-**ATSM** (^{64}Cu-**L9**) uptake has been correlated with topoisomerase II expression,[574] fatty acid synthase expression,[575] tissue oxygenation[576] and uptake of other PET tracers currently used in the clinic. For example, Dence et al. performed dual tracer experiments that combined autoradiography and small animal PET/CT to correlate the imaging information obtained from ^{64}Cu-**ATSM** (^{64}Cu-**L9**) imaging with those from ^{18}F-FMISO, ^{18}F-FDG and ^{18}F-FLT which are clinically-approved tracers for imaging hypoxia, metabolism and cellular proliferation, respectively.[577] ^{64}Cu-**ATSM** (^{64}Cu-**L9**) correlated well with the ^{18}F-FMISO and ^{18}F-FLT, but not strongly with ^{18}F-FDG. This provides a good example of how dual-tracer imaging can yield more detailed information to the clinician about the physiological processes occurring within the imaged tumor.

5.0. Conclusion

Metal-based radiopharmaceutical research has progressed rapidly since the first ^{99}Mo/^{99m}Tc generator was produced more than 50 years ago. Since that time great strides have been made in radioisotope production, the coordination chemistry of radiometals, and in correlating the chemical structure of metal based radiopharmaceuticals with their behavior *in vivo*. For example, radio-copper chelate stability is paramount when developing tumor targeting radiopharmaceuticals so that optimum image quality can be achieved. However, the opposite is true when considering radio-copper radiopharmaceuticals for hypoxia and perfusion imaging. As a result researchers now have the ability to match the physical characteristics of a specific radiometal with the biokinetics of a particular biological targeting molecule leading to the development of diagnostic and therapeutic radiopharmaceuticals which can be tailored to individual disease processes. This impressive achievement has occurred not by chance, but by the dedicated and collaborative efforts of physicists, chemists, biologists, engineers and physicians. Furthermore, as this scientific discipline advances further into the 21st century, this collaboration must continue and is essential if the transition of more of these radiopharmaceuticals from bench to bedside is to occur.

Acknowledgments

The authors gratefully acknowledge Dr. Riccardo Ferdani, Ph.D. for assistance with the creation of Figure 1, the financial support of NIH grants R01 CA064475 (CJA), CA093375 (EHW) and F32 CA115148 (TJW) and the Gloria G. & Robert E. Lyle Professorship endowment (GRW).

Author Biographies

Carolyn Anderson was born in Superior, WI in 1962, and remained there throughout her school years. In 1985 she graduated Summa Cum Laude with a B.S. in Chemistry from the University of Wisconsin-Superior. In 1984 she received a fellowship to attend the Summer School in Nuclear Chemistry at San Jose State University, and this is where her interest in nuclear and radiochemistry began. She pursued her Ph.D. in Inorganic Chemistry with Prof. Gregory R. Choppin, studying the electrochemistry and spectroscopy of uranium complexes in room temperature molten salts. On completion of her Ph.D. in 1990, she moved to Washington University School of Medicine (WUSM) in St. Louis, MO to carry out postdoctoral research with Prof. Michael J. Welch in the development of radiopharmaceuticals for PET imaging. In 1993 she was promoted to Assistant Professor of Radiology, and she is currently Professor in the departments of Radiology, Biochemistry & Molecular Biophysics and Chemistry. Her research interests include the development of radiometal-labeled tumor receptor-based radiopharmaceuticals for PET imaging and targeted radiotherapy of cancer and cancer metastasis. She greatly enjoys the productive collaboration with Edward Wong and Gary Weisman on the development of novel chelation systems for attaching metal radionuclides to biomolecules for nuclear medicine imaging applications.

Thaddeus J. Wadas was born in Nanticoke, PA in 1974. He received his B.S. degree in Biology from King's College, Wilkes-Barre, Pa in 1996, and while working in the environmental science industry, completed his second major in Chemistry in 1998. After completing his second major, he pursued graduate studies at the University of Rochester, Rochester, NY where he received his M.S. and Ph.D. degrees in Chemistry under the supervision of Richard Eisenberg, Ph.D. His Ph.D. work focused on the synthesis and characterization of luminescent Pt(II) acetylide complexes for photo-induced charge transfer and light-to-chemical energy conversion. On completion of his Ph.D. he moved to the Washington University School of Medicine in St. Louis, MO to pursue postdoctoral studies with Carolyn Anderson, Ph.D. and develop targeted radiopharmaceuticals for diagnostic imaging and radiotherapy. In 2005 he

was the recipient of a National Institutes of Health National Research Service Award (NRSA) Fellowship to study bone metastasis imaging with copper-64-labeled peptides, and in 2009 he was promoted to the position of Instructor at the School of Medicine. His current research interests include the application of combinatorial display methods to radiopharmaceutical development and understanding the respective roles gadolinium based contrast agents and renal insufficiency play in the development of Nephrogenic Systemic Fibrosis.

Edward H. Wong was born in Wuhan, China in 1946 but was raised in Hong Kong where he discovered the joy of mixing chemicals at St. Louis High School. He then majored in chemistry at the University of California at Berkeley and obtained his PhD doing boron hydride synthesis

with William N. Lipscomb at Harvard University in 1974. After a post-doctoral stint with M. Frederick Hawthorne at the University of California, Los Angeles, he began his academic career at Fordham University in 1976 before moving to the University of New Hampshire in 1978. He has performed research in main group boron and phosphorus chemistry as well as metal-phosphine coordination chemistry. In recent years, with his colleague Gary Weisman he has focused on the coordination chemistry of cross-bridged tetraamine macrocycles. Together they have also explored applications of these chelators in copper-based radiopharmaceuticals with Carolyn Anderson and her research group.

Gary R. Weisman was born in Mason, Ohio in 1949, receiving his primary and secondary education in the public school system there. He was interested in chemistry from a young age, working with his cousin Thomas J. Richardson in their substantial home laboratories. He earned his B.S. in Chemistry With Distinction at the University of Kentucky in 1971, carrying out research with Robert D. Guthrie. At the University of Wisconsin – Madison, he worked on conformational analysis of hydrazines and their radical cations under the mentorship of Stephen F. Nelsen, earning the Ph.D. in Organic Chemistry in 1976. After a post-doctoral with Donald J. Cram at the University of California, Los Angeles in 1976-1977, he started his independent academic career at the University of New Hampshire, where he has enjoyed both teaching and research. He was Gloria G. and Robert E. Lyle Professor at UNH from 2005-2009 and has been the recipient of Outstanding Teaching awards in 1995 and 2009. He has been a visiting professor at the University of Wisconsin (1986), University of Bristol (1987, 1998), University of Melbourne (2005), and Australian National University (2005). He was a Wilsmore Fellow at the University of Melbourne in 2002. His research interests are in both physical organic and synthetic organic chemistry, with special emphasis on stereochemical aspects. His recent research has centered on the chemistry of polyaza molecules, ligand design and synthesis, and biomedical applications of coordination complexes. He has enjoyed a productive collaboration with Edward H. Wong for almost two decades and more recently with Carolyn J. Anderson.

6.0. Glossary

%IDG	percent injected dose per gram
aa	amino acid
BBB	blood brain barrier
BBN	bombesin
BFC	bifunctional chelator
CAV	rat caveolin 1-α
CN	coordination number
CT	computed tomography
DBP	di-(n-butylphosphate)
Df or DFO	desferrioxamine
DMF	dimethylformamide
EDC	1-ethyl-3-(3-dimethyl-aminopropyl)-carbodiimide
EGF	epidermal growth factor
Fab	fragment, antigen binding region
Fc	fragment crystallizable
FDA	Food and Drug Administration
FDG	[^{18}F]-fluorodeoxy glucose
FLT	[^{18}F]-fluoro-L-thymidine
FMISO	[^{18}F]-fluoromisonidazole
FPR	formyl peptide receptor
Fv	fragment variable
GBq	gigabecquerel

GFAP	rat glial fibrillary acidic protein
GRP	gastrin releasing peptide
GRPR	gastrin releasing peptide receptor
h	hours
HDEHP	bis-(2-ethylhexyl)-phosphate
HEK	human embryonic kidney
HMPAO	hexamethylpropyleneamine oxime
HNSCC	head and neck squamous cell carcinoma
hnTf	human transferrin
HOPO	hydroxypyridinone
hplc	high performance liquid chromatography
IGF	insulin like growth factor
IGFR	insulin like growth factor receptor
IgG	immunoglobulin gamma
kBq	kilobecquerel
keV	kiloelectron volt
LTB4	leukotriene B4
LTB4R	leukotriene B4 receptor
mAb	monoclonal antibody
MBq	megabecquerel
MC-1	melanocortin-1
MC-1R	melanocortin-1 receptor
MeV	megaelectron volt
MRI	magnetic resonance imaging
NCA	no carrier added
NET	neuroendocrine tumor
NIR	near infrared
N-sucDF	N-Succinyldesferrioxamine B
NTMF	nuclear track micro filters
OC	octreotide
ODNS	oligodeoxynucleotides
p.i.	post injection
PEG	polyethylene glycol
PET	positron emission tomography
PlGF	placental growth factor
PNA	protein nucleic acid

QD	quantum dot
RIT	radioimmunotherapy
RP-hplc	reversed phase high performance liquid chromatography
SA	square antiprismatic
SCID	severly combined immunodeficiency
SPECT	single photon emission computed tomography
SST	somatostatin
SSTR	somatostatin receptor
Sulfo-SMCC	sulfosuccinimidyl 4-(n-maleimidomethyl)cyclohexane-1-carboxylate
TATE	octreotate
TBP	tributylphosphate
TFP	10-(3-(4-methyl-piperazin-1-yl)-propyl)-2-trifluoromethyl-10h-phenothiazine
TOA	trioctyl amine
TSA	twisted square antiprismatic
TTA	4,4,4-trifluoro-1-(2-thienyl)-1,3-butanedione
VEGF	vascular endothelial growth factor
VEGFR	vascular endothelial growth factor receptor
Y^3-OC	tyrosine-3-octreotide
Y^3-TATE	tyrosine-3-octreotate
α-MSH	alpha melanocyte stimulating hormone
β^-	beta - particle
β^+	positron
γ	gamma ray

8.0. References

(1). Society of Nuclear Medicine. 2009. http://interactive.snm.org/index.cfm?PageID=5571&RPID=969

(2). Welch, MJ.; Redvanly, CS., editors. Handbook of Radiopharmaceuticals: Radiochemistry and Applications. John Wiley & Sons Inc.; Hoboken, NJ: 2003.

(3). Blower PJ, Lewis JS, Zweit J. Nucl. Med. Biol 1996;23(8):957. [PubMed: 9004284]

(4). Wadas TJ, Wong EH, Weisman GR, Anderson CJ. Curr. Pharm. Des 2007;13(1):3. [PubMed: 17266585]

(5). Smith SV. IDrugs 2005;8(10):827. [PubMed: 16254803]

(6). Smith SV. J. Inorg. Biochem 2004;98(11):1874. [PubMed: 15522415]

(7). Shokeen M, Anderson CJ. Acc. Chem. Res 2009;42(7):832. [PubMed: 19530674]

(8). Zwanziger D, Beck-Sickinger AG. Curr. Pharm. Des 2008;14(24):2385. [PubMed: 18781989]

(9). de Jong M, Breeman WAP, Kwekkeboom DJ, Valkema R, Krenning EP. Acc. Chem. Res 2009;42(7):873. [PubMed: 19445476]

(10). Liu S. Adv. Drug Delivery Rev 2008;60(12):1347.

(11). Heeg MJ, Jurisson SS. Acc. Chem. Res 1999;32(12):1053.

(12). Anderson CJ, Welch MJ. Chem. Rev 1999;99(9):2219. [PubMed: 11749480]

(13). Anderson CJ, Wadas TJ, Wong EH, Weisman GR. Q. J. Nucl. Med. Mol. Imaging 2008;52(2):185. [PubMed: 18043536]

(14). Rowland DJ, Lewis JS, Welch MJ. J. Cell. Biochem 2002;(Suppl. 39):110.

(15). McQuade P, Rowland DJ, Lewis JS, Welch MJ. Curr. Med. Chem 2005;12(7):807. [PubMed: 15853713]

(16). McQuade, P.; McCarthy, DW.; Welch, MJ.; Valk, PE. Metal radionuclides for PET imaging. In: Bailey, DL.; Townsend, DW.; Maisey, MN., editors. Positron Emission Tomography. Springer-Verlag; London: 2003. p. 251

(17). Hoffman TJ, Smith CJ. Nucl. Med. Biol 2009;36(6):579. [PubMed: 19647163]

(18). Meares, CF. Capturing copper for molecular imaging and therapy. In: Chen, X., editor. Recent Advances of Bioconjugation Chemistry in Molecular Imaging. Research Signpost; Kerala, India: 2009. p. 227

(19). Verel I, Visser GWM, Boellaard R, Stigter-van Walsum M, Snow GB, van Dongen GAMS. J. Nucl. Med 2003;44(8):1271. [PubMed: 12902418]

(20). Bass LA, Wang M, Welch MJ, Anderson CJ. Bioconjugate Chem 2000;11(4):527.

(21). Boswell CA, Sun X, Niu W, Weisman GR, Wong EH, Rheingold AL, Anderson CJ. J. Med. Chem 2004;47(6):1465. [PubMed: 14998334]

(22). Harrison A, Walker CA, Parker D, Jankowski KJ, Cox JPL, Craig AS, Sansom JM, Beeley NRA, Boyce RA. Nucl. Med. Biol 1991;18(5):469.

(23). Camera L, Kinuya S, Garmestani K, Wu C, Brechbiel MW, Pai LH, McMurry TJ, Gansow OA, Pastan I, Paik CH. J. Nucl. Med 1994;35(5):882. [PubMed: 8176477]

(24). Stimmel JB, Kull FC. Nucl. Med. Biol 1998;25(2):117. [PubMed: 9468026]

(25). Stimmel JB, Stockstill ME, Kull FC Jr. Bioconjugate Chem 1995;6(2):219.

(26). Byegard J, Skarnemark G, Skalberg M. J. Radioanal. Nucl. Chem 1999;241(2):281.

(27). Kukis DL, DeNardo SJ, DeNardo GL, O'Donnell RT, Meares CF. J. Nucl. Med 1998;39(12):2105. [PubMed: 9867151]

(28). Jang YH, Blanco M, Dasgupta S, Keire DA, Shively JE, Goddard WA III. J. Am. Chem. Soc 1999;121(26):6142.

(29). Liu S, Edwards DS. Bioconjugate Chem 2001;12(1):7.

(30). Moreau J, Guillon E, Pierrard J-C, Rimbault J, Port M, Aplincourt M. Chem.--Eur. J 2004;10(20):5218.

(31). Chong, H.-s.; Garmestani, K.; Ma, D.; Milenic, DE.; Overstreet, T.; Brechbiel, MW. J. Med. Chem 2002;45(16):3458. [PubMed: 12139456]

(32). Li WP, Ma DS, Higginbotham C, Hoffman T, Ketring AR, Cutler CS, Jurisson SS. Nucl. Med. Biol 2001;28(2):145. [PubMed: 11295425]

(33). Yoo J, Reichert DE, Welch MJ. J. Med. Chem 2004;47(26):6625. [PubMed: 15588098]

(34). Barnard PJ, Bayly SR, Holland JP, Dilworth JR, Waghorn PA. Q. J. Nucl. Med. Mol. Imaging 2008;52(3):235. [PubMed: 18551094]

(35). Jurisson S, Cutler C, Smith SV. Q. J. Nucl. Med. Mol. Imaging 2008;52(3):222. [PubMed: 18480740]

(36). McMurry TJ, Pippin CG, Wu C, Deal KA, Brechbiel MW, Mirzadeh S, Gansow OA. J. Med. Chem 1998;41(18):3546. [PubMed: 9719608]

(37). Broan CJ, Cox J,PL, Craig AS, Kataky R, Parker D, Harrison A, Randall A, Ferguson G. J. Chem. Soc. Perkin Trans. 2 1991;1:87.

(38). Achour B, Costa J, Delgado R, Garrigues E, Geraldes CFGC, Korber N, Nepveu F, Prata MI. Inorg. Chem 1998;37(25):6552.

(39). Pulukkody KP, Norman TJ, Parker D, Royle L, Broan CJ. J. Chem. Soc., Perkin Trans. 2 1993;4:605.

(40). Rae TD, Schmidt PJ, Pufahl RA, Culotta VC, O'Halloran TV. Science 1999;284(5415):805. [PubMed: 10221913]

(41). Kim B-E, Nevitt T, Thiele DJ. Nat. Chem. Biol 2008;4(3):176. [PubMed: 18277979]

(42). Arnesano F, Banci L, Bertini I, Ciofi-Baffoni S. Eur. J. Inorg. Chem 2004;8:1583.

(43). Rosenzweig AC. Acc. Chem. Res 2001;34(2):119. [PubMed: 11263870]
(44). Perk LR, Visser GWM, Vosjan MJWD, Stigter-van Walsum M, Tijink BM, Leemans CR, van Dongen GAMS. J. Nucl. Med 2005;46(11):1898. [PubMed: 16269605]
(45). Perk LR, Visser OJ, Stigter-Van Walsum M, Vosjan MJWD, Visser GWM, Zijlstra JM, Huijgens PC, Dongen GAMS. Eu. J. Nucl. Med. Mol. Imaging 2006;33(11):1337.
(46). Harris WR, Pecoraro VL. Biochemistry 1983;22(2):292. [PubMed: 6402006]
(47). Liu S, Pietryka J, Ellars CE, Edwards DS. Bioconjugate Chem 2002;13(4):902.
(48). Boswell CA, McQuade P, Weisman GR, Wong EH, Anderson CJ. Nucl. Med. Biol 2005;32(1):29. [PubMed: 15691659]
(49). Jalilian AR, Rowshanfarzad P, Sabet M, Kamalidehlghan M, Mirzaii M, Rajamand AA. Maj. Ulum va Funun-i Hastah-i 2005;33:1.
(50). Cordero B, Gomez V, Platero-Prats AE, Reves M, Echeverria J, Cremades E, Barragan F, Alvarez S. Dalton Trans 2008;21:2832. [PubMed: 18478144]
(51). Pasquarello A, Petri I, Salmon PS, Parisel O, Car R, Toth E, Powell DH, Fischer HE, Helm L, Merbach AE. Science 2001;291(5505):856. [PubMed: 11157161]
(52). Mukherjee, R. Copper. In: Constable, EC.; Dilworth, J., editors. Comprehensive Coordination Chemistry II: Transition Metal Groups 7 and 8. Vol. 6. Elsevier Limited; San Diego: 2004. p. 747
(53). Cabbiness DK, Margerum DW. J. Amer. Chem. Soc 1969;91(23):6540.
(54). Bencini A, Bianchi A, Paoletti P, Paoli P. Coord. Chem. Rev 1992;120(1):51.
(55). Curtis, NF. Nitrogen Ligands. In: Constable, EC.; Dilworth, J., editors. Comprehensive Coordination Chemistry II: Funudamentals. Vol. 1. Elsevier Limited; San Diego: 2004. p. 447
(56). Liang X, Sadler PJ. Chem. Soc. Rev 2004;33(4):246. [PubMed: 15103406]
(57). Delgado R, Felix V, Lima LMP, Price DW. Dalton Trans 2007;26:2734. [PubMed: 17592589]
(58). Hall MD, Hambley TW. Coord. Chem. Rev 2002;232(1-2):49.
(59). Fry FH, Jacob C. Curr. Pharm. Des 2006;12(34):4479. [PubMed: 17168755]
(60). Hall MD, Failes TW, Yamamoto N, Hambley TW. Dalton Trans 2007;36:3983. [PubMed: 17828357]
(61). Reisner E, Arion VB, Keppler BK, Pombeiro AJL. Inorg. Chim. Acta 2008;361(6):1569.
(62). Obata A, Yoshimi E, Waki A, Lewis JS, Oyama N, Welch MJ, Saji H, Yonekura Y, Fujibayashi Y. Ann. Nucl. Med 2001;15(6):499. [PubMed: 11831397]
(63). Vavere AL, Lewis JS. Dalton Trans 2007;43:4893. [PubMed: 17992274]
(64). Holland JP, Barnard PJ, Collison D, Dilworth JR, Edge R, Green JC, McInnes EJL. Chem.--Eur. J 2008;14(19):5890.
(65). Holland JP, Giansiracusa JH, Bell SG, Wong L-L, Dilworth JR. Phys. Med. Biol 2009;54(7):2103. [PubMed: 19287086]
(66). Holland JP, Hickin JA, Grenville-Mathers E, Nguyen TN, Peach JM. J. Chem. Res 2008;12:702.
(67). Heroux KJ, Woodin KS, Tranchemontagne DJ, Widger PCB, Southwick E, Wong EH, Weisman GR, Tomellini SA, Wadas TJ, Anderson CJ, Kassel S, Golen JA, Rheingold AL. Dalton Trans 2007;21:2150. [PubMed: 17514336]
(68). Dhungana S, Taboy CH, Zak O, Larvie M, Crumbliss AL, Aisen P. Biochemistry 2004;43(1):205. [PubMed: 14705946]
(69). Mies KA, Wirgau JI, Crumbliss AL. BioMetals 2006;19(2):115. [PubMed: 16718598]
(70). Bakaj M, Zimmer M. J. Mol. Struct 1999;508(1-3):59.
(71). Kaden, TA.; Gokel, GW. Advances in Supramolecular Chemistry. Vol. 3. Elsevier Limited; San Diego: 1993. Functional tetraazamacrocycles: Ligands with many aspects; p. 65
(72). Bridger GJ, Skerlj RT, Padmanabhan S, Thornton D. J. Org. Chem 1996;61(4):1519.
(73). Meyer M, Dahaoui-Gindrey V, Lecomte C, Guilard R. Coord. Chem. Rev 1998;178-180(Pt. 2): 1313.
(74). Guilard R, Bessmertnykh AG, Beletskaya IP. Synlett 1997;10:1190.
(75). Konig B, Pelka M, Klein M, Dix I, Jones PG, Lex J. J. Inclusion Phenom. Macrocyclic Chem 2000;37(1-4):39.

(76). Kaden TA. Chimia 2000;54(10):574.
(77). Lewis EA, Allan CC, Boyle RW, Archibald SJ. Tetrahedron Lett 2004;45(15):3059.
(78). Massue J, Plush SE, Bonnet CS, Moore DA, Gunnlaugsson T. Tetrahedron Lett 2007;48(45):8052.
(79). Suchy M, Hudson RHE. Eur. J. Org. Chem 2008;29:4847.
(80). Bharadwaj PK, Potenza JA, Schugar HJ. J. Am. Chem. Soc 1986;108(6):1351.
(81). Holland JP, Barnard PJ, Collison D, Dilworth JR, Edge R, Green JC, Heslop JM, McInnes EJL, Salzmann CG, Thompson AL. Eur. J. Inorg. Chem 2008;22:3549.
(82). Bu XH, Zhang ZH, An DL, Chen YT, Shionoya M, Kimura E. Inorg. Chim. Acta 1996;249(1):125.
(83). Polyakova IN, Poznyak AL, Sergienko VS. Kristallografiya 2000;45(1):41.
(84). Fomenko VV, Polynova TN, Porai-Koshits MA, Varlamova GL, Pechurova NI. Zh. Strukt. Khim 1973;14(3):571.
(85). Borzel H, Comba P, Hagen KS, Katsichtis C, Pritzkow H. Chem.--Eur. J 2000;6(5):914.
(86). Juran S, Walther M, Stephan H, Bergmann R, Steinbach J, Kraus W, Emmerling F, Comba P. Bioconjugate Chem 2009;20(2):347.
(87). Park G, Dadachova E, Przyborowska A, Lai S.-j. Ma D, Broker G, Rogers RD, Planalp RP, Brechbiel MW. Polyhedron 2001;20(26-27):3155.
(88). Ma D, Lu F, Overstreet T, Milenic DE, Brechbiel MW. Nucl. Med. Biol 2002;29(1):91. [PubMed: 11786280]
(89). Siegfried L, Kaden TA. Dalton Trans 2005;6:1136. [PubMed: 15739018]
(90). Papini G, Alidori S, Lewis JS, Reichert DE, Pellei M, Gioia Lobbia G, Biddlecombe GB, Anderson CJ, Santini C. Dalton Trans 2009;1:177. [PubMed: 19081987]
(91). Kreher U, Hearn MTW, Moubaraki B, Murray KS, Spiccia L. Polyhedron 2007;26(13):3205.
(92). Wieghardt K, Bossek U, Chaudhuri P, Herrmann W, Menke BC, Weiss J. Inorg. Chem 1982;21 (12):4308.
(93). Pavlishchuk V, Birkelbach F, Weyhermueller T, Wieghardt K, Chaudhuri P. Inorg. Chem 2002;41 (17):4405. [PubMed: 12184757]
(94). Packard AB, Kronauge JF, Day PJ, Treves ST. Nucl. Med. Biol 1998;25(6):531. [PubMed: 9751419]
(95). Packard AB, Kronauge JF, Barbarics E, Kiani S, Treves ST. Nucl. Med. Biol 2002;29(3):289. [PubMed: 11929697]
(96). Kiani S, Staples RJ, Ted Treves S, Packard AB. Polyhedron 2009;28(4):775. [PubMed: 20161333]
(97). Kiani S, Staples RJ, Packard AB. Acta Crystallogr., Sect. C 2002;C58(12):m593. [PubMed: 12466608]
(98). Walker PS, Bergin PM, Grossel MC, Horton PN. Inorg. Chem 2004;43(14):4145. [PubMed: 15236526]
(99). Motekaitis RJ, Sun Y, Martell AE, Welch MJ. Can. J. Chem 1999;77(5-6):614.
(100). Barnard PJ, Holland JP, Bayly SR, Wadas TJ, Anderson CJ, Dilworth JR. Inorg. Chem 2009;48 (15):7117. [PubMed: 19588930]
(101). Riesen A, Zehnder M, Kaden TA. Helv. Chim. Acta 1986;69(8):2067.
(102). Kumar K, Tweedle MF, Malley MF, Gougoutas JZ. Inorg. Chem 1995;34(26):6472.
(103). Sun X, Wuest M, Kovacs Z, Sherry AD, Motekaitis R, Wang Z, Martell AE, Welch MJ, Anderson CJ. J. Biol. Inorg. Chem 2003;8(1-2):217. [PubMed: 12459917]
(104). Kalman FK, Baranyai Z, Toth I, Banyai I, Kiraly R, Bruecher E, Aime S, Sun X, Sherry AD, Kovacs Z. Inorg. Chem 2008;47(9):3851. [PubMed: 18380456]
(105). Aneetha H, Lai Y-H, Lin S-C, Panneerselvam K, Lu T-H, Chung C-S. J. Chem. Soc., Dalton Trans 1999;16:2885.
(106). Tonei DM, Ware DC, Brothers PJ, Plieger PG, Clark GR. Dalton Trans 2006;1:152. [PubMed: 16357971]
(107). Chapman J, Ferguson G, Gallagher JF, Jennings MC, Parker D. J. Chem. Soc., Dalton Trans 1992;3:345.
(108). Silversides JD, Allan CC, Archibald SJ. Dalton Trans 2007;9:971. [PubMed: 17308678]

(109). Moi MK, Yanuck M, Deshpande SV, Hope H, DeNardo SJ, Meares CF. Inorg. Chem 1987;26 (21):3458.

(110). Sprague JE, Peng Y, Fiamengo AL, Woodin KS, Southwick EA, Weisman GR, Wong EH, Golen JA, Rheingold AL, Anderson CJ. J. Med. Chem 2007;50(10):2527. [PubMed: 17458949]

(111). Wong EH, Weisman GR, Hill DC, Reed DP, Rogers ME, Condon JP, Fagan MA, Calabrese JC, Lam K-C, Guzei IA, Rheingold AL. J. Am. Chem. Soc 2000;122(43):10561.

(112). Woodin KS, Heroux KJ, Boswell CA, Wong EH, Weisman GR, Niu W, Tomellini SA, Anderson CJ, Zakharov LN, Rheingold AL. Eu. J. Inorg. Chem 2005;23:4829.

(113). Lewis EA, Boyle RW, Archibald SJ. Chem. Comm 2004;19:2212. [PubMed: 15467877]

(114). Kotek J, Lubal P, Hermann P, Cisarova I, Lukes I, Godula T, Svobodova I, Taborsky P, Havel J. Chem.-Eur. J 2003;9(1):233.

(115). Boswell CA, Regino CAS, Baidoo KE, Wong KJ, Milenic DE, Kelley JA, Lai CC, Brechbiel MW. Bioorg. Med. Chem 2009;17(2):548. [PubMed: 19101152]

(116). Sargeson AM. Pure Appl. Chem 1986;58(11):1511.

(117). Bottomley GA, Clark IJ, Creaser II, Engelhardt LM, Geue RJ, Hagen KS, Harrowfield JM, Lawrance GA, Lay PA. Aust. J. Chem 1994;47(1):143.

(118). Bernhardt PV, Bramley R, Engelhardt LM, Harrowfield JM, Hockless DCR, Korybut-Daszkiewicz BR, Krausz ER, Morgan T, Sargeson AM. Inorg. Chem 1995;34(14):3589.

(119). Di Bartolo NM, Sargeson AM, Donlevy TM, Smith SV. J. Chem. Soc., Dalton Trans 2001;15:2303.

(120). Voss SD, Smith SV, DiBartolo N, McIntosh LJ, Cyr EM, Bonab AA, Dearling JLJ, Carter EA, Fischman AJ, Treves ST, Gillies SD, Sargeson AM, Huston JS, Packard AB. Proc. Natl. Acad. Sci. U. S. A 2007;104(44):17489. [PubMed: 17954911]

(121). Smith SV. Q. J. Nucl. Med. Mol. Imaging 2008;52(2):193. [PubMed: 18174877]

(122). Cai W, Guzman R, Hsu AR, Wang H, Chen K, Sun G, Gera A, Choi R, Bliss T, He L, Li Z-B, Maag A-LD, Hori N, Zhao H, Moseley M, Steinberg GK, Chen X. Stroke 2009;40(1):270. [PubMed: 18948613]

(123). Cai H, Fissekis J, Conti PS. Dalton Trans 2009;27:5395. [PubMed: 19565091]

(124). Ma MT, Karas JA, White JM, Scanlon D, Donnelly PS. Chem. Commun 2009;22:3237.

(125). Donnelly PS, Harrowfield JM, Skelton BW, White AH. Inorg. Chem 2001;40(22):5645. [PubMed: 11599965]

(126). Donnelly PS, Harrowfield JM, Skelton BW, White AH. Inorg. Chem 2000;39(25):5817. [PubMed: 11151385]

(127). Bandoli G, Dolmella A, Tisato F, Porchia M, Refosco F. Coord. Chem. Rev 2009;253(1+2):56.

(128). Harris WR, Chen Y, Wein K. Inorg. Chem 1994;33(22):4991.

(129). Jarjayes O, Mortini F, du Moulinet d'Hardemare A, Philouze C, Serratrice G. Eur. J. Inorg. Chem 2005;21:4417.

(130). Motekaitis RJ, Martell AE, Koch SA, Hwang J, Quarless DA Jr. Welch MJ. Inorg. Chem 1998;37 (22):5902.

(131). Francesconi LC, Liu BL, Billings JJ, Carroll PJ, Graczyk G, Kung HF. J. Chem. Soc., Chem. Commun 1991;2:94.

(132). Zheng YY, Saluja S, Yap GPA, Blumenstein M, Rheingold AL, Francesconi LC. Inorg. Chem 1996;35(23):6656. [PubMed: 11666826]

(133). Li Y, Martell AE, Hancock RD, Reibenspies JH, Anderson CJ, Welch MJ. Inorg. Chem 1996;35 (2):404. [PubMed: 11666222]

(134). Jung W-S, Chung YK, Shin DM, Kim S-D. Bull. Chem. Soc. Jpn 2002;75(6):1263.

(135). Ma R, Motekaitis RJ, Martell AE. Inorg. Chim. Acta 1994;224(1-2):151.

(136). Schuhmacher J, Kaul S, Klivenyi G, Junkermann H, Magener A, Henze M, Doll J, Haberkorn U, Amelung F, Bastert G. Cancer Res 2001;61(9):3712. [PubMed: 11325843]

(137). Eder M, Waengler B, Knackmuss S, LeGall F, Little M, Haberkorn U, Mier W, Eisenhut M. Eu. J. Nucl. Med. Mol. Imaging 2008;35(10):1878.

(138). Ma R, Murase I, Martell AE. Inorg. Chim. Acta 1994;223(1-2):109.

(139). Wong E, Caravan P, Liu S, Rettig SJ, Orvig C. Inorg. Chem 1996;35(3):715.

(140). Blend MJ, Stastny JJ, Swanson SM, Brechbiel MW. Cancer Biother. Radiopharm 2003;18(3):355. [PubMed: 12954122]

(141). Wei L, Zhang X, Gallazzi F, Miao Y, Jin X, Brechbiel MW, Xu H, Clifford T, Welch MJ, Lewis JS, Quinn TP. Nucl. Med. Biol 2009;36(4):345. [PubMed: 19423001]

(142). Tsang BW, Mathias CJ, Fanwick PE, Green MA. J. Med. Chem 1994;37(25):4400. [PubMed: 7996552]

(143). Sharma V, Beatty A, Wey SP, Dahlheimer J, Pica CM, Crankshaw CL, Bass L, Green MA, Welch MJ, Piwnica-Worms D. Chem. Biol 2000;7(5):335. [PubMed: 10801474]

(144). Hsiao Y-M, Mathias CJ, Wey S-P, Fanwick PE, Green MA. Nucl. Med. Biol 2009;36(1):39. [PubMed: 19181267]

(145). Martell AE, Motekaitis RJ, Clarke ET, Delgado R, Sun Y, Ma R. Supramol. Chem 1996;6(3-4): 353.

(146). Moore DA, Fanwick PE, Welch MJ. Inorg. Chem 1990;29(4):672.

(147). Clarke ET, Martell AE. Inorg. Chim. Acta 1991;181(2):273.

(148). Prata MIM, Santos AC, Geraldes CFGC, Lima J. J. P. d. Nucl. Med. Biol 1999;26(6):707. [PubMed: 10587111]

(149). McMurry TJ, Brechbiel MW, Wu C, Gansow OA. Bioconjugate Chem 1993;4(3):236.

(150). Cox JPL, Craig AS, Helps IM, Jankowski KJ, Parker D, Eaton MAW, Millican AT, Millar K, Beeley NRA, Boyce BA. J. Chem Soc. Perkin Trans 1 1999:2567.

(151). Studer M, Meares CF. Bioconjugate Chem 1992;34(4):3691.

(152). Brechbiel MW, McMurry TJ, Gansow OA. Tetrahedron Lett 1993;34(23):3691.

(153). Andre JP, Macke HR, Zehnder M, Macko L, Acyel KG. Chem. Commun 1998;12:1301.

(154). Eisenwiener K-P, Prata MIM, Buschmann I, Zhang H-W, Santos AC, Wenger S, Reubi JC, Maecke HR. Bioconjugate Chem 2002;13(3):530.

(155). Viola NA, Rarig RS, Ouellette W, Doyle RP. Polyhedron 2006;25(18):3457.

(156). Heppeler A, Andre JP, Buschmann I, Wang X, Reubi J-C, Hennig M, Kaden TA, Maecke HR. Chem.-Eur. J 2008;14(10):3026.

(157). Heppeler A, Froidevaux S, Macke HR, Jermann E, Behe M, Powell P, Hennig M. Chem.--Eur. J 1999;5(7):1974.

(158). Yang C-T, Li Y, Liu S. Inorg. Chem 2007;46(21):8988. [PubMed: 17784751]

(159). Fani M, Andre JP, Maecke HR. Contrast Media Mol. Imaging 2008;3(2):67. [PubMed: 18383558]

(160). Clarke ET, Martell AE. Inorg. Chim. Acta 1991;190(1):37.

(161). Decristoforo C, Petrik M, von Guggenberg E, Carlsen J, Huisman M, Wester H-J, Virgolini I, Haubner R. J. Lab. Compd. Radiopharm 2007;50:S23.

(162). Niu W, Wong EH, Weisman GR, Peng Y, Anderson CJ, Zakharov LN, Golen JA, Rheingold AL. Eur. J. Inorg. Chem 2004;16:3310.

(163). Terova, O. Synthesis, Characterization and Inertness Studies of Gallium(III) and Indium(III) Complexes of Dicarboxymethyl Pendant-armed Cross-bridged Cyclam. MS, University of New Hampshire; Durham, NH: 2008.

(164). Ward MC, Roberts KR, Babich JW, Bukhari MA, Coghlan G, Westwood JH, McCready VR, Ott RJ. Int. J. Rad. Appl. Instrum. B 1986;13(5):505. [PubMed: 3818312]

(165). Smith-Jones PM, Stolz B, Bruns C, Albert R, Reist HW, Fridrich R, Mäcke HR. J. Nucl. Med 1994;35(2):317. [PubMed: 8295005]

(166). Mathias CJ, Lewis MR, Reichert DE, Laforest R, Sharp TL, Lewis JS, Yang Z-F, Waters DJ, Snyder PW, Low PS, Welch MJ, Green MA. Nucl. Med. Biol 2003;30(7):725. [PubMed: 14499330]

(167). Govindan SV, Michel RB, Griffiths GL, Goldenberg DM, Mattes MJ. Nucl. Med. Biol 2005;32 (5):513. [PubMed: 15982582]

(168). Ye Y, Liu M, Kao JLF, Marshall GR. Biopolymers 2006;84(5):472. [PubMed: 16705688]

(169). Banin E, Lozinski A, Brady KM, Berenshtein E, Butterfield PW, Moshe M, Chevion M, Greenberg EP, Banin E. Proc. Natl. Acad. Sci. U. S. A 2008;105(43):16761. [PubMed: 18931304]

(170). Borgias B, Hugi AD, Raymond KN. Inorg. Chem 1989;28(18):3538.

(171). Borgias BA, Barclay SJ, Raymond KN. J. Coord. Chem 1986;15(2):109.

(172). Motekaitis RJ, Sun Y, Martell AE. Inorg. Chem 1991;30(7):1554.
(173). Rose DJ, Zubieta J, Fischman AJ, Hillier S, Babich JW. Inorg. Chem. Commun 1998;1(5):164.
(174). Ilyukhin AB, Malyarik MA, Petrosyants SP, Davidovich RL, Samsonova IN. Zh. Neorg. Khim 1995;40(7):1125.
(175). Ilyukhin AB, Malyarik MA, Porai-Koshits MA, Davidovich RL, Logvinova VB. Kristallografiya 1995;40(4):656.
(176). Maecke HR, Riesen A, Ritter W. J. Nucl. Med 1989;30(7):1235. [PubMed: 2738704]
(177). Parker D, Pulukkody K, Smith FC, Batsanov A, Howard JAK. J. Chem. Soc., Dalton Trans 1994;5:689.
(178). Hsieh W-Y, Liu S. Inorg. Chem 2004;43(19):6006. [PubMed: 15360250]
(179). Craig AS, Helps IM, Parker D, Adams H, Bailey NA, Williams MG, Smith JMA, Ferguson G. Polyhedron 1989;8(20):2481.
(180). Matthews RC, Parker D, Ferguson G, Kaitner B, Harrison A, Royle L. Polyhedron 1991;10(16): 1951.
(181). Cole E, Copley RCB, Howard JAK, Parker D, Ferguson G, Gallagher JF, Kaitner B, Harrison A, Royle L. J. Chem. Soc., Dalton Trans 1994;11:1619.
(182). Bossek U, Hanke D, Wieghardt K, Nuber B. Polyhedron 1993;12(1):1.
(183). Clarke ET, Martell AE. Inorg. Chim. Acta 1991;186(1):103.
(184). Liu S, He Z, Hsieh W-Y, Fanwick PE. Inorg. Chem 2003;42(26):8831. [PubMed: 14686864]
(185). Riesen A, Kaden TA, Ritter W, Maecke HR. J. Chem. Soc., Chem. Commun 1989;8:460.
(186). Clarke ET, Martell AE. Inorg. Chim. Acta 1991;190(1):27.
(187). Moerlein SM, Welch MJ. Int. J. Nucl. Med. Biol 1981;8(4):277. [PubMed: 6460006]
(188). Mistryukov VE, Sergeev AV, Chuklanova EB, Mikhailov YN, Shchelokov RN. Zh. Neorg. Khim 1997;42(6):969.
(189). Wang J, Zhao J, Zhang X, Gao J. Rare Met 2000;19(4):241.
(190). Amin S, Marks C, Toomey LM, Churchill MR, Morrow JR. Inorg. Chim. Acta 1996;246(1-2):99.
(191). Chang CA, Francesconi LC, Malley MF, Kumar K, Gougoutas JZ, Tweedle MF, Lee DW, Wilson LJ. Inorg. Chem 1993;32(16):3501.
(192). Vojtisek P, Cigler P, Kotek J, Rudovsky J, Hermann P, Lukes I. Inorg. Chem 2005;44(16):5591. [PubMed: 16060608]
(193). Corneillie TM, Fisher AJ, Meares CF. J. Am. Chem. Soc 2003;125(49):15039. [PubMed: 14653738]
(194). Schlesinger J, Koezle I, Bergmann R, Tamburini S, Bolzati C, Tisato F, Noll B, Klussmann S, Vonhoff S, Wuest F, Pietzsch H-J, Steinbach J. Bioconjugate Chem 2008;19(4):928.
(195). Kodama M, Koike T, Mahatma AB, Kimura E. Inorg. Chem 1991;30(6):1270.
(196). Cox JPL, Jankowski KJ, Kataky R, Parker D, Beeley NRA, Boyce BA, Eaton MAW, Millar K, Millican AT. J. Chem. Soc., Chem. Commun 1989;12:797.
(197). Spirlet MR, Rebizant J, Loncin MF, Desreux JF. Inorg. Chem 1984;23(25):4278.
(198). Kang J-G, Na M-K, Yoon S-K, Sohn Y, Kim Y-D, Suh I-H. Inorg. Chim. Acta 2000;310(1):56.
(199). Maecke HR, Scherer G, Heppeler A, Henig M. Eu. J. Nucl. Med 2001;28:967.
(200). Onthank DC, Liu S, Silva PJ, Barrett JA, Harris TD, Robinson SP, Edwards DS. Bioconjugate Chem 2004;15(2):235.
(201). Liu S, Edwards DS. Bioconjugate Chem 2001;12(4):630.
(202). Singhal A, Toth LM, Lin JS, Affholter K. J. Am. Chem. Soc 1996;118(46):11529.
(203). Ekberg C, Kaellvenius G, Albinsson Y, Brown PL. J. Solution Chem 2004;33(1):47.
(204). Pozhidaev AI, Porai-Koshits MA, Polynova TN. Zh. Strukt. Khim 1974;15(4):644.
(205). Davidovich RL, Logvinova VB, Teplukhina LV. Koord. Khim 1992;18(6):580.
(206). Meijs WE, Herscheid JDM, Haisma HJ, Pinedo HM. Appl. Radiat. Isot 1992;43(12):1443.
(207). Takahashi A, Yamaguchi H, Igarashi S. Bunseki Kagaku 1997;46(1):55.
(208). Verel I, Visser GWM, Boellaard R, Boerman OC, van Eerd J, Snow GB, Lammertsma AA, van Dongen GAMS. J. Nucl. Med 2003;44(10):1663. [PubMed: 14530484]

(209). Boerjesson PKE, Jauw YWS, Boellaard R, de Bree R, Comans EFI, Roos JC, Castelijns JA, Vosjan MJWD, Kummer JA, Leemans CR, Lammertsma AA, van Dongen GAMS. Clin. Cancer Res 2006;12(7, Pt. 1):2133. [PubMed: 16609026]

(210). Nagengast WB, de Vries EG, Hospers GA, Mulder NH, de Jong JR, Hollema H, Brouwers AH, van Dongen GA, Perk LR, Lub-de-Hooge MN. J. Nucl. Med 2007;48(8):1313. [PubMed: 17631557]

(211). Datta A, Raymond KN. Acc. Chem. Res 2009;42(7):938. [PubMed: 19505089]

(212). Piel H, Qaim SM, Stocklin G. Radiochim. Acta 1992;57:1.

(213). Williams HA, Robinson S, Julyan P, Zweit J, Hastings D. Eu. J. Nucl. Med. Mol. Imaging 2005;32 (12):1473.

(214). Fujibayashi Y, Matsumoto K, Yonekura Y, Konishi J, Yokayama A. J. Nucl. Med 1989;30(11): 1838. [PubMed: 2809748]

(215). Zweit J, Gordall R, Cox M, Babich JW, Petter GA, Sharma HL, Ott RJ. Eu. J. Nucl. Med 1992;19 (6):418.

(216). Haynes NG, Lacy JL, Nayak N, Martin CS, Dai D, Mathias CJ, Green MA. J. Nucl. Med 2000;41 (2):309. [PubMed: 10688116]

(217). Fukumura T, Okada K, Suzuki H, Nakao R, Mukai K, Szelecsenyi F, Kovacs Z, Suzuki K. Nucl. Med. Biol 2006;33(6):821. [PubMed: 16934701]

(218). Rowshanfarzad P, Sabet M, Reza Jalilian A, Kamalidehghan M. Appl. Radiat. Isot 2006;64(12): 1563. [PubMed: 16377202]

(219). McCarthy DW, Bass LA, Cutler PD, Shefer RE, Klinkowstein RE, Herrero P, Lewis JS, Cutler CS, Anderson CJ, Welch MJ. Nucl. Med. Biol 1999;26(4):351. [PubMed: 10382836]

(220). Szelecsenyi F, Kovacs Z, Suzuki K, Okada K, Fukumura T, Mukai K. Nucl. Instrum. Methods Phys. Res., Sect. B 2004;222(3-4):364.

(221). Fukumura T, Okada K, Szelecsenyi F, Kovacs Z, Suzuki K. Radiochim. Acta 2004;92(4-6):209.

(222). Szelecsenyi F, Suzuki K, Kovacs Z, Takei M, Okada K. Nucl. Instrum. Methods Phys. Res., Sect. B 2002;187(2):153.

(223). Novak-Hofer I, Schubiger PA. Eu. J. Nucl. Med. Mol. Imaging 2002;29(6):821.

(224). Schwarzbach R, Zimmermann K, Blauenstein P, Smith A, Schubiger PA. Appl. Radiat. Isot 1995;46(5):329. [PubMed: 7581290]

(225). Alekseev IE, Darmograi VV, Marchenkov NS. Radiochem 2005;47(5):502.

(226). Dasgupta AK, Mausner LF, Srivastava SC. Appl. Radiat. Isot 1991;42:371.

(227). Kroger LA, DeNardo GL, Gumerlock PH, Xiong CY, Winthrop MD, Shi XB, Mack PC, Leshchinsky T, DeNardo SJ. Cancer Biother. Radiopharm 2001;16(3):213. [PubMed: 11471486]

(228). Wun T, Kwon DS, Tuscano JM. BioDrugs 2001;15(3):151. [PubMed: 11437681]

(229). Zimmermann K, Gianollini S, Schubiger PA, Novak-Hofer I. Nucl. Med. Biol 1999;26(8):943. [PubMed: 10708309]

(230). Frier M. Mini-Rev. Med. Chem 2004;4(1):61. [PubMed: 14754444]

(231). Zimmermann K, Grunberg J, Honer M, Ametamey S, August Schubiger P, Novak-Hofer I. Nucl. Med. Biol 2003;30(4):417. [PubMed: 12767399]

(232). DeNardo GL, DeNardo SJ, Kukis DL, O'Donnell RT, Shen S, Goldstein DS, Kroger LA, Salako Q, DeNardo DA, Mirick GR, Mausner LF, Srivastava SC, Meares CF. Anticancer Res 1998;18:2779. [PubMed: 9713461]

(233). O'Donnell RT, DeNardo GL, Kukis DL, Lamborn KR, Shen S, Yuan A, Goldstein DS, Mirick GR, DeNardo SJ. Clin. Cancer Res 1999;5(10):3330s. [PubMed: 10541382]

(234). Mirick GR, O'Donnell RT, DeNardo SJ, Shen S, Meares CF, DeNardo GL. Nucl. Med. Biol 1999;26(7):841. [PubMed: 10628566]

(235). O'Donnell RT, DeNardo GL, Kukis DL, Lamborn KR, Shen S, Yuan A, Goldstein DS, Carr CE, Mirick GR, DeNardo SJ. J. Nucl. Med 1999;40(12):2014. [PubMed: 10616879]

(236). Sun X, Anderson CJ. Methods Enzymol 2004;386:237. [PubMed: 15120255]

(237). McCarthy DW, Shefer RE, Klinkowstein RE, Bass LA, Margenau WH, Cutler CS, Anderson CJ, Welch MJ. Nucl. Med. Biol 1997;24(1):35. [PubMed: 9080473]

(238). McCarthy DW, Shefer RF, Klinkowstein RF, Cutler CS, Anderson CJ, Welch MJ. J. Labeled Compd. Radiopharm 1995;37(9):830.

(239). Kim JY, Park H, Lee JC, Kim KM, Lee KC, Ha HJ, Choi TH, An GI, Cheon GJ. Appl. Radiat. Isot 2009;67(7-8):1190. [PubMed: 19299153]

(240). Le VS, Howse J, Zaw M, Pellegrini P, Katsifis A, Greguric I, Weiner R. Appl. Radiat. Isot 2009;67 (7-8):1324. [PubMed: 19307129]

(241). Hermanne A, Tarkanyi F, Takacs S, Kovalev SF, Ignatyuk A. Nucl. Instrum. Methods Phys. Res., Sect. B 2007;258(2):308.

(242). Hou X, Jacobsen U, Jorgensen JC. Appl. Radiat. Isot 2002;57(6):773. [PubMed: 12406615]

(243). Watanabe S, Iida Y, Suzui N, Katabuchi T, Ishii S, Kawachi N, Hanaoka H, Watanabe S, Matsuhashi S, Endo K, Ishioka NS. J. Radioanal. Nucl. Chem 2009;280(1):199.

(244). Obata A, Kasamatsu S, McCarthy DW, Welch MJ, Saji H, Yonekura Y, Fujibayashi Y. Nucl. Med. Biol 2003;30(5):535. [PubMed: 12831992]

(245). Avila-Rodriguez MA, Nye JA, Nickles RJ. Appl. Radiat. Isot 2007;65(10):1115. [PubMed: 17669663]

(246). Szajek LP, Meyer W, Plascjak P, Eckleman WC. Radiochim. Acta 2005;93(4):239.

(247). So L, Pellegrini P, Katsifis A, Howse J, Greguric I. J. Radioanal. Nucl. Chem 2008;277(2):451.

(248). Spahn I, Coenen HH, Qaim SM. Radiochim. Acta 2004;92(3):183.

(249). Hilgers K, Stoll T, Skakun Y, Coenen HH, Qaim SM. Appl. Radiat. Isot 2003;59(5-6):343. [PubMed: 14622933]

(250). Abbas K, Kozempel J, Bonardi M, Groppi F, Alfarano A, Holzwarth U, Simonelli F, Hofman H, Horstmann W, Menapace E, Leseticky L, Gibson N. Appl. Radiat. Isot 2006;64(9):1001. [PubMed: 16500108]

(251). Kozempel J, Abbas K, Simonelli F, Zampese M, Holzwarth U, Gibson N, Leseticky L. Radiochim. Acta 2007;95(2):75.

(252). Hassanein MA, El-Said H, El-Amir MA. J. Radioanal. Nucl. Chem 2006;269(1):75.

(253). Little FE, Lagunas-Solar MC. Int. J. Appl. Radiat. Isot 1983;34(3):631.

(254). Nagame Y, Unno M, Nakahara H, Murakami Y. Int. J. Appl. Radiat. Isot 1978;29(11):615.

(255). Steyn J, Meyer BR. Int. J. Appl. Radiat. Isot 1973;24(7):369.

(256). Naidoo C, van der Walt TN. Appl. Radiat. Isot 2001;54(6):915. [PubMed: 11300404]

(257). van der Meulen NP, van der Walt TN. Z. Naturforsch., B: Chem. Sci 2007;62(3):483.

(258). Nayak D, Lahiri S. Appl. Radiat. Isot 2001;54(2):189. [PubMed: 11200879]

(259). Nayak D, Banerjee A, Lahiri S. Appl. Radiat. Isot 2007;65(8):891. [PubMed: 17531499]

(260). Dacosta ACA, Lelite SGF. Biotechnol. Lett 1991;13:559.

(261). Yamamoto F, Tsukamoto E, Nakada K, Takei T, Zhao S, Asaka M, Tamaki N. Ann. Nucl. Med 2004;18(6):519. [PubMed: 15515753]

(262). Lambrecht R, Sajjad M. Radiochim. Acta 1988;43(1):171.

(263). Mirzadeh S, Lambrecht R. J. Radioanal. Nucl. Chem 1996;202(1-2):7.

(264). Zhernosekov KP, Filosofov DV, Baum RP, Aschoff P, Bihl H, Razbash AA, Jahn M, Jennewein M, Rosch F. J. Nucl. Med 2007;48(10):1741. [PubMed: 17873136]

(265). Velikyan I, Beyer GJ, Langstrom B. Bioconjugate Chem 2004;15(3):554.

(266). Breeman WA, de Jong M, de Blois E, Bernard BF, Konijnenberg M, Krenning EP. Eu. J. Nucl. Med. Mol. Imaging 2005;32(4):478.

(267). Azhdarinia A, Yang DJ, Chao C, Mourtada F. Nucl. Med. Biol 2007;34(1):121. [PubMed: 17210469]

(268). Lewis MR, Reichert DE, Laforest R, Margenau WH, Shefer RE, Klinkowstein RE, Hughey BJ, Welch MJ. Nucl. Med. Biol 2002;29(6):701. [PubMed: 12234596]

(269). Lundqvist H, Tolmachev V, Bruskin A, Einarsson L, Malmborg P. Appl. Radiat. Isot 1995;46(9): 859.

(270). Schlyer, DJ. Production of radionuclides in accelerators. In: Welch, MJ.; Redvanly, CS., editors. Handbook of Radiopharmaceuticals: Radiochemistry and Applications. John Wiley & Sons Inc.; Hoboken: 2003. p. 1

(271). Lubberink M, Tolmachev V, Widstroem C, Bruskin A, Lundqvist H, Westlin J-E. J. Nucl. Med 2002;43(10):1391. [PubMed: 12368379]

(272). Tolmachev V, Bernhardt P, Forssell-Aronsson E, Lundqvist H. Nucl. Med. Biol 2000;27(2):183. [PubMed: 10773548]

(273). Nortier FM, Mills SJ, Steyn GF. Appl. Radiat. Isot 1990;41(12):1201.

(274). Thakare SV, Nair GC, Chakrabarty S, Tomar BS. J. Radioanal. Nucl. Chem 1999;242(2):537.

(275). Mukhopadhyay B, Lahiri S, Mukhopadhyay K, Ramaswami A. J. Radioanal. Nucl. Chem 2003;256 (2):307.

(276). Shikano K, Katoh M, Shigematsu T, Yonezawa H. J. Radioanal. Nucl. Chem 1987;119(6):433.

(277). Lewis JS, Laforest R, Lewis MR, Anderson CJ. Cancer Biother. Radiopharm 2000;15(6):593. [PubMed: 11190491]

(278). Casella VR, Grant PM, O'Brien HA Jr. Radiochim. Acta 1975;22(1-2):31.

(279). Claessens RAMJ, Janssen AGM, Van den Bosch RLP, De Goeij JJM. Dev. Nucl. Med 1986;10:46.

(280). Janssen AGM, Claessens RAMJ, Van den Bosch RLP, De Goeij JJM. Appl. Radiat. Isot 1986;37 (4):297.

(281). Abbasi IA, Zaidi JH, Arif M, Waheed S, Subhani MS. Radiochim. Acta 2006;94(8):381.

(282). Bray LA, Wheelwright EJ, Wester DW, Carson KJ, Elovich RJ, Shade EH, Alexander DL, Culley GE, Atkin SD. Radioact. Radiochem 1992;3(4):22.

(283). Hsieh BT, Ting G, Hsieh HT, Shen LH. Radioact. Radiochem 1992;3(4):26.

(284). Happel S, Streng R, Vater P, Ensinger W. Radiat. Meas 2003;36(1-6):761.

(285). Rane AT, Bhatki KS. Anal. Chem 1966;38:1598.

(286). Kawashima T. Int. J. Appl. Radiat. Isot 1969;20(11):806.

(287). Suzuki Y. Int. J. Appl. Radiat. Isot 1964;15(10):599. [PubMed: 14219006]

(288). Doering RF, Tucker WD, Stang LGJ. J. Nucl. Med 1963;4:54. [PubMed: 14028354]

(289). Chinol M, Hnatowich DJ. J. Nucl. Med 1987;28(9):1465. [PubMed: 3625298]

(290). Skraba WJ, Arino H, Kramer HH. Int. J. Appl. Radiat. Isot 1978;29(2):91.

(291). Chakravarty R, Pandey U, Manolkar RB, Dash A, Venkatesh M, Pillai MRA. Nucl. Med. Biol 2008;35(2):245. [PubMed: 18312836]

(292). Pal S, Chattopadhyay S, Das MK, Sudersanan M. Appl. Radiat. Isot 2006;64(12):1521. [PubMed: 16822676]

(293). Roesch F, Qaim SM, Stoecklin G. Appl. Radiat. Isot 1993;44(4):677.

(294). Sadeghi M, Aboudzadeh M, Zali A, Mirzaii M, Bolourinovin F. Appl. Radiat. Isot 2009;67(1):7. [PubMed: 18930657]

(295). Sadeghi M, Aboudzadeh M, Zali A, Mirzaii M, Bolourinovin F. Appl. Radiat. Isot 2008;67(1):7. [PubMed: 18930657]

(296). Garmestani K, Milenic DE, Plascjak PS, Brechbiel MW. Nucl. Med. Biol 2002;29(5):599. [PubMed: 12088731]

(297). Park LS, Szajek LP, Wong KJ, Pascjak PS, Garmestani K, Googins S, Eckelman WC, Carrasquillo JA, Paik CH. Nucl. Med. Biol 2004;31(2):297. [PubMed: 15013497]

(298). Reischl G, Rosch F, Machulla HJ. Radiochim. Acta 2002;90(4):225.

(299). Yoo J, Tang L, Perkins Todd A, Rowland Douglas J, Laforest R, Lewis Jason S, Welch Michael J. Nucl. Med. Biol 2005;32(8):891. [PubMed: 16253815]

(300). Lukic D, Tamburella C, Buchegger F, Beyer G-J, Comor Jozef J, Seimbille Y. Appl. Radiat. Isot 2009;67(4):523. [PubMed: 19181533]

(301). Saha GB, Porile NT, Yaffe L. Phys. Rev 1966;144(3):962.

(302). Link JM, Krohn KA, Eary JF, Kishore R, Lewellen TK, Johnson MW, Badger CC, Richter KY, Nelp WB. J. Labeled Compd. Radiopharm 1986;23(10-12):1297.

(303). DeJesus OT, Nickles RJ. Appl. Radiat. Isot 1990;41(8):789.

(304). Zweit J, Downey S, Sharma HL. Appl. Radiat. Isot 1991;42(2):199.

(305). Hohn A, Zimmermann K, Schaub E, Hirzel W, Schubiger PA, Schibli R. Q. J. Nucl. Med. Mol. Imaging 2008;52(2):145. [PubMed: 18174878]

(306). Meijs WE, Herscheid JDM, Haisma HJ, van Leuffen PJ, Mooy R, Pinedo HM. Appl. Radiat. Isot 1994;45:1143.

(307). Sharma V, Prior JL, Belinsky MG, Kruh GD, Piwnica-Worms D. J. Nucl. Med 2005;46(2):354. [PubMed: 15695797]

(308). Sharma V. Bioconjugate Chem 2004;15(6):1464.

(309). Jacob R, Smith T, Prakasha B, Joannides T. Rheumatol. Inter 2003;23(5):216.

(310). Turkmen C, Ozturk S, Unal SN, Zulfikar B, Taser O, Sanli Y, Cefle K, Kilicoglu O, Palanduz S. Cancer Biother. Radiopharm 2007;22(3):393. [PubMed: 17651045]

(311). Cancer Research UK Home Page. [accessed August 2009]. http://info.cancerresearchuk.org

(312). Gonsalves CF, Brown DB, Carr BI. Exp. Rev. Gastroenterol. Hepatol 2008;2(4):453.

(313). Nelson K, Vause PE Jr. Koropova P. Health Phys 2008;95(5, Suppl.):S156. [PubMed: 18849708]

(314). Khodjibekova M, Szyszko T, Khan S, Nijran K, Tait P, Al-Nahhas A. Rev. Recent Clin. Trials 2007;2(3):212. [PubMed: 18474007]

(315). Dijkgraaf I, Boerman OC, Oyen WJG, Corstens FHM, Gotthardt M. Anti-Cancer Agents Med. Chem 2007;7(5):543.

(316). Vente MAD, Hobbelink MGG, van het Schip AD, Zonnenberg BA, Nijsen JFW. Anti-Cancer Agents Med. Chem 2007;7(4):441.

(317). Mier W, Haberkorn U, Eisenhut M. Signaling Mol. Targets Cancer Ther 2007:215.

(318). Gates VL, Atassi B, Lewandowski RJ, Ryu RK, Sato KT, Nemcek AA, Omary R, Salem R. Future Oncol 2007;3(1):73. [PubMed: 17280504]

(319). Salem R, Hunter RD. Int. J. Radiat. Oncol., Biol., Phys 2006;66(2, Suppl.):S83. [PubMed: 16979447]

(320). Welsh JS, Kennedy AS, Thomadsen B. Int. J. Radiat. Oncol., Biol., Phys 2006;66(2, Suppl.):S62. [PubMed: 16979443]

(321). Pohlman B, Sweetenham J, Macklis RM. Expert Rev. Anticancer Ther 2006;6(3):445. [PubMed: 16503861]

(322). Rao AV, Akabani G, Rizzieri DA. Clin. Med. Res 2005;3(3):157. [PubMed: 16160070]

(323). Stolz, B. Expanding Role of Octreotide I; Presented at the 1st Advances in Oncology, Symposium; Noordwijk, Netherlands. 2002; p. 203

(324). de Herder WW, Lamberts SWJ. Endocrine 2003;20(3):285. [PubMed: 12721509]

(325). Behr TM, Behe M, Sgouros G. Cancer Biother. Radiopharm 2002;17(4):445. [PubMed: 12396708]

(326). Podoloff DA. Curr. Pharm. Des 2002;8(20):1809. [PubMed: 12171532]

(327). Virgolini I, Traub T, Novotny C, Leimer M, Fuger B, Li SR, Patri P, Pangerl T, Angelberger P, Raderer M, Burggasser G, Andreae F, Kurtaran A, Dudczak R. Curr. Pharm. Des 2002;8(20):1781. [PubMed: 12171531]

(328). Nijsen JFW, Van het Schip AD, Hennink WE, Rook DW, Van Rijk PP, De Klerk JMH. Curr. Med. Chem 2002;9(1):73. [PubMed: 11860349]

(329). Vriesendorp HM, Quadri SM. Cancer Biother. Radiopharm 2000;15(5):431. [PubMed: 11155816]

(330). Bal CS, Kumar A. Trop. Gastroenterol 2008;29(2):62. [PubMed: 18972764]

(331). Price TJ, Townsend A. Arch. Surg 2008;143(3):313. [PubMed: 18347282]

(332). Shimoni A, Nagler A. Leuk Lymphoma 2007;48(11):2110. [PubMed: 17891639]

(333). Salem R, Thurston KG. J. Vasc. Interv. Radiol 2006;17(10):1571. [PubMed: 17056999]

(334). Salem R, Thurston Kenneth G. J. Vasc. Interv. Radiol 2006;17(9):1425. [PubMed: 16990462]

(335). Salem R, Thurston Kenneth G. J. Vasc. Interv. Radiol 2006;17(8):1251. [PubMed: 16923973]

(336). Murthy R, Nunez R, Szklaruk J, Erwin W, Madoff David C, Gupta S, Ahrar K, Wallace Michael J, Cohen A, Coldwell Douglas M, Kennedy Andrew S, Hicks Marshall E. Radiographics 2005;25 (Suppl 1):S41. [PubMed: 16227496]

(337). Stipsanelli E, Valsamaki P. Hell. J. Nucl. Med 2005;8(2):103. [PubMed: 16142251]

(338). Mulcahy MF. Curr. Treat. Opt. Oncol 2005;6(5):423.

(339). Hagenbeek A, Lewington V. Ann. Oncol 2005;16(5):786. [PubMed: 15802280]

(340). Hernandez MC, Knox SJ. Sem. Oncol 2003;30(6 Suppl 17):6.

(341). Mahmoud-Ahmed AS, Suh JH. Pituitary 2002;5(3):175. [PubMed: 12812309]

(342). Salem R, Thurston Kenneth G, Carr Brian I, Goin James E, Geschwind Jean-Francois H. J. Vasc. Interv. Radiol 2002;13(9 Pt 2):S223. [PubMed: 12354840]

(343). Pharmacother EO, Illidge TM, Bayne MC. Expt. Opin. Pharm 2001;2(6):953.

(344). Riva P, Franceschi G, Riva N, Casi M, Santimaria M, Adamo M. Eu. J. Nucl. Med 2000;27(5): 601.

(345). Sims E, Doughty D, Macaulay E, Royle N, Wraith C, Darlison R, Plowman PN. Clin. Oncol 1999;11(5):303.

(346). Muller C, Schibli R, Krenning Eric P, de Jong M. J. Nucl. Med 2008;49(4):623. [PubMed: 18344429]

(347). Mathias CJ, Wang S, Low PS, Waters DJ, Green MA. Nucl. Med. Biol 1998;26(1):23. [PubMed: 10096497]

(348). de Visser M, Janssen PJ, Srinivasan A, Reubi JC, Waser B, Erion JL, Schmidt MA, Krenning EP, de Jong M. Eu. J. Nucl. Med. Mol. Imaging 2003;30(8):1134.

(349). Hillairet de Boisferon M, Raguin O, Thiercelin C, Dussaillant M, Rostene W, Barbet J, Pelegrin A, Gruaz-Guyon A. Bioconjugate Chem 2002;13(3):654.

(350). Bussolati G, Chinol M, Chini B, Nacca A, Cassoni P, Paganelli G. Cancer Res 2001;61(11):4393. [PubMed: 11389066]

(351). Schoenberger J, Bauer J, Moosbauer J, Eilles C, Grimm D. Curr. Med. Chem 2008;15(2):187. [PubMed: 18220774]

(352). Sarda-Mantel L, Hervatin F, Michel J-B, Louedec L, Martet G, Rouzet F, Lebtahi R, Merlet P, Khaw B-A, Le Guludec D. Eu. J. Nucl. Med. Mol. Imaging 2008;35(1):158.

(353). Sarda-Mantel L, Michel J-B, Rouzet F, Martet G, Louedec L, Vanderheyden J-L, Hervatin F, Raguin O, Vrigneaud J-M, Khaw BA, Guludec D. Eu. J. Nucl. Med. Mol. Imaging 2006;33(3):239.

(354). Ke S, Wen X, Wu Q-P, Wallace S, Charnsangavej C, Stachowiak AM, Stephens CL, Abbruzzese JL, Podoloff DA, Li C. J. Nucl. Med 2004;45(1):108. [PubMed: 14734682]

(355). Wen X, Wu Q-P, Ke S, Wallace S, Charnsangavej C, Huang P, Liang D, Chow D, Li C. Cancer Biother. Radiopharm 2003;18(5):819. [PubMed: 14629830]

(356). Liu D, Overbey D, Watkinson L, Giblin MF. Bioconjugate Chem 2009;20(5):888.

(357). Hanaoka H, Mukai T, Habashita S, Asano D, Ogawa K, Kuroda Y, Akizawa H, Iida Y, Endo K, Saga T, Saji H. Nucl. Med. Biol 2007;34(5):503. [PubMed: 17591550]

(358). Giersing BK, Rae MT, Carballido BM, Williamson RA, Blower PJ. Bioconjugate Chem 2001;12:964.

(359). Perk LR, Stigter-van Walsum M, Visser GWM, Kloet RW, Vosjan MJWD, Leemans CR, Giaccone G, Albano R, Comoglio PM, van Dongen GAMS. Eu. J. Nucl. Med. Mol. Imaging 2008;35(10): 1857.

(360). Borjesson PKE, Jauw YWS, Boellaard R, de Bree R, Comans EFI, Roos JC, Castelijns JA, Vosjan MJWD, Kummer JA, Leemans CR, Lammertsma AA, van Dongen GAMS. Clin. Cancer Res 2006;12(7):2133. [PubMed: 16609026]

(361). Murata Y, Ishida R, Umehara I, Ishikawa N, Komatsuzaki A, Kurabayashi T, Ishii Y, Ogura I, Ishii J, Okada N, Shibuya H. Nucl. Med. Commun 1999;20(7):599. [PubMed: 10423761]

(362). Kotani J, Kawabe J, Higashiyama S, Kawamura E, Oe A, Hayashi T, Kurooka H, Tsumoto C, Kusuki M, Yamane H, Shiomi S. Ann. Nucl. Med 2008;22(4):297. [PubMed: 18535880]

(363). Van Den Bossche B, Lambert B, De Winter F, Kolindou A, Dierckx RA, Noens L, Van De Wiele C. Nucl. Med. Commun 2002;23(11):1079. [PubMed: 12411836]

(364). Ballani NS, Khan HA, Al-Mohannadi SH, Abu Al-Huda F, Usmani S, Tuli MM, Al-Shemmari SH, Al-Sawagh HF, Al-Enezi FH. Nucl. Med. Commun 2008;29(6):527. [PubMed: 18458599]

(365). Kita T, Watanabe S, Yano F, Hayashi K, Yamamoto M, Iwasaki Y, Kosuda S. Ann. Nucl. Med 2007;21(9):499. [PubMed: 18030581]

(366). Even-Sapir E, Israel O. Eu. J. Nucl. Med. Mol. Imaging 2003;30(Suppl. 1):S65.

(367). Nejmeddine F, Raphael M, Martin A, Le Roux G, Moretti J-L, Caillat-Vigneron N. J. Nucl. Med 1999;40(1):40. [PubMed: 9935054]

(368). Herman M, Paucek B, Raida L, Myslivecek M, Zapletalova J. Eu. J. Radiol 2007;64(3):432.

(369). Sun S-S, Lin C-Y, Chuang F-J, Kao C-H. Clin. Nucl. Med 2003;28(10):869. [PubMed: 14508290]

(370). Israel O, Mekel M, Bar-Shalom R, Epelbaum R, Hermony N, Haim N, Dann EJ, Frenkel A, Ben-Arush M, Gaitini D. J. Nucl. Med 2002;43(10):1295. [PubMed: 12368366]

(371). Rehm PK. Cancer Biother. Radiopharm 1999;14(4):251. [PubMed: 10850311]

(372). Watanabe R, Iizuka H, Kaira K, Mori T, Takise A, Ito J, Motegi A, Onozato Y, Ishihara H. Radiat. Med 2006;24(6):456. [PubMed: 16958428]

(373). Nakahara T, Togawa T, Nagata M, Kikuchi K, Hatano K, Yui N, Kubo A. Eu. J. Nucl. Med. Mol. Imaging 2002;29(8):1072.

(374). Horton MA. Int. J. Biochem. Cell Biol 1997;29(5):721. [PubMed: 9251239]

(375). Albelda SM, Buck CA. FASEB J 1990;4(11):2868. [PubMed: 2199285]

(376). Hausner SH, Kukis DL, Gagnon MKJ, Stanecki CE, Ferdani R, Marshall JF, Anderson CJ, Sutcliffe JL. Mol. Imaging 2009;8(2):111. [PubMed: 19397856]

(377). Sutcliffe JL, Liu R, Peng L, DeNardo SJ, Cherry SR, Kukis DL, Hausner SH, Lam KS. J. Nucl. Med 2007;48(1):69P.

(378). Denardo SJ, Liu R, Albrecht H, Natarajan A, Sutcliffe JL, Anderson C, Peng L, Ferdani R, Cherry SR, Lam KS. J. Nucl. Med 2009;50(4):625. [PubMed: 19289419]

(379). Clezardin P. Cell. Mol. Life Sci 1998;54(6):541. [PubMed: 9676573]

(380). Jin H, Varner J. Br. J. Cancer 2004;90(3):561. [PubMed: 14760364]

(381). Kimura RH, Cheng Z, Gambhir S, Cochran JR. Cancer Res 2009;69(6):2435. [PubMed: 19276378]

(382). McQuade P, Knight LC, Welch MJ. Bioconjugate Chem 2004;15(5):988.

(383). Harris TD, Cheesman E, Harris AR, Sachleben R, Edwards DS, Liu S, Bartis J, Ellars C, Onthank D, Yalamanchili P, Heminway S, Silva P, Robinson S, Lazewatsky J, Rajopadhye M, Barrett J. Bioconjugate Chem 2007;18(4):1266.

(384). Harris TD, Kalogeropoulos S, Nguyen T, Dwyer G, Edwards DS, Liu S, Bartis J, Ellars C, Onthank D, Yalamanchili P, Heminway S, Robinson S, Lazewatsky J, Barrett J. Bioconjugate Chem 2006;17(5):1294.

(385). Harris TD, Kalogeropoulos S, Nguyen T, Liu S, Bartis J, Ellars C, Edwards S, Onthank D, Silva P, Yalamanchili P, Robinson S, Lazewatsky J, Barrett J, Bozarth J. Cancer Biother. Radiopharm 2003;18(4):627. [PubMed: 14503959]

(386). Jang B-S, Lim E, Park SH, Shin IS, Danthi SN, Hwang IS, Le N, Yu S, Xie J, Li KCP, Carrasquillo JA, Paik CH. Nucl. Med. Biol 2007;34(4):363. [PubMed: 17499725]

(387). Shin IS, Jang B-S, Danthi SN, Xie J, Yu S, Le N, Maeng J-S, Hwang IS, Li KCP, Carrasquillo JA, Paik CH. Bioconjugate Chem 2007;18(3):821.

(388). Yoshimoto M, Ogawa K, Washiyama K, Shikano N, Mori H, Amano R, Kawai K. Int. J. Cancer 2008;123(3):709. [PubMed: 18498129]

(389). van Hagen PM, Breeman WAP, Bernard HF, Schaar M, Mooij CM, Srinivasan A, Schmidt MA, Krenning EP, de Jong M. Int. J. Cancer 2000;90(4):186. [PubMed: 10993959]

(390). Dumont RA, Hildebrandt I, Su H, Haubner R, Reischl G, Czernin JG, Mischel PS, Weber WA. Cancer Res 2009;69(7):3173. [PubMed: 19318569]

(391). Wu Y, Zhang X, Xiong Z, Cheng Z, Fisher DR, Liu S, Gambhir SS, Chen X. J. Nucl. Med 2005;46(10):1707. [PubMed: 16204722]

(392). Cao Q, Cai W, Li Z-B, Chen K, He L, Li H-C, Hui M, Chen X. Eu. J. Nucl. Med. Mol. Imaging 2007;34(11):1832.

(393). Chen X, Sievers E, Hou Y, Park R, Tohme M, Bart R, Bremner R, Bading JR, Conti PS. Neoplasia 2005;7(3):271. [PubMed: 15799827]

(394). Cao F, Li Z, Lee A, Liu Z, Chen K, Wang H, Cai W, Chen X, Wu JC. Cancer Res 2009;69(7):2709. [PubMed: 19318556]

(395). Li Z-B, Cai W, Cao Q, Chen K, Wu Z, He L, Chen X. J. Nucl. Med 2007;48(7):1162. [PubMed: 17574975]

(396). Shi J, Kim Y-S, Zhai S, Liu Z, Chen X, Liu S. Bioconjugate Chem 2009;20(4):750.

(397). Lee H-Y, Li Z, Chen K, Hsu Andrew R, Xu C, Xie J, Sun S, Chen X. J. Nucl. Med 2008;49(8): 1371. [PubMed: 18632815]

(398). Cai W, Chen K, Li Z-B, Gambhir SS, Chen X. J. Nucl. Med 2007;48(11):1862. [PubMed: 17942800]

(399). Wei L, Ye Y, Wadas TJ, Lewis JS, Welch MJ, Achilefu S, Anderson CJ. Nucl. Med. Biol 2009;36 (3):277. [PubMed: 19324273]

(400). Sprague JE, Kitaura H, Zou W, Ye Y, Achilefu S, Weilbaecher KN, Teitelbaum SL, Anderson CJ. J. Nucl. Med 2007;48(2):311. [PubMed: 17268030]

(401). Jeong Jae M, Hong Mee K, Chang Young S, Lee Y-S, Kim Young J, Cheon Gi J, Lee Dong S, Chung J-K, Lee Myung C. J. Nucl. Med 2008;49(5):830. [PubMed: 18413379]

(402). Li Z-B, Chen K, Chen X. Eu. J. Nucl. Med. Mol. Imaging 2008;35(6):1100.

(403). Liu Z, Niu G, Shi J, Liu S, Wang F, Liu S, Chen X. Eu. J. Nucl. Med. Mol. Imaging 2009;36(6): 947.

(404). Reubi JC. Endocr. Rev 2003;24(4):389. [PubMed: 12920149]

(405). Reubi JC, Waser B, Schaer J-C, Laissue JA. Eu. J. Nucl. Med 2001;28(7):836.

(406). Rogers BE, Zinn KR, Buchsbaum DJ. Q. J. Nucl. Med 2000;44(3):208. [PubMed: 11105586]

(407). Kwekkeboom DJ, Kooij PP, Bakker WH, Maecke HR, Krenning EP. J. Nucl. Med 1999;40(5): 762. [PubMed: 10319747]

(408). Kwekkeboom DJ, Bakker WH, Kooij PPM, Konijnenberg MW, Srinivasan A, Erion JL, Schmidt MA, Bugaj JE, de Jong M, Krenning EP. Eu. J. Nucl. Med 2001;28(9):1319.

(409). Lebtahi R, Moreau S, Marchand-Adam S, Debray M-P, Brauner M, Soler P, Marchal J, Raguin O, Gruaz-Guyon A, Reubi J-C, Le Guludec D, Crestani B. J. Nucl. Med 2006;47(8):1281. [PubMed: 16883006]

(410). Lebtahi R, Le Cloirec J, Houzard C, Daou D, Sobhani I, Sassolas G, Mignon M, Bourguet P, Le Guludec D. J. Nucl. Med 2002;43(7):889. [PubMed: 12097458]

(411). Traub T, Petkov V, Ofluoglu S, Pangerl T, Raderer M, Fueger BJ, Schima W, Kurtaran A, Dudczak R, Virgolini I. J. Nucl. Med 2001;42(9):1309. [PubMed: 11535718]

(412). Cremonesi M, Ferrari M, Zoboli S, Chinol M, Stabin MG, Orsi F, Maecke HR, Jermann E, Robertson C, Fiorenza M, Tosi G, Paganelli G. Eu. J. Nucl. Med 1999;26(8):877.

(413). Forrer F, Uusijarvi H, Waldherr C, Cremonesi M, Bernhardt P, Mueller-Brand J, Maecke HR. Eu. J. Nucl. Med. Mol. Imaging 2004;31(9):1257.

(414). Rodrigues M, Gabriel M, Heute D, Putzer D, Griesmacher A, Virgolini I. Eu. J. Nucl. Med. Mol. Imaging 2008;35(10):1796.

(415). Rodrigues M, Traub-Weidinger T, Leimer M, Li S, Andreae F, Angelberger P, Dudczak R, Virgolini I. Eu. J. Nucl. Med. Mol. Imaging 2005;32(10):1144.

(416). Becherer A, Szabo M, Karanikas G, Wunderbaldinger P, Angelberger P, Raderer M, Kurtaran A, Dudczak R, Kletter K. J. Nucl. Med 2004;45(7):1161. [PubMed: 15235062]

(417). Decristoforo C, Mather SJ, Cholewinski W, Donnemiller E, Riccabona G, Moncayo R. Eu. J. Nucl. Med 2000;27(9):1318.

(418). Meisetschlager G, Poethko T, Stahl A, Wolf I, Scheidhauer K, Schottelius M, Herz M, Wester Hans J, Schwaiger M. J. Nucl. Med 2006;47(4):566. [PubMed: 16595488]

(419). Gabriel M, Decristoforo C, Donnemiller E, Ulmer H, Rychlinski CW, Mather SJ, Moncayo R. J. Nucl. Med 2003;44(5):708. [PubMed: 12732671]

(420). Anderson CJ, Dehdashti F, Cutler PD, Schwarz SW, Laforest R, Bass LA, Lewis JS, McCarthy DW. J. Nucl. Med 2001;42(2):213. [PubMed: 11216519]

(421). Parry JJ, Eiblmaier M, Andrews R, Meyer LA, Higashikubo R, Anderson CJ, Rogers BE. Mol. Imaging 2007;6(1):56. [PubMed: 17311765]

(422). Wang M, Caruano AL, Lewis MR, Ballard L, Kelly K, Vanderwaal RP, Anderson CJ. Q. J. Nucl. Med 2001;45(2):S12.

(423). Wang M, Caruano AL, Lewis MR, Meyer LM, VanderWaal RP, Anderson CJ. Cancer Res 2003;63 (20):6864. [PubMed: 14583484]

(424). Li WP, Lewis JS, Kim J, Bugaj JE, Johnson MA, Erion JL, Anderson CJ. Bioconjugate Chem 2002;13(4):721.

(425). Edwards WB, Xu B, Akers W, Cheney PP, Liang K, Rogers BE, Anderson C,J, Achilefu S. Bioconjugate Chem 2008;19(1):192.

(426). de Jong M, Breeman WAP, Bernard BF, van Gameren A, de Bruin E, Bakker WH, van der Pluijm ME, Visser TJ, Macke HR, Krenning EP. Eu. J. Nucl. Med 1999;26(7):693.

(427). Lewis JS, Lewis MR, Cutler PD, Srinivasan A, Schmidt MA, Schwarz SW, Morris MM, Miller JP, Anderson CJ. Clin. Cancer Res 1999;5(10):3608. [PubMed: 10589778]

(428). Lewis JS, Srinivasan A, Schmidt MA, Anderson CJ. Nucl. Med. Biol 1999;26(3):267. [PubMed: 10363797]

(429). Weisman GR, Rogers ME, Wong EH, Jasinski JP, Paight ES. J. Am. Chem. Soc 1990;112(23): 8604.

(430). Sprague JE, Peng Y, Sun X, Weisman GR, Wong EH, Achilefu S, Anderson CJ. Clin. Cancer Res 2004;10(24):8674. [PubMed: 15623652]

(431). Eiblmaier M, Andrews R, Laforest R, Rogers BE, Anderson CJ. J. Nucl. Med 2007;48(8):1390. [PubMed: 17631550]

(432). Milenic DE, Brady ED, Brechbiel MW. Nat. Rev. Drug Discovery 2004;3(6):488.

(433). Clifford T, Boswell CA, Biddlecombe GB, Lewis JS, Brechbiel MW. J. Med. Chem 2006;49(14): 4297. [PubMed: 16821789]

(434). Lincke T, Singer J, Kluge R, Sabri O, Paschke R. Thyroid 2009;19(4):381. [PubMed: 19355828]

(435). Fanti S, Ambrosini V, Tomassetti P, Castellucci P, Montini G, Allegri V, Grassetto G, Rubello D, Nanni C, Franchi R. Biomed. Pharmacother 2008;62(10):667. [PubMed: 18358680]

(436). Koukouraki S, Strauss LG, Georgoulias V, Eisenhut M, Haberkorn U, Dimitrakopoulou-Strauss A. Eu. J. Nucl. Med. Mol. Imaging 2006;33(10):1115.

(437). Wild D, Schmitt JS, Ginj M, Maecke HR, Bernard BF, Krenning E, de Jong M, Wenger S, Reubi J-C. Eu. J. Nucl. Med. Mol. Imaging 2003;30(10):1338.

(438). Froidevaux S, Eberle AN, Christe M, Sumanovski L, Heppeler A, Schmiti JS, Eisenwiener K, Beglinger C, Macke HR. Int. J. Cancer 2002;98(6):930. [PubMed: 11948475]

(439). Hofmann M, Maecke H, Boerner AR, Weckesser E, Schoeffski P, Oei ML, Schumacher J, Henze M, Heppeler A, Meyer GJ, Knapp WH. Eu. J. Nucl. Med 2001;28(12):1751.

(440). Gabriel M, Decristoforo C, Kendler D, Dobrozemsky G, Heute D, Uprimny C, Kovacs P, Von Guggenberg E, Bale R, Virgolini IJ. J. Nucl. Med 2007;48(4):508. [PubMed: 17401086]

(441). Henze M, Schuhmacher J, Hipp P, Kowalski J, Becker DW, Doll J, Macke HR, Hofmann M, Debus J, Haberkorn U. J. Nucl. Med 2001;42(7):1053. [PubMed: 11438627]

(442). Kayani I, Bomanji JB, Groves A, Conway G, Gacinovic S, Win T, Dickson J, Caplin M, Ell PJ. Cancer 2008;112(11):2447. [PubMed: 18383518]

(443). Ugur O, Kothari PJ, Finn RD, Zanzonico P, Ruan S, Guenther I, Maecke HR, Larson SM. Nucl. Med. Biol 2002;29(2):147. [PubMed: 11823119]

(444). Ginj M, Zhang H, Waser B, Cescato R, Wild D, Wang X, Erchegyi J, Rivier J, Macke HR, Reubi JC. Proc. Natl. Acad. Sci. U.S.A 2006;103(44):16436. [PubMed: 17056720]

(445). Wadas TJ, Eiblmaier M, Zheleznyak A, Sherman CD, Ferdani R, Liang K, Achilefu S, Anderson CJ. J. Nucl. Med 2008;49(11):1819. [PubMed: 18927338]

(446). Slamon DJ, Godolphin W, Jones LA, Holt JA, Wong SG, Keith DE, Levin WJ, Stuart SG, Udove J, Ullrich A. Science 1989;244(4905):707. [PubMed: 2470152]

(447). Pauletti G, Dandekar S, Rong H, Ramos L, Peng H, Seshadri R, Slamon DJ. J. Clin. Oncol 2000;18 (21):3651. [PubMed: 11054438]

(448). Perik PJ, Lub-De Hooge MN, Gietema JA, van der Graaf WTA, de Korte MA, Jonkman S, Kosterink JGW, van Veldhuisen DJ, Sleijfer DT, Jager PL, de Vries EGE. J. Clin. Oncol 2006;24 (15):2276. [PubMed: 16710024]

(449). Lub-de Hooge MN, Kosterink JGW, Perik PJ, Nijnuis H, Tran L, Bart J, Suurmeijer AJH, de Jong S, Jager PL, de Vries EGE. Br. J. Pharmacol 2004;143(1):99. [PubMed: 15289297]

(450). Sampath L, Kwon S, Ke S, Wang W, Schiff R, Mawad ME, Sevick-Muraca EM. J. Nucl. Med 2007;48(9):1501. [PubMed: 17785729]

(451). Tang Y, Scollard D, Chen P, Wang J, Holloway C, Reilly RM. Nucl. Med. Commun 2005;26(5): 427. [PubMed: 15838425]

(452). Tang Y, Wang J, Scollard DA, Mondal H, Holloway C, Kahn HJ, Reilly RM. Nucl. Med. Biol 2005;32(1):51. [PubMed: 15691661]

(453). Dennis MS, Jin H, Dugger D, Yang R, McFarland L, Ogasawara A, Williams S, Cole MJ, Ross S, Schwall R. Cancer Res 2006;67(1):254. [PubMed: 17210705]

(454). Orlova A, Tolmachev V, Pehrson R, Lindborg M, Tran T, Sandstroem M, Nilsson FY, Wennborg A, Abrahmsen L, Feldwisch J. Cancer Res 2007;67(5):2178. [PubMed: 17332348]

(455). Wallberg H, Orlova A. Cancer Biother. Radiopharm 2008;23(4):435. [PubMed: 18771347]

(456). Breeman WAP, De Jong M, Bernard BF, Kwekkeboom DJ, Srinivasan A, Van Der Pluijm ME, Hofland LJ, Visser TJ, Krenning EP. Int. J. Cancer 1999;83(5):657. [PubMed: 10521803]

(457). Hoffman TJ, Gali H, Smith CJ, Sieckman GL, Hayes DL, Owen NK, Volkert WA. J. Nucl. Med 2003;44(5):823. [PubMed: 12732685]

(458). Garrison JC, Rold TL, Sieckman GL, Naz F, Sublett SV, Figueroa SD, Volkert WA, Hoffman TJ. Bioconjugate Chem 2008;19(9):1803.

(459). Schuhmacher J, Zhang H, Doll J, Maecke HR, Matys R, Hauser H, Henze M, Haberkorn U, Eisenhut M. J. Nucl. Med 2005;46(4):691. [PubMed: 15809493]

(460). Dimitrakopoulou-Strauss A, Hohenberger P, Eisenhut M, Maecke HR, Haberkorn U, Strauss L. J. Nucl. Med 2006;47(S1):102P.

(461). Biddlecombe GB, Rogers BE, de Visser M, Parry JJ, de Jong M, Erion JL, Lewis JS. Bioconjugate Chem 2007;18(3):724.

(462). Gasser G, Tjioe L, Graham B, Belousoff MJ, Juran S, Walther M, Kuenstler J-U, Bergmann R, Stephan H, Spiccia L. Bioconjugate Chem 2008;19(3):719.

(463). Rogers BE, Bigott HM, McCarthy DW, Della Manna D, Kim J, Sharp TL, Welch MJ. Bioconjugate Chem 2003;14(4):756.

(464). Parry JJ, Andrews R, Rogers BE. Breast Cancer Res. Treat 2007;101(2):175. [PubMed: 16838112]

(465). Parry JJ, Kelly TS, Andrews R, Rogers BE. Bioconjugate Chem 2007;18(4):1110.

(466). Chen X, Park R, Hou Y, Tohme M, Shahinian AH, Bading JR, Conti PS. J. Nucl. Med 2004;45 (8):1390. [PubMed: 15299066]

(467). Prasanphanich AF, Nanda PK, Rold TL, Ma L, Lewis MR, Garrison JC, Hoffman TJ, Sieckman GL, Figueroa SD, Smith CJ. Proc. Natl. Acad. Sci. U. S. A 2007;104(30):12462. [PubMed: 17626788]

(468). Prasanphanich AF, Retzloff L, Lane SR, Nanda PK, Sieckman GL, Rold TL, Ma L, Figueroa SD, Sublett SV, Hoffman TJ, Smith CJ. Nucl. Med. Biol 2009;36(2):171. [PubMed: 19217529]

(469). Klein S, Levitzki A. Curr. Opin. Cell Biol 2009;21(2):185. [PubMed: 19216065]

(470). Klijn JGM, Berns PMJJ, Schmitz PIM, Foekens JA. Endo. Rev 1992;13(1):3.

(471). Kurihara A, Pardridge WM. Cancer Res 1999;59(24):6159. [PubMed: 10626807]

(472). Kurihara A, Deguchi Y, Pardridge WM. Bioconjugate Chem 1999;10(3):502.

(473). Reilly RM, Kiarash R, Sandhu J, Lee YW, Cameron RG, Hendler A, Vallis K, Gariepy J. J. Nucl. Med 2000;41(5):903. [PubMed: 10809207]

(474). Reilly RM, Kiarash R, Cameron RG, Porlier N, Sandhu J, Hill RP, Vallis K, Hendler A, Gariepy J. J. Nucl. Med 2000;41(3):429. [PubMed: 10716315]

(475). Chen P, Cameron R, Wang J, Vallis KA, Reilly RM. J. Nucl. Med 2003;44(9):1469. [PubMed: 12960194]

(476). Reilly RM, Chen P, Wang J, Scollard D, Cameron R, Vallis KA. J. Nucl. Med 2006;47(6):1023. [PubMed: 16741313]

(477). Hu M, Scollard D, Chan C, Chen P, Vallis K, Reilly RM. Nucl. Med. Biol 2007;34(8):887. [PubMed: 17998090]

(478). Reilly RM, Scollard DA, Wang J, Mondal H, Chen P, Henderson LA, Bowen BM, Vallis KA. J. Nucl. Med 2004;45(4):701. [PubMed: 15073268]

(479). Velikyan I, Sundberg AL, Lindhe O, Hoeglund AU, Eriksson O, Werner E, Carlsson J, Bergstroem M, Laangstroem B, Tolmachev V. J. Nucl. Med 2005;46(11):1881. [PubMed: 16269603]

(480). Niu G, Cai W, Chen K, Chen X. Mol. Imaging Biol 2008;10(2):99. [PubMed: 18157579]

(481). Cai W, Chen K, He L, Cao Q, Koong A, Chen X. Eu. J. Nucl. Med. Mol. Imaging 2007;34(6): 850.

(482). Li WP, Meyer LA, Capretto DA, Sherman CD, Anderson CJ. Cancer Biother. Radiopharm 2008;23 (2):158. [PubMed: 18454685]

(483). Wen X, Wu QP, Ke S, Ellis L, Charnsangavej C, Delpassand AS, Wallace S, Li C. J. Nucl. Med 2001;42(10):1530. [PubMed: 11585869]

(484). Eiblmaier M, Meyer LA, Watson MA, Fracasso PM, Pike LJ, Anderson CJ. J. Nucl. Med 2008;49 (9):1472. [PubMed: 18703609]

(485). Lohela M, Bry M, Tammela T, Alitalo K. Curr. Opin. Cell Biol 2009;21(2):154. [PubMed: 19230644]

(486). Kaplan RN, Rafii S, Lyden D. Cancer Res 2006;66(23):11089. [PubMed: 17145848]

(487). Kaplan RN, Riba RD, Zacharoulis S, Bramley AH, Vincent L, Costa C, MacDonald DD, Jin DK, Shido K, Kerns SA, Zhu Z, Hicklin D, Wu Y, Port JL, Altorki N, Port ER, Ruggero D, Shmelkov SV, Jensen KK, Rafii S, Lyden D. Nature 2005;438(7069):820. [PubMed: 16341007]

(488). Chan C, Sandhu J, Guha A, Scollard DA, Wang J, Chen P, Bai K, Lee L, Reilly RM. J. Nucl. Med 2005;46(10):1745. [PubMed: 16204726]

(489). Cai W, Chen K, Mohamedali KA, Cao Q, Gambhir SS, Rosenblum MG, Chen X. J. Nucl. Med 2006;47(12):2048. [PubMed: 17138749]

(490). Wang H, Cai W, Chen K, Li Z-B, Kashefi A, He L, Chen X. Eu. J. Nucl. Med. Mol. Imaging 2007;34(12):2001.

(491). Chen K, Li Z-B, Wang H, Cai W, Chen X. Eu. J. Nucl. Med. Mol. Imaging 2008;35(12):2235.

(492). Hsu AR, Cai W, Veeravagu A, Mohamedali KA, Chen K, Kim S, Vogel H, Hou LC, Tse V, Rosenblum MG, Chen X. J. Nucl. Med 2007;48(3):445. [PubMed: 17332623]

(493). Backer MV, Levashova Z, Patel V, Jehning BT, Claffey K, Blankenberg FG, Backer JM. Nat. Med 2007;13(4):504. [PubMed: 17351626]

(494). Jemal A, Siegel R, Ward R, Murray T, Xu J, Thun MJ. Cancer J. Clin 2007;57:43.

(495). Miao Y, Quinn TP. Front. Biosci 2007;12(12):4514. [PubMed: 17485393]

(496). Chen J, Cheng Z, Owen NK, Hoffman TJ, Miao Y, Jurisson SS, Quinn TP. J. Nucl. Med 2001;42 (12):1847. [PubMed: 11752084]

(497). Cheng Z, Chen J, Miao Y, Owen NK, Quinn TP, Jurisson SS. J. Med. Chem 2002;45(14):3048. [PubMed: 12086490]

(498). Chen J, Cheng Z, Miao Y, Jurisson SS, Quinn TP. Cancer 2002;94(4, Suppl.):1196. [PubMed: 11877745]

(499). Bapst J-P, Calame M, Tanner H, Eberle AN. Bioconjugate Chem 2009;20(5):984.

(500). McQuade P, Miao Y, Yoo J, Quinn TP, Welch MJ, Lewis JS. J. Med. Chem 2005;48(8):2985. [PubMed: 15828837]

(501). Cheng Z, Xiong Z, Subbarayan M, Chen X, Gambhir SS. Bioconjugate Chem 2007;18(3):765.

(502). Froidevaux S, Calame-Christe M, Schuhmacher J, Tanner H, Saffrich R, Henze M, Eberle AN. J. Nucl. Med 2004;45(1):116. [PubMed: 14734683]

(503). Wei L, Miao Y, Gallazzi F, Quinn TP, Welch MJ, Vavere AL, Lewis JS. Nucl. Med. Biol 2007;34 (8):945. [PubMed: 17998097]

(504). Wei L, Butcher C, Miao Y, Gallazzi F, Quinn TP, Welch MJ, Lewis JS. J. Nucl. Med 2007;48(1): 64. [PubMed: 17204700]

(505). Misek DE, Imafuku Y, Hanash SM. Pharmacogenom. J 2004;5(8):1129.

(506). Giannios J, Ioannidou-Mouzaka L. Eu. J. Gyn. Oncol 1997;18(5):387.

(507). Lendvai G, Velikyan I, Estrada S, Eriksson B, Laangstroem B, Bergstroem M. Oligonucleotides 2008;18(1):33. [PubMed: 18321161]

(508). Lendvai G, Velikyan I, Bergstroem M, Estrada S, Laryea D, Vaelilae M, Salomaeki S, Langstroem B, Roivainen A. Eur. J. Pharm. Sci 2005;26(1):26. [PubMed: 15941654]

(509). Schlesinger J, Bergmann R, Klussmann S, Wuest F. Lett. Drug Disc 2006;3(5):330.

(510). Wang J, Chen P, Mrkobrada M, Hu M, Vallis KA, Reilly RM. Eu. J. Nucl. Med. Mol. Imaging 2003;30(9):1273.

(511). Roivainen A, Tolvanen T, Salomaki S, Lendvai G, Velikyan I, Numminen P, Valila M, Sipila H, Bergstrom M, Harkonen P, Lonnberg H, Langstrom B. J. Nucl. Med 2004;45(2):347. [PubMed: 14960659]

(512). Tian X, Aruva MR, Zhang K, Shanthly N, Cardi CA, Thakur ML, Wickstrom E. J. Nucl. Med 2007;48(10):1699. [PubMed: 17909257]

(513). Tian X, Aruva MR, Qin W, Zhu W, Duffy KT, Sauter ER, Thakur ML, Wickstrom E. J. Nucl. Med 2004;45(12):2070. [PubMed: 15585484]

(514). Suzuki T, Zhang Y, Zhang Y.-f. Schlachetzki F, Pardridge WM. Mol. Imaging 2004;3(4):356. [PubMed: 15802053]

(515). Suzuki T, Wu D, Schlachetzki F, Li JY, Boado RJ, Pardridge WM. J. Nucl. Med 2004;45(10): 1766. [PubMed: 15471847]

(516). Boerman OC, Dams ETM, Oyen WJG, Corstens FHM, Storm G. Inflammation Res 2001;50(2): 55.

(517). Hughes DK. J. Nucl. Med. Technol 2003;31(4):196. [PubMed: 14657285]

(518). Liu S-F, Liu J-W, Lin M-C, Lee C-H, Huang H-H, Lai Y-F. Am. J. Roentgenol 2007;188(5):W403. [PubMed: 17449733]

(519). Hang LW, Hsu WH, Tsai JJP, Jim YF, Lin CC, Kao A. Rheumatol. Inter 2004;24(3):153.

(520). Lazzeri E, Pauwels EKJ, Erba PA, Volterrani D, Manca M, Bodei L, Trippi D, Bottoni A, Cristofani R, Consoli V, Palestro CJ, Mariani G. Eu. J. Nucl. Med. Mol. Imaging 2004;31(11):1505.

(521). Lazzeri E, Manca M, Molea N, Marchetti S, Consoli V, Bodei L, Bianchi R, Chinol M, Paganelli G, Mariani G. Eu. J. Nucl. Med 1999;26(6):606.

(522). van Eerd JEM, Oyen WJG, Harris TD, Rennen HJJM, Edwards DS, Liu S, Ellars CE, Corstens FHM, Boerman OC. J. Nucl. Med 2003;44(7):1087. [PubMed: 12843226]

(523). Broekema M, Van Eerd JJEM, Oyen WJG, Corstens FHM, Liskamp RMJ, Boerman OC, Harris TD. J. Med. Chem 2005;48(20):6442. [PubMed: 16190770]

(524). Bhargava KK, Gupta RK, Nichols KJ, Palestro CJ. Nucl. Med. Biol 2009;36(5):545. [PubMed: 19520295]

(525). Locke LW, Chordia MD, Zhang Y, Kundu B, Kennedy D, Landseadel J, Xiao L, Fairchild KD, Berr SS, Linden J, Pan D. J. Nucl. Med 2009;50(5):790. [PubMed: 19372473]

(526). Heusch G. Br. J. Pharmacol 2008;153(8):1589. [PubMed: 18223669]

(527). Moustafa RR, Baron JC. Br. J. Pharmacol 2008;153(Suppl. 1):S44. [PubMed: 18037922]

(528). Hardee ME, Dewhirst MW, Agarwal N, Sorg BS. Curr. Mol. Med 2009;9(4):435. [PubMed: 19519401]

(529). Hwang, D-R.; Bergmann, SR. Radiopharmaceuticals for studying the heart. In: Welch, MJ.; Redvanly, CS., editors. Handbook of Radiopharmaceuticals: Radiochemistry and Applications. John Wiley & Sons Inc.; Hoboken: 2003. p. 529

(530). Keng FY. J. Ann. Acad. Med. Singapore 2004;33(2):175.

(531). Yetkin FZ, Mendelsohn D. Neuroimag. Clin. North Amer 2002;12(4):537.

(532). Hoffend J, Mier W, Schuhmacher J, Schmidt K, Dimitrakopoulou-Strauss A, Strauss LG, Eisenhut M, Kinscherf R, Haberkorn U. Nucl. Med. Biol 2005;32(3):287. [PubMed: 15820764]

(533). Kiratli PO, Tuncel M, Ozkutlu S, Caglar M. Nucl. Med. Commun 2008;29(10):907. [PubMed: 18769309]

(534). Kinuya S, Li XF, Yokoyama K, Mori H, Shiba K, Watanabe N, Shuke N, Bunko H, Michigishi T, Tonami N. Nucl. Med. Commun 2004;25(1):49. [PubMed: 15061264]

(535). Takahashi N, Fujibayashi Y, Yonekura Y, Welch MJ, Waki A, Tsuchida T, Sadato N, Sugimoto K, Nakano A, Lee JD, Itoh H. Ann. Nucl. Med 2001;15(3):293. [PubMed: 11545205]

(536). Fujibayashi Y, Cutler CS, Anderson CJ, McCarthy DW, Jones LA, Sharp T, Yonekura Y, Welch MJ. Nucl. Med. Biol 1999;26(1):117. [PubMed: 10096511]

(537). Plossl K, Chandra R, Qu W, Lieberman Brian P, Kung M-P, Zhou R, Huang B, Kung Hank F. Nucl. Med. Biol 2008;35(1):83. [PubMed: 18158947]

(538). Cutler CS, Giron MC, Reichert DE, Snyder AZ, Herrero P, Anderson CJ, Quarless DA, Koch SA, Welch MJ. Nucl. Med. Biol 1999;26(3):305. [PubMed: 10363802]

(539). Wallhaus TR, Lacy J, Stewart R, Bianco J, Green MA, Nayak N, Stone CK. J. Nucl. Cardiol 2001;8 (1):67. [PubMed: 11182711]

(540). Flower MA, Zweit J, Hall AD, Burke D, Davies MM, Dworkin MJ, Young HE, Mundy J, Ott RJ, McCready VR, Carnochan P, Allen-Mersh TG. Eu. J. Nucl. Med 2001;28(1):99.

(541). Holschneider DP, Yang J, Sadler TR, Galifianakis NB, Bozorgzadeh MH, Bading JR, Conti PS, Maarek JMI. Brain Res 2008;1234(9):32. [PubMed: 18687316]

(542). Yang DJ, Ilgan S, Higuchi T, Zareneyrizi F, Oh CS, Liu CW, Kim EE, Podoloff DA. Pharm. Res 1999;16(5):743. [PubMed: 10350019]

(543). Ito M, Yang David J, Mawlawi O, Mendez R, Oh C-S, Azhdarinia A, Greenwell AC, Yu D-F, Kim EE. Acad. Radiol 2006;13(5):598. [PubMed: 16627201]

(544). Fujibayashi Y, Taniuchi H, Yonekura Y, Ohtani H, Konishi J, Yokoyama A. J. Nucl. Med 1997;38 (7):1155. [PubMed: 9225812]

(545). Holland JP, Aigbirhio FI, Betts HM, Bonnitcha PD, Burke P, Christlieb M, Churchill GC, Cowley AR, Dilworth JR, Donnelly PS, Green JC, Peach JM, Vasudevan SR, Warren JE. Inorg. Chem 2007;46(2):465. [PubMed: 17279826]

(546). Bonnitcha PD, Vavere AL, Lewis JS, Dilworth JR. J. Med. Chem 2008;51(10):2985. [PubMed: 18416544]

(547). Barnard P, Bayly S, Betts H, Bonnitcha P, Christlieb M, Dilworth J, Holland J, Pascu S. Q. J. Nucl. Med. Mol. Imaging 2008;52(2):174. [PubMed: 18354370]

(548). Ackerman LJ, West DX, Mathias CJ, Green MA. Nucl. Med. Biol 1999;26(5):551. [PubMed: 10473194]

(549). McQuade P, Martin KE, Castle TC, Went MJ, Blower PJ, Welch MJ, Lewis JS. Nucl. Med. Biol 2005;32(2):147. [PubMed: 15721760]

(550). Cowley AR, Dilworth JR, Donnelly PS, Heslop JM, Ratcliffe SJ. Dalton Trans 2007;2:209. [PubMed: 17180189]

(551). Cowley AR, Dilworth JR, Donnelly PS, White JM. Inorg. Chem 2006;45(2):496. [PubMed: 16411680]

(552). Cowley AR, Dilworth JR, Donnelly PS, Gee AD, Heslop JM. Dalton Trans 2004;16:2404. [PubMed: 15303151]

(553). Blower PJ, Castle TC, Cowley AR, Dilworth JR, Donnelly PS, Labisbal E, Sowrey FE, Teat SJ, Went MJ. Dalton Trans 2003;23:4416.

(554). Castle TC, Maurer RI, Sowrey FE, Went MJ, Reynolds CA, McInnes EJL, Blower PJ. J. Am. Chem. Soc 2003;125(33):10040. [PubMed: 12914467]

(555). Maurer RI, Blower PJ, Dilworth JR, Reynolds CA, Zheng Y, Mullen GED. J. Med. Chem 2002;45 (7):1420. [PubMed: 11906283]

(556). Dearling JLJ, Lewis JS, Mullen GED, Welch MJ, Blower PJ. J. Biol. Inorg. Chem 2002;7(3):249. [PubMed: 11935349]

(557). Burgman P, O'Donoghue JA, Lewis JS, Welch MJ, Humm JL, Ling CC. Nucl. Med. Biol 2005;32 (6):623. [PubMed: 16026709]

(558). Laforest R, Dehdashti F, Lewis JS, Schwarz SW. Eu. J. Nucl. Med. Mol. Imaging 2005;32(7):764.

(559). Lewis JS, McCarthy DW, McCarthy TJ, Fujibayashi Y, Welch MJ. J. Nucl. Med 1999;40(1):177. [PubMed: 9935074]

(560). Yuan H, Schroeder T, Bowsher JE, Hedlund LW, Wong T, Dewhirst MW. J. Nucl. Med 2006;47 (6):989. [PubMed: 16741309]

(561). Obata A, Yoshimoto M, Kasamatsu S, Naiki H, Takamatsu S, Kashikura K, Furukawa T, Lewis JS, Welch MJ, Saji H, Yonekura Y, Fujibayashi Y. Nucl. Med. Biol 2003;30(5):529. [PubMed: 12831991]

(562). Dehdashti F, Mintun MA, Lewis JS, Bradley J, Govindan R, Laforest R, Welch MJ, Siegel BA. Eu. J. Nucl. Med. Mol. Imaging 2003;30(6):844.

(563). Dehdashti F, Grigsby PW, Mintun MA, Lewis JS, Siegel BA, Welch MJ. Int. J. Radiat. Oncol. Biol. Phys 2003;55(5):1233. [PubMed: 12654432]

(564). Dehdashti F, Grigsby PW, Lewis JS, Laforest R, Siegel BA, Welch MJ. J. Nucl. Med 2008;49(2): 201. [PubMed: 18199612]

(565). Grigsby PW, Malyapa RS, Higashikubo R, Schwarz JK, Welch MJ, Huettner PC, Dehdashti F. Mol. Imaging Biol 2007;9(5):278. [PubMed: 17431727]

(566). Lewis JS, Laforest R, Dehdashti F, Grigsby PW, Welch MJ, Siegel BA. J. Nucl. Med 2008;49(7): 1177. [PubMed: 18552145]

(567). Lewis JS, Connett JM, Garbow JR, Buettner TL, Fujibayashi Y, Fleshman JW, Welch MJ. Cancer Res 2002;62(2):445. [PubMed: 11809694]

(568). Aft RL, Lewis JS, Zhang F, Kim J, Welch MJ. Cancer Res 2003;63(17):5496. [PubMed: 14500386]

(569). Lewis JS, Laforest R, Buettner TL, Song SK, Fujibayashi Y, Connett JM, Welch MJ. Proc. Natl. Acad. Sci. U.S.A 2001;98(3):1206. [PubMed: 11158618]

(570). Obata A, Kasamatsu S, Lewis JS, Furukawa T, Takamatsu S, Toyohara J, Asai T, Welch MJ, Adams SG, Saji H. Nucl. Med. Biol 2005;32(1):21. [PubMed: 15691658]

(571). Lewis JS, Dearling JLJ, Sosabowski JK, Zweit J, Carnochan P, Kelland LR, Coley HM, Blower PJ. Eu. J. Nucl. Med 2000;27(6):638.

(572). Black NF, McJames S, Rust TC, Kadrmas DJ. Phys.Med. Biol 2008;53(1):217. [PubMed: 18182698]

(573). Green MA, Mathias CJ, Willis LR, Handa RK, Lacy JL, Miller MA, Hutchins GD. Nucl. Med. Biol 2007;34(3):247. [PubMed: 17383574]

(574). Wei L, Easmon J, Nagi RK, Muegge BD, Meyer LA, Lewis JS. J. Nucl. Med 2006;47(12):2034. [PubMed: 17138747]

(575). Vavere AL, Lewis JS. Nucl. Med. Biol 2008;35(3):273. [PubMed: 18355682]

(576). Lewis JS, Sharp TL, Laforest R, Fujibayashi Y, Welch MJ. J. Nucl. Med 2001;42(4):655. [PubMed: 11337556]

(577). Dence CS, Ponde DE, Welch MJ, Lewis JS. Nucl. Med. Biol 2008;35(6):713. [PubMed: 18678357]

(578). Lederer, CM.; Shirley, VS., editors. Table of Isotopes. 7 ed.. John Wiley & Sons; New York: 1978.

(579). Shannon RD. Acta Crystallogr., Sect. A 1976;A32(5):751.

(580). Baes, CF., Jr.; Mesmer, RE. The Hydrolysis of Cations. Wiley-Interscience; New York: 1976.

(581). Martell, AE.; Smith, RM. Critical Stability Constants, Vol. 3: Other Organic Ligands. Plenum Press; New York: 1977.

(582). Wulfsberg, G. Inorganic Chemistry. University Science Books; Sausalito: 2000.

(583). Douglas, B.; McDaniel, D.; Alexander, J. Concepts and Models of Inorganic Chemistry. Third ed.. John Wiley & Sons; New York: 1994.

(584). Hancock RD, McDougall GJ. J. Am. Chem. Soc 1980;102(21):6551.

(585). Hancock RD, McDougall GJ. Adv. Mol. Relaxation Interact. Processes 1980;18(2):99.

(586). Martell, AE.; Hancock, RD. Metal Complexes in Aqueous Solutions. Plenum Press; New York: 1996.

(587). Martell, AE.; Smith, RM. Editors Critical Stability Constants, Vol. 1: Amino Acids. Plenum Press; New York: 1974.

(588). Delgado R, De Carmo FM, Quintino S. Talanta 1997;45(2):451. [PubMed: 18967026]

(589). Martell, AE.; Smith, RM. Critical Stability Constants. Plenum Press; New York: 1982.

(590). Bleiholder C, Boerzel H, Comba P, Ferrari R, Heydt M, Kerscher M, Kuwata S, Laurenczy G, Lawrance GA, Lienke A, Martin B, Merz M, Nuber B, Pritzkow H. Inorg. Chem 2005;44(22):8145. [PubMed: 16241165]

(591). Bevilacqua A, Gelb RI, Hebard WB, Zompa LJ. Inorg. Chem 1987;26(16):2699.

(592). Garcia, E. Synthesis of TACN-derived Chelators and Studies of their Metal Complexes. University of New Hampshire; Durham, NH: 2009. Unpublished work

(593). Smith, RM.; Martell, AE. Critical Stability Contants. Plenum Press; New York: 1989.

(594). Delgado R, Frausto da Silva JJR. Talanta 1982;29(10):815. [PubMed: 18963244]

(595). Chaves S, Delgado R, Dasilva JJRF. Talanta 1992;39(3):249. [PubMed: 18965370]

(596). Sun X, Wuest M, Weisman GR, Wong EH, Reed DP, Boswell CA, Motekaitis R, Martell AE, Welch MJ, Anderson CJ. J. Med. Chem 2002;45(2):469. [PubMed: 11784151]

(597). Delgado R, Sun Y, Motekaitis RJ, Martell AE. Inorg. Chem 1993;32(15):3320.

(598). Motekaitis RJ, Sun Y, Martell AE, Welch MJ. Inorg. Chem 1991;30(13):2737.

(599). Evers A, Hancock RD, Martell AE, Motekaitis RJ. Inorg. Chem 1989;28(11):2189.

(600). Bottari E, Anderegg G. Helv. Chim. Acta 1967;50(8):2349.

(601). Kumar K, Chang CA, Francesconi LC, Dischino DD, Malley MF, Gougoutas JZ, Tweedle MF. Inorg. Chem 1994;33(16):3567.

(602). Koudelkova M, Vinsova H, Jedinakova-Krizova V. Czech. J. Phys 2003;53(Suppl. A, Pt. 2):A769.

(603). Lovqvist A, Humm JL, Sheikh A, Finn RD, Koziorowski J, Ruan S, Pentlow KS, Jungbluth A, Welt S, Lee FT, Brechbiel MW, Larson SM. J. Nucl. Med 2001;42(8):1281. [PubMed: 11483692]

(604). Dimitrakopoulou-Strauss A, Hohenberger P, Haberkorn U, Macke HR, Eisenhut M, Strauss LG. J. Nucl. Med 2007;48(8):1245. [PubMed: 17631559]

(605). Asti M, De Pietri G, Fraternali A, Grassi E, Sghedoni R, Fioroni F, Roesch F, Versari A, Salvo D. Nucl. Med. Biol 2008;35(6):721. [PubMed: 18678358]

(606). Hofmann M, Weitzel T, Krause T. Nucl. Instrum. Methods Phys. Res., Sect. A 2006;569(2):522.

(607). van Eerd JEM, Oyen WJG, Harris TD, Rennen HJJM, Edwards DS, Corstens FHM, Boerman OC. J. Nucl. Med 2005;46(5):786. [PubMed: 15872352]

(608). Xu H, Baidoo K, Gunn AJ, Boswell CA, Milenic DE, Choyke PL, Brechbiel MW. J. Med. Chem 2007;50(19):4759. [PubMed: 17725340]

(609). Li WP, Lewis JS, Srinivasan A, Schmidt MA, Anderson CJ. J. Labeled Compd. Radiopharm 2001;44(suppl. 1):S948.

(610). Lewis JS, Lewis MR, Srinivasan A, Schmidt MA, Wang J, Anderson CJ. J. Med. Chem 1999;42 (8):1341. [PubMed: 10212119]

(611). Wadas TJ, Anderson CJ. Nat. Protoc 2006;1(6):3062. [PubMed: 17406569]

(612). Liu Z, Yan Y, Liu S, Wang F, Chen X. Bioconjugate Chem 2009;20(5):1016.

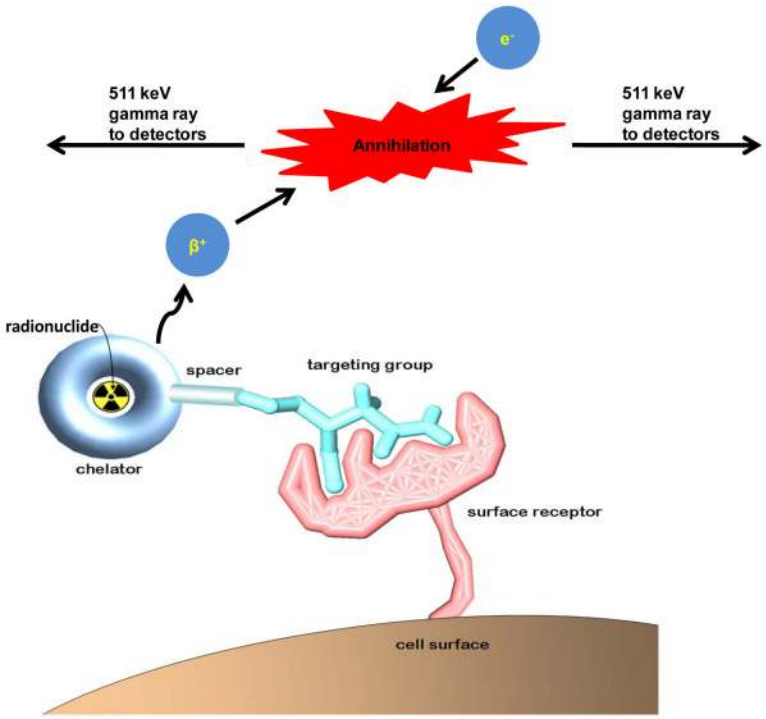

Figure 1.

Cartoon depicting the fundamental principle of Positron Emission Tomography (PET). As the targeting group interacts with the cell surface receptor, the positron emitting radio-metal decays by ejecting β^+ particles from its nucleus. After traveling a short distance in the electron rich tissue, the positron recombines with an electron in a process called annihilation. During annihilation, the mass of the positron and electron are converted into two high energy photons (511 keV gamma rays), which are released approximately 180° apart to ensure that energy and momentum are conserved. Although attenuation is possible, these two gamma rays are usually energetic enough to escape the organism and be collected by the detectors of a PET scanner.

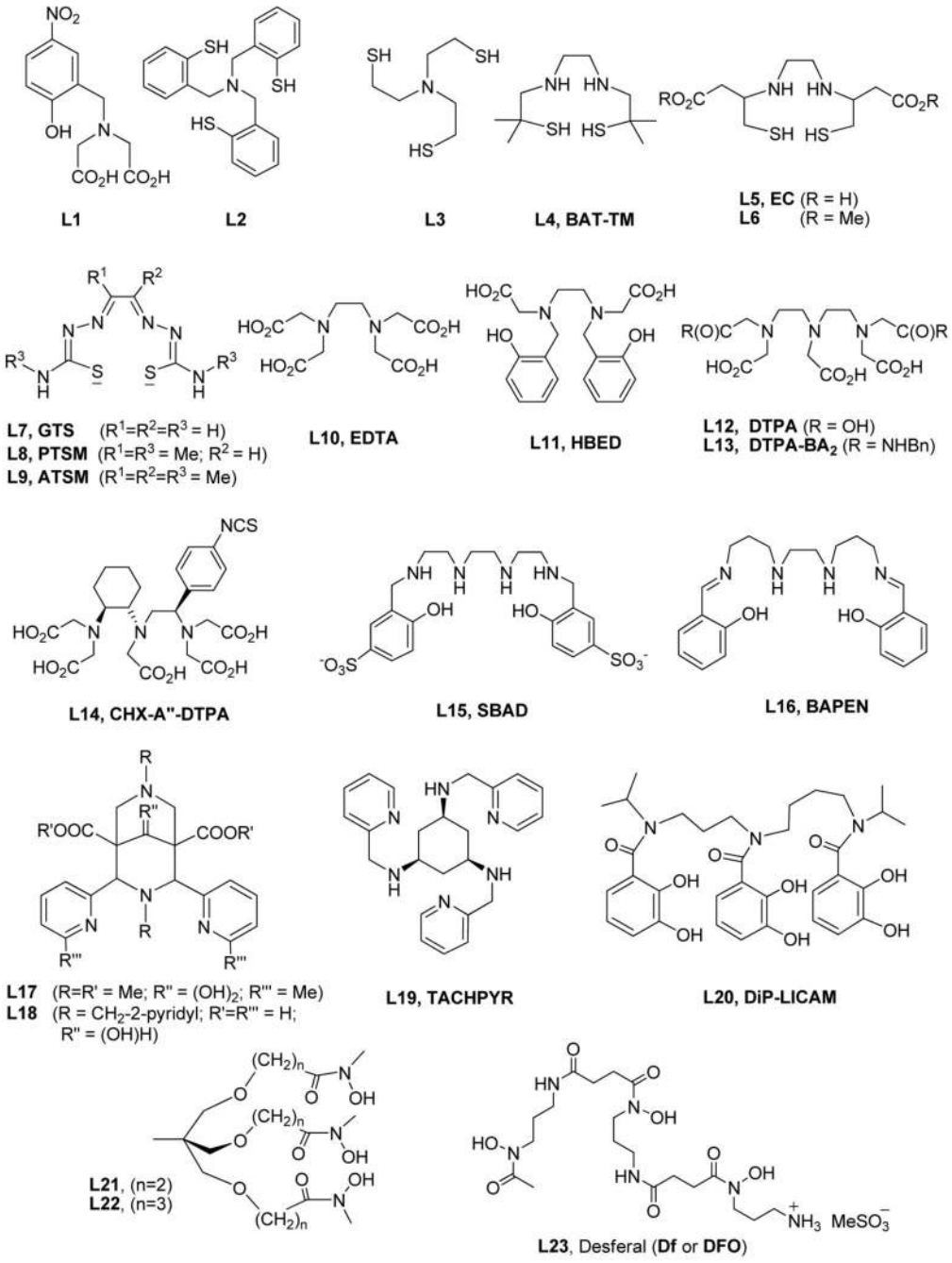

Figure 2.
Selected acyclic chelators

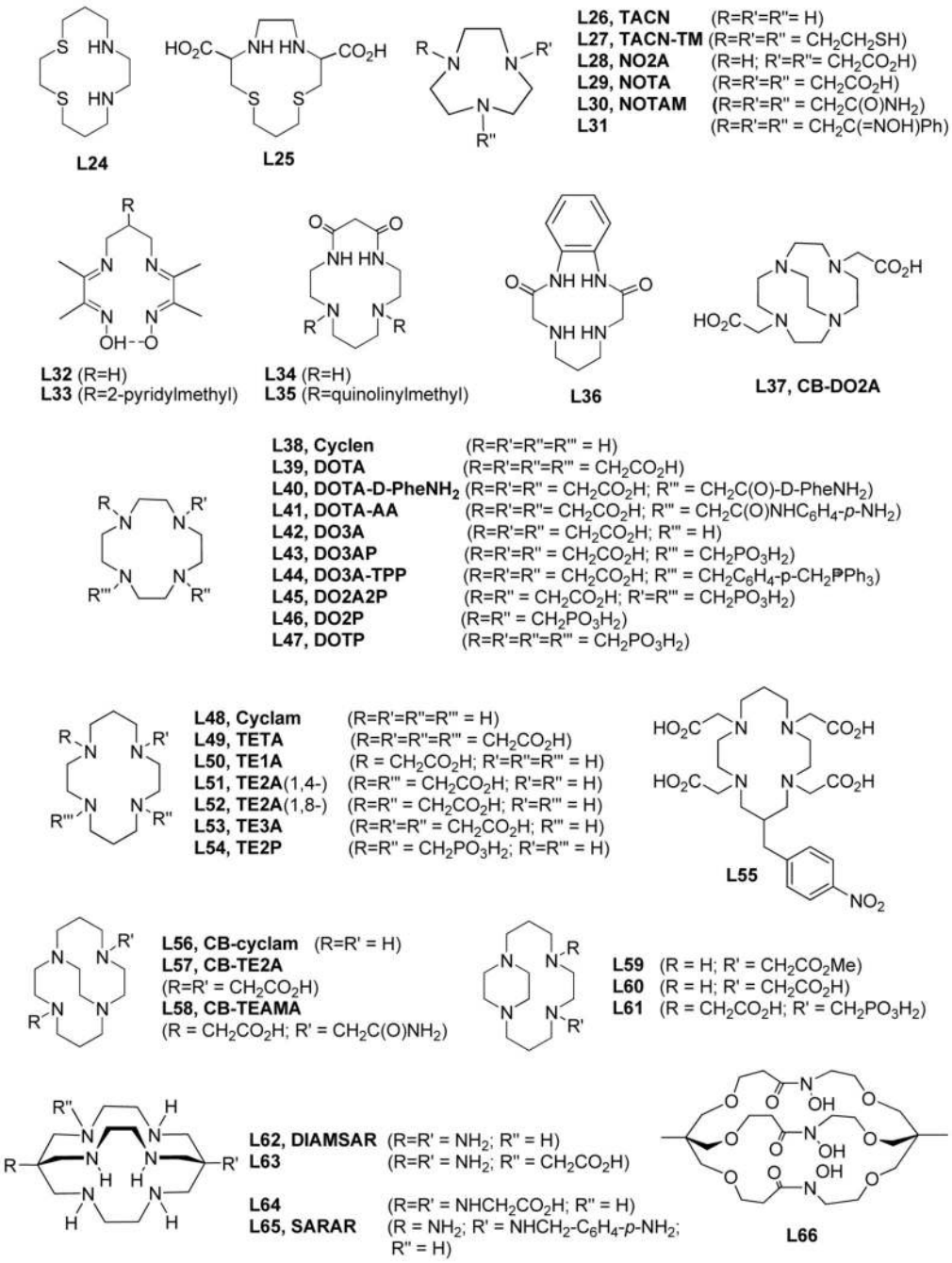

Figure 3.
Selected macrocyclic chelators

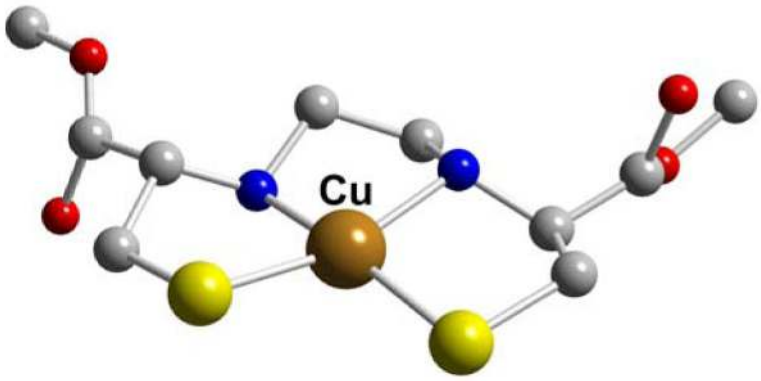

Figure 4.
Cu-**L6**

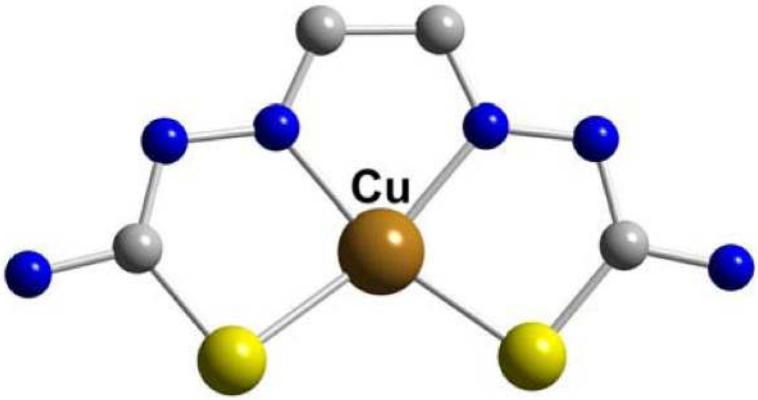

Figure 5.
Cu-**GTS** (**L7**)

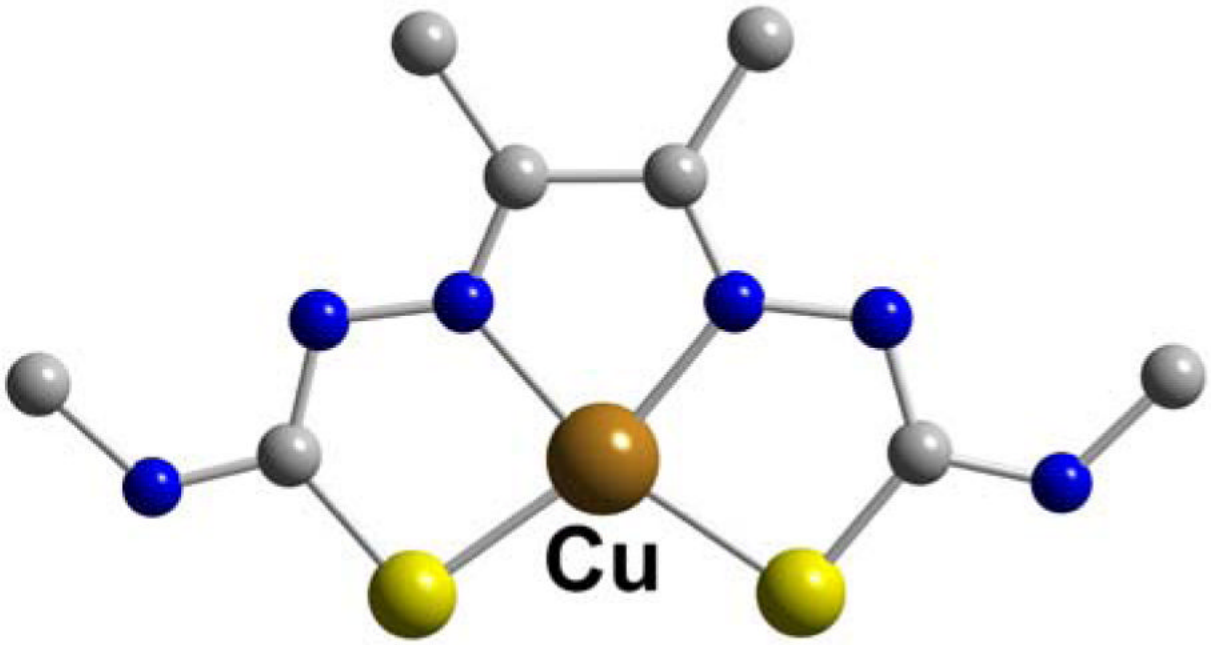

Figure 6.
Cu-**PTSM** (**L8**)

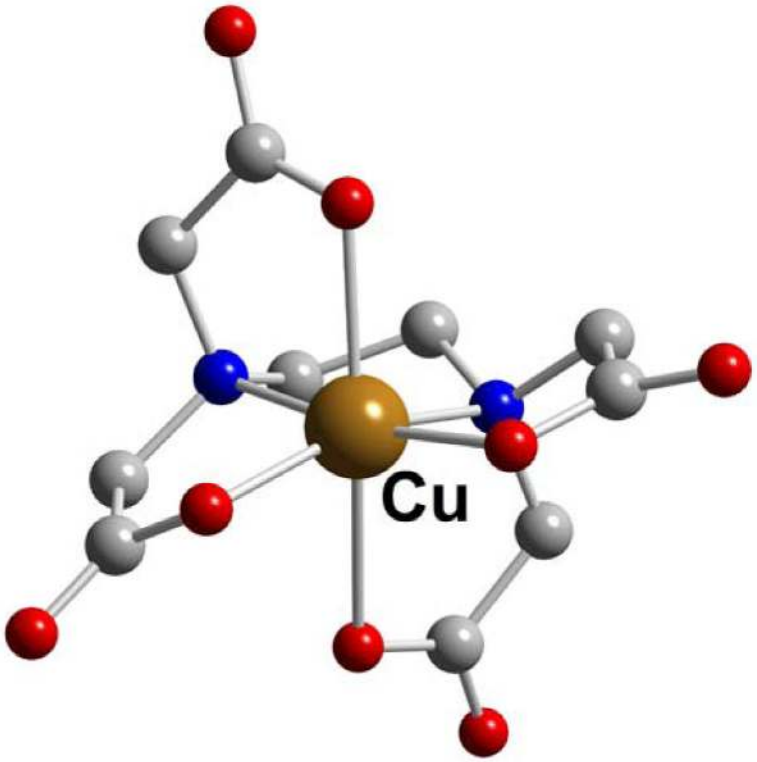

Figure 7.
Cu-**EDTA** (**L10**)

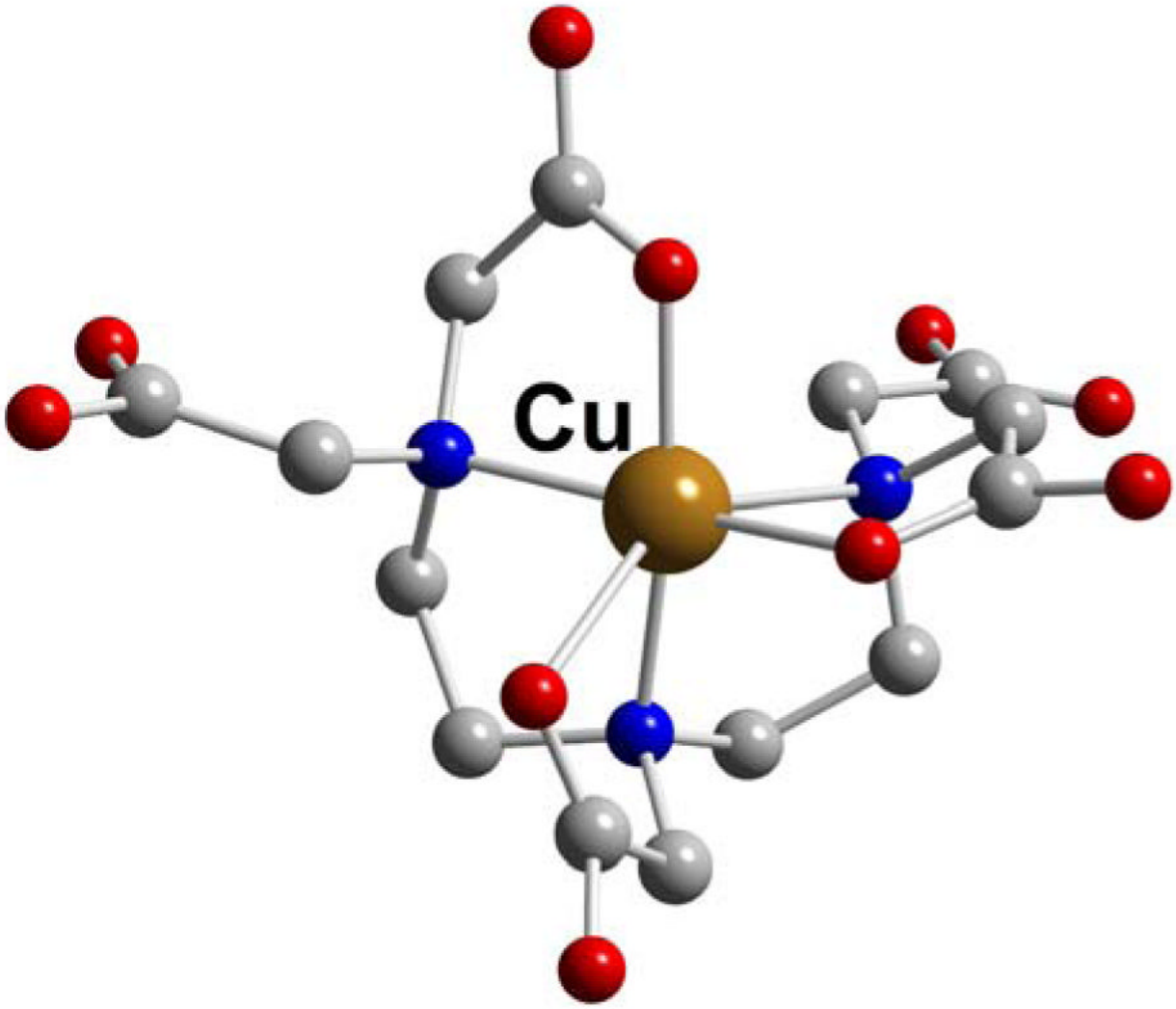

Figure 8.
Cu-**DTPA** (**L12**)

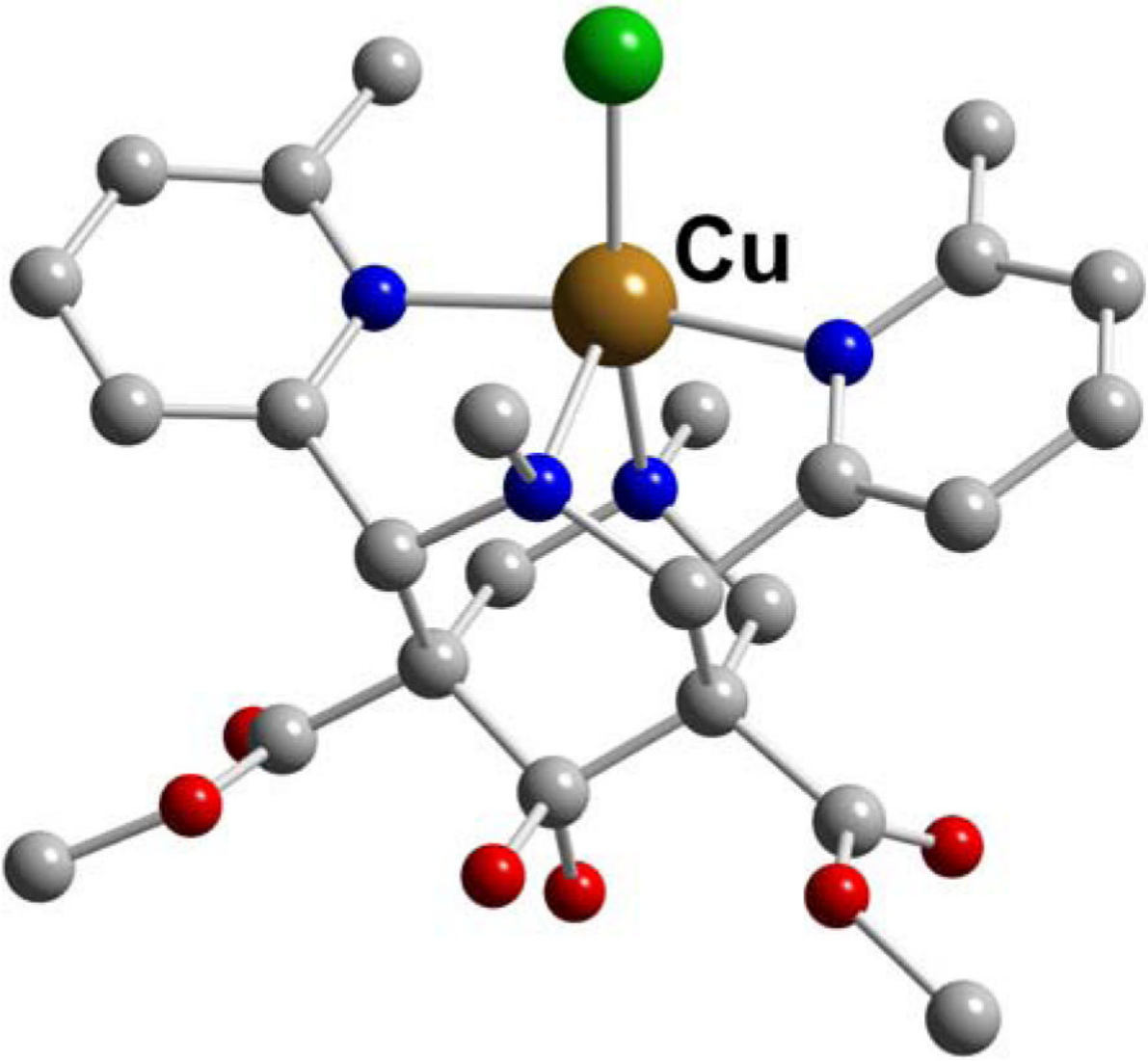

Figure 9.
Cu-**L17**

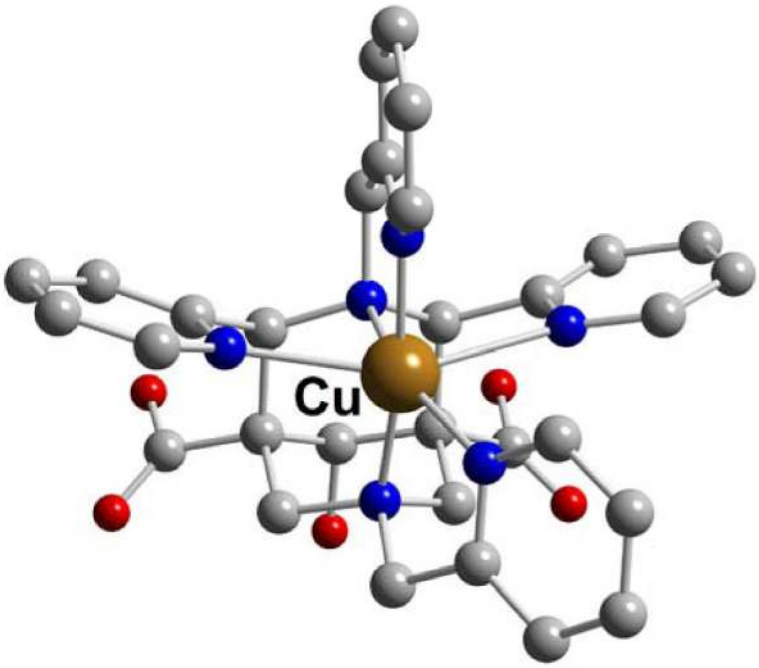

Figure 10.
Cu-**L18**

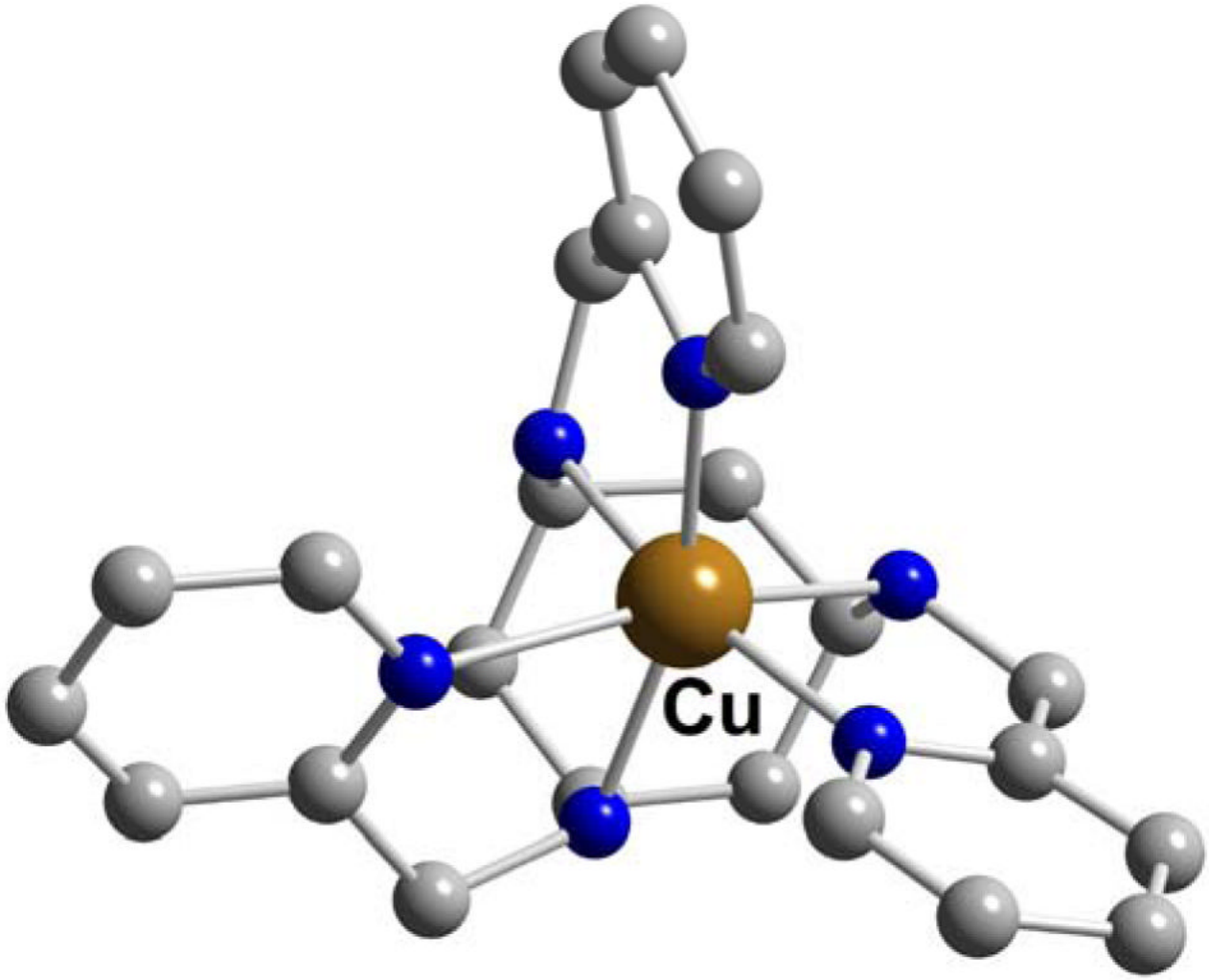

Figure 11.
Cu-**TACHPYR** (**L19**)

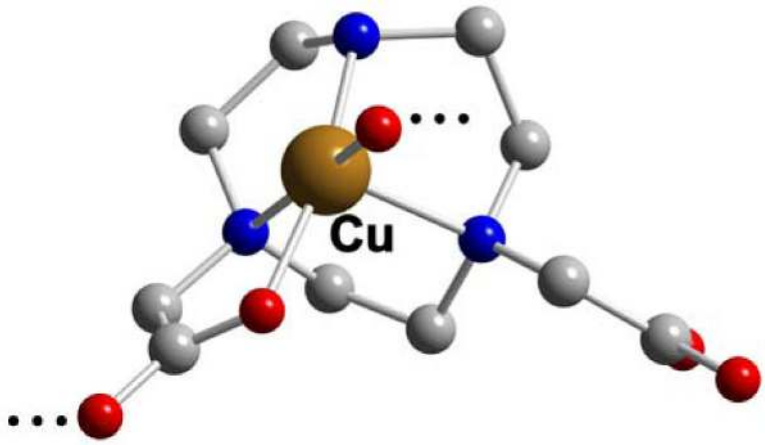

Figure 12.
Cu-**NO2A** (**L28**)

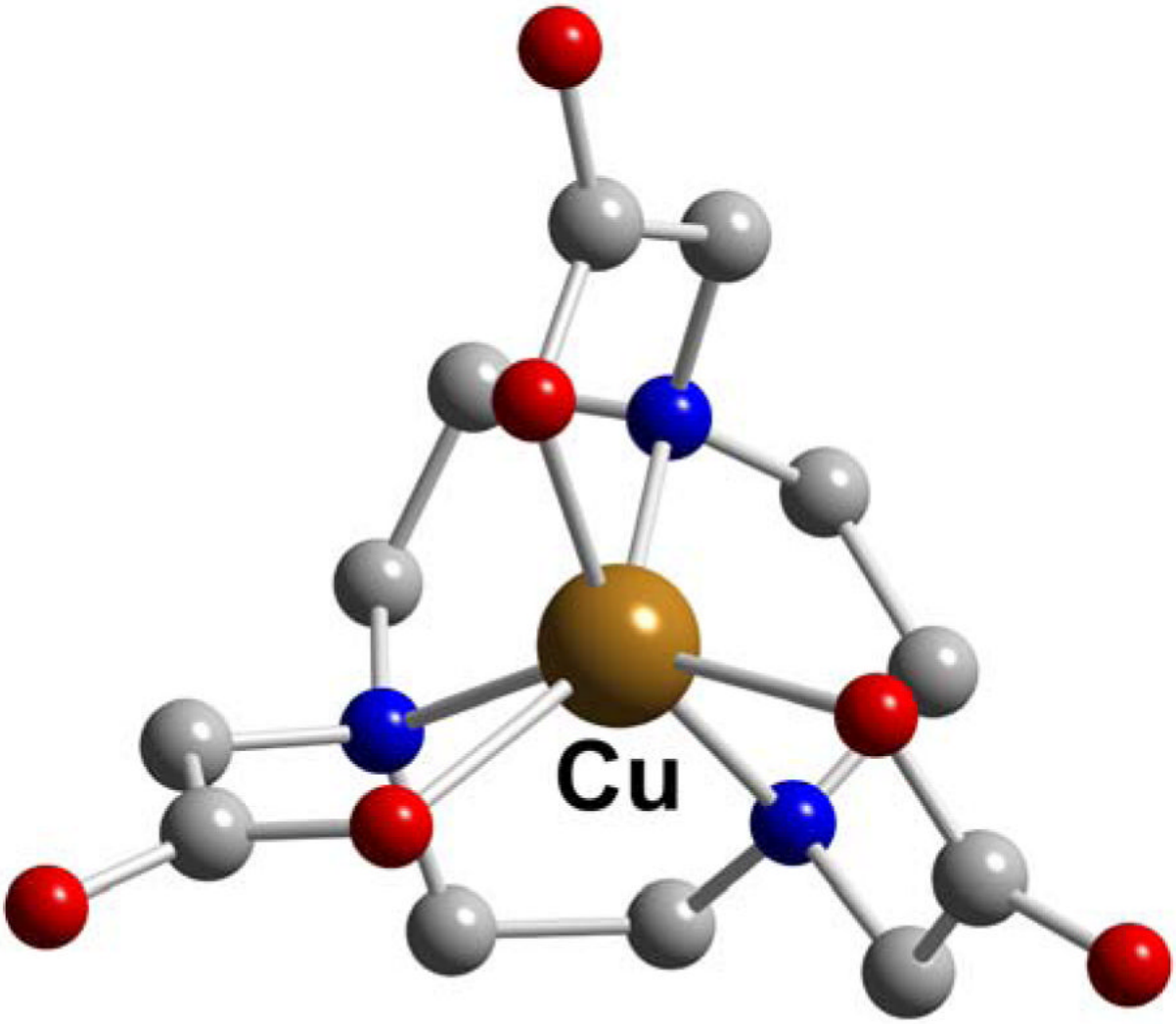

Figure 13.
Cu-**NOTA** (**L29**)

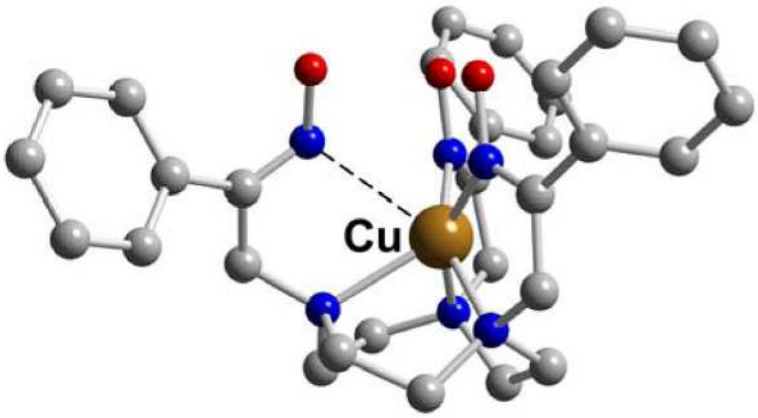

Figure 14.
Cu-**NOTAM (L30)**

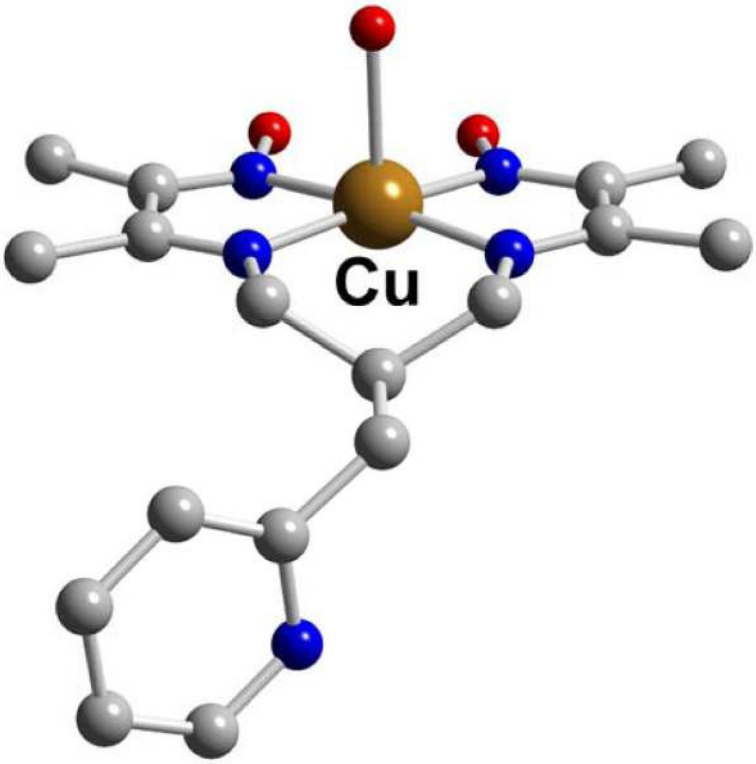

Figure 15.
Cu-**L33**

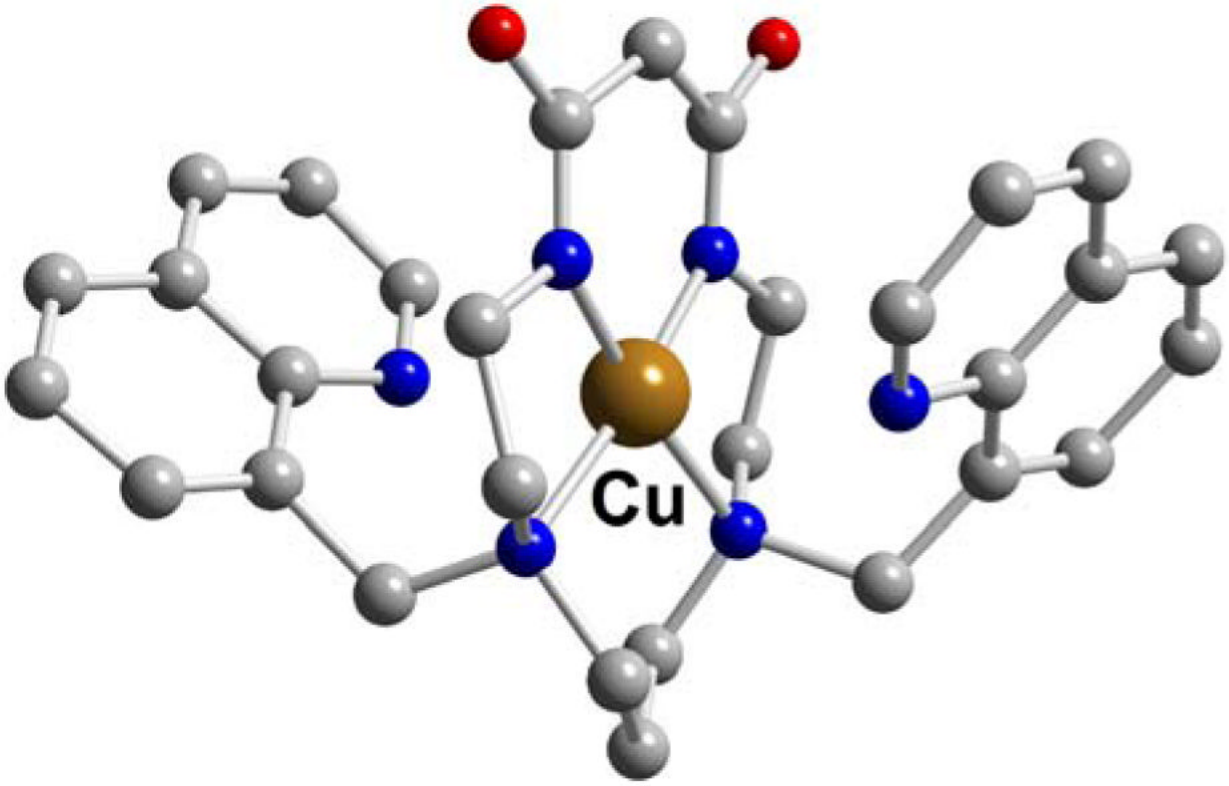

Figure 16.
Cu-**L35**

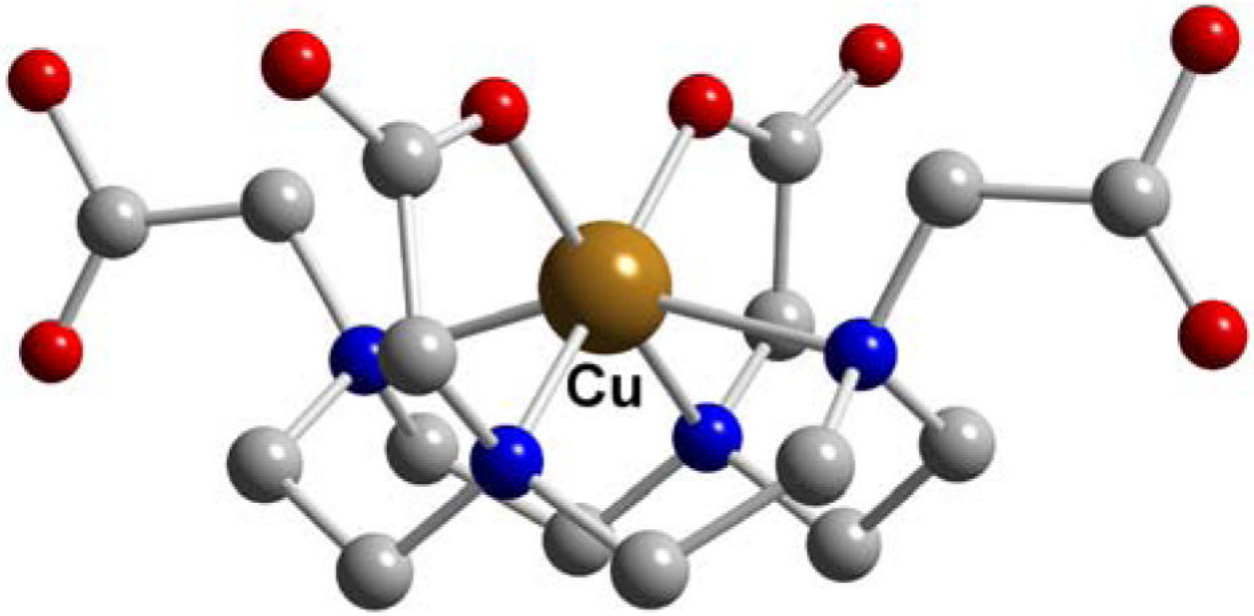

Figure 17.
Cu-**DOTA** (**L39**)

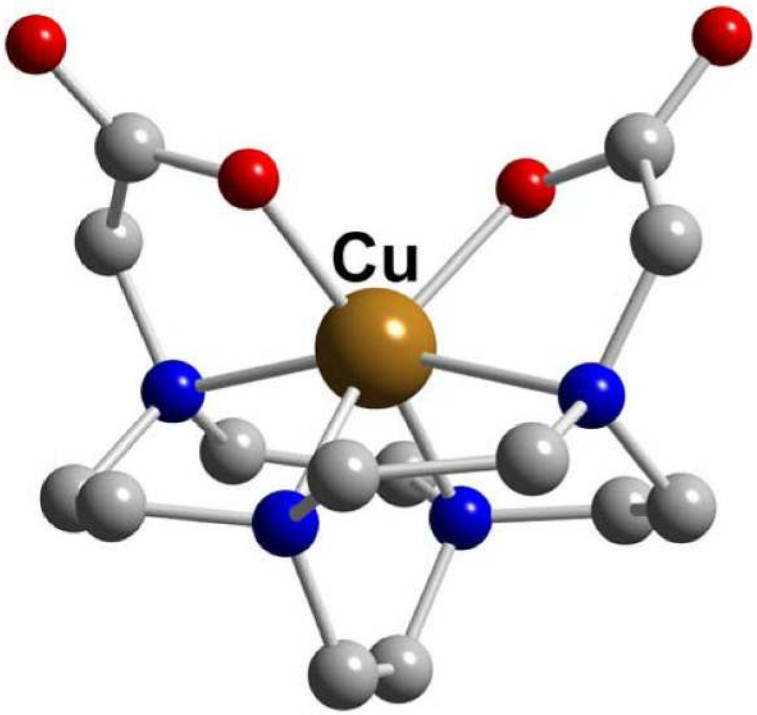

Figure 18.
Cu-**CB-DO2A** (**L37**)

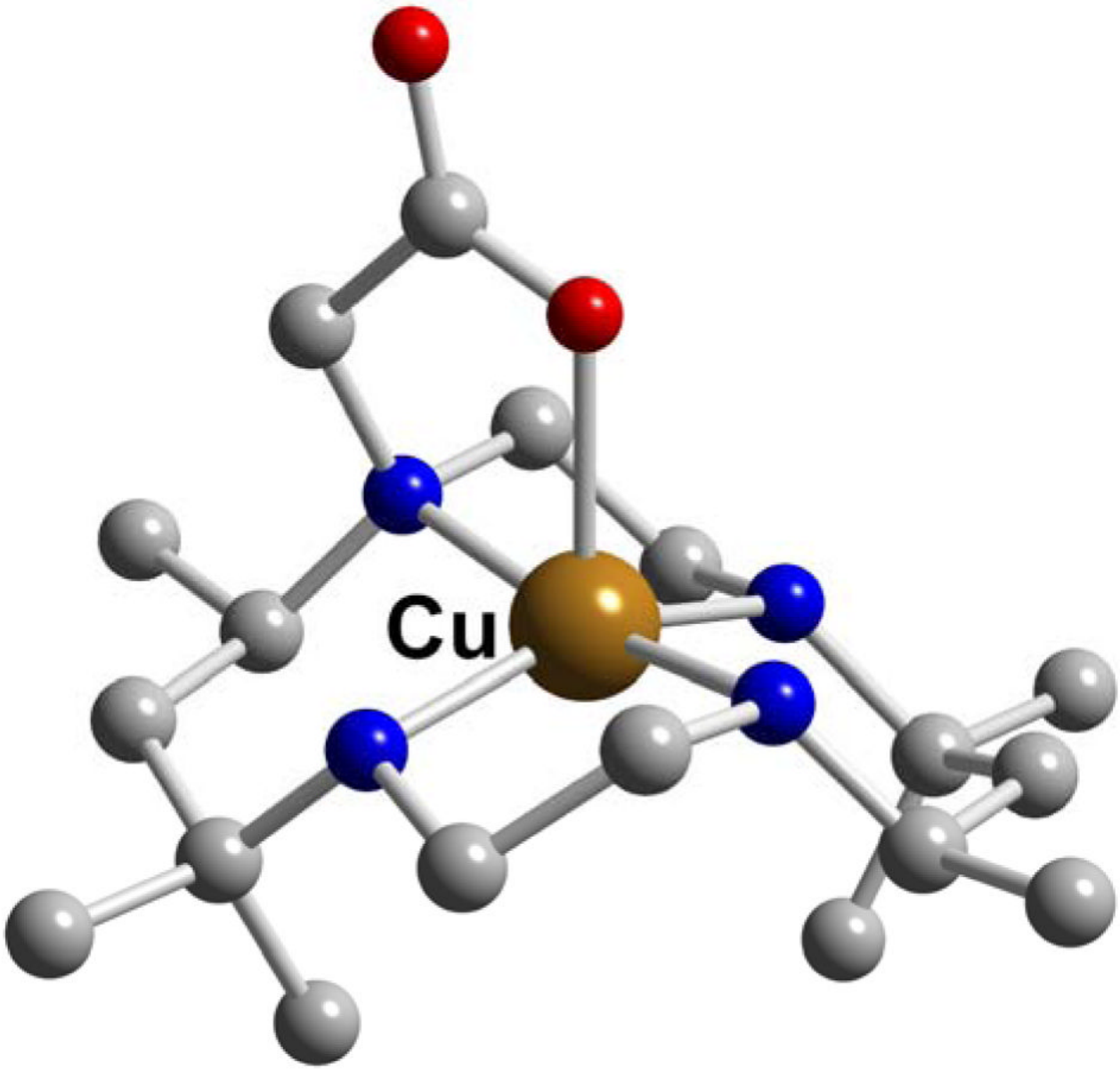

Figure 19.
Cu-**TE1A (L50)**

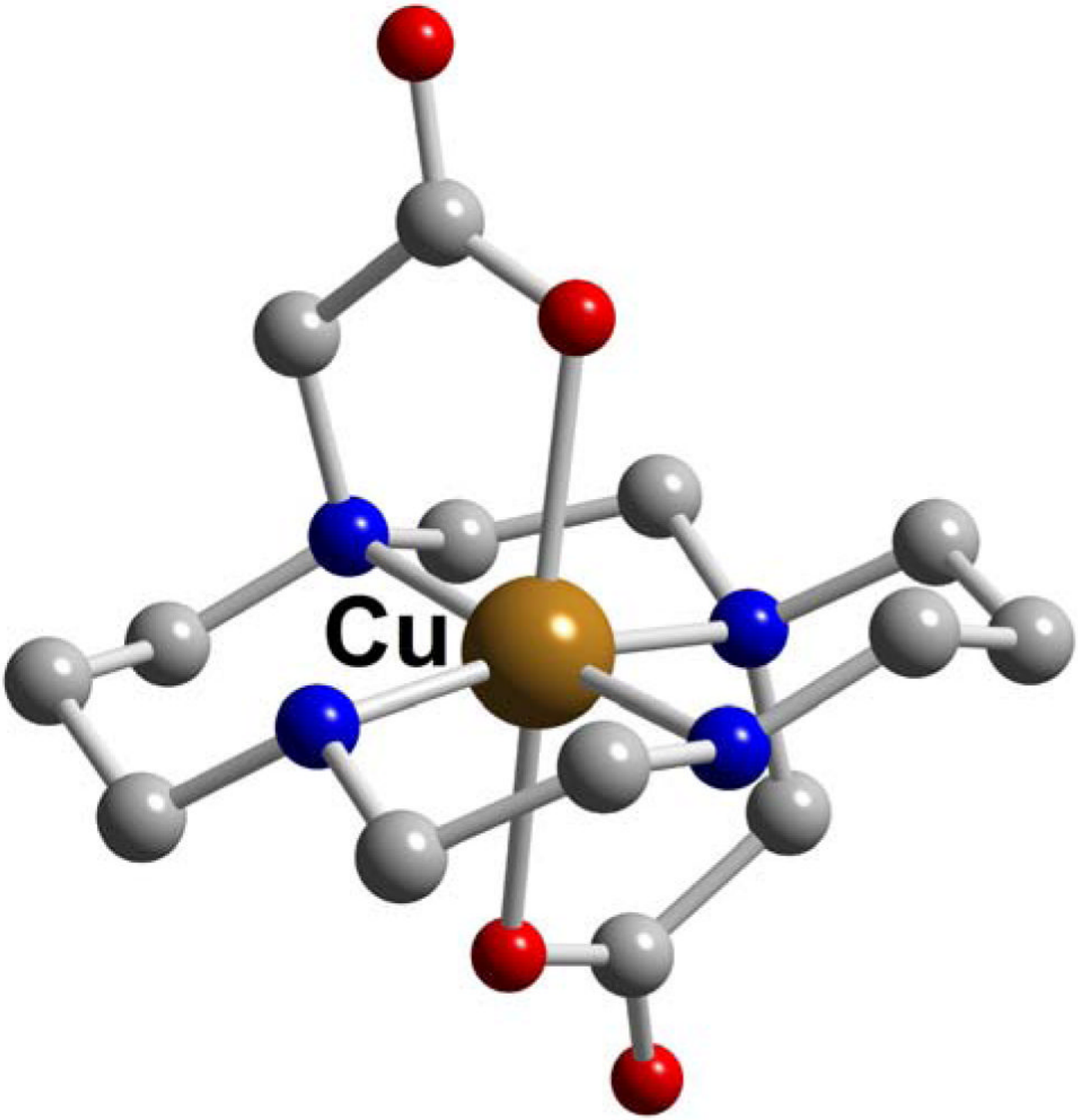

Figure 20.
Cu-**L51**

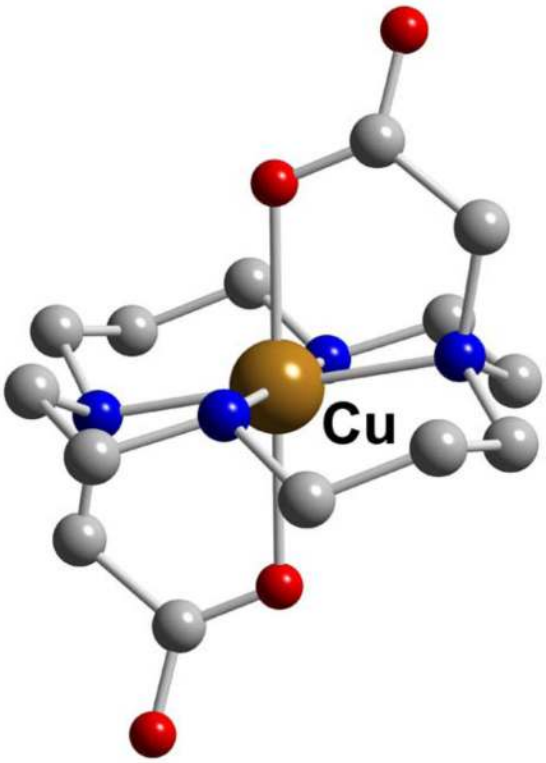

Figure 21.
Cu-**L52**

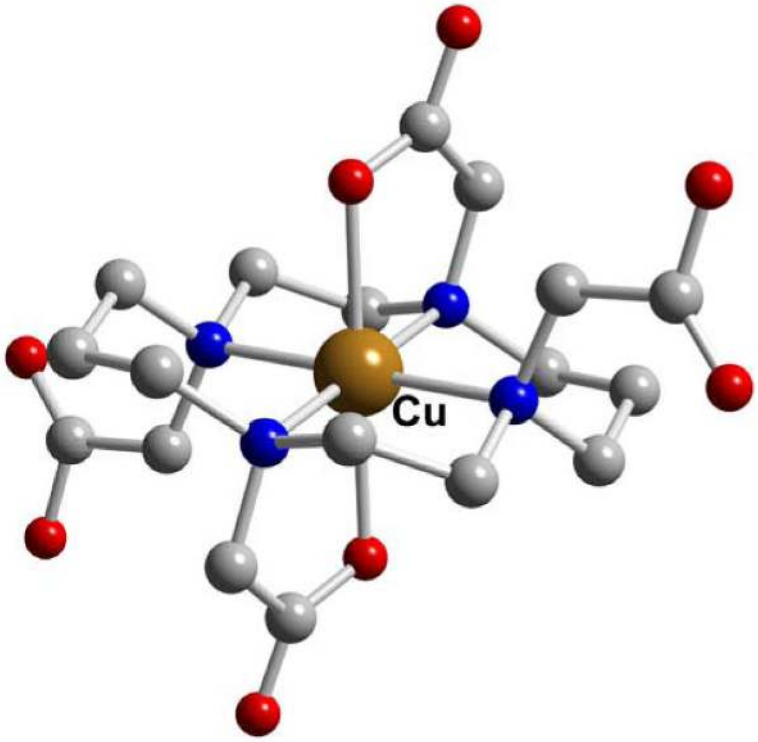

Figure 22.
Cu-H_2**TETA** (**L49**)

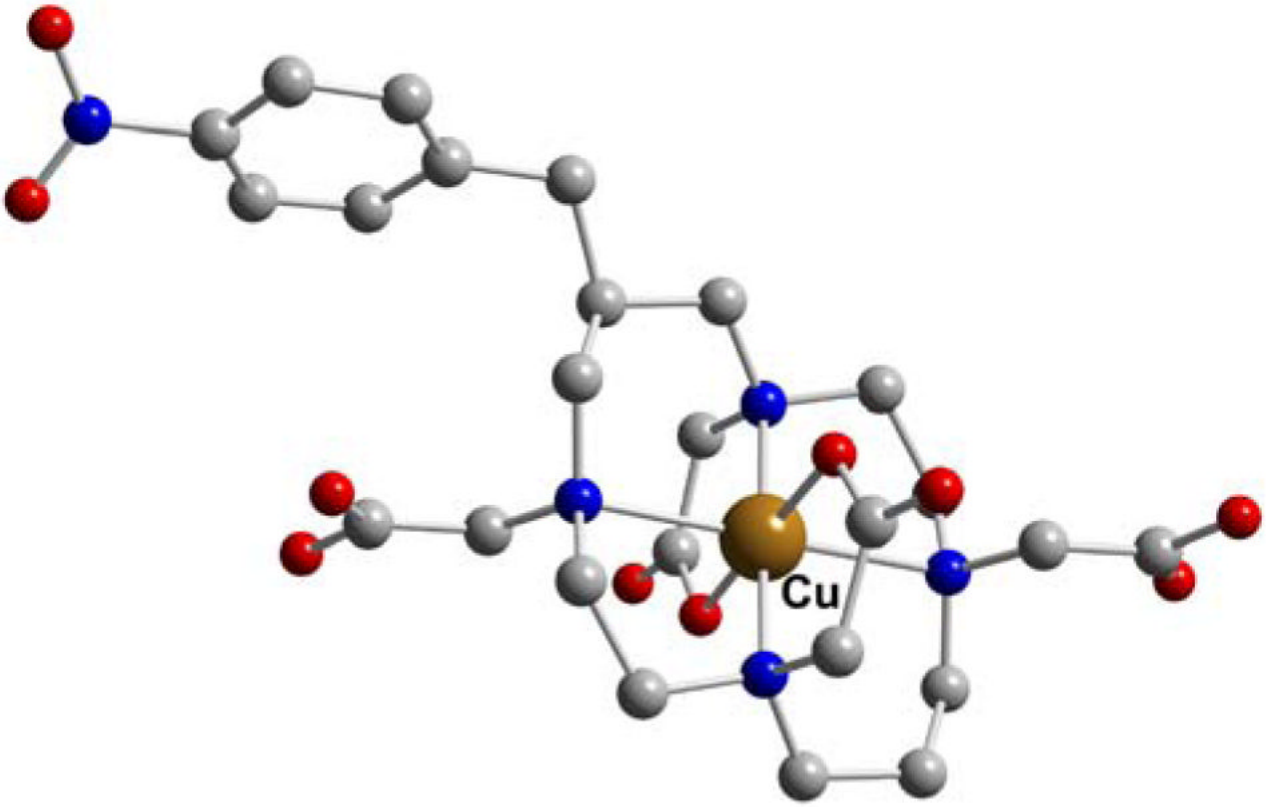

Figure 23.
Cu-**L55**

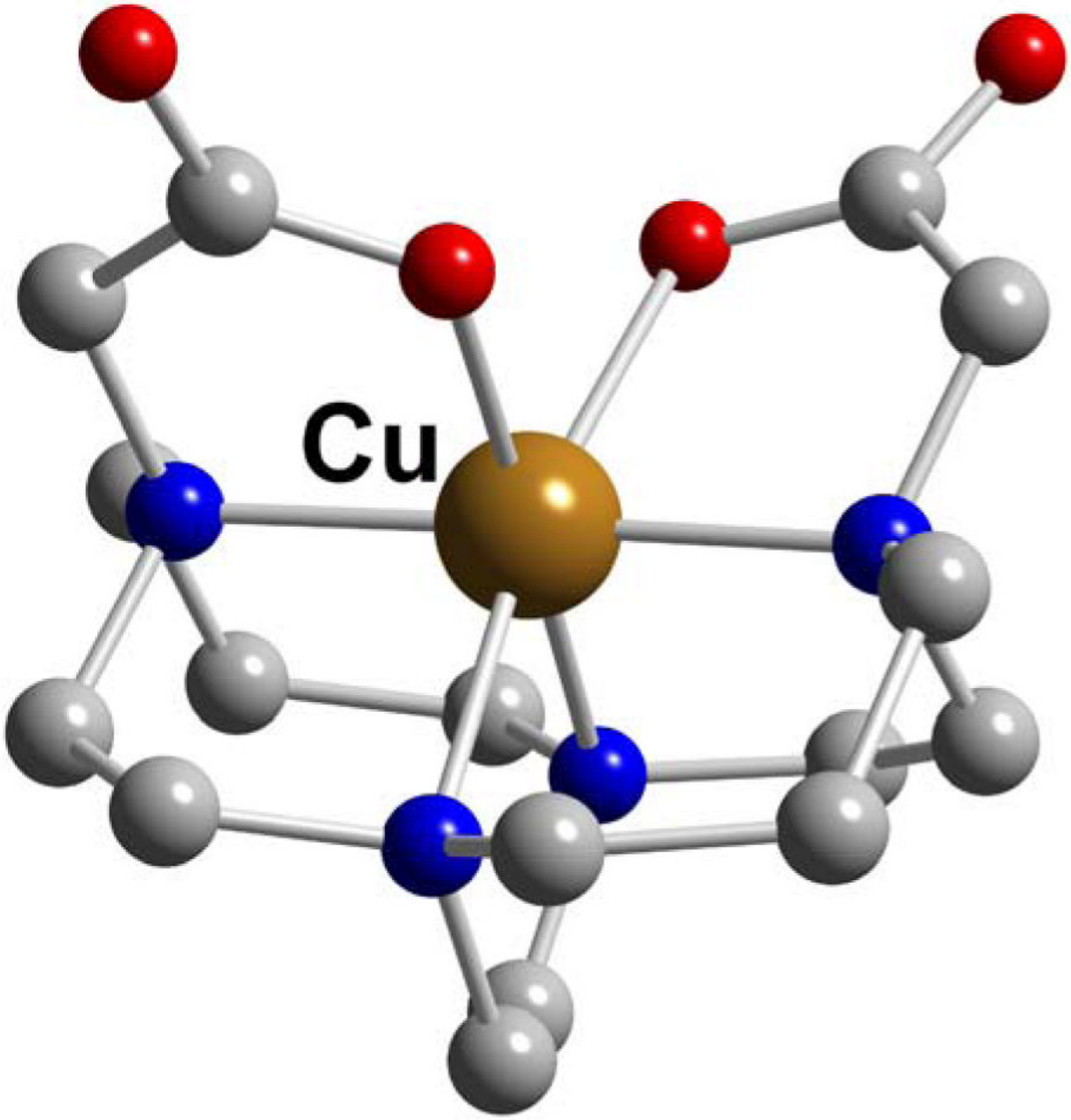

Figure 24.
Cu-**CB-TE2A** (**L57**)

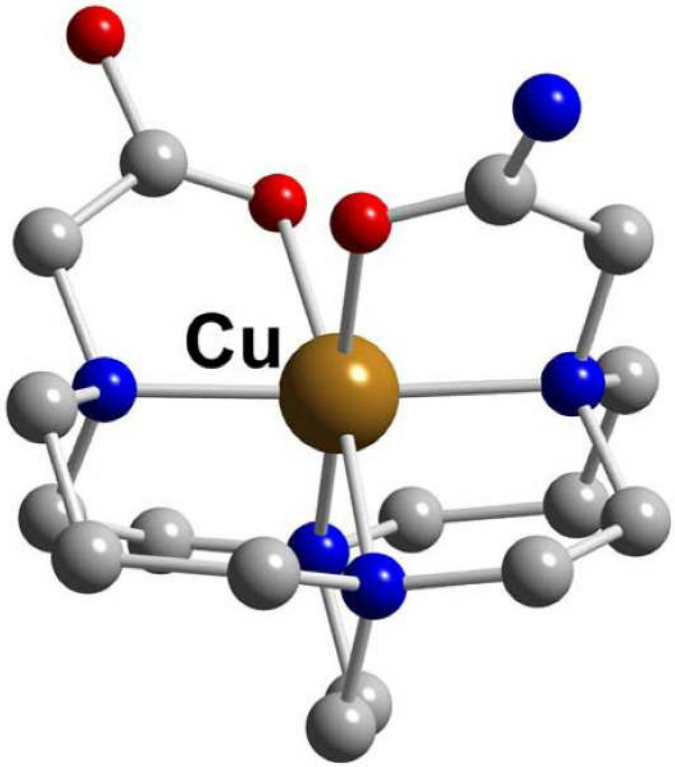

Figure 25.
Cu-**CB-TEAMA** (**L58**)

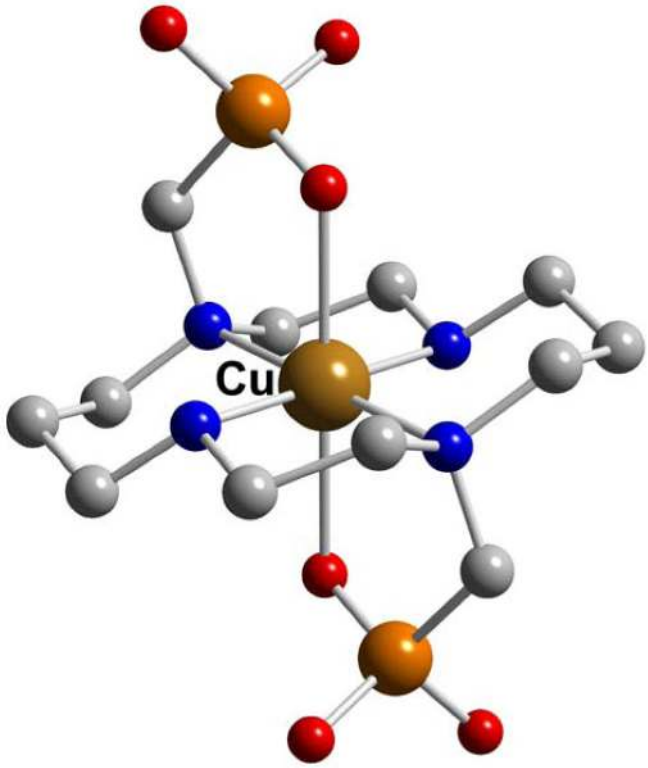

Figure 26.
Cu-**TE2P** (**L54**)

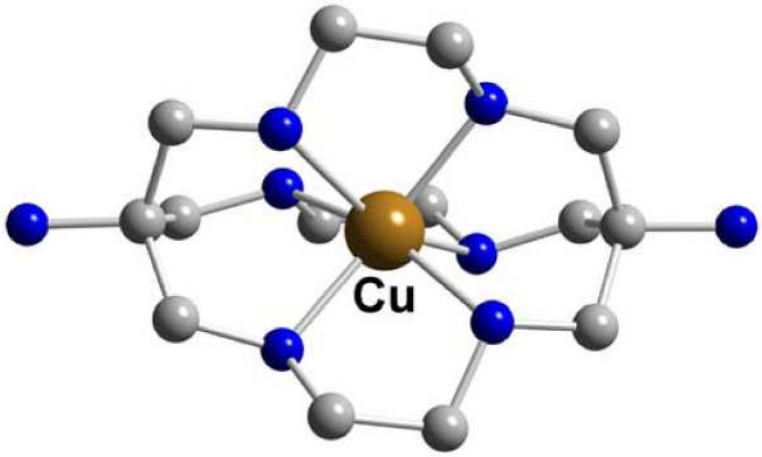

Figure 27.
Cu-**L62**

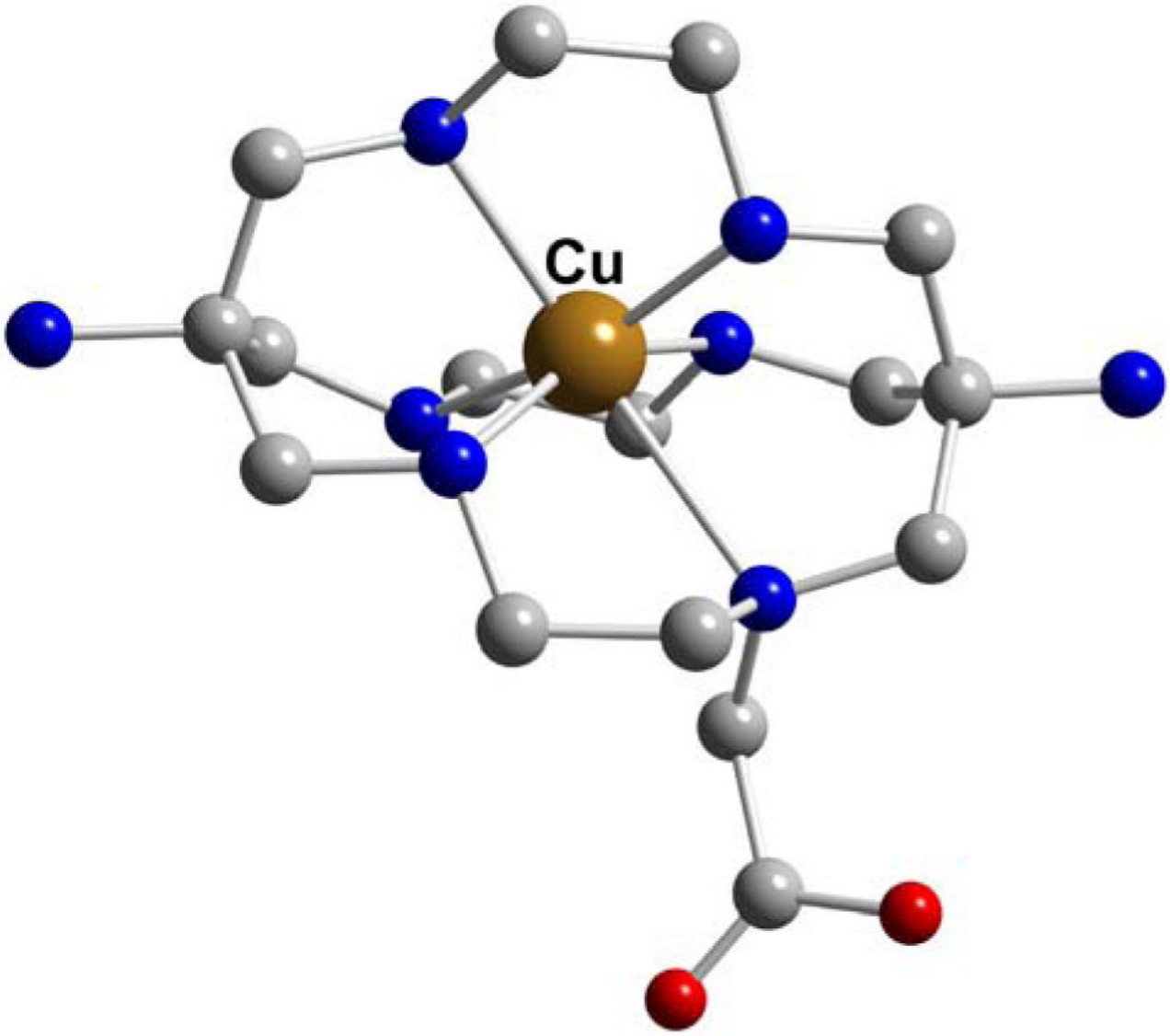

Figure 28.
Cu-**L63**

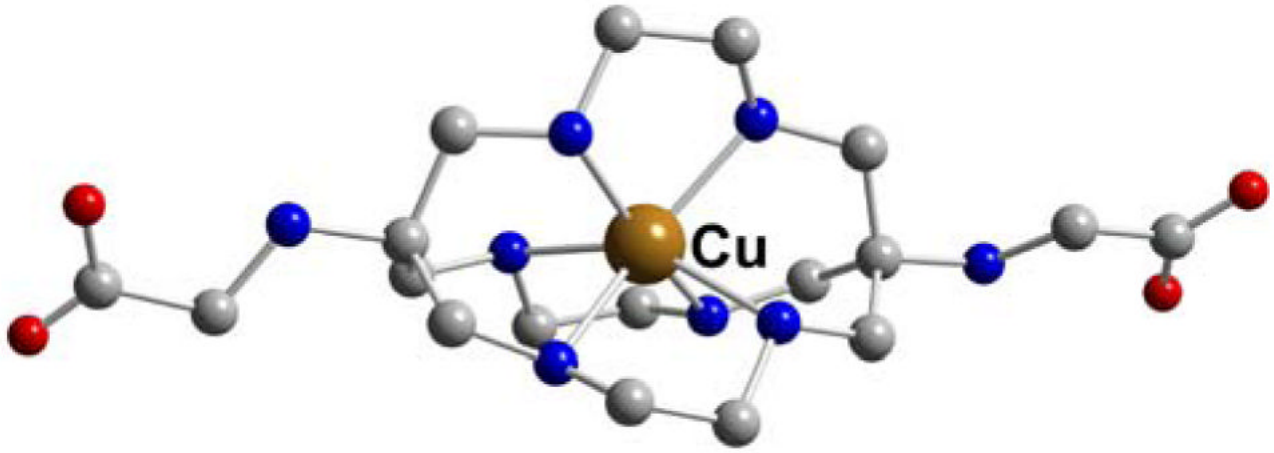

Figure 29.
Cu-**L64**

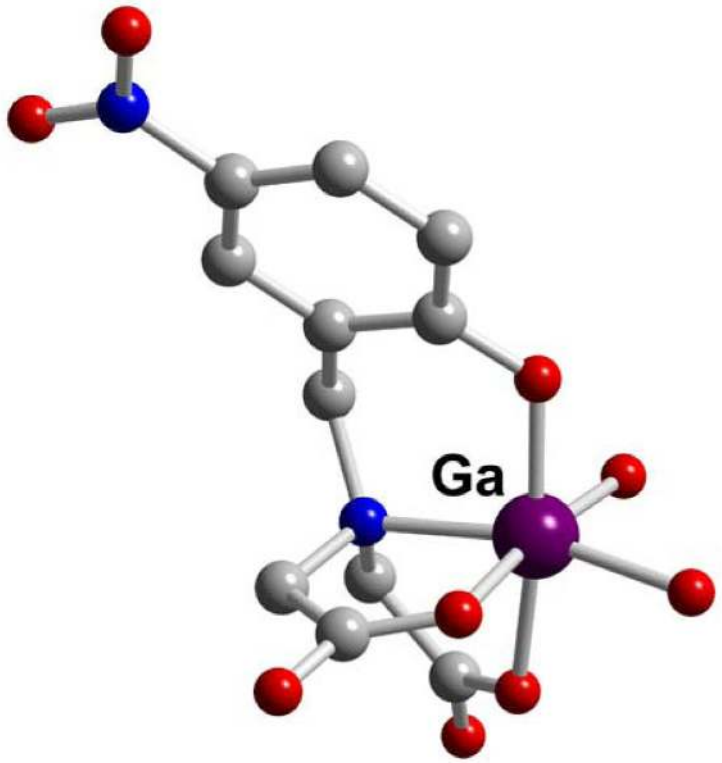

Figure 30.
Ga-**L1**

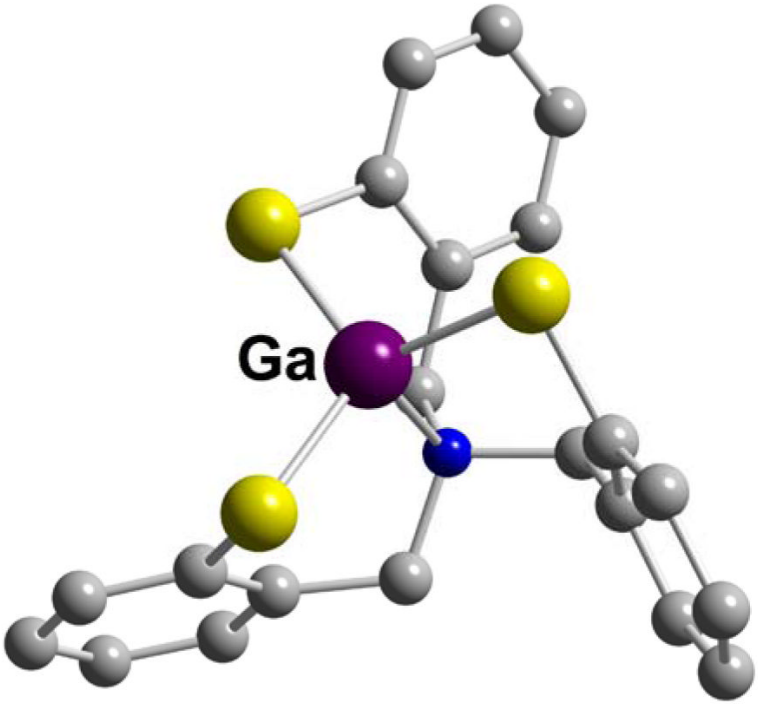

Figure 31.
Ga-**L2**

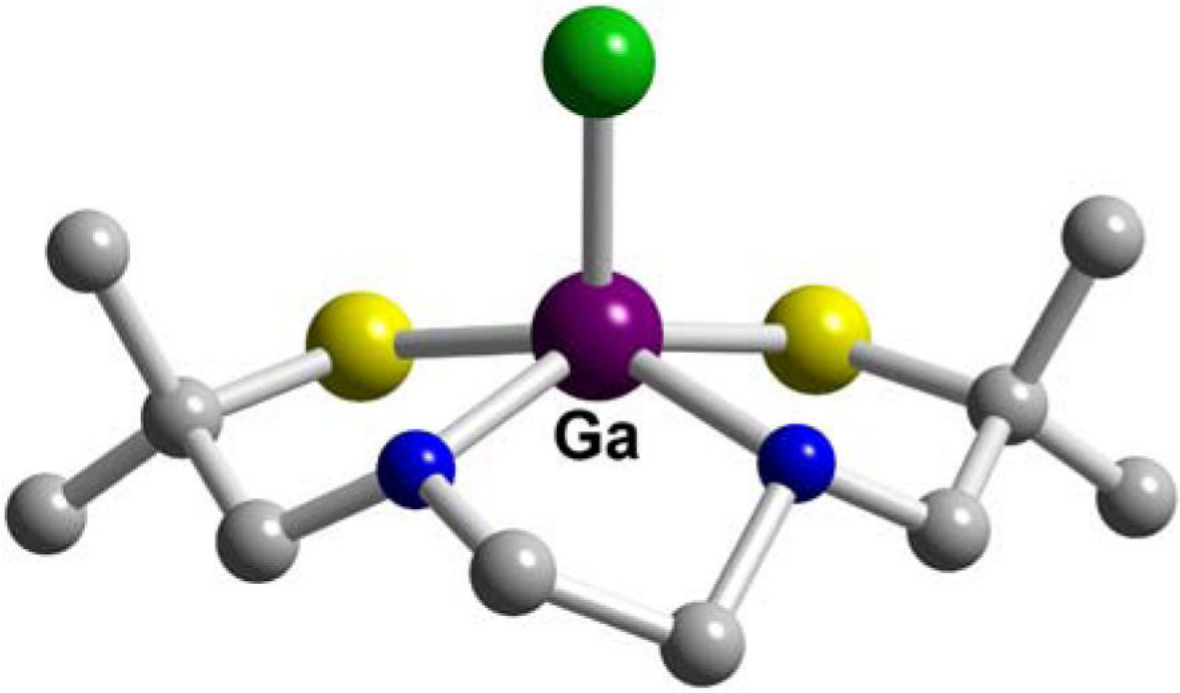

Figure 32.
Ga-**BAT-TM** (**L4**)

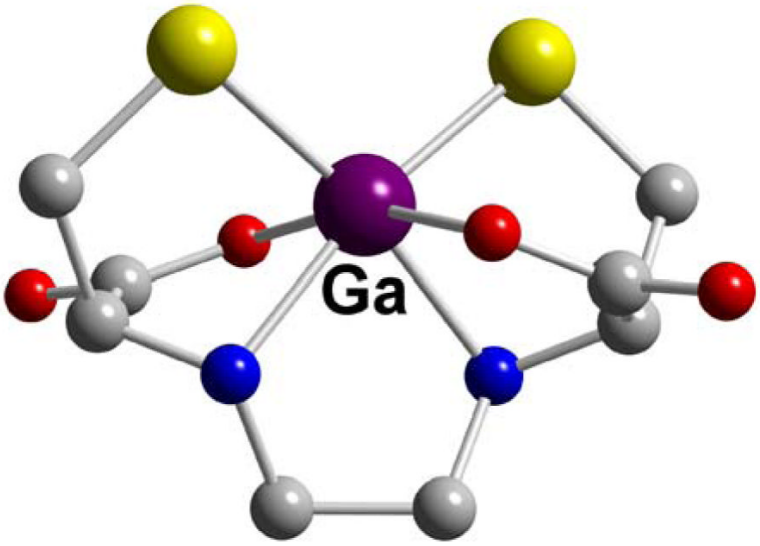

Figure 33.
Ga-**EC** (**L5**)

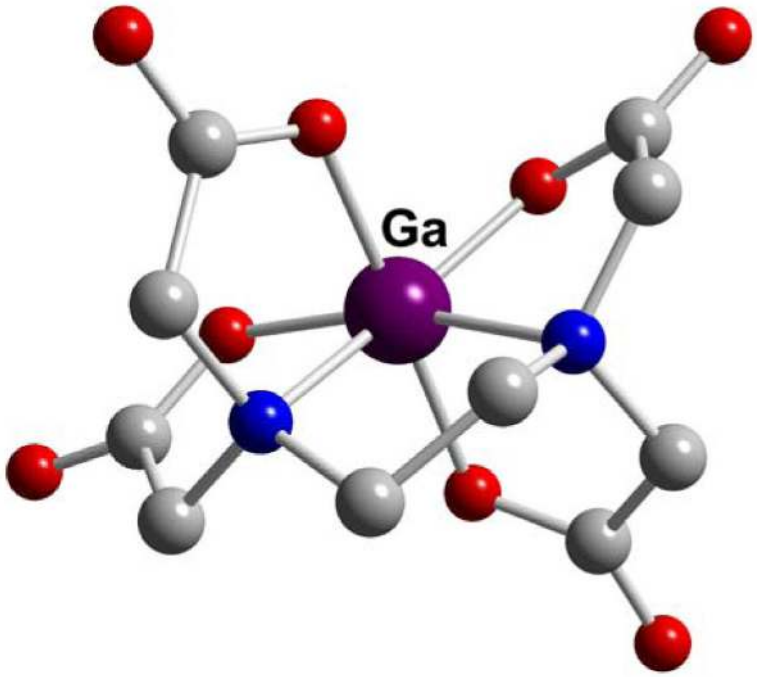

Figure 34.
Ga-**EDTA** (**L10**)

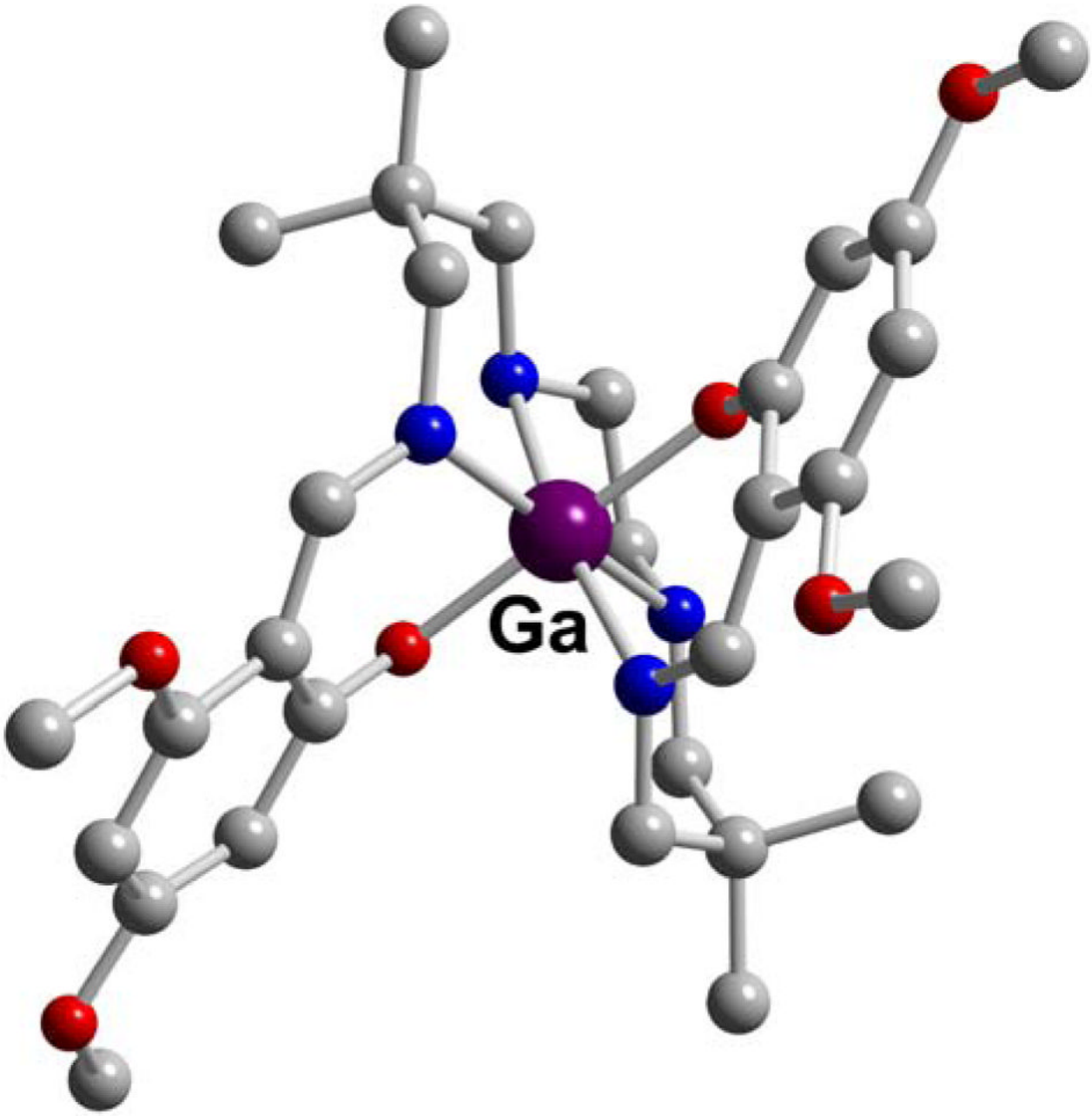

Figure 35.
Ga-**BAPEN** (**L16**)

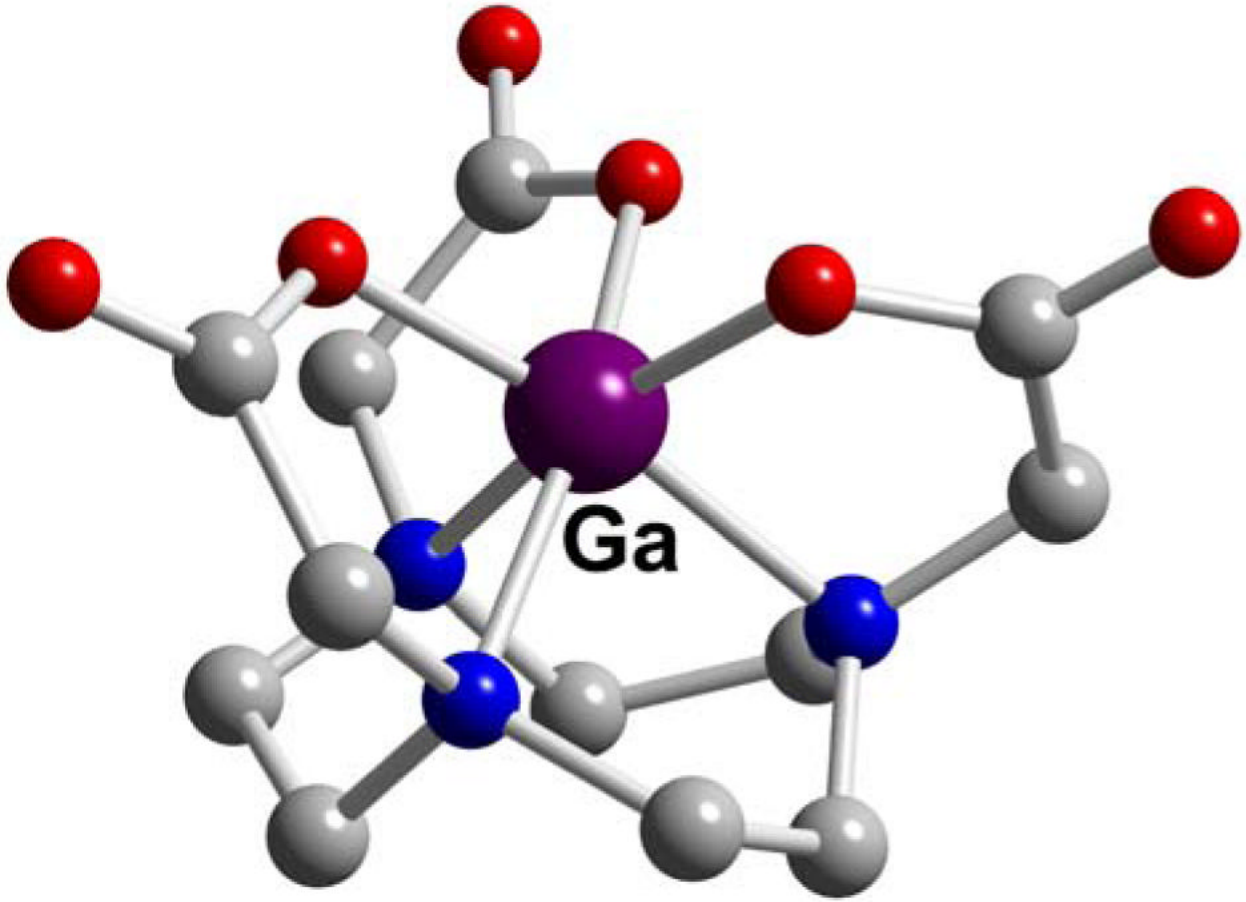

Figure 36.
Ga-**NOTA** (**L29**)

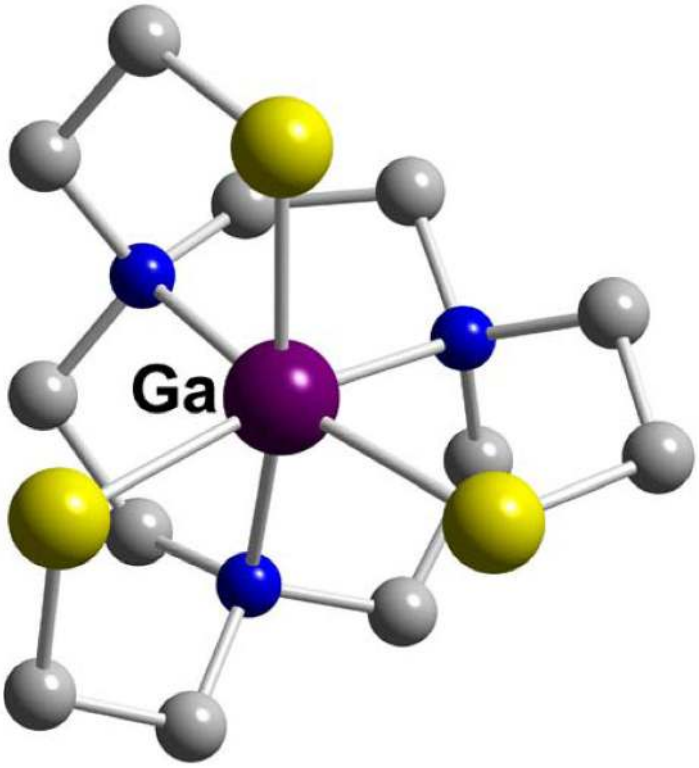

Figure 37.
Ga-**TACN-TM** (**L27**)

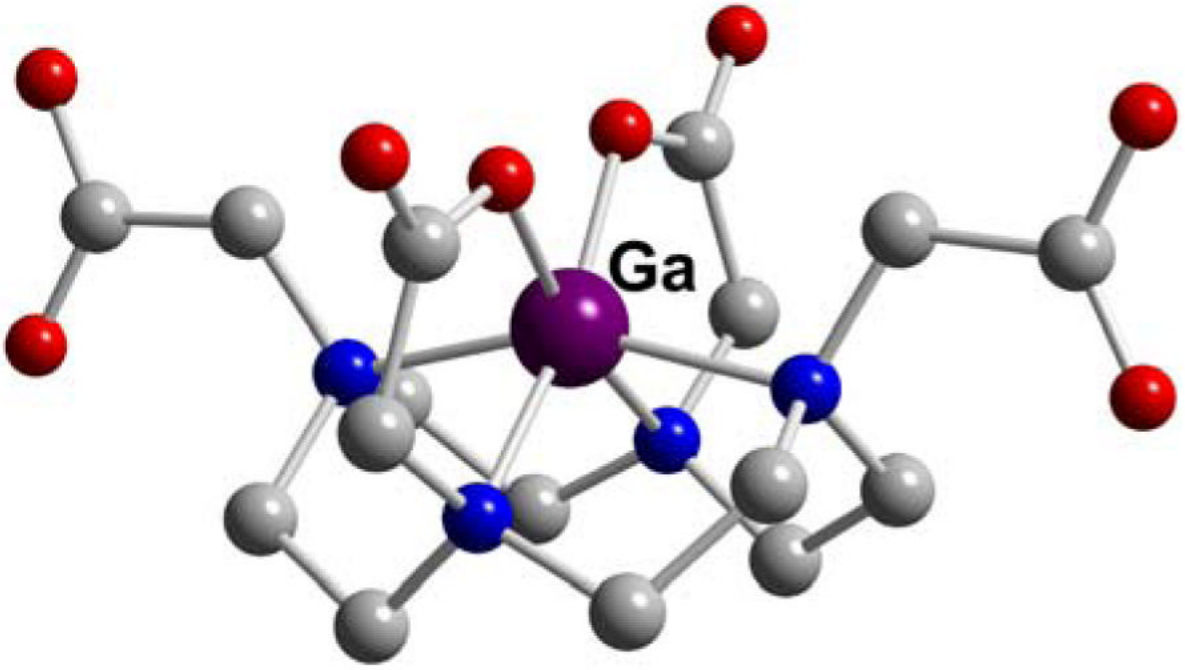

Figure 38.
Ga-**DOTA** (**L39**)

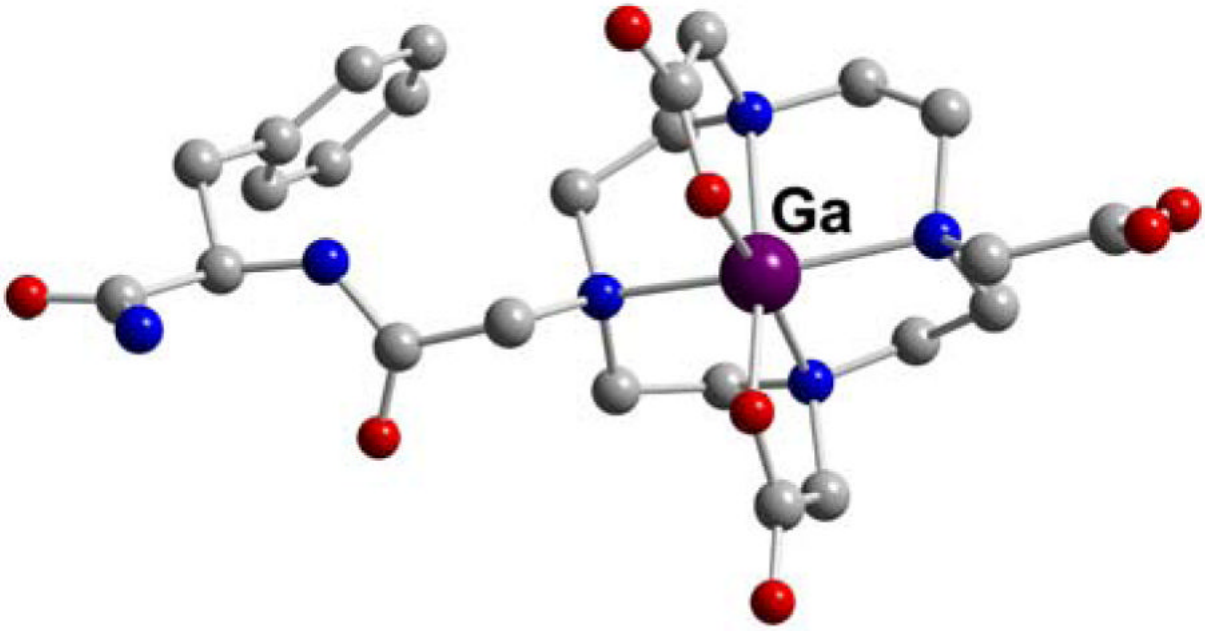

Figure 39.
Ga-**DOTA-D-PheNH$_2$** (**L40**)

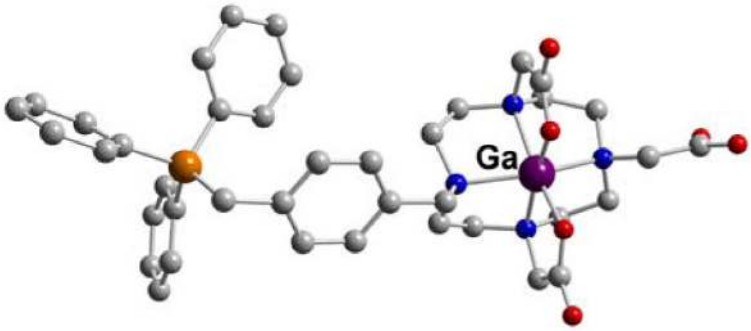

Figure 40.
Ga-**DO3A-TPP (L44)**

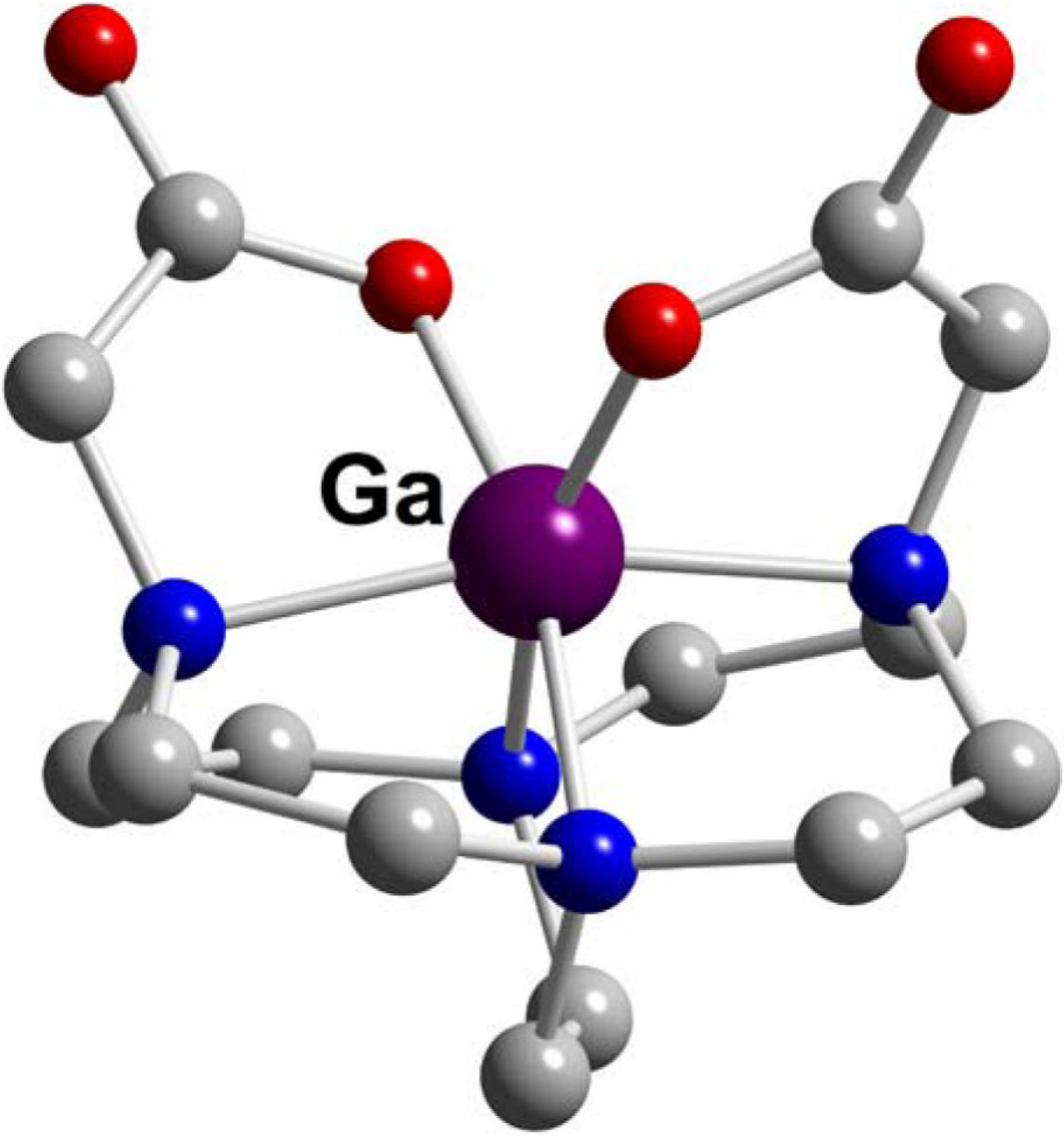

Figure 41.
Ga-**CB-DO2A (L37)**

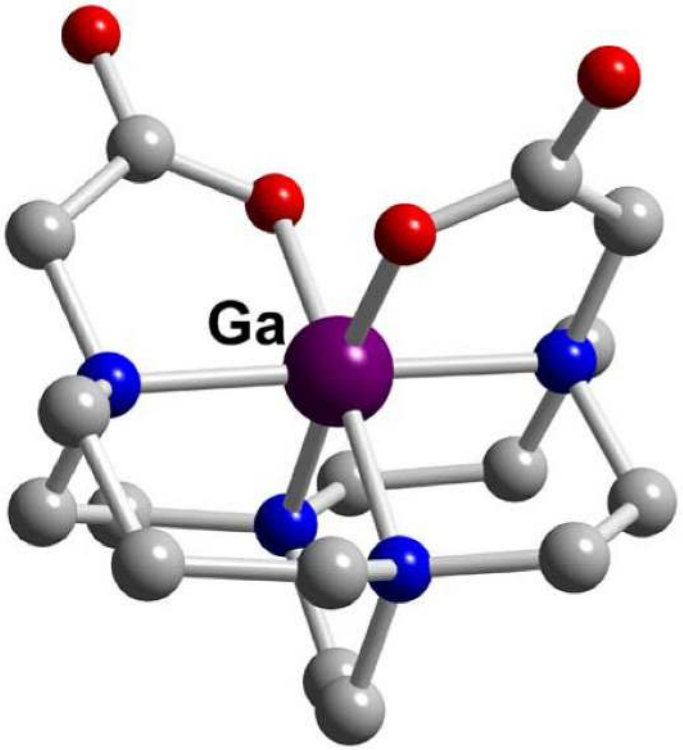

Figure 42.
Ga-**CB-TE2A (L57)**

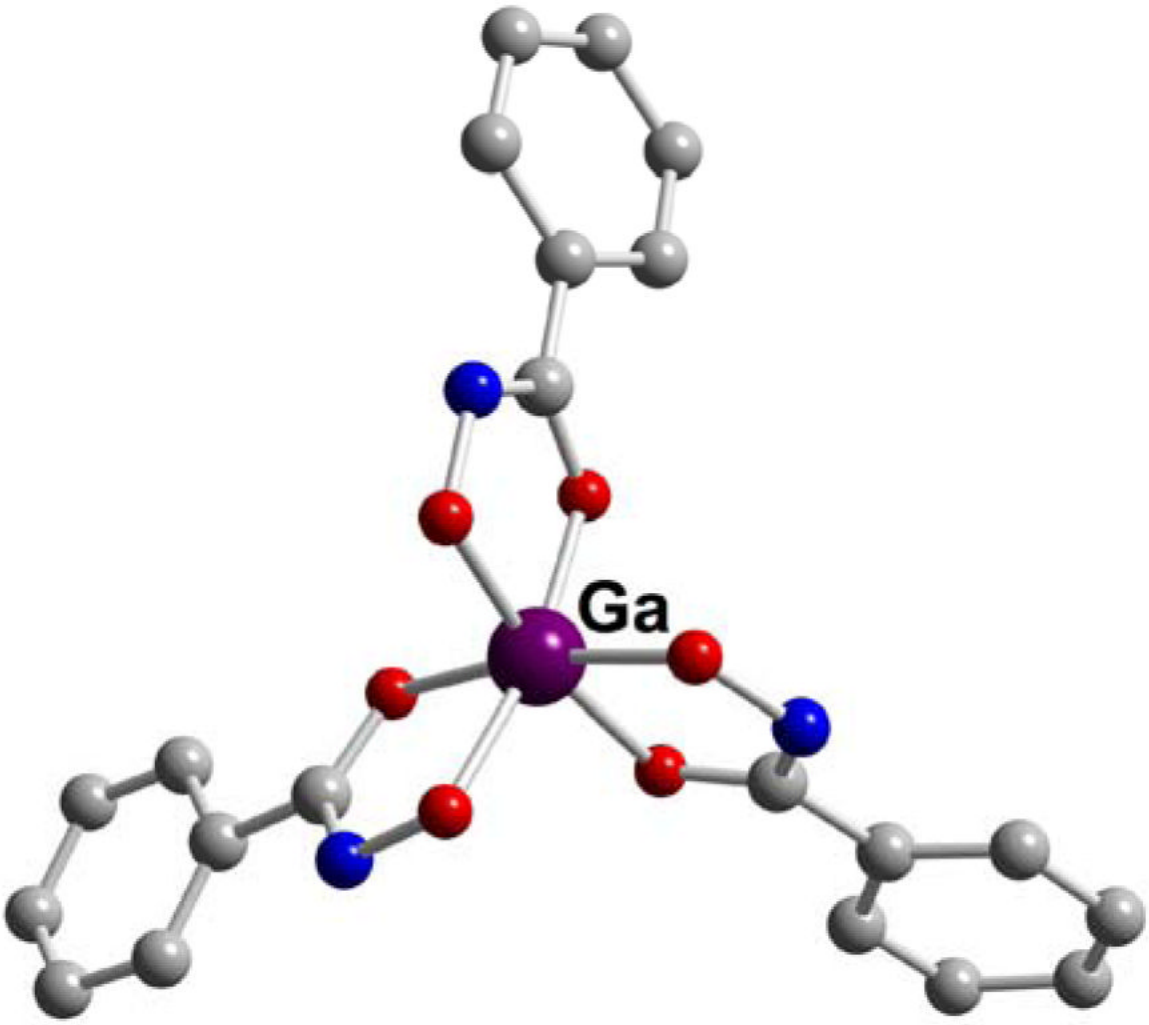

Figure 43.
Ga-*tris*(benzohydroxamate)

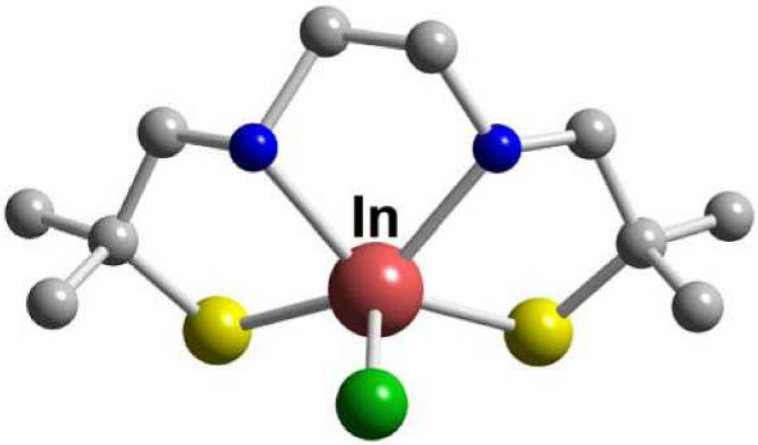

Figure 44.
InCl-**BAT-TM** (**L4**)

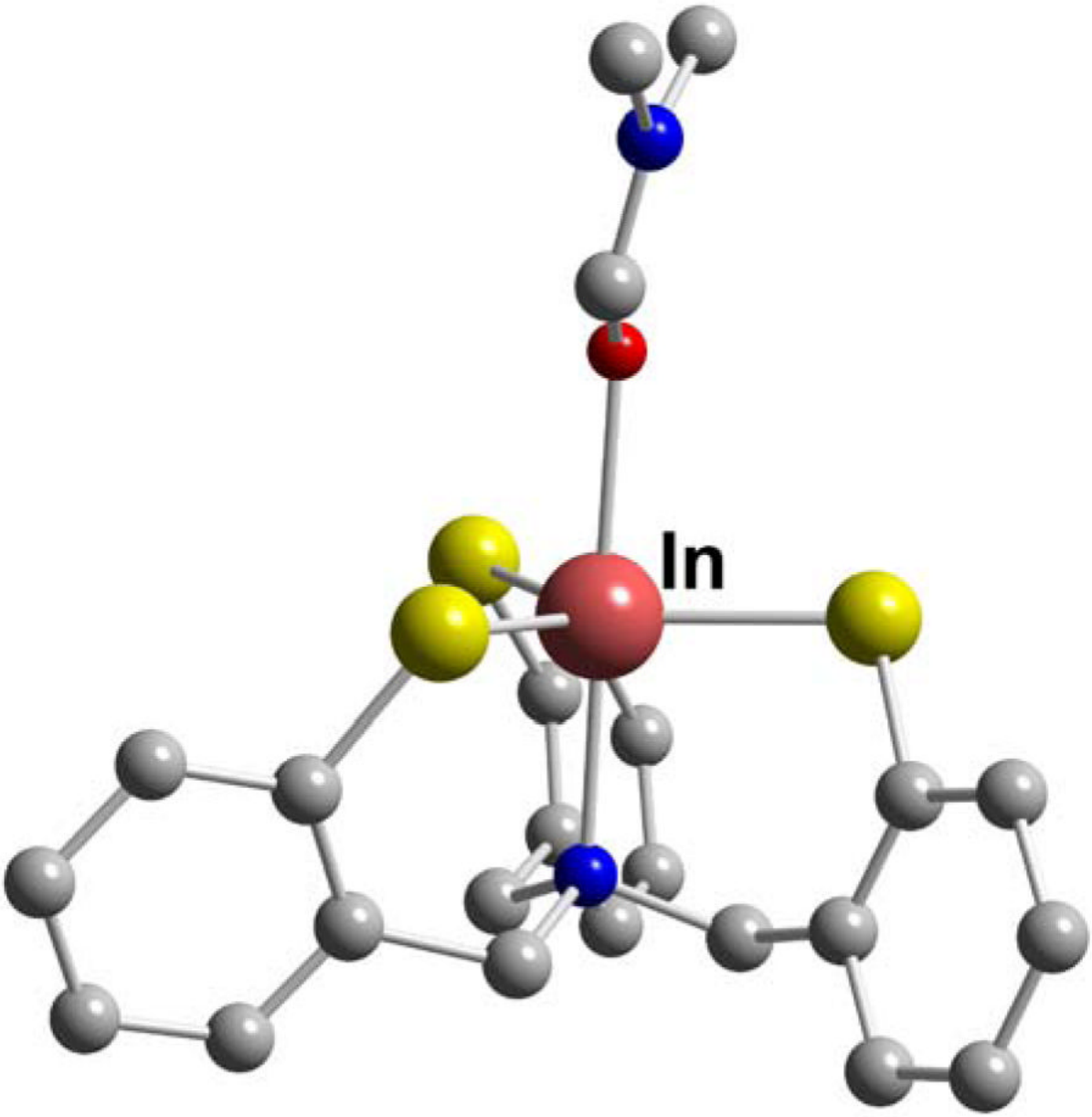

Figure 45.
In-**L2**•DMF

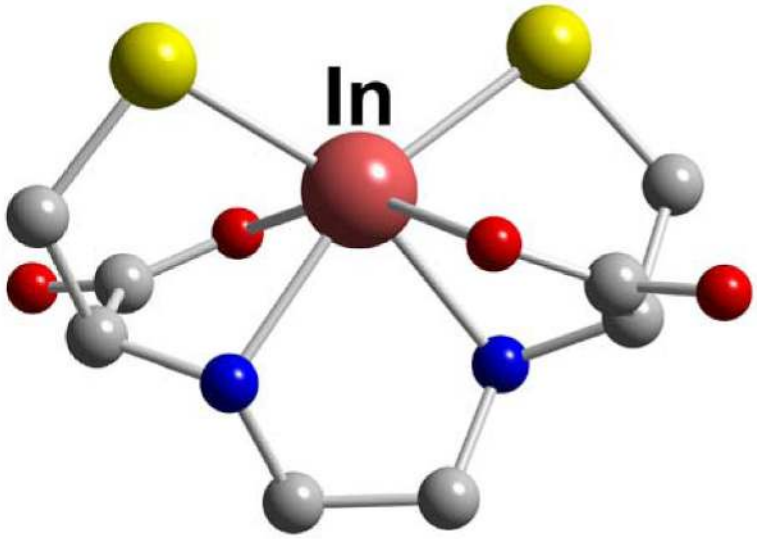

Figure 46.
In-**EC** (**L5**)

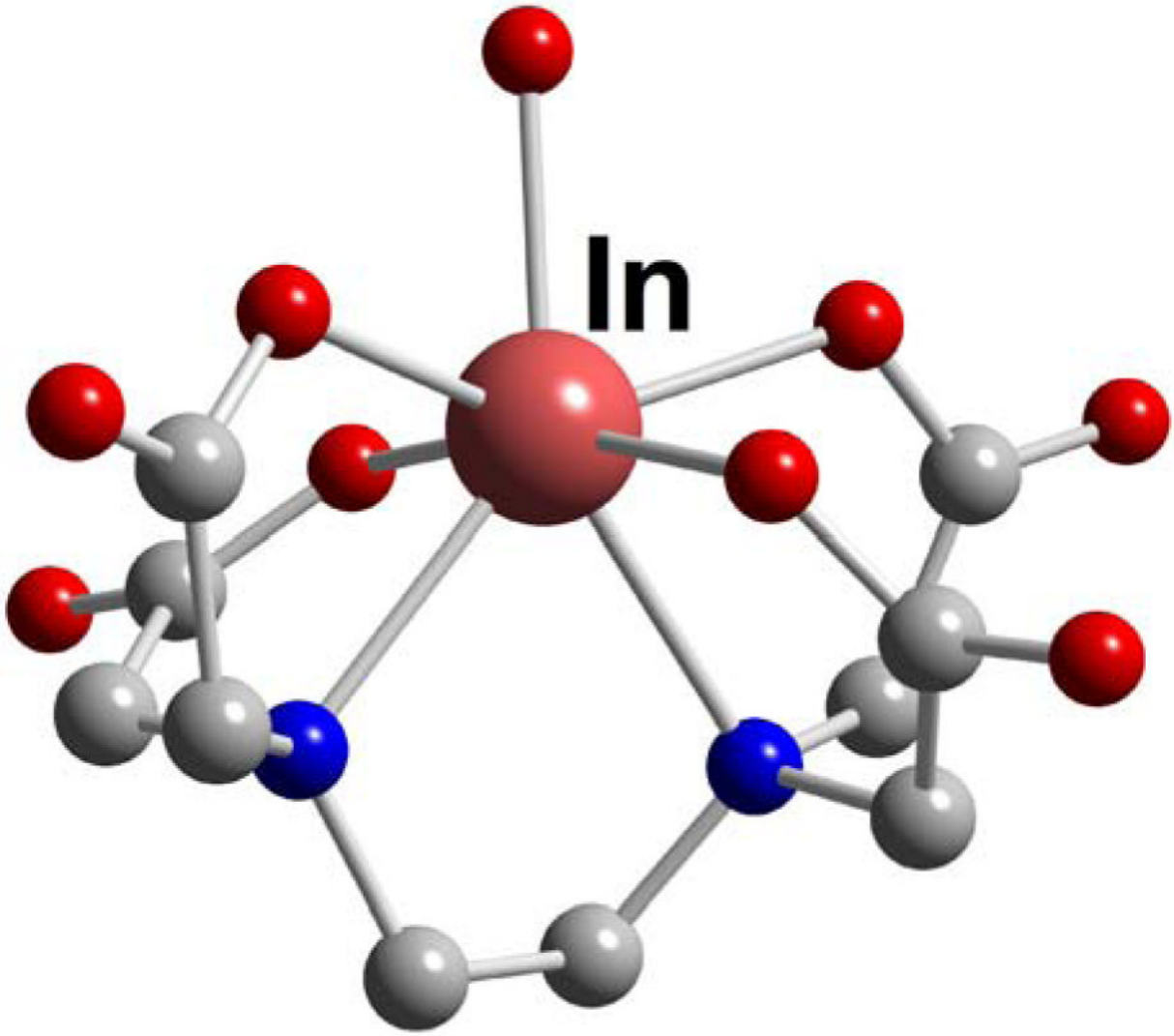

Figure 47.
In-**EDTA** (**L9**)

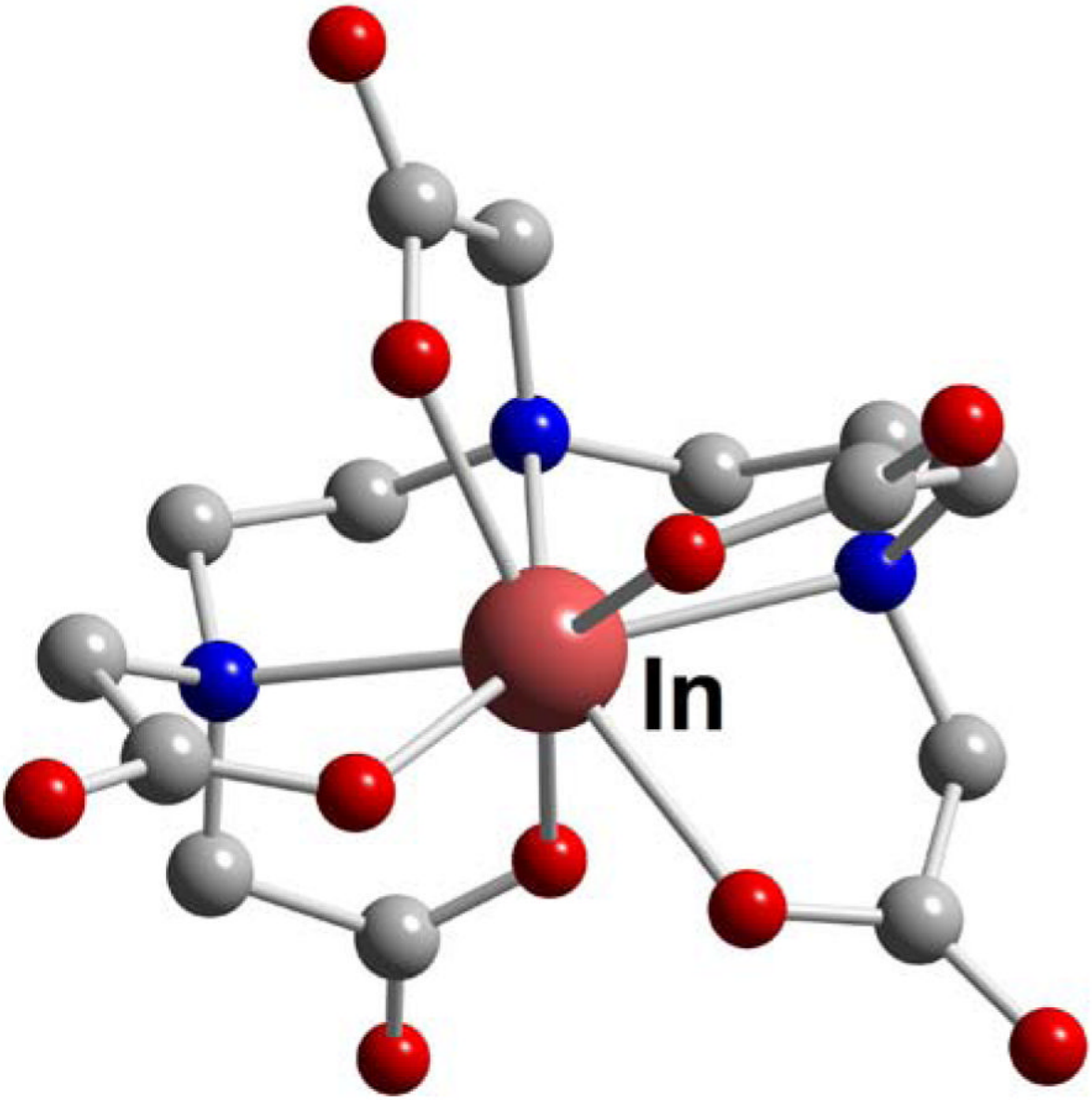

Figure 48.
In-**DTPA** (**L12**)

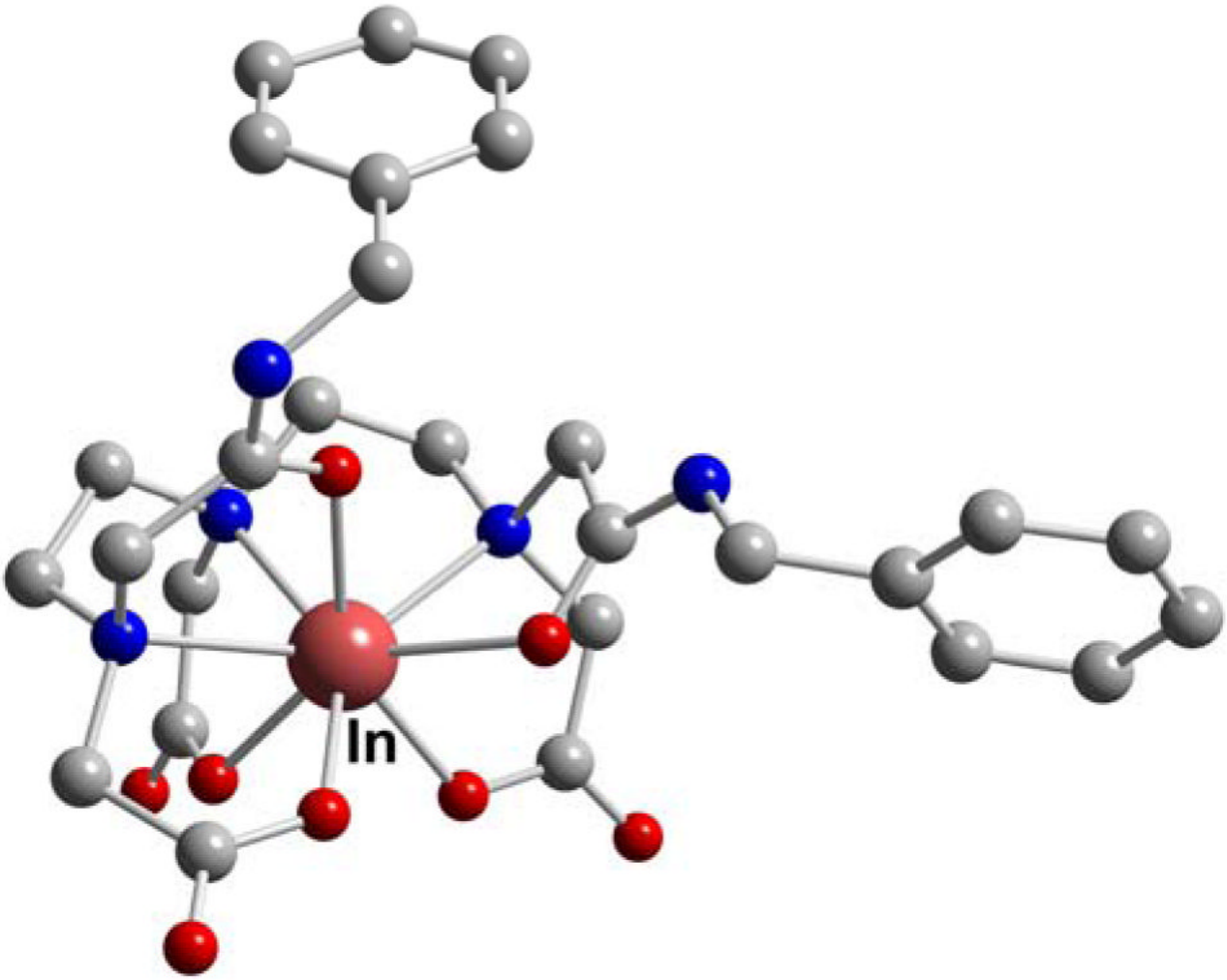

Figure 49.
In-**DTPA-BA$_2$** (**L13**)

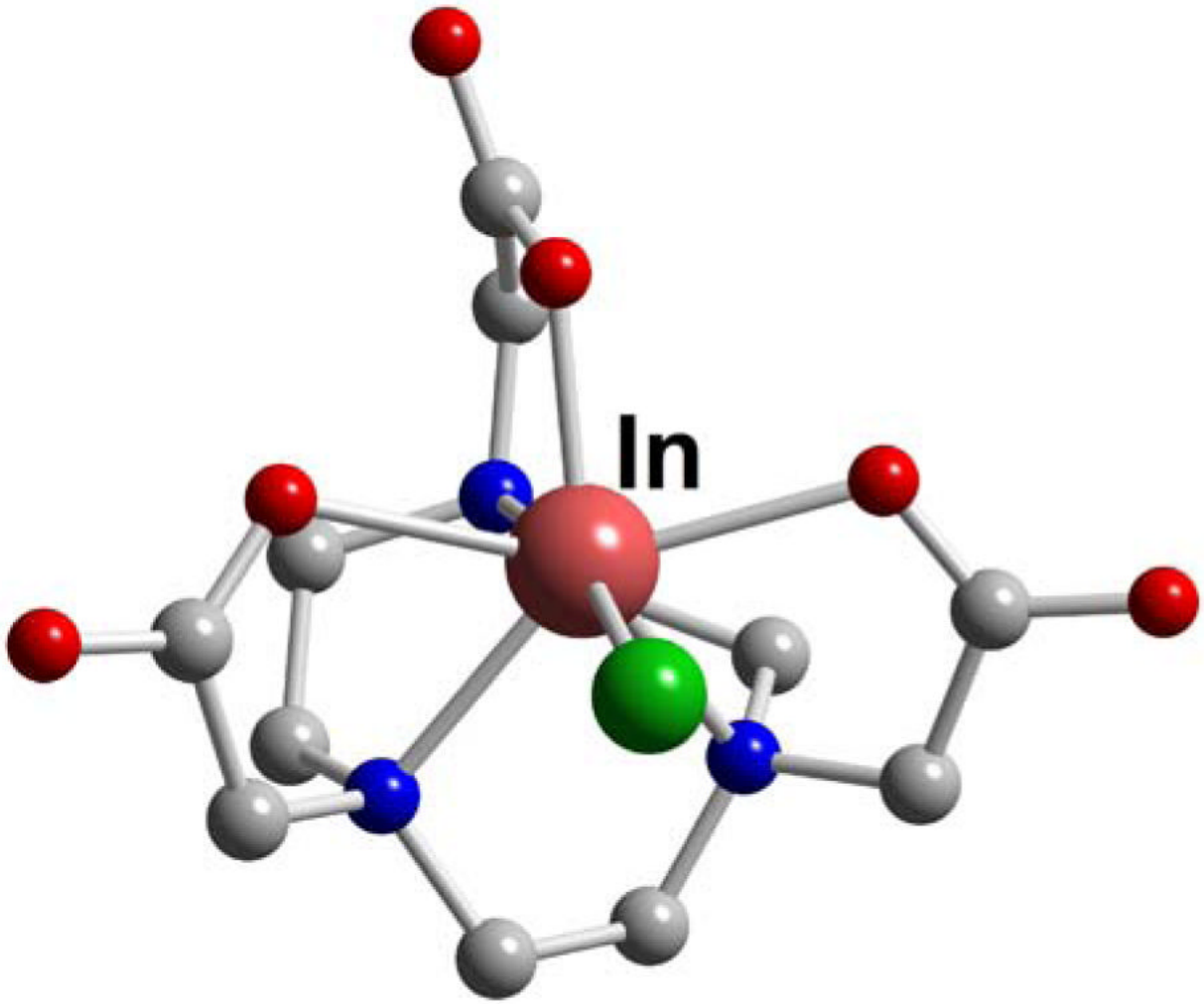

Figure 50.
InCl-H**NOTA** (**L29**)

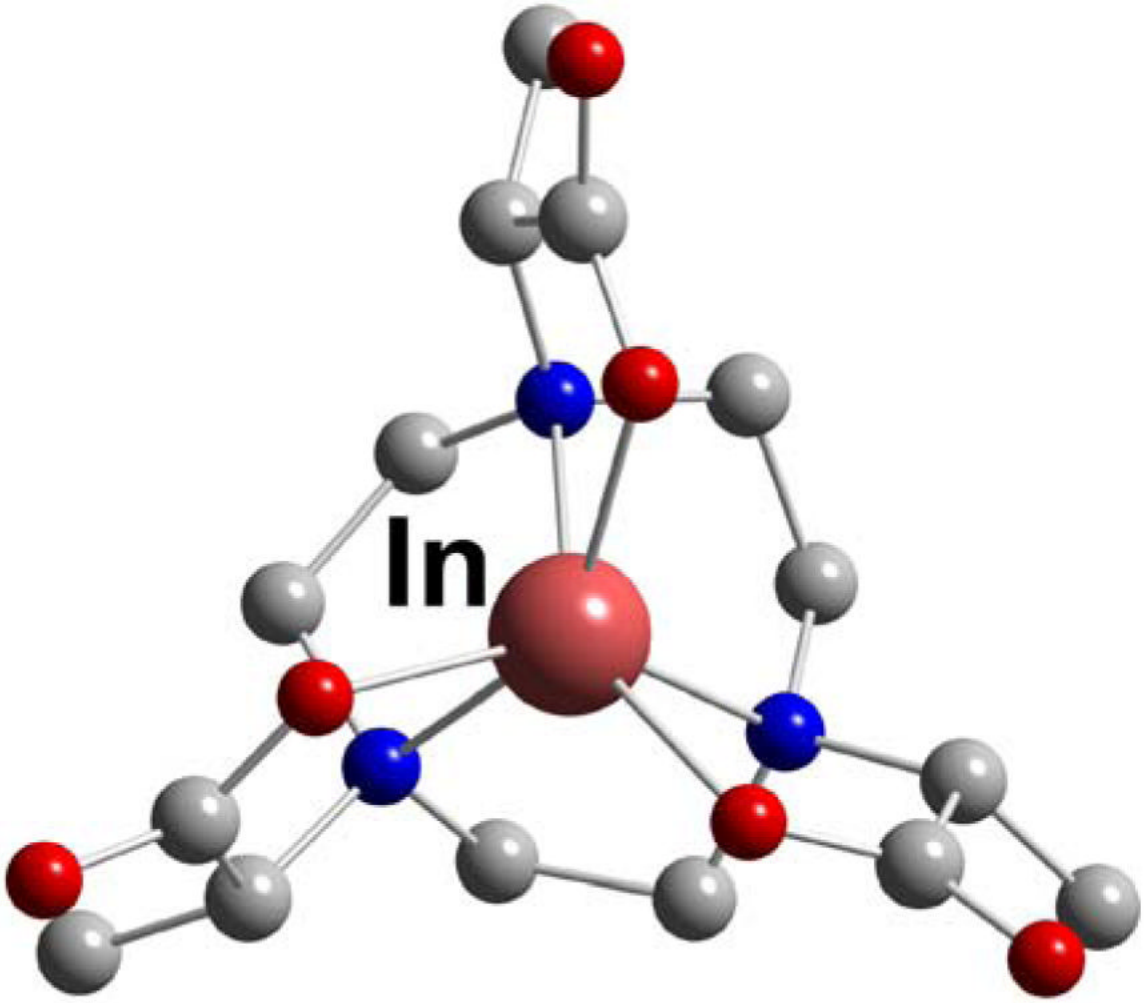

Figure 51.
In-**TACN (L26)**-*tris*(2′-methylcarboxylmethyl)

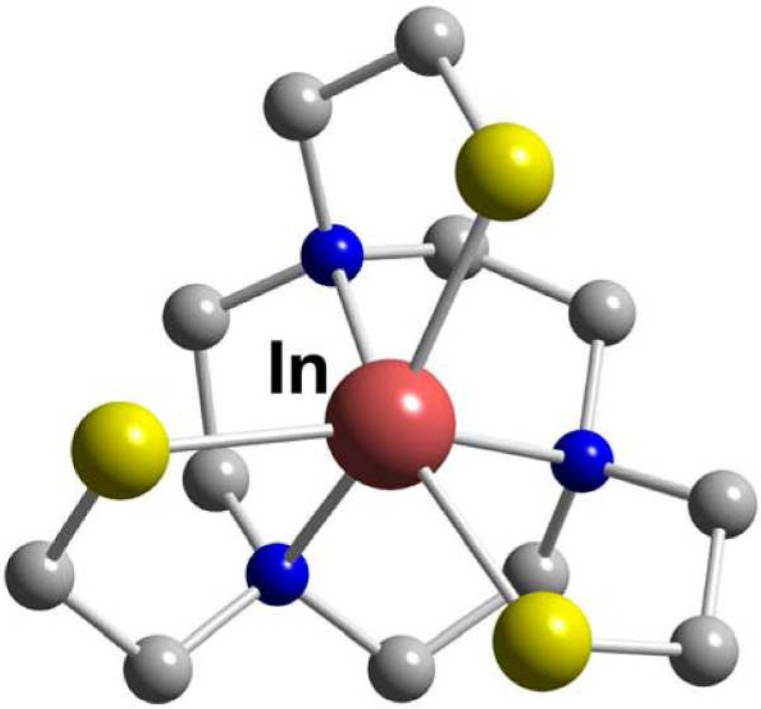

Figure 52.
In-**TACN-TM** (**L27**)

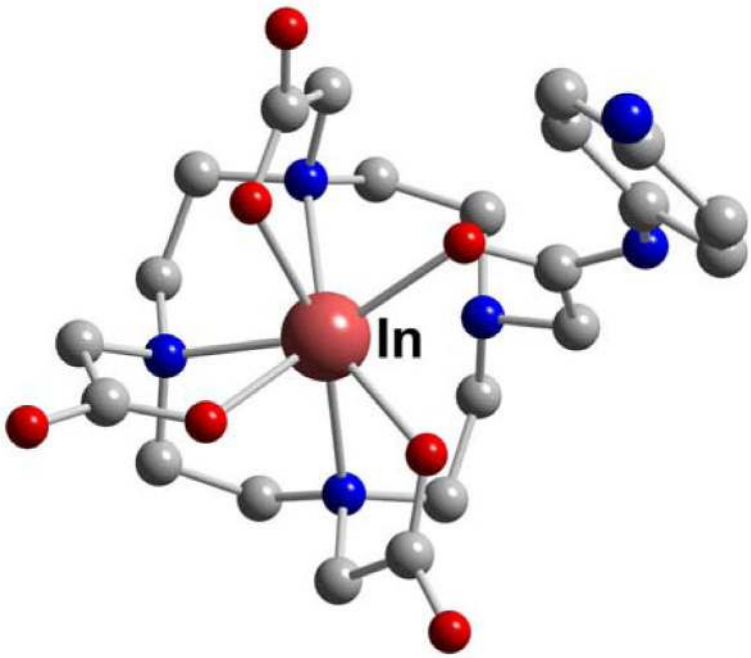

Figure 53.
In-**DOTA-AA** (**L41**)

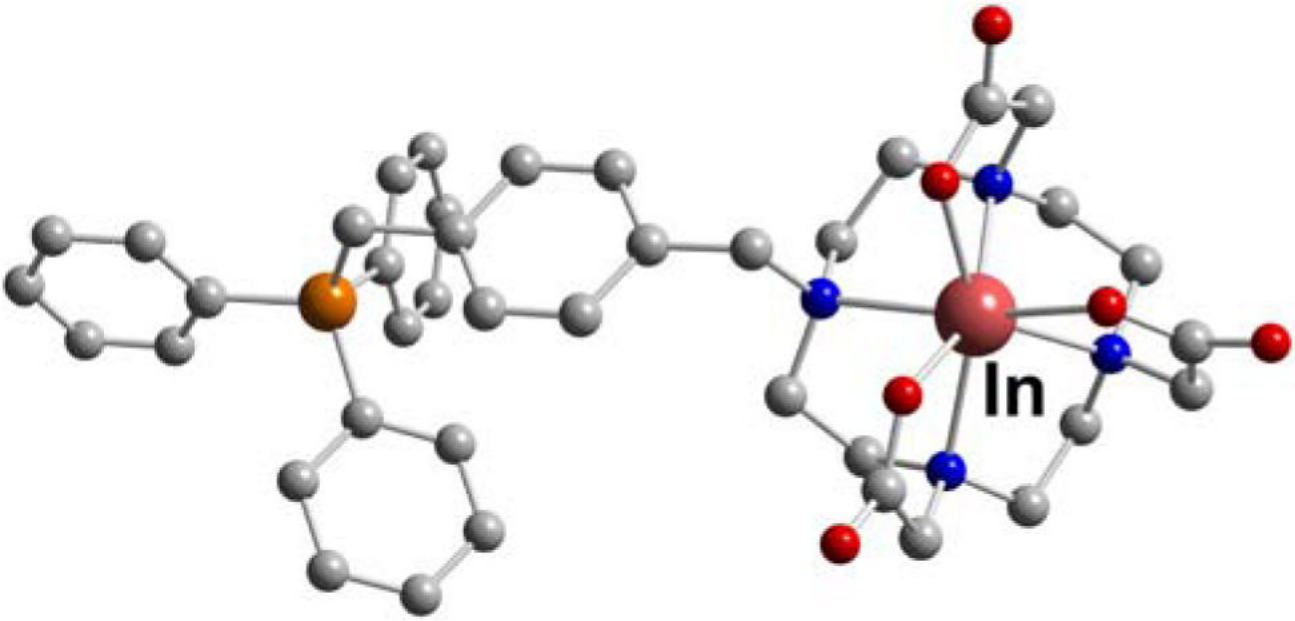

Figure 54.
In-**DOTA-TPP** (**L44**)

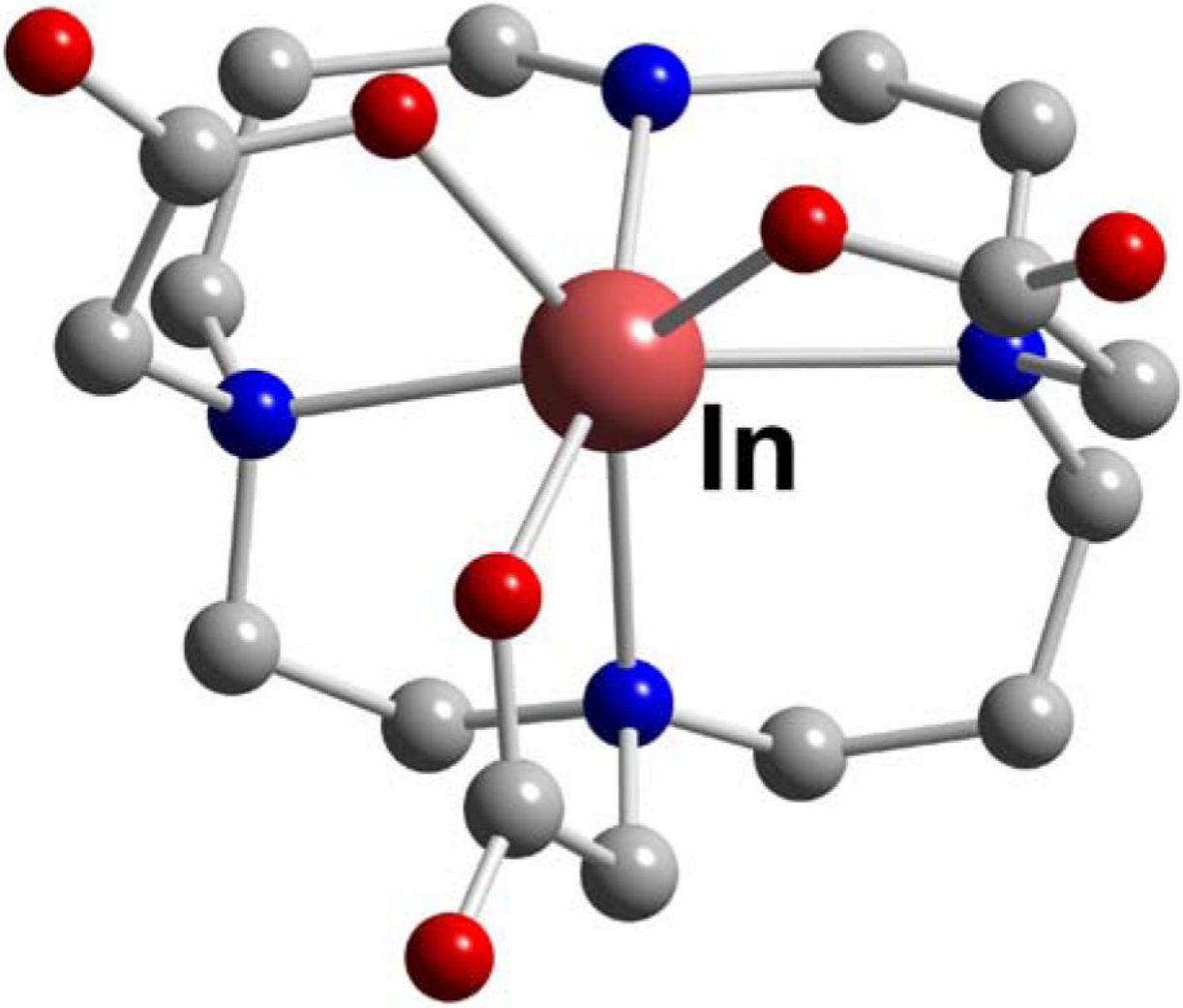

Figure 55.
In-**TE3A** (**L53**)

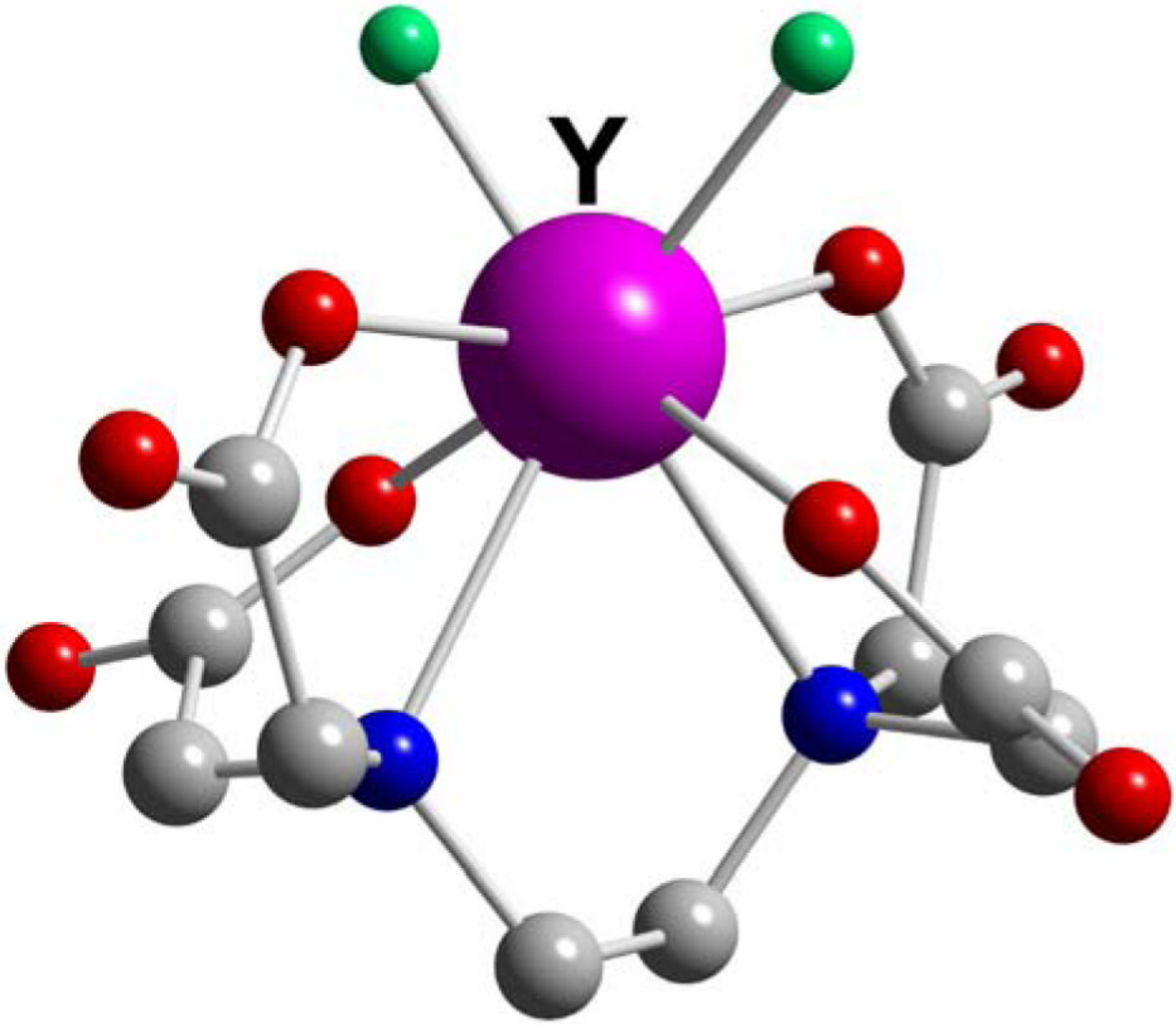

Figure 56.
YF_2-**EDTA** (**L10**)

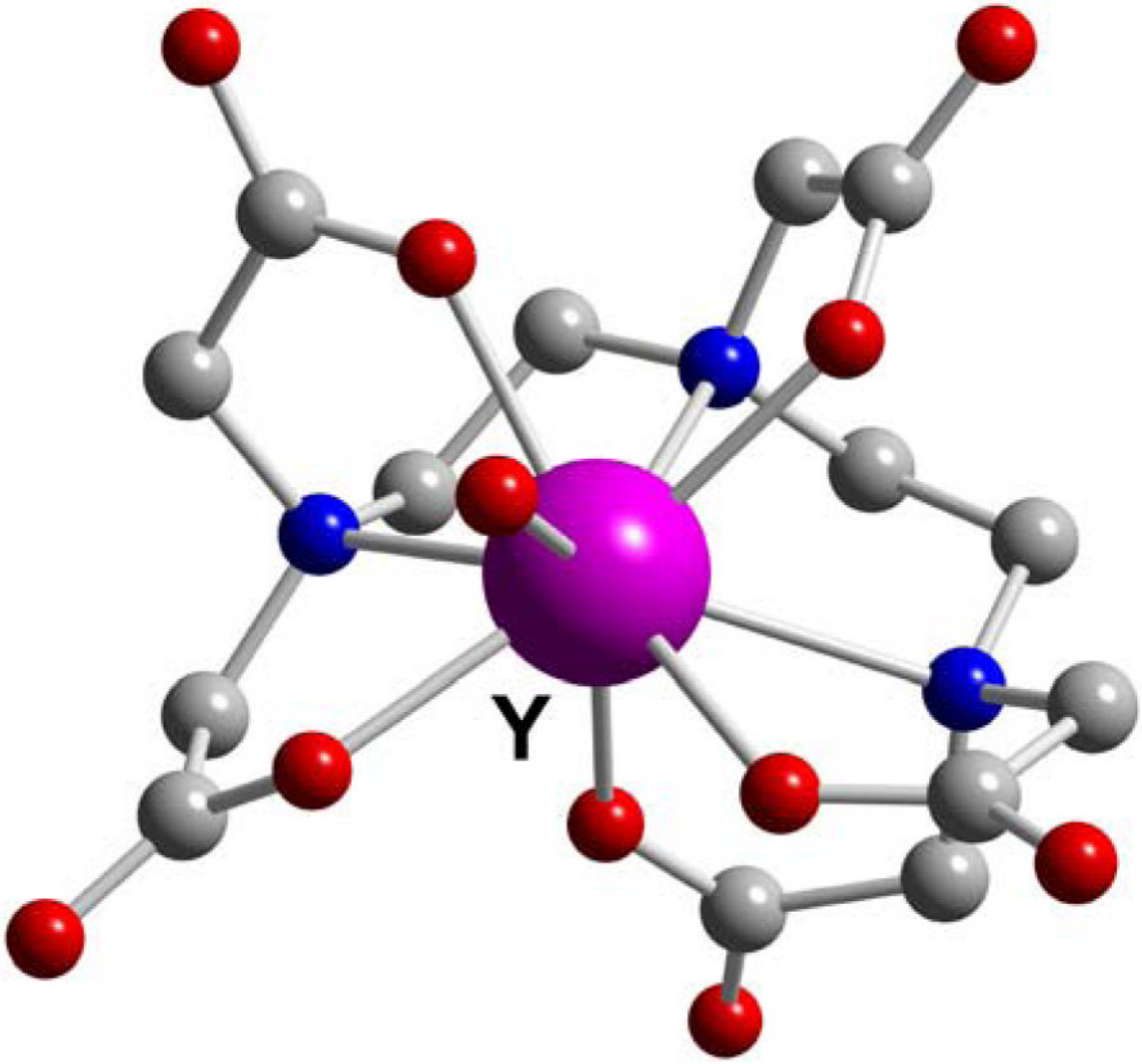

Figure 57.
Y-**DTPA** (**L12**)

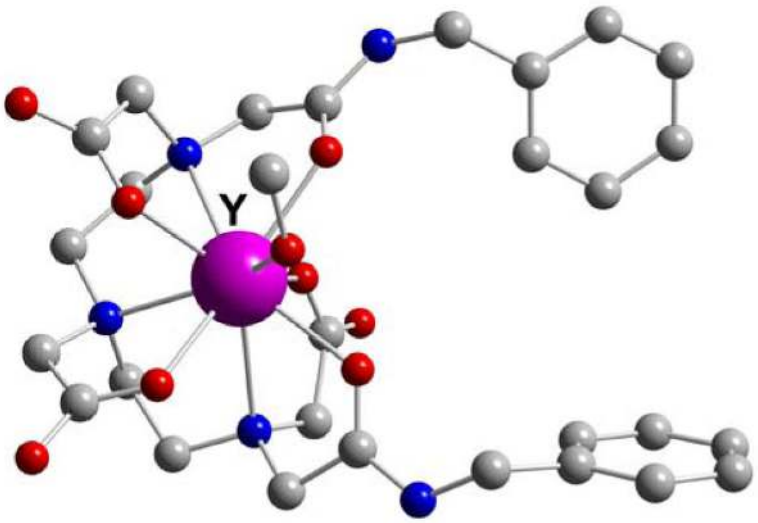

Figure 58.
Y-**DTPA-BA$_2$ (L13)**

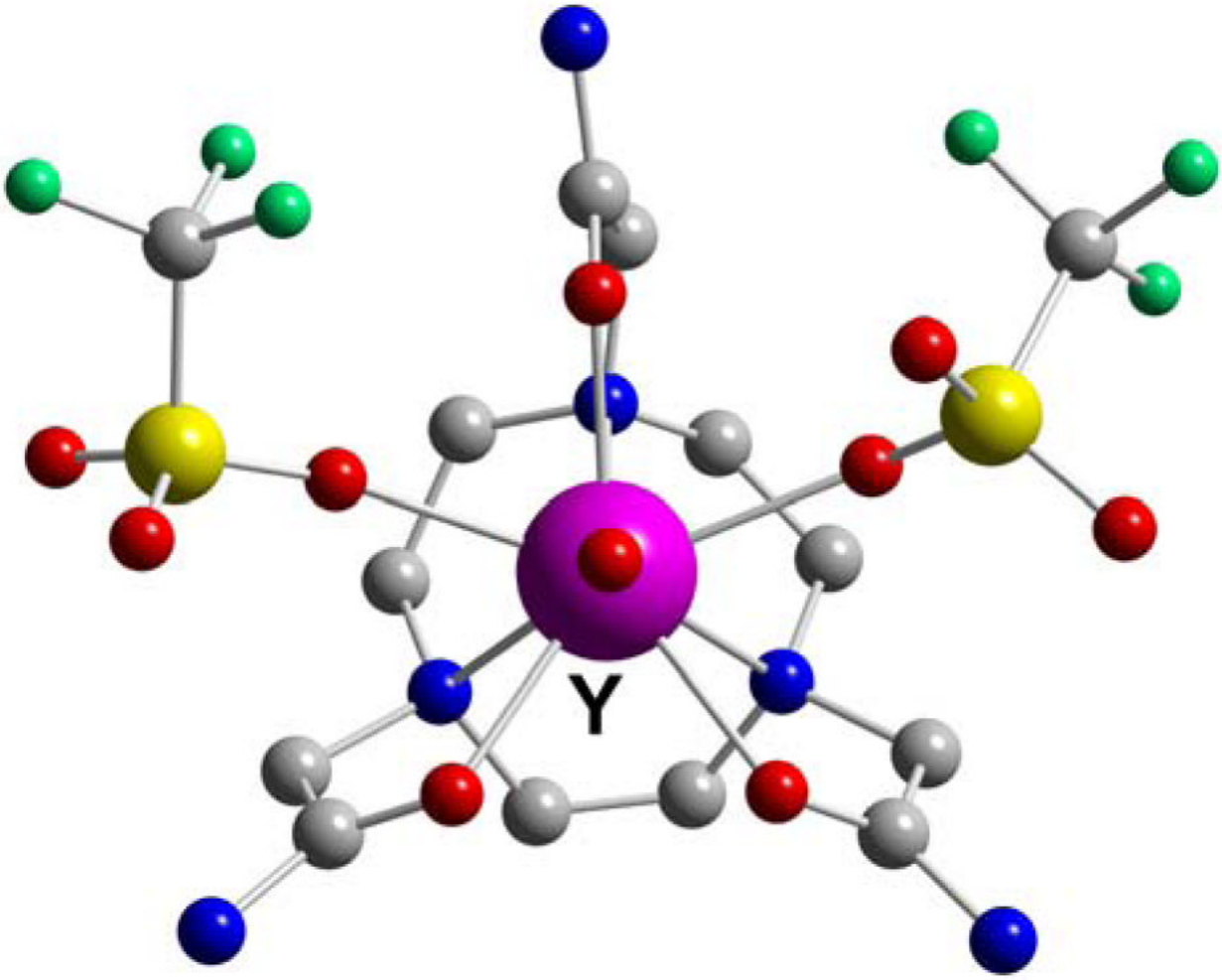

Figure 59.
Y(triflate)$_2$-**NOTAM** (**L30**)

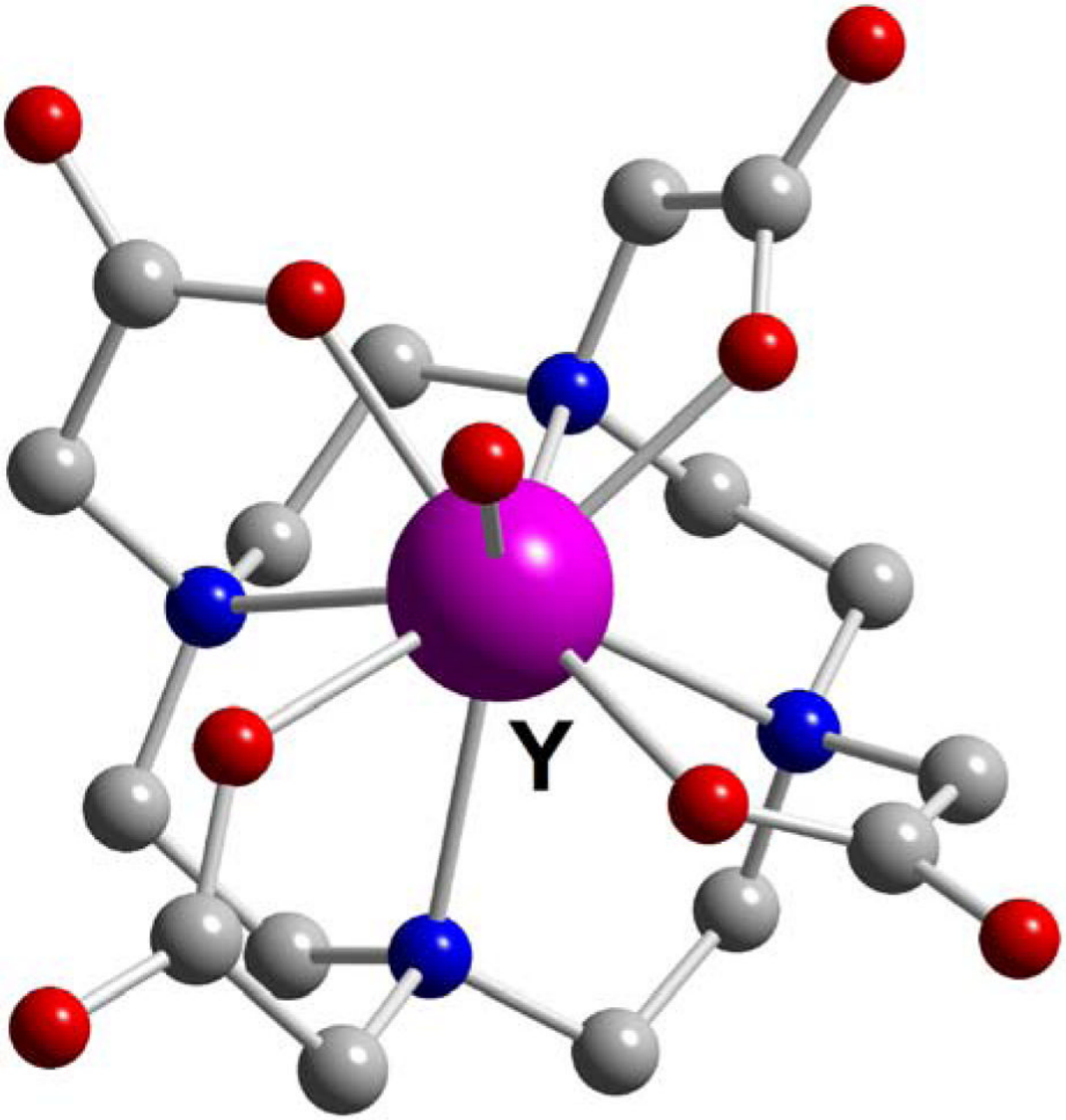

Figure 60.
[Y-**DOTA**]$^{-}$ (**L39**)

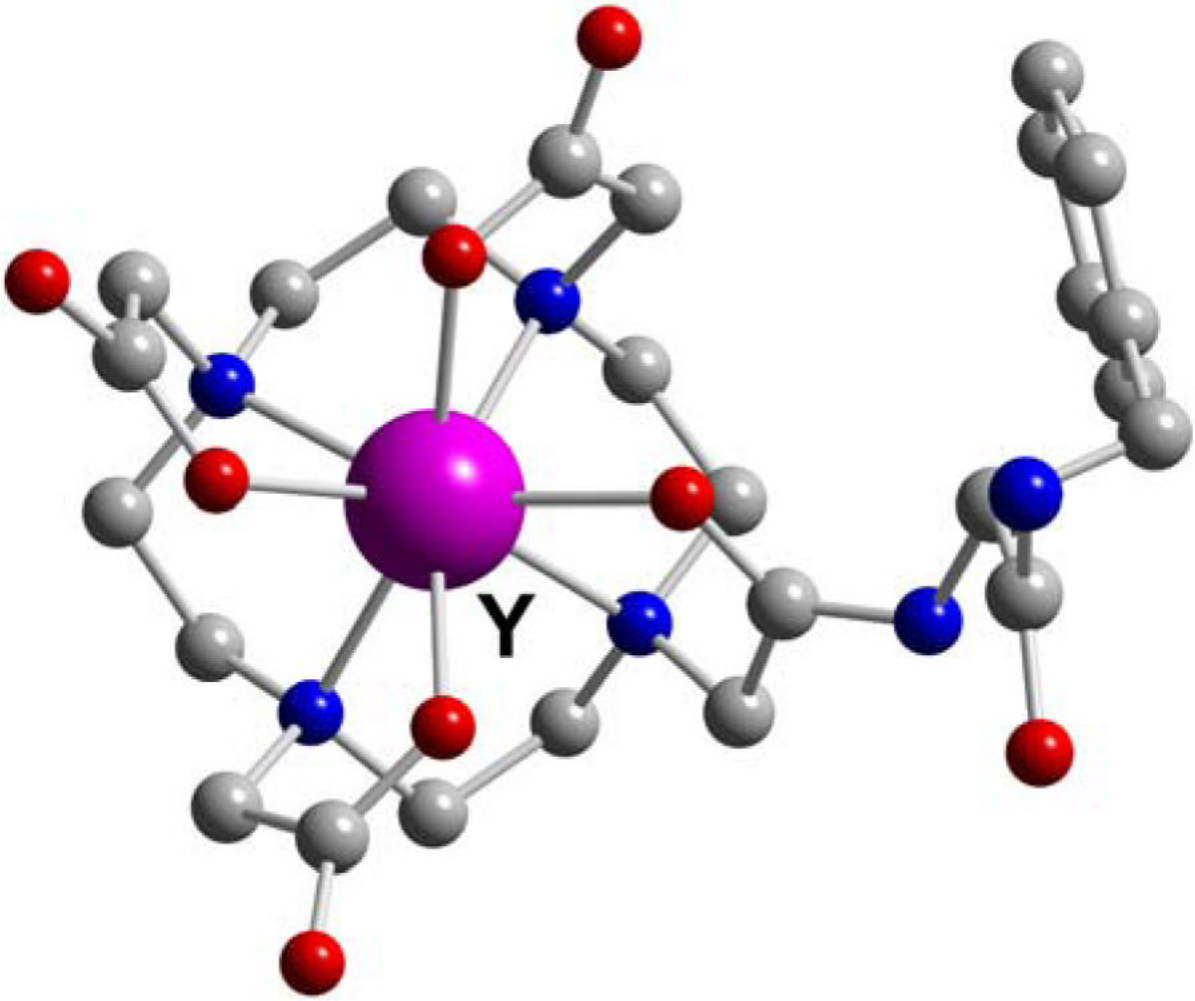

Figure 61.
Y-**DOTA-D-Phe-NH$_2$ (L40)**

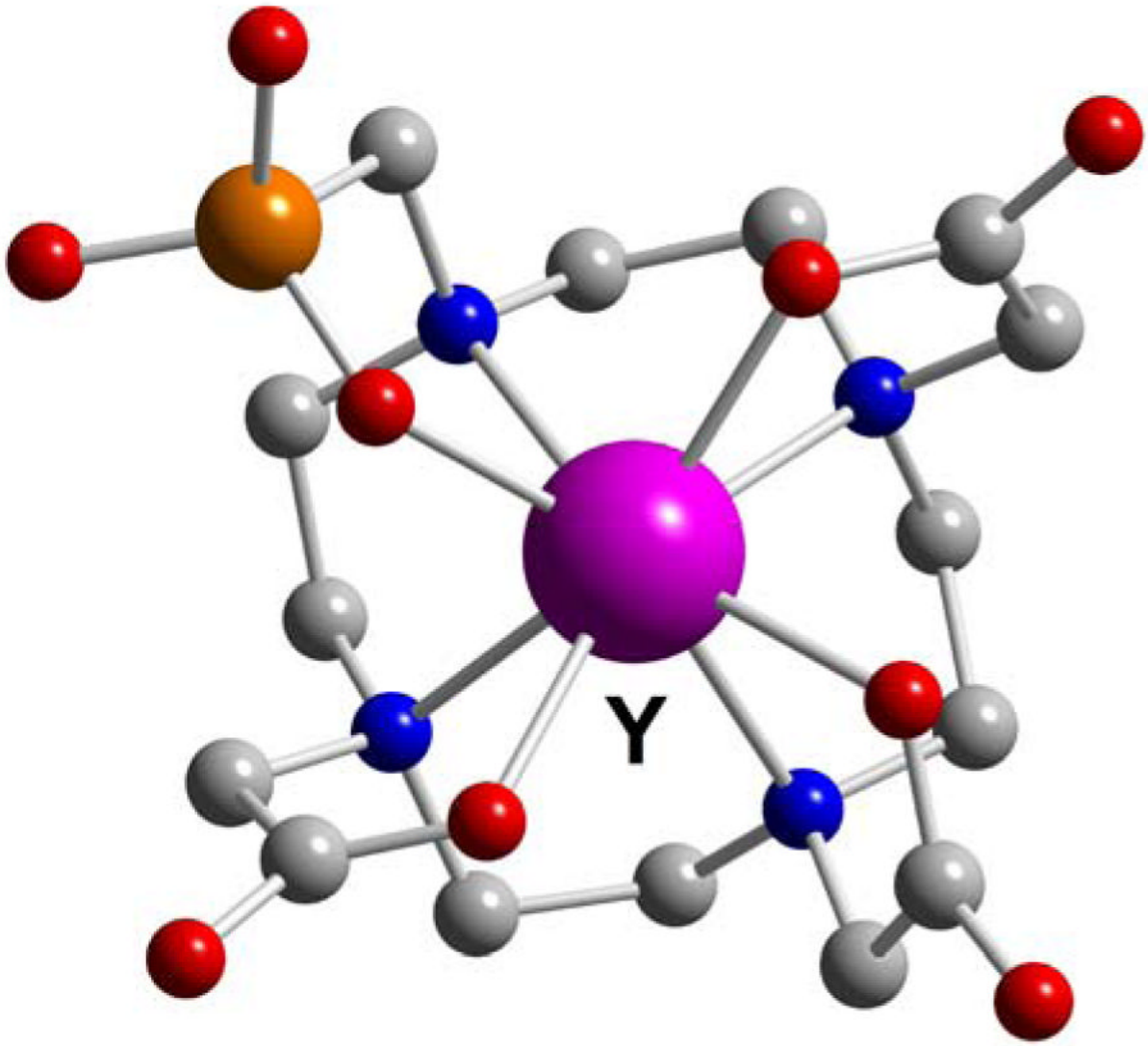

Figure 62.
Y-**DO3AP** (**L42**)

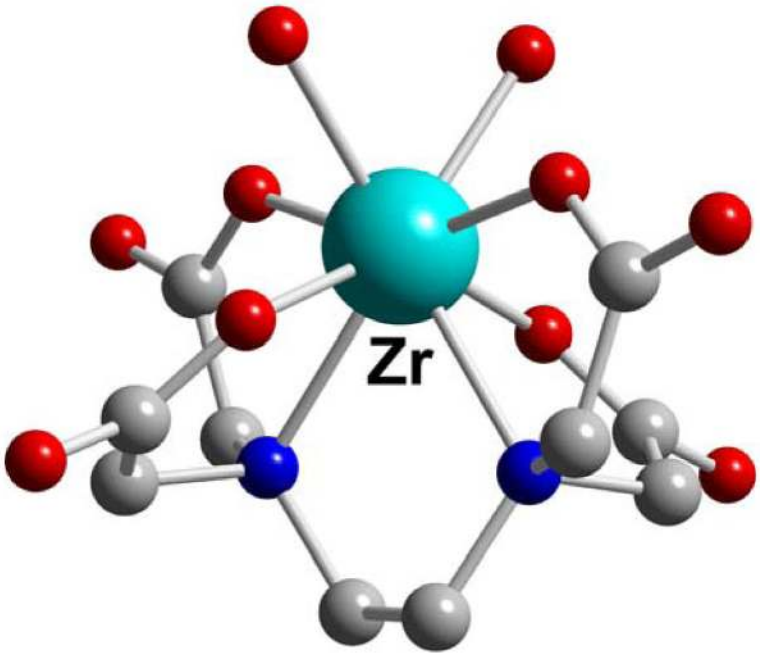

Figure 63.
Zr-**EDTA** (**L10**)

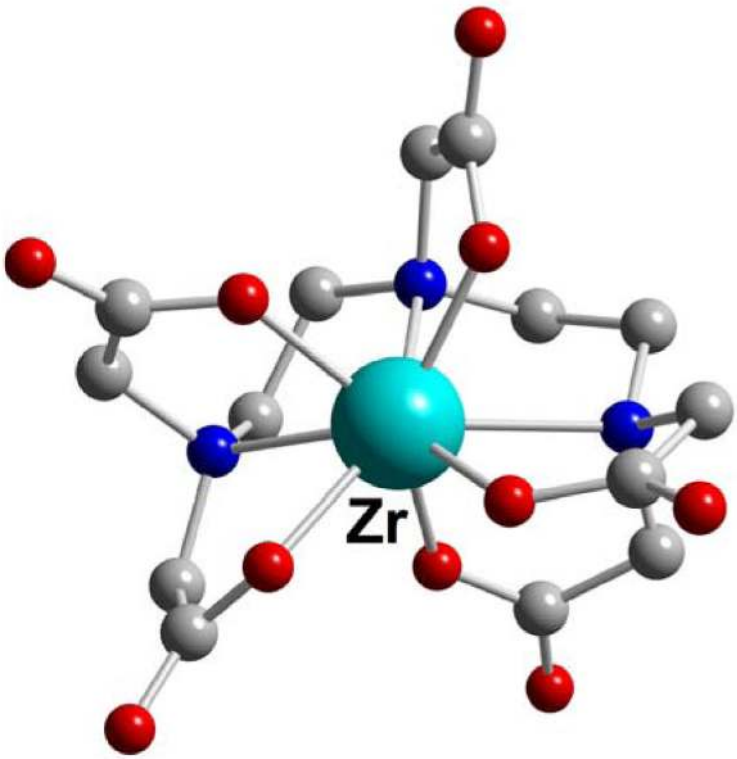

Figure 64.
Zr-**DTPA** (**L12**)

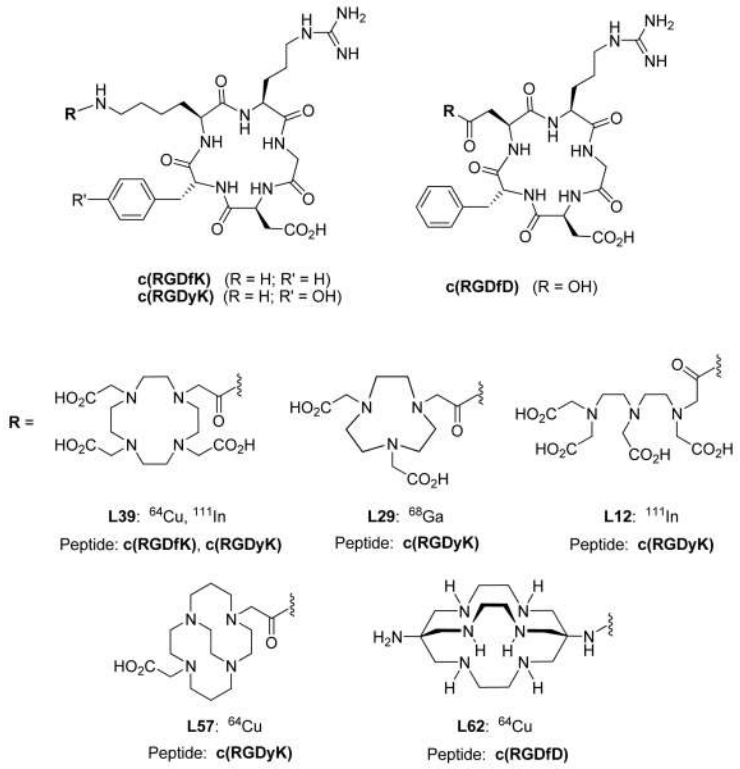

Figure 65.
Selected RGD analogues used in $\alpha_v\beta_3$ targeting radiopharmaceuticals.

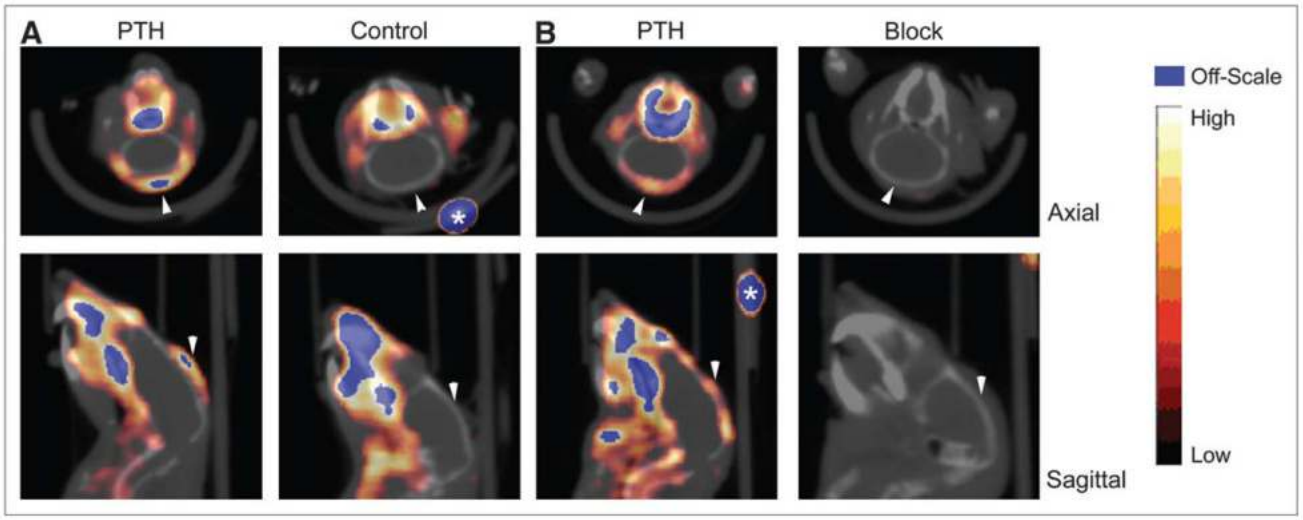

Figure 66.

Small-animal PET/CT of PTH-treated mice. Calvarium uptake of ^{64}Cu-CB-TE2A-c(RGDyK) was higher in PTH-treated mice (7.4 MBq [199 mCi],115 ng, SUV 0.53) than in control mice (7.7 MBq [209 mCi], 121 ng, SUV 0.22) (50- to 60-min summed dynamic image). (A) In PTH-treated mice, uptake was reduced in all tissues, including calvarium, after injection of c (RGDyK) (PTH[left]: 159 mCi, 84 ng, SUV 5 0.33; block [right]: 164 mCi, 87 ng, SUV 5 0.18) (static image obtained 60 min after injection, 10-minscan). (B) Arrowheads indicate calvarium of each animal. Fiducials (*) are indicated. Reprinted with permission from reference [400]. Copyright 2007 Society of Nuclear Medicine.

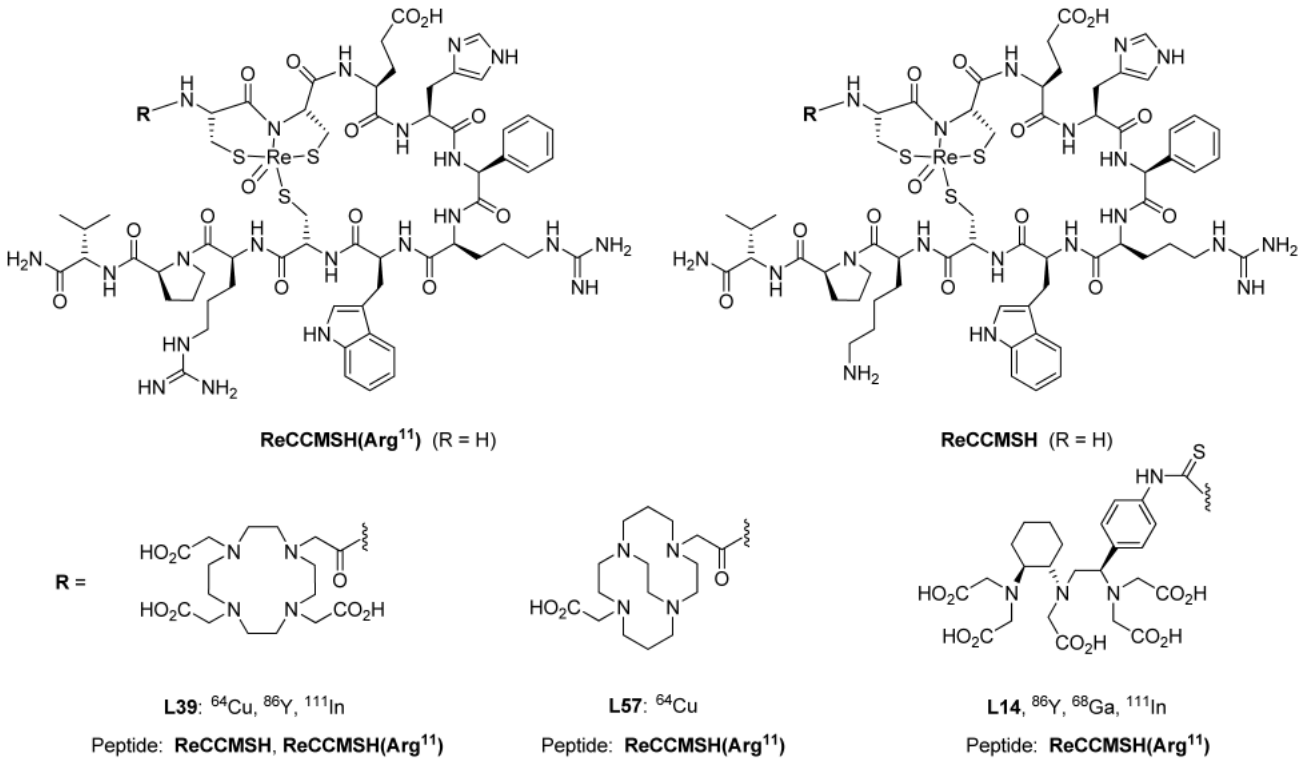

Figure 67.
Selected somatostatin analogues used in somatostatin receptor targeting radiopharmaceuticals.

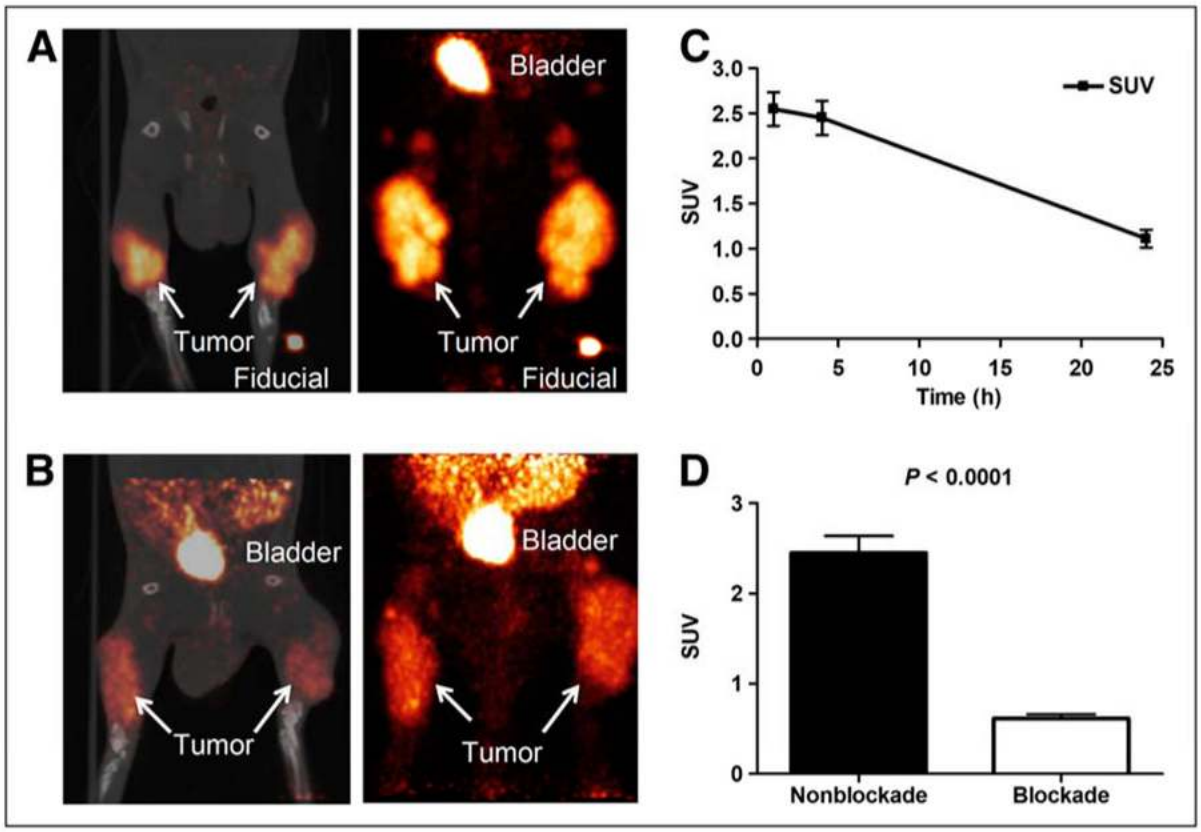

Figure 68.

(A) Representative small animal PET image at 4 h of rat injected with ^{64}Cu-CB-TE2A-sst$_2$-ANT. Left image is representative slice from small-animal PET/CT fusion image and right image is small-animal PET projection view of same animal. Calculated SUV for the tumor in left hind limb was determined to be 2.7 and SUV for tumor in right hind limb was determined to be 2.8. (B) Representative small-animal PET image at 4 h of rat injected with ^{64}Cu-CB-TE2Asst$_2$-ANT and sst$_2$-ANT as blocking agent. Left image is representative slice from small-animal PET/CT fusion image and right image is small-animal PET projection view of same animal. In animal receiving blockade, SUV for tumor in left hind limb was calculated to be 0.74 and SUV for tumor in right hind limb was calculated to be 0.51. (C) Graphical plot of change in average SUV over time. Even after 24 h, SUV remains high, suggesting enhanced binding of ^{64}Cu-CB-TE2A-sst$_2$-ANT for SST2 receptor. (D) Graphical representation that demonstrates change in observed SUV when excess cold sst$_2$-ANT is coinjected with radiopharmaceutical, indicating that binding of radiopharmaceutical to SSTR-positive tumor is receptor-mediated. Reprinted with permission from reference [445]. Copyright 2008 Society of Nuclear Medicine.

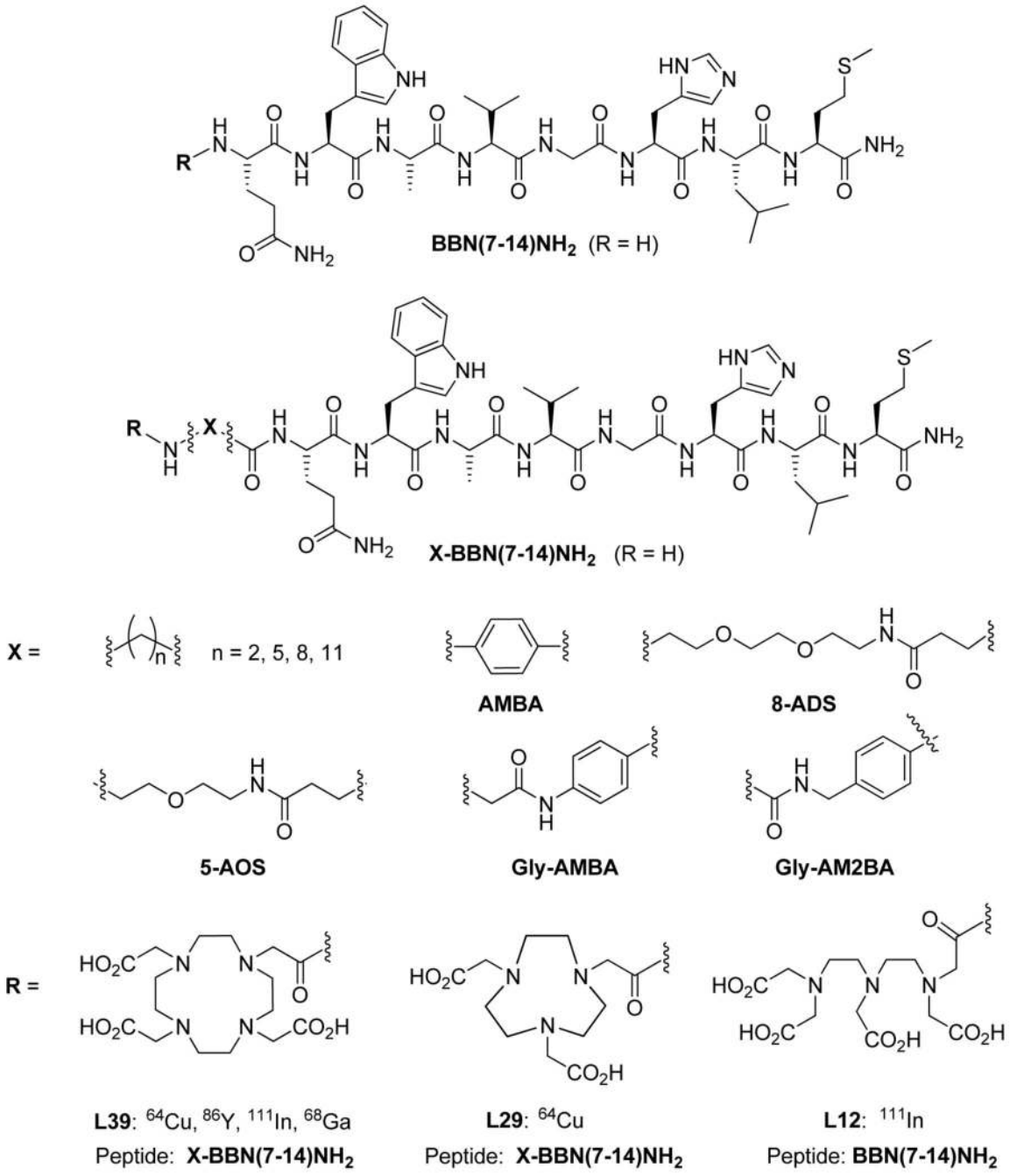

Figure 69.
Selected bombesin analogues used in targeting the GRP receptor.

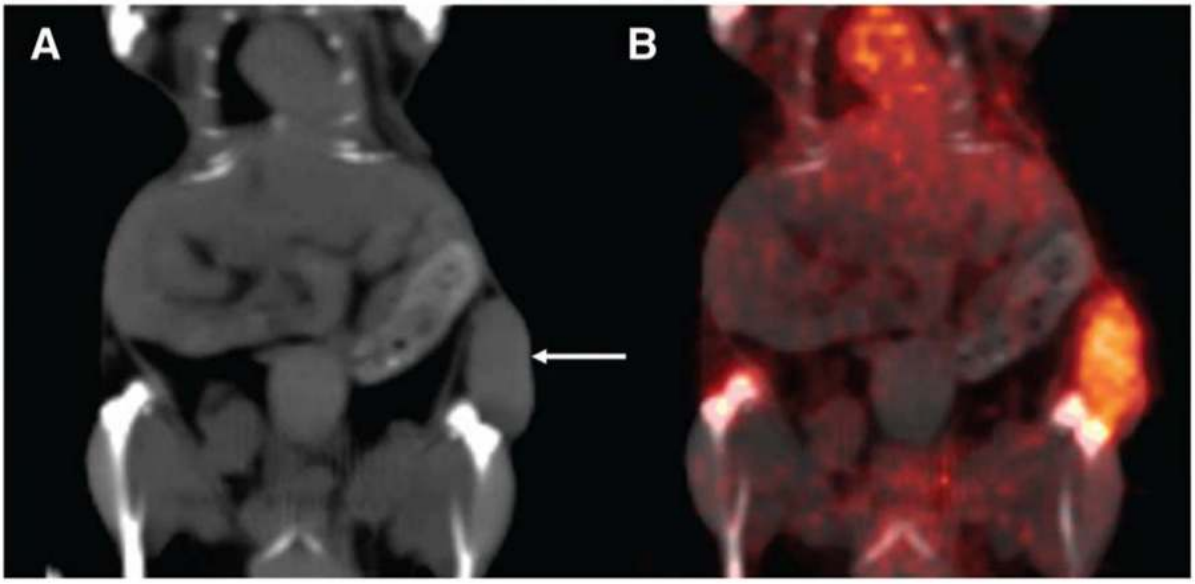

Figure 70.
Coronal CT image (A) with clear subcutaneous localization of SKOV-3 tumor (arrow). Fusion of microPET and CT images (B) (168 h after injection) enables adequate quantitative measurement of ^{89}Zr-bevacizumab in the tumor. Reprinted with permission from reference [210]. Copyright 2007 Society of Nuclear Medicine.

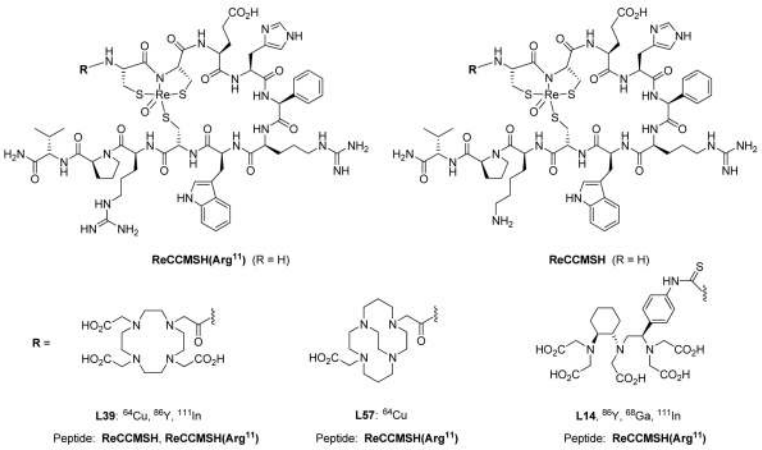

Figure 71.
Selected α-MSH analogues that target the melanocortin-1 (MC-1) receptor.

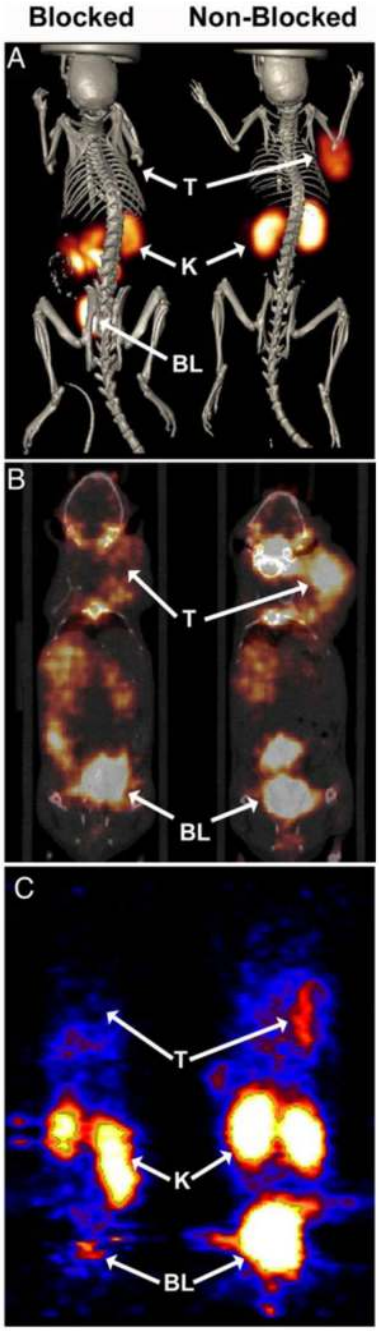

Figure 72.

Whole-body SPECT/CT, PET/CT and PET images of B16 melanoma tumor-bearing C57 mice 2 h post tail vein injection of radiolabeled CHX-A”-Re(Arg^{11})CCMSH. (A) SPECT/CT images of tumor-bearing mice injected intravenously with 12.95 MBq (350 μCi) of ^{111}In-CHX-A”-Re(Arg^{11})CCMSH with (blocked) or without (nonblocked) a 20-μg nonradiolabeled peptide block. PET/CT and PET imaging of melanoma-bearing mice 2 h post tail vein injection of (B) 4.44 MBq (120 μCi) of ^{86}Y-CHX-A”-Re(Arg^{11})CCMSH with a 20-μg NDP block (blocked) and without block (nonblocked) or (C) 3.7 MBq (100 μCi) of ^{68}Ga-CHX-A”-Re(Arg^{11}) CCMSH with (blocked) and without (nonblocked) a 60-μg NDP block, respectively. Tumor

(T), kidney (K) and (BL) bladder locations are highlighted for each mouse. Reprinted with permission from reference [141]. Copyright 2009 Elsevier Limited.

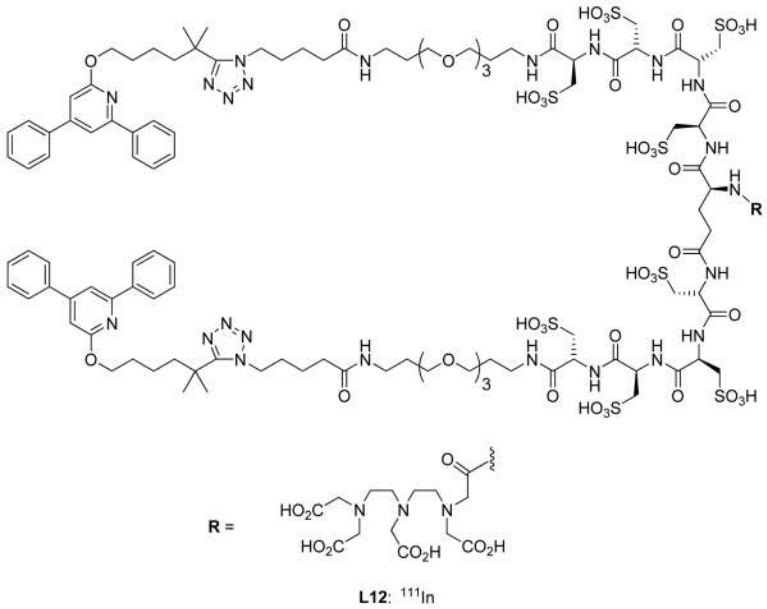

Figure 73.
The synthetic antagonist DPC11870 targets the leukotriene B4 (LTB4) receptor.

Table 1

Gamma- and Beta-Emitting Radiometals

Isotope	$T_{1/2}$ (h)	Production Methods	Decay Mode	E_γ (keV)	E_{β^-} (keV)	Reference
^{67}Cu	62.01	accelerator $^{67}Zn(n,p)$	β^- (100%)	91, 93, 185	577, 484,395	578
^{67}Ga	78.26	cyclotron	EC (100%)	91, 93, 185, 296, 388		578
^{90}Y	64.06	$^{90}Sr/^{90}Y$ generator	β^- (72%)		2288	578
^{111}In	67.9	cyclotron, $^{111}Cd(p,n)^{111}n$	EC (100%)	245, 172		578

Table 2

Positron-Emitting Radiometals

Isotope	$T_{1/2}$ (h)	Methods of Production	Decay Mode	E_{β^+} (keV)	Reference
^{60}Cu	0.4	cyclotron, $^{60}Ni(p,n)^{60}Cu$	β^+ (93%) EC (7%)	3920, 3000 2000	578
^{61}Cu	3.3	cyclotron, $^{61}Ni(p,n)^{61}Cu$	β^+ (62%) EC (38%)	1220, 1150 940, 560	578
^{62}Cu	0.16	$^{62}Zn/^{62}Cu$ generator	β^+ (98%) EC (2%)	2910	578
^{64}Cu	12.7	cyclotron, $^{64}Ni(p,n)^{64}Cu$	β^+ 19(%) EC (41%) β^- (40%)	656	578
^{66}Ga	9.5	cyclotron, $^{63}Cu(\alpha,n\gamma)^{66}Ga$	β^+ (56%) EC (44%)	4150, 935	578
^{68}Ga	1.1	$^{68}Ge/^{68}Ga$ generator	β^+ (90%) EC (10%)	1880, 770	578
^{86}Y	14.7	cyclotron, $^{86}Sr(p,n)^{86}Y$	β^+ (33%) EC (66%)	2335, 2019 1603, 1248 1043	578
^{89}Zr	78.5	$^{89}Y(p,n)^{89}Zr$	β^+ (22.7%) EC (77%)	897 909, 1675, 1713, 1744	208,578

Table 3

Properties of Relevant Metal Cations

Cation/Electron Configuration	Ionic Radius,[a] (CN)	pK_a[b]	$k_{exchange}$ s^{-1}[c]	E_{red}[d] V (acid)	*Hardness Classification* (I_A)[e]
Cu(II)/[Ar]$3d^9$	57 (4) 65 (5) **73 (6)**	7.53	2×10^8	+0.34 (Cu^0) +0.16 (Cu^I)	Borderline (2.68)
Ga(III)/[Ar]$3d^{10}$	47 (4) 55 (5) **62 (6)**	2.6	7.6×10^2	−0.56 (Ga^0) −0.65 (Ga^{II})	Hard (7.07)
In(III)/[Kr]$4d^{10}$	62 (4) **80 (6)** 92 (8)	4.0	4.0×10^4	−0.34 (In^0) −0.49 (In^{II})	Hard (6.30)
Y(III)/[Kr]	**90 (6)** 102 (8) 108 (9)	7.7	1.3×10^7	−2.37 (Y^0)	Hard (10.64)
Zr(IV)/[Kr]	59 (4) **72 (6)** 84 (8) 89 (9)	0.22		−1.54 (Zr^0)	Hard

[a] picometers.[579]

[b] as hydrated cation.[580]

[c] H_2O.[581]

[d] vs. NHE; Table 6.2, p.267;[582] Appendix E.[583]

[e] $I_A = E_A/C_A$;[584,585] Table 2.3.[586]

Table 4

Data on Selected Cu(II)-Chelator Complexes

Chelator	Donor Set (Total CN)	Cation Coordination Geometry	$\log K_{ML}$ [a]	E_{red} or E_p [b,c]	Acid Inertness, $t_{1/2}$ (Conditions)	Reference
L6	N_2S_2 (4)	distorted square planar				80
L9, ATSM	N_2S_2 (4)	distorted square planar		−0.40 (q-rev)		81,82
L10, EDTA	N_2O_4 (6)		18.8 19.2			587,588
L12, DTPA	N_3O_3 (6)		21.4			589
L17	N_6 (6)	distorted octahedron	16.3	0.08 (q-rev)		590
L19, TACHPYR	N_6 (6)	distorted octahedron				88
L29, NOTA	N_3O_3 (6)	distorted trigonal prsim	19.8 21.6	~−0.70 (irrev)	< 3 min (5M HCl, 30°)	586,591,592
L38, CYCLEN	N_4 (5)	square pyramid	24.6		< 3 min (5M HCl, 30°)	112,593
L34	N_4	distorted square pyramid	8.3	~−1.60 [b](irrev)		99,100
L36	(5)					
L39, DOTA	N_4O_2 (6)	distorted octahedron	22.2 22.7	~−0.74 (irrev)	< 3 min (5M HCl, 90°)[112]	145,594,595
L46, DO2P	N_4O_2 (6?)		28.7			103
L48, CYCLAM	N_4 (5-6)	square pyramid, tetragonally elongated octahedral	27.2	~−0.48 (irrev)	3.8 min (5M HCl, 90°)[112]	593
L49, TETA	N_4O_2 (6)	distorted octahedron	21.1 21.9	~−0.98 (irrev)	< 3 min (5M HCl, 90°)[112]	145,594,595
L54, TE2P	N_4O_2 (6)	tetragonally-distorted octahedron	26.5	~−0.45 (irrev)	1.7 h (1M HCl, 60°)	114
L56, CB-CYCLAM	N_4 (5)	distorted square pyramid	27.1	−0.32 (q-rev)	11.8 min (1M HCl, 90°)	111,112,596

Chelator	Donor Set (Total CN)	Cation Coordination Geometry	$\log K_{ML}$ [a]	E_{red} or E_p [b,c]	Acid Inertness, $t_{1/2}$ (Conditions)	Reference
L37, CB-DO2A	N_4O_2	distorted octahedron		~−0.72 (irrev)	4.0 h (1M HCl, 30°)	21,112
L57, CB-TE2A	N_4O_2 (6)	distorted octahedron		−0.88 (q-rev)	154 h (5M HCl, 90°)	111,112
L62, DIAMSAR	N_6 (6)	distorted octahedron or trigonal prism		~−0.90 (irrev)[13]	40 h (5M HCl, 90°)[13]	118

[a] K_{ML} = [ML]/[M][L].

[b] (q-rev) = quasi-reversible; E_{red} = reduction potential; (irrev) = irreversible reduction, E_p = peak potential only.

[c] vs. NHE.

Table 5

Data for Selected Ga(III)-Chelator Complexes

Chelator	Donor Set (Total CN)	Cation Coordination Geometry	$\log K_{ML}$ [a]	Reference
L1	NO_3 (6)	distorted octahedron	19.1 (*p*-NO_2) 25.2 (*p*-OMe)	129
L2	NS_3 (4)	distorted tetrahedron	20.5	130
L4, BAT-TM	N_2S_2 (5)	distorted square pyramid		132
Transferrin	NO_5 (6)		20.3 19.8	46,128
L5, EC	$N_2O_2S_2$ (6)	distorted octahedron	31.5	133,586
L10, EDTA	N_2O_4 (6)	distorted octahedron	21.0 22.0	588,593
L11, HBED	N_2O_4 (6)		37.7 38.5	135,172
L12, DTPA	N_3O_3 (6?)		25.5	593
L15, SBAD	N_4O_2 (6)	distorted octahedron	28.3	139
L16, BAPEN	N_4O_2 (6)	distorted octahedron		143,144
L29, NOTA	N_3O_3 (6)	distorted octahedron	31.0	145,597
L27, TACN-TM	N_3S_3 (6)	distorted octahedron	34.2	145
L39, DOTA	N_4O_2 (6)	distorted octahedron	21.3	145
L49, TETA	N_4O_2 (6)	distorted octahedron	19.7	145
L37, CB-DO2A	N_4O_2 (6)	distorted octahedron		162
L57, CB-TE2A	N_4O_2 (6)	distorted octahedron		163
L20, DiP-LICAM	O_6 (6)		38.6	187
L66	O_6 (6)		27.5	
L21			25.6	598
L22			27.3	
L23, DFO	O_6 (6)		28.6	599

[a] $K_{ML} = [ML]/[M][L]$.

Table 6
Data for Selected In(III)-Chelator Complexes

Chelator	Donor Set (Total CN)	Cation Coordination Geometry	$log K_M$[a]	Reference
L2	NS_3 (5)	~trigonal bipyramid	21.2	130,173
L3	NS_3 (5)	~trigonal bipyramid		
L4, BAT-TM	N_2S_2 (5)	square pyramid		132
Transferrin	NO_5 (6)	distorted octahedron(?)	18.7	128
L5, EC	$N_2O_2S_2$ (6)	distorted octahedron	33.0	133
L11, HBED	N_2O_4 (6)		27.9 27.8	138,172
L10, EDTA	N_2O_4 (7)	~pentagonal bipyramid	24.9 25.1 25.3	593 588,600
L12, DTPA	N_3O_4 (7) N_3O_5 (8)	~pentagonal bipyramid ~square antiprism	29.5 29.0 29.0	587,588,600
L15, SBAD	N_4O_2		24.5	139
L29, NOTA	N_3O_3 (6)	distorted octahedron	26.2	37,147
L27, TACN-TM	N_3S_3 (6)	distorted octahedron	36.1	145
L39, DOTA	N_4O_2 (8?)		23.9	186
L49, TETA	N_4O_2		21.89	186
L57, CB-TE2A	N_4O_2 (6)	distorted octahedron		155
L23, DFO	O_6		21.4	599
L20, DiP-LICAM	O_6		39.2	187

[a] $K_{ML} = [ML]/[M][L]$.

Table 7
Data for Selected Y(III)-Chelator Complexes

Chelator	Donor Set (Total CN)	Cation Coordination Geometry	$\log K_{ML}$ [a]	Reference
L10, EDTA	N_2O_4 (8)	distorted dodecahedron	18.1 18.5	593,601
L12, DTPA	N_3O_5 (8)	monocapped square antiprism	21.2 22.0 22.5	587,601,602
L30, NOTAM	N_3O_3 (9)	monocapped square antiprism		190
L39, DOTA	N_4O_4 (8)	square antiprism	24.3 24.4 24.9	37,601,602
L49, TETA	N_4O_2 (8?)	distorted dodecahedron (?)	14.8	195

[a] K_{ML} = [ML]/[M][L].

Table 8

Data for Selected Zr(IV)-Chelator Complexes

Chelator	Donor Set (Total CN)	Cation Coordination Geometry	$\log K_{ML}$ [a]	Reference
L10, EDTA	N_2O_4 (8)	~ dodecahedron	27.7 29.4	589,600
L12, DTPA	N_3O_5 (8)	~ dodecahedron	35.8 36.9	587,600
L39, DOTA	N_4O_4 (8?)	square anti-prism(?)		177

[a] K_{ML} = [ML]/[M][L].

Table 9

Biologically Targeted Radiopharmaceuticals Developed with Zr, Y, Ga, In and Cu Radiometals

Metal	Bifunctional Chelator	Targeting Molecule	Target	Preparatory Notes[a]
Zr	**L23, DFO**	antibody	HNSCC[19,208] Met expression[359] non-hodgkin's lymphoma[45]	Labeling in oxalate solution requires a strong, indifferent buffer (HEPES (pH 7.2)) required.
			EGFR[44]	
			VEGF[210]	Tetrafluorophenyl ester modified DfO facilitates coupling to targeting molecule.
Y	**L14, CHX-A"-DTPA**	peptide antibody	SSTR[433] Lewis Y antigen[603]	acetate buffer (pH 5.5), 25°C
	L39, DOTA	peptide ODNS	MC-1R[500] GRPR[461] gene expression[194,509]	acetate buffer (pH 5.5-7); reaction temperature: 60-90°C (peptides) 25-37°C (antibody)
				DOTA-NHS facilitates coupling to peptides and antibodies.
	L23, DFO	peptide	folate receptor[347]	Tris buffered saline (pH 7.4), 25°C, 24 h is suggested.
Ga	L11, HBED	peptide antibody	EGFR[137] MUC1[136]	Tetrafluorophenyl ester modified HBED facilitates coupling to targeting molecule.
				Low final pH (4.1-4.5) is necessary for Ga complexation.
	L39, DOTA	peptide ODNS	MC-1R[502] GRPR.[459,604] K-ras oncogene.[511] EGFR[479]	Anion exchange chromatography can be used to concentrate generator eluates.[605]
			SSTR [268,439,441-443,605,606]	The use of acetate or HEPES buffer is suggested.
				The final pH of the reaction solution should be 4-5.5.
				High reaction temperatures required (85-100°C).
				Microwave heating reduces reaction time.
	L29, NOTA	peptide	SSTR[154] integrin $\alpha_v\beta_3$[395,401]	Labeling can occur at 25°C over a pH range of 3.5-6 in less than 30 min.
	L12, DTPA	peptide ODNS/PNA peptidomimetic antibody	GRPR[456] EGFR[449,473,474] p21[WAF-1CIP-1510] mRNA[515]	Labeling can occur at 25°C with reaction times no longer than 60 min.
			LTB4R.[523,607] SSTR[9]	Acetate buffers (pH 5.5-6.5) are recommended.

Metal	Bifunctional Chelator	Targeting Molecule	Target	Preparatory Notes[a]
In	**L39, DOTA**	peptide peptidomimetic	GRPR[457] MC-1R.[496] SSTR[9,407]	Final solution pH should be 5.0-7.0. Acetate buffer is recommended.
			integrin $\alpha_v\beta_3$ [383,386]	
			integrin $\alpha_4\beta_1$ [378]	Reaction conditions are 30-60 min. at 65-100°C.
	L12, DTPA	peptide peptidomimetic	inflammation	Acetate buffer (pH 5.5) is recommended.
				Final solution pH is 4.5-5.0.
	L14, CHX-A”-DTPA	antibody	hEGFR-2[608]	Acetate buffer is recommended.
				Reaction conditions are 30-60 min. at 25°C.
Cu	**L39, DOTA**	peptide antibody peptidomimetic	integrin $\alpha_v\beta_3$ [397] $\alpha_v\beta_6$[376] VEGFR(various)[489 490,493]	Acetate buffer recommended. Final solution pH should be 5.5-8.0.
			MC-1R.[500,501] EGFR[480]	Reaction temperatures are 25-100°C depending on conjugate.
		GRPR[466461464,465]		
			SSTR[7,425,609]	PD-10 or Waters SepPak light C18 can be used for antibody or peptide purification, respectively.
	L49, TETA	peptide	SSTR[431,610,611]	Acetate buffer recommended (pH 5.5-6.5).
				Reaction conditions of 60 min. at 25-37 °C are recommended.
				Gentisic acid (1mg/mL) can be used to counteract radioloysis.
	L57, CB-TE2A	peptide peptidomimetic	integrin $\alpha_v\beta_3$ 399,611 integrin $\alpha_v\beta_6$[376] MC-1R[504]	Acetate buffer (pH 7.5-8.5), 95°C; 1-2 h is recommended.
	L62, DIAMSAR	peptide	$\alpha_v\beta_3$[121,399]	Acetate buffer (pH 5.0-8.0) 25°C; 60 min. is recommended.
	L29, NOTA	peptide	GRPR[462467,468,612]	Acetate buffer; final pH 6.5 60 min. at 70 °C is recommended.

[a]Presented as an initial reference for radiopharmaceutical preparation.